

Developing tools for the characterisation of host-pathogen interactions in amoebic gill disease (AGD) of Atlantic salmon (Salmo salar)

Thesis submitted for the degree of
Doctor of Philosophy in Aquaculture

By

Carolina Fernandez-Senac

BSc. in Biology

Parasitology Research Group

Institute of Aquaculture, University of Stirling

Stirling, Scotland, UK

March, 2020



Declaration

I hereby declare that the work and results presented in this thesis was conducted by me at the Institute of Aquaculture, University of Stirling, Scotland. The work presented in this thesis has not been previously submitted for any other degree or qualification.

The literature consulted has been cited and where appropriated, collaborative assistance has been acknowledged.

Word count: Approximately 52614 words



Carolina Fernandez-Senac

Stirling, Scotland, UK

February 8th, 2021

This is to certify that this thesis for the degree of Doctor of Philosophy entitled “Characterising host-pathogen interactions in amoebic gill disease (AGD) of Atlantic salmon (*Salmo salar*)” submitted to the University of Stirling (UK), is an original work carried out by Carolina Fernández-Senac under our supervision.



Prof. James E. Bron

Stirling, UK

February 8th, 2021



Prof. Alexandra Adams

Stirling, UK

February 8th, 2021

Acknowledgements

I would first express my immense appreciation to Ana Corrochano. You know that without your crazy idea of moving to Scotland in 2015, I would have not been here in the first place. The chance of working as a trainee under the wing of Dr. Giuseppe Paladini brought me the opportunity to learn all I know about parasites so thanks for giving me the chance and push me towards the right direction.

Likewise, to my principal supervisors, Professor James E. Bron and Professor Alexandra Adams for making me a better and independent researcher. Also, to Dr. Sophie Fridman, who taught me all about culturing the amoebae and, although we have not always been on the same page, I appreciate her for helping me along the way.

Nevertheless, all my lab work would not have been possible without the constant help, but above all patience, from the technical staff at the Institute of Aquaculture: Debbie Faichney, Karen Snedden, Hilary McEwan, Jacquie Ireland and Kerrie Bartie, but also from all the technical staff at MERL and to my partners in the ParaFishControl project.

While getting the results is important, their understanding and analysis is key and for that I would like to voice my deepest gratitude to Dr. Michäel Bekaert, Dr. Teresa Garzon, Dr. Johanna L. Baily, Dr. Monica Betancor and Dr. Lynn Chalmers.

Especially I would like to warmheartedly thank my friend and, in essence, supervisor, Dr. Sean J. Monaghan. You know how much you helped me all the way. In getting the results, two key students have helped me and have been part of my thesis as much as I have, for that thanks to my office and project colleague Jadwiga Sokolowska and to Dr. Dario Mascolo, which I can also call a friend after all these years.

Nonetheless, the path of doing a doctoral thesis is sometimes isolating and for that I would like to all the people I have met through the years and have helped me from going insane. Firstly, all the people from the University of Stirling Triathlon and Cycling Clubs. You helped me get fit but also had tons of fun learning about these two great sports. Especially I would like to thank my sporty ladies Iona Hamilton,

Emily Boardman, Yana Semerdjieva, Sarah King and Phoebe Lloyd-Evans. Thanks for taking me out on bike rides and swims and, least favourite, runs.

I would also like to mention the people who offered me a job during my last year of PhD which helped me with my living costs. Thanks to my CIAO family, Marco, Hayley and all my co-workers, especially Kennedy McCall and Biagio Celiento.

To my Stirling family, Dr. Sanne and Dr. Matthijs Metselaar, their amazing children Fleur and Anna-Fay, and Dr. Marie Smedley and Dr. Sean J. Monaghan, and their wee one Euan Daniel Smedley-Monaghan. Thanks for always making me feel like home when I'm so far from mine. I will never forget that.

A huge thanks to my colleagues and friends at the University of Stirling, especially to Dr. Bernat Morro, Dr. Kristina Ulrich, Ana Corrochano, Irene M. Martin, Lewis Warren, I cannot explain with words how much you helped me grow into the person I am today through coffee breaks, pub and sporadic hangouts. You have been through good and bad and for that I hold a huge gratitude towards you.

To all my friends back home and the ones that have visited me through this period away from home. Your support from the distance was much needed during this time of my life. Great thanks to my childhood friends Alba, Ana, Adri, Yoli, Susi, Alba, Miguel, Jess, and Cris. My friends from uni, Marta, Guille, Sergio, Jhorman, Nico, Zuazu, and Rafa. To the Kappa Crew for always bring a smile to my face from far away and the Dark Lord Sauron, you know why. To my second family back home, Chus, Enrique, Marisa, Manolo, Los Setienes, Laurita, Susana, and Paloma. My immense wholehearted thanks. Also, to David, even though you were still not in my life during the process, your support through the time spent on my corrections was much appreciated and I'm so glad I met you. Good luck with your own thesis, my dearest friend.

Lastly, I would like to dedicate my work to my parents and sister, Mercedes, Pepo and Gloria. Without your constant support and words of appreciation I would not be the person I am today. Thanks for always believing in me and encourage me to take on this adventure and more to come across my life, even though it could mean I'm far away from home.

Peer-reviewed publications

1. Fernandez, C., Mascolo, D., Monaghan, S. J., Baily, J. L., Chalmers, L., Paladini, G., Adams, S., Bron, J. E. & Fridman, S. (2019). Methacarn preserves mucus integrity and improves visualization of amoebae in gills of Atlantic salmon (*Salmo salar* L.). *Journal of Fish Diseases*, 42(6), 883-894.
2. Fernandez-Senac, C., Fridman, S., Sokolowska, J., Monaghan, S. J., Garzon, T., Betancor, M., Adams, S. & Bron, J. E. (2020). A comparison of the use of different swab materials for optimal diagnosis of amoebic gill disease (AGD) in Atlantic salmon (*Salmo salar* L.). *Journal of Fish Diseases*.

Scientific conferences and meetings

1. Fernandez, C., Paladini, G., Fridman, S., Garzon, T., Adams, A., Bekaert, M., Migaud, H., Monaghan, S.J. & Bron, J.E. A comparison of different swabbing methods for optimised diagnosis of amoebic gill disease (AGD) in the Atlantic salmon (*Salmo salar*). 18th International Conference on Diseases of Fish & Shellfish. 4-8th September 2017, Belfast, UK (Poster presentation).
2. Fernandez C., Monaghan S.M., Mascolo D., Baily J.L., Betancor M.B., Chalmers L., Paladini G., Adams A., Fridman S. and Bron J.E. H₂O₂ treatment impacts immune activity in Atlantic salmon gills and causes similar mucin disruption to high grade AGD affected fish. 19th International Conference on Diseases of Fish and Shellfish. 9-12th September 2019, Porto, Portugal (Oral presentation).
3. Fernandez, C., Mascolo, D., Monaghan, S. J., Baily, J. L., Chalmers, L., Paladini, G., Adams, S., Bron, J. E. & Fridman, S. Methacarn preserves mucus integrity and improves visualisation of amoebae in gills of Atlantic salmon (*Salmo salar* L.). 19th International Conference on Diseases of Fish and Shellfish. 9-12th September 2019, Porto, Portugal (Poster presentation).

Trainings and workshops

1. ScotPil Personal Licence training course, 23rd October 2017, Glasgow, UK.
2. Teaching Assistant course, 22nd October 2018, Stirling, UK.

Grants

1. Travel grant for the 19th EAAP, Porto, Portugal. Amount: £1,000

List of abbreviations

| | |
|--------------------|---|
| µg | Micrograms |
| µl | Microliters |
| µm | Micrometres |
| AB/PAS | Alcian blue-Periodic Acid Schiff stain |
| AGD | Amoebic gill disease |
| ANOVA | Analysis of variance |
| AN | Accession number |
| aq | Aqueous |
| asAG-2 | Atlantic salmon anterior gradient-2 protein |
| ASPA | Animals Scientific Procedures Act 1986 |
| ATP | Adenosine triphosphate |
| AWERB | Animal Welfare and Ethical Review Body |
| β-actin | Beta-actin |
| BCP | 1-Bromo-3-chloropropane |
| BLAST | Basic Local Alignment Search Tool |
| BSA | Bovine serum albumin |
| β-tubulin | Beta-tubulin |
| cat | catalase |
| cDNA | Complementary DNA |
| CD3 | Cluster of differentiation 3 |
| CD3γδ-B | Cluster of differentiation 3γδ-B |
| CD4-2α | Cluster of differentiation 4-2α |
| CD8α | Cluster of differentiation 8α |
| CDS | Coding region |
| cm | Centimetre |
| CPA | Cytopathic effect |
| CS | Cleavage site |
| C _t | Cycle threshold |
| d | Days |
| DBA | <i>Dolichos biflorus</i> agglutinin lectin |
| ddH ₂ O | Double distilled water |
| DNA | Deoxyribonucleic acid |
| dNTP | Deoxyribonucleotide triphosphate |
| DO | Dissolved oxygen |
| dpi | Days post-infection |
| dpt | Days post-treatment |
| EDTA | Ethylenediaminetetraacetic acid |
| EF1α | Elongation factor 1α |
| e.g. | <i>Exempli gratia</i> (for example) |
| F | F value |
| FSW | Filtered seawater |
| FW | Freshwater |
| GADD45β | Growth arrest and DNA-damage-inducible beta protein |
| GalNac | N-acetyl-D-galactosamine |
| GC | Guanine/cytosine ratio |
| GO | Gene ontology |
| Gpx1 | Glutathione peroxidase 1 |

| | |
|-------------------------------|---|
| GlcNAc | N-Acetylglucosamine |
| h | Hours |
| H ₂ O ₂ | Hydrogen proxide |
| hsp70 | Heat shock protein 90 |
| <i>i.e.</i> | Id est (in other words) |
| IFN- γ | Interferon gamma |
| IgG | Immunoglobulin G |
| IgM | Immunoglobulin M |
| IgT | Immunoglobulin T |
| IHC | Immunohistochemistry |
| IL1 β | Interleukin 1 β |
| IL-4/13 | Interleukin 4/13 |
| IL-4/13 β 2 | Interleukin 4/13 beta 2 |
| IL-10 | Interleukin 10 |
| IL-22 | Interleukin 22 |
| KEGG | Kyoto Encyclopedia of Genes and Genomes |
| KHV | Koi herpesvirus |
| kg | Kilogram |
| L | Litre |
| LWB | Lectin wash buffer |
| M | Molar |
| MDAB | Modified Davidson's solution with 2% (w/v) Alcian blue |
| MDS | Modified Davidson's solution |
| MERL | The Marine Environmental Research Laboratory |
| mg | Milligrams |
| m IgM | Mucosal immunoglobulin M |
| min | Minutes |
| mL | Millilitres |
| mM | Millimolar |
| mRNA | Messenger RNA |
| MS | Methacarn solution |
| MSAB | Methacarn solution supplemented with 2% (w/v) Alcian blue |
| MS-222 | Tricaine mesylate |
| Muc1 | Mucin 1 |
| Muc17 | Mucin 17 |
| Muc2 | Mucin 2 |
| Muc5ac | Mucin 5ac |
| MYB | Malt yeast broth |
| N | Normality |
| NBF | 10% Neutral buffered formalin solution |
| NCBI | National Centre for Biotechnology Information |
| nt | Nucleotides |
| <i>p</i> | p-value |
| PAS | Periodic Acid Schiff stain |
| PCNA | Proliferating cell nuclear antigen |
| PCR | Conventional polymerase chain reaction |
| ppt | Parts per thousand |
| ppm | Parts per million |
| <i>r</i> | Correlation coefficient |

| | |
|-----------------|-------------------------------------|
| rDNase I | Recombinant DNase I |
| REST | Randomisation test |
| rRNA | Ribosomal ribonucleic acid |
| RNA | Ribonucleic acid |
| RT | Room temperature |
| R. T. | Recombinant transcriptase |
| RT-PCR or qPCR | Real-time polymerase chain reaction |
| s | Seconds |
| s.d. | Standard deviation |
| s.e.m | Standard error of the mean |
| SEM | Scanning electron microscopy |
| Sig. | Significance |
| SP | Signal peptide |
| SW | Seawater |
| SWA | Seawater agar |
| TBS | Tris-buffered saline |
| TBST | Tris-buffered saline with Tween-20 |
| TCR α | T-cell receptor alpha |
| Th | T helper cells |
| Th1 | T helper cells 1 |
| Th17 | T helper cells 17 |
| Th2 | T helper cells 2 |
| TNF- α 2 | Tumor necrosis factor alpha 2 |
| TNF- α 3 | Tumor necrosis factor alpha 3 |
| v/v | Volume/volume |
| w/v | Weight/volume |
| WGA | Wheat germ agglutinin lectin |
| x g | Centrifugal force |

Abstract

Atlantic salmon production (*Salmo salar*) has increased in-line with global population growth and changes in consumption patterns, causing the emergence of several infectious diseases. Gill disorders, such as amoebic gill disease (AGD), have posed a particular problem. Thus, limiting the levels of infection by its causative agent, *Neoparamoeba perurans*, is considered to be one of the main challenges for salmon producers worldwide. Current treatments often lead to re-infection and may eventually cause indirect and direct economic losses. Hence, the development of alternative treatments is required.

Therefore, this study focused on the search and development of tools for the characterisation of host-pathogen interactions between Atlantic salmon and *N. perurans*. Firstly, an improved quantification of amoebae was accomplished through the comparison of different swab materials and the swabbing of different gill arches, showing a potential advantage by sampling the 4th gill arch and by using alginate-fibre tipped swabs in contrast to the other gill arches and swab materials. Additionally, the study of a better *in-situ* method for the preservation of mucus was explored through the use of a range of fixatives. Methacarn solution provided significantly greater retention of the mucus covering of the gill epithelium while aiding the preservation of amoeba trophozoites embedded in the mucus.

In addition, the potential effect of the commonly applied hydrogen peroxide (H₂O₂) treatment was assessed through use of a range of molecular tools to examine the gills of H₂O₂-treated fish and of AGD-infected fish. Results suggested evidence of a T-cell response after treatment, while a possible immunomodulation by the parasite was found in the AGD-infected fish. Lastly, the *in-silico* screening and identification of potential vaccine candidates within the *N. perurans* transcriptome provided a final list of cell membrane proteins, enzymes and structural proteins which could potentially serve as ideal candidates for vaccine development.

Table of Contents

| | |
|--|-----------|
| Declaration..... | i |
| Acknowledgements..... | ii |
| Peer-reviewed publications..... | iv |
| Scientific conferences and meetings | iv |
| Trainings and workshops..... | v |
| Grants..... | v |
| List of abbreviations | vi |
| Abstract..... | ix |
| List of tables | xiv |
| List of figures | xvii |
| Chapter 1 : General introduction | 1 |
| 1.1. Aquaculture industry: background..... | 1 |
| 1.2. Amoebic Gill Disease (AGD)..... | 2 |
| 1.2.1. Biology and taxonomy of <i>N. perurans</i> | 3 |
| 1.2.2. Pathology and clinical signs..... | 7 |
| 1.2.3. Diagnosis..... | 7 |
| 1.2.4. Current treatments and management | 9 |
| 1.3. Teleost fish immune system..... | 11 |
| 1.3.1. Mucosal immunity: gills..... | 13 |
| 1.3.2. Host response to AGD | 18 |
| 1.4. Vaccine development in the aquaculture industry | 22 |
| 1.4.1. Reverse vaccinology and the challenges in vaccine development against parasitic infections..... | 24 |
| 1.5. Aims and Objectives | 29 |
| Chapter 2 : A comparison of different swabbing methods for optimised diagnosis of amoebic gill disease (AGD) in Atlantic salmon (<i>Salmo salar</i>)..... | 30 |
| 2.1. Introduction | 30 |
| 2.2. Materials and Methods..... | 33 |

| | |
|---|-----------|
| 2.2.1. Clinical swabs | 33 |
| 2.2.2. Clonal development and culture conditions of <i>N. perurans</i> | 33 |
| 2.2.3. Evaluation of the potential inhibition of PCR by sodium citrate | 36 |
| 2.2.4. <i>In vitro</i> testing for the swabbing and spiking of the three clinical swabs .. | 36 |
| 2.2.5. <i>In vivo</i> testing of the three clinical swabs | 38 |
| 2.2.6. Swab digestion, DNA extraction and qPCR quantification | 40 |
| 2.2.7. Statistical analysis | 42 |
| 2.3. Results | 42 |
| 2.3.1. Evaluation of the preservation capacity of <i>N. perurans</i> in sodium citrate by PCR..... | 42 |
| 2.3.2. Detection of <i>N. perurans</i> from the <i>in vitro</i> and <i>in vivo</i> testing..... | 43 |
| 2.4. Discussion | 55 |
| Chapter 3 : Methacarn preserves mucus integrity and improves visualisation of amoebae in gills of Atlantic salmon (<i>Salmo salar</i> L.)..... | 60 |
| 3.1. Introduction | 60 |
| 3.2. Materials and Methods..... | 62 |
| 3.2.1. Fish and sampling..... | 62 |
| 3.2.2. Histology processing..... | 63 |
| 3.2.3. Staining for mucus layer evaluation | 65 |
| 3.2.4. Comparison of the different fixatives for semi-quantitative analysis of mucus and mucous cells | 66 |
| 3.2.5. Confirmation of mucus presence with fluorescent lectin labelling | 68 |
| 3.2.6. Statistical analysis | 69 |
| 3.3. Results | 70 |
| 3.3.1. Evaluation of different fixatives for the conservation of gill mucus | 70 |
| 3.3.2. Semi-quantitative analysis study for mucus and mucous cells | 73 |
| 3.3.3. Examination of the relationship between amoebae and mucus during an AGD infection | 75 |
| 3.3.4. Confirmation of mucus preservation using lectin histochemistry..... | 78 |
| 3.4. Discussion | 82 |

| | |
|---|------------|
| Chapter 4 : H2O2 treatment impacts on the T-cell response in Atlantic salmon gills and causes similar mucin disruption to fish during a late stage AGD-infection | 87 |
| 4.1. Introduction | 87 |
| 4.2. Material and Methods..... | 91 |
| 4.2.1. Experimental fish | 91 |
| 4.2.2. Sampling collection and hydrogen peroxide treatment | 92 |
| 4.2.3. TaqMan RT-qPCR analysis for <i>N. perurans</i> quantification | 93 |
| 4.2.4. SYBR® green RT-qPCR analysis for gene expression on gill tissue..... | 94 |
| 4.2.5. Mucous cell semi-quantitative analysis..... | 99 |
| 4.2.6. Immunohistochemistry (IHC) for evaluation of CD3+ cells expression and localisation in sampled gill tissue..... | 99 |
| 4.2.7. Image analysis for CD3+ cell expression quantification..... | 100 |
| 4.2.8. Statistical analysis | 102 |
| 4.3. Results | 103 |
| 4.3.1. Macroscopic analysis of gill pathology..... | 103 |
| 4.3.2. TaqMan RT-qPCR: <i>N. perurans</i> load quantification..... | 106 |
| 4.3.3. Gill gene expression | 106 |
| 4.3.4. Mucous cells semi-quantitative analysis and qualitative assessment of mucus production | 113 |
| 4.3.5. Immunohistochemistry for CD3+ cell expression quantification..... | 117 |
| 4.4. Discussion | 121 |
| Chapter 5 : Characterisation of <i>N. perurans</i> transcriptome for the <i>in-silico</i> prediction of potential vaccine candidates | 128 |
| 5.1. Introduction | 128 |
| 5.2. Materials and Methods..... | 132 |
| 5.2.1. Preparation of <i>N. perurans</i> cultures for transcriptomic analysis..... | 132 |
| 5.2.2. Sampling of high infected AGD fish for transcriptomic analysis | 132 |
| 5.2.3. RNA extraction and quality control..... | 132 |
| 5.2.4. RNAseq libraries preparation, sequencing data processing and <i>de novo</i> assembly | 133 |
| 5.2.5. Annotation and functional classification | 134 |
| 5.2.6. Selection of potential vaccine candidates through <i>in-silico</i> search | 134 |

| | |
|--|------------|
| 5.3. Results | 136 |
| 5.3.1. RNA isolation and quality control | 136 |
| 5.3.2. RNAseq libraries preparation..... | 137 |
| 5.3.3. Illumina sequencing and <i>de novo</i> assembly of the cultured <i>N. perurans</i> transcriptome..... | 138 |
| 5.3.4. Annotation and functional characterisation of the cultured <i>N. perurans</i> transcriptome..... | 140 |
| 5.3.5. Illumina sequencing and de novo assembly of the AGD-infected gill transcriptome..... | 142 |
| 5.3.6. Selection of potential vaccine candidates from the cultured <i>N. perurans</i> | 142 |
| 5.3.7. Selection of the potential vaccine candidates from the salmon AGD-infected gills..... | 148 |
| 5.3.8. Selection of potential vaccine candidates from literature survey..... | 152 |
| 5.4. Discussion | 156 |
| Chapter 6 : General Discussion | 163 |
| Appendices | 173 |
| I. Protocol for the cryopreservation of <i>N. perurans</i> | 173 |
| Cryopreservation methodology..... | 173 |
| Preliminary results from the cryopreservation of <i>N. perurans</i> | 173 |
| II. Annotation of the amoebae-cultured transcriptome with matching cell membrane proteins before blasting against the host's transcriptome. In blue and green the proteins that didn't match salmon's transcriptome . | 175 |
| III. Alignments of all the mRNA sequences with the <i>N. perurans</i> transcriptome | 183 |
| References..... | 189 |

List of tables

| | |
|---|----|
| Table 1.1. Key parasitic infections affecting Atlantic salmon globally in the aquaculture industry..... | 2 |
| Table 1.2. Summary of the studies that have investigated the host response to AGD in Atlantic salmon (▼ Indicates significant down-regulation, ▲ significant up-regulation and ▲▲ significant over expression). | 20 |
| Table 1.3. Different vaccination approaches performed against AGD. | 27 |
| Table 2.1. Method for swabbing the gills of AGD-infected fish: gills were sampled with different swab types (e.g. Cotton 2.1: cotton is the swab type; 2 is the 2nd gill arch; 1 is the replicate number)..... | 40 |
| Table 2.2. Results from the two-way ANOVA for the interaction: Swab type vs amoebae load vs Ct values for the spiked samples (A) and swabbed samples (B). F: F-test. Sig.: statistical significance. Bold values represent the significance of interactions ($p < 0.001$), while underlined values represent the non-significant interactions ($p > 0.001$). | 44 |
| Table 2.3. Results from the first experiment <i>in vivo</i> during December 2018. Scoring of all fish and Ct values are described in this table. Negative results are underlined and when no Ct value was detected during the qPCR, a value of 37 was assigned as this is the limit value when diagnosing AGD in the industry. | 47 |
| Table 2.4. Results from the second experiment <i>in vivo</i> during April 2019. Scoring of all fish and Ct values are described in this table. Negative results are underlined and when no Ct value was detected during the qPCR, a value of 37 was assigned as this is the limit value when diagnosing AGD in the industry..... | 48 |
| Table 2.5. Percentages of positives and negative results during both trials: (A) First trial in December. (B) Second trial in April. Isohelix® and CalgiSwab® present higher percentages of positive results throughout the experiment. | 49 |
| Table 2.6. December 2018 trial results from the two-way ANOVA for the interaction: Swab type vs gill arches vs Ct values. F: F-test. Sig.: statistical significance. Bold values represent the significance of interactions ($p < 0.05$), while underlined values represent the non-significant interactions ($p > 0.05$).. | 49 |
| Table 2.7. April 2019 trial results from the two-way ANOVA for the interaction: Swab type vs gill arches vs Ct values. F: F-test. Sig.: statistical significance. Bold values | |

represent the significance of interactions ($p > 0.05$), while underlined values represent the not significant interactions ($p < 0.05$)..... 49

Table 3.1. Preparation and maintenance of the distinct fixatives. RT: room temperature..... 65

Table 3.2. Lectins used and their specificity to glycoproteins present in gill mucus. 69

Table 4.1. Table representing means \pm s.e.m of the weight (kg), fork length (length; cm) and AGD score (according to modified AGD grading criteria of Taylor et al. 2009) of each fish used for the H₂O₂ treatment experiment (n= 48 fish). The Table shows data from the control group and from the AGD challenged group. Time 0 sub-groups are H₂O₂ untreated Atlantic salmon, whilst time 4, 24 and 14d are the post-H₂O₂ treatment sub-groups named after the time point at which they were sampled (namely 4 h, 24 h and 14d). 91

Table 4.2. Thermocycler conditions for cDNA synthesis of the RNA samples. 95

Table 4.3. List of primers (5' → 3') used for the immune and mucin gene expression analysis in control fish treated with hydrogen peroxide and fish infected with AGD. 97

Table 5.1. Summary statistics of sequencing and assembly of cultured *N. perurans* transcriptome. *based of the longest transcript for each unigene..... 139

Table 5.3. Statistics of annotation results for *N. perurans* unigenes. *Interpro covers 12 databases (CATH-Gene3D, CDD, HAMAP, PANTHER, PIRSF, PRINTS, ProDom, PROSITE (patterns and profiles), SFLD, SMART, SUPERFAMILY, TIGRFAMs)..... 140

Table 5.4. Summary statistics of sequencing and assembly of AGD-infected gill transcriptome 142

Table 5.5. List of the best twenty selected proteins from the in-silico search of the cultured *N. perurans* transcriptome from low to high E-values. 144

Table 5.6. Summary of the best vaccine candidates from the *in-silico* search of the cultured *N. perurans* transcriptome. These candidates were selected after blasting the sequences against the host's transcriptome, *S. salar*; remaining four proteins presented no homology with the host..... 145

Table 5.7. Summary of the remaining proteins from the cultured *N. perurans* transcriptome with the details of signal peptide presence and antigenicity. 146

Table 5.8. List of the best ten proteins from the *in-silico* search of the AGD-infected gill transcriptome from low to high E-values. 149

Table 5.9. Summary of the best vaccine candidates from the *in-silico* search of the AGD-infected gill transcriptome. These candidates were selected after blasting the sequences against the host's transcriptome *S. salar*; the remaining two proteins presented no homology with the host..... 150

Table 5.10. Summary of the remaining proteins from the AGD-infected gill transcriptome with the details of signal peptide presence and antigenicity. 151

Table 5.11. List of proteins investigated within both transcriptome assemblies (cultured amoebae and AGD-infected gills)..... 152

Table 5.12. Summary of the best vaccine candidates from the *in-silico* search of the cultured *N. perurans* and AGD-infected gill transcriptome assemblies. These candidates were selected after blasting the sequences against the host's transcriptome, *S. salar*. 153

Table 5.13. Summary of the remaining proteins from both transcriptome assemblies (cultured amoebae and AGD-infected gills) with the details of signal peptide presence and antigenicity..... 154

Table 5.14. Summary of the six best vaccine candidates identified in this experimental chapter according to its homology to known proteins, antigenicity, presence of signal peptide and proposed function. 155

List of figures

- Figure 1.1.** Different morphologies observed in the cultured *N. perurans*: attached trophozoites (a), floating trophozoites (b) and pseudocyst/cyst (c). Image taken with light microscope. 3
- Figure 1.2.** Images taken during the study by Tanifuji *et al.* (2017). (A) Atlantic salmon gill infected with *Paramoeba* spp. trophozoites found attached to gill epithelium. Eosin and haematoxylin staining to differentiate NP (nucleus of the host amoeba) from En (*Perkinsela* sp. endosymbiont). (B) Trophozoites of *P. pemaquidensis* with contrast microscopy. (C) Scanning electron microscopy (SEM) of a *P. pemaquidensis* trophozoite with endosymbiont (MP = plasma membrane of *P. pemaquidensis*). 5
- Figure 1.3.** Phylogenetic tree of some of the best known parasitic amoebic species using their 18S ribosomal RNA sequences. This was developed through the online tool Phylogeny.fr (Dereeper *et al.*, 2008)..... 6
- Figure 1.4.** Schematic representation of teleost fish gill mucosal surface. The mucus layer is shown containing antibodies (IgM and IgT) along with AMPs (antimicrobial peptides). The gill epithelium comprises epithelial cells along with mucous / goblet cells and B T cells. This diagram is simplified from Gomez *et al.* (2013)..... 14
- Figure 1.5.** Schematic representation of the mucosal immunity of the mucosal surface of the teleost gill. When a pathogen gets through the first barriers (mucus and gill epithelium), the recognition of this pathogen is facilitated by the pathogen-associated molecules (PAMPs) within these organisms. PRRs/TLRs localised on the macrophages recognise them and the antigen presentation takes place. As part of the adaptive immunity, dendritic cells present foreign antigens to T cells that will produce cytokines; B cells also do the same and also activate T cells. Subsequently the release of specific antibodies occurs by B cell produced plasma cells in the blood. This is a simplified version of the schematic representation featured in Beck & Peatman (2015)..... 17
- Figure 2.1.** Physical changes to the calcium alginate matrix after sodium citrate addition: Following sodium citrate treatment, trapped amoebae would become detached from the material due to matrix disintegration allowing improved access for diagnostic tools. Image modified from www.jchs.edu. 32

| | |
|--|----|
| Figure 2.2. Different types of swabs: (A) Cotton wool tipped swabs; (B) CalgiSwab®; (C) Isohelix® DNA buccal swabs. | 33 |
| Figure 2.3. Excised AGD-affected gill from Atlantic salmon showing white lesions (white arrows) caused by <i>N. perurans</i> | 34 |
| Figure 2.4. Culture of <i>N. perurans</i> . Different morphologies including attached (1), the latent stage, pseudocyst (2) and floating trophozoite (3). Observed with microscope Olympus BX53M and images were taken with Olympus SC100 camera. | 35 |
| Figure 2.5. Swabbing method: amoebae were swabbed on a seawater agar plate in two perpendicular directions..... | 38 |
| Figure 2.6. PCR results after preservation of amoebae in 0.2 M sodium citrate for 7 days (lanes S1-S3) and 14 days (S4-S6). M: 100 bp DNA ladder. +ve control: <i>N. perurans</i> 18S rRNA sequence. –ve control: ddH ₂ O. | 43 |
| Figure 2.7. Spiked amoebae: qPCR <i>Ct</i> values of <i>N. perurans</i> for three clinical swab types spiked with different concentrations of amoebae (10, 100 and 1,000/swab). Swabbed amoebae: qPCR <i>Ct</i> values of <i>N. perurans</i> for three clinical swab types used to detect amoebae from MYA plates seeded with different concentrations of amoebae (10, 100 and 1,000/plate). Bars represent the mean <i>Ct</i> values (n = 10 per concentration) (± s.e.m). Different letters represent statistically significant differences between swab type (p < 0.05). | 44 |
| Figure 2.8. Scores and number of fish for the first trial in December 2018 (A) and second trial in April 2019 (B) (n = 30 fish per trial). | 46 |
| Figure 2.9. Results of the qPCR detection of <i>N. perurans</i> 18S rRNA sequences when only gill arches were compared, regardless of the swab type during both trials (December 2018 and April 2019). Bars represent the mean <i>Ct</i> values (n= 30) (± s.e.m). Different letters represent statistically significant differences (<i>post-hoc</i> Tukey HSD Test; p < 0.05) and same letters mean no statistical differences (p > 0.05). Different colours in letters represent statistically significant differences between gill arches (p < 0.05)..... | 50 |
| Figure 2.10. Results of the qPCR detection of <i>N. perurans</i> 18S rRNA sequences when only gill arches were compared, regardless of the swab type during both trials (December 2018 and April 2019). Bars represent the average <i>Ct</i> values (n= 30) (± s.e.m). Different letters represent statistically significant differences (<i>post-hoc</i> Tukey HSD Test; p < 0.05) and same letters mean no statistical differences (p > 0.05)..... | 52 |

Figure 2.11. Scatterplot showing the relationship between the gill score (mean of left and right arches), measured during both trials in December and April, and the Ct values quantified through qPCR. Different trend line equations show the correspondent correlation coefficient (R^2); n= 30 per swab type. 54

Figure 3.1. Method of semi-quantitative analysis for mucus and mucous cell quantification. Mucus was quantified by counting the absence (A) or presence (B, arrows) of mucus traces (blue) in twenty inter-lamellar spaces from twelve random mid-sections of the primary lamellae. This method was used for all the fixation and staining techniques (e.g. A. NBF fixation with AB/PAS staining. B. Methacarn fixation with AB/PAS staining). For the mucous cell counts, the same method was performed by counting the presence (asterisk) or absence of mucous cells in twenty inter-lamellar spaces from twelve random mid-sections of the primary lamellae. Images taken by slide scanner, Axio Scan.Z1 (ZEISS, Cambridge, UK). 67

Figure 3.2. Evaluation of aqueous-based and solvent-based fixatives to preserve mucus layer in Atlantic salmon gills. A) Lower magnification and B) higher magnification of gill sample fixed with 10% neutral buffered formalin (10% NBF) stained with Alcian blue and Periodic acid-Schiff's reagent (AB/PAS). Note that there is no evidence of overlying mucus on epithelial layers or associated secretions from mucous cells (black arrow); C) lower magnification and D) higher magnification of gill sample fixed with modified Davidson's solution, stained with AB/PAS. There is some evidence of patchy preservation of mucus between the secondary lamellae (arrow heads) with some mucus secretions from mucous cells (black arrows); E) lower magnification and F) higher magnification of gill sample fixed with modified Davidson's and 2% Alcian blue (AB) solution stained with PAS. Note increased amount of mucus evident between lamellae (arrow heads) and some mucus secretions from mucous cells (black arrows)..... 71

Figure 3.3. Transverse sections of methacarn fixed Atlantic salmon gills stained with Alcian blue and Periodic acid-Schiff reagent (AB/PAS). A) Transverse section of gill from Atlantic salmon showing interlamellar mucus) and B) higher magnification of boxed area from A) with mucous cells (black arrows) and mucus layer (arrowheads). 73

Figure 3.4. Effects of different fixation methods on presence of mucus and mucous cells on Atlantic salmon gills. A) Graph showing the proportion of examined interlamellar spaces showing mucus traces and B) graph showing number of

mucous cells in gill fixed with 10% NBF, modified Davidson's solution and methacarn solution. Different superscript letters indicate significant differences between fixatives (mean \pm s.e.m, n = 6 control fish, 12 random fields of 20 interlamellar spaces; ANOVA test: $p < 0.05$)..... 74

Figure 3.5. Comparison of histological stains of methacarn fixed Atlantic salmon gill infected with AGD (gill score 2.5) with H&E and AB/PAS staining. A) & B) Epithelial hyperplastic lesions with lacuna formation (lac) from AGD-infected gill stained with A) H&E stain and B) Alcian blue and Periodic acid-Schiff reagent (AB/PAS); C) & D) advanced hyperplastic lesions with associated amoeba trophozoites (arrows) stained with C) routine H&E stain and D) Alcian blue and Periodic acid-Schiff reagent (AB/PAS). Amoebae trophozoites (arrows) between lacuna formation (lac) in a hyperplastic lamella..... 75

Figure 3.6. Gills of Atlantic salmon infected with AGD fixed in methacarn and stained with AB/PAS. A) & B) Hyperplastic gill epithelial tissue with mucous cells and mucus throughout (asterisks), in addition to numerous amoeba trophozoites (black arrows) associated in the periphery of the lesion surface and showing close interaction with overlying mucus (asterisk); C) trophozoites are found attached to the gill epithelium (black arrows) and a mucous cell (arrow head) and D) trophozoite found between a lacuna formation (black arrow) surrounded by mucus and mucous cells (arrow heads). 76

Figure 3.7. Gills of Atlantic salmon infected with AGD fixed in methacarn and stained with AB/PAS. A) Lacunae formations (lac) across the hyperplastic epithelial tissue with mucous cells (arrows) and amoebae trophozoites (asterisks); B) more lacunae formations (lac) with additional mucus; C) trophozoite (arrow) between a lacuna formation (lac) in hyperplastic gill tissue and D) transverse section of gill with lacunae formations (lac) and amoebae attached to the epithelium (arrows) surrounded by a mucus layer (arrow heads)..... 77

Figure 3.8. Lectin labelling of Atlantic salmon gills. A) Section of gill fixed in methacarn; negative control using lectin wash buffer. Note very faint presence of mucus or mucous cells (arrows); B) section of gill fixed in 10% neutral buffered formalin (NBF) labelled with wheat germ agglutinin (WGA); faint traces of mucus visible in inter-lamellar spaces (arrows); C) lower magnification and D) higher magnification of section of gills fixed in methacarn and labelled with wheat germ agglutinin (WGA); visible mucous cells (arrows) and overlay of mucus (asterisks).. 78

Figure 3.9. Lectin histochemistry using wheat germ agglutinin (WGA) on AGD-infected Atlantic salmon gills. A) Section of gill showing an amoeba trophozoite found between a lacuna formation (lac) (white arrowhead); visible mucus layer (arrows) and counterstaining with DAPI highlighting host and parasite nuclei in blue; B) section of gill showing thick mucus layer in inter-lamellar spaces (arrows) and overlying hyperplastic tissue (asterisk); C) transverse section of gill showing interlamellar mucus (arrows) and D) section of gill showing lacuna formation within hyperplastic tissue and thick mucus layer (arrows). **79**

Figure 3.10. Confocal microscopy images of the lectin labelling of non-AGD infected Atlantic salmon gills. A) Section of gill fixed in methacarn; negative control using lectin wash buffer; faint traces are observed (arrows); B) section of gill fixed in 10% neutral buffered formalin (NBF) labelled with wheat germ agglutinin (WGA); no mucus visible (asterisk); C) and D) gills fixed in methacarn and labelled with wheat germ agglutinin (WGA); visible mucous cells (arrowheads) and overlay of mucus (arrows). **80**

Figure 3.11. Confocal microscopy images of the lectin labelling of high AGD-infected Atlantic salmon gills. A) and B) sections of high hyperplastic gills fixed with methacarn solution and labelled with wheat germ agglutinin (WGA); high level of mucus traces visible in inter-lamellar spaces (arrows) along with high numbers of mucous cells (arrowheads). **81**

Figure 4.1. Formula for the calculation of H₂O₂ concentration prior to the treatment. **92**

Figure 4.2. Image analysis for the semi-quantitative analysis of CD3⁺ cells expression in control and 14 dpt *A. salmon* gills. A) Control slide without CD3 antibodies. Note no red coloured cells were observed within the selected 10 lamellae inside the red rectangle. B) Antibody labelled slide showing CD3 antibody labelling (red coloured cells) within the selected 10 lamellae described inside the red rectangle (arrows). C) Selection of the blue channel image after separation of the image into different channels for image analysis. Arrows show the intense black coloured cells (positive for CD3 antibodies). D) Resulting image after applying a 0 – 120 threshold range, masking the CD3⁺ cells in red (arrows). **101**

Figure 4.3. Equation used for the calculation of the CD3⁺ cell expression. **102**

Figure 4.4. Light micrograph of PAS staining of Davidson’s fixed gills. Control (0h) non-AGD- challenged fish presenting no signs of pathology. **104**

Figure 4.5. Light micrograph of PAS staining of Davidson’s fixed gills. H₂O₂ treated fish from the non-AGD- challenged group 4 h post-treatment presenting some epithelial lifting and oedema (arrows) and some aneurism in secondary lamellae tips (arrow heads). 104

Figure 4.6. Light micrograph of PAS staining of Davidson’s fixed gills. H₂O₂ treated fish from the non-AGD- challenged group 24 h post-treatment presenting some epithelial lifting and oedema (arrows). 105

Figure 4.7. Light micrograph of PAS staining of Davidson’s fixed gills. H₂O₂ treated fish from the non-AGD- challenged group 14 dpt presenting some epithelial lifting and oedema (arrows). 105

Figure 4.8. Quantitative RT-PCR analysis of (A) T-cell, (B) B-cell, and (C) Th1/Th17 and Th2 pathway-related transcript expression in gill samples from non-AGD-infected Atlantic salmon after hydrogen peroxide treatment at different time points (0h, 4h, 24h and 14 d). Statistical differences were determined by a one-way ANOVA and subsequent *post-hoc* Tukey HSD test. Results are normalized expression ratios (mean ± s.e.m, n = 5) of the expression of these transcripts in relation to untreated fish time point 0h. Asterisk (*) denotes statistically significant regulation in target transcript expression relative to the time zero fish ($p < 0.05$) while double asterisks (**) represent highly significant regulation ($p < 0.001$). 107

Figure 4.9. Quantitative RT-PCR analysis of mucin-related transcript expression in gill samples from non-AGD-infected Atlantic salmon after hydrogen peroxide treatment within different time points (0h, 4h, 24h and 14 d). Statistical differences were determined by a one-way ANOVA and subsequent *post-hoc* Tukey HSD test. Results are normalized expression ratios (mean ± s.e.m, n = 5) of the expression of these transcripts in relation to untreated fish time point 0h. Asterisk (*) denotes statistically significant regulation in target transcript expression relative to the time zero fish ($p < 0.05$) while double asterisks (**) represent highly significant regulation ($p < 0.001$). 108

Figure 4.10. Quantitative RT-PCR analysis of (A) T-cell, (B) B-cell, and (C) Th1/Th17 and Th2 pathway related transcript expression in gill samples from fish during an early AGD infection stage (7 dpi) (Low AGD; scores 1-2) and control fish. Statistical differences were determined by a one-way ANOVA and subsequent *post-hoc* Tukey HSD test. Results are normalized expression ratios (mean ± s.e.m, n = 5) of the expression of these genes in relation to untreated fish time point 0h. Asterisk

(*) denotes statistically significant regulation in target gene expression relative to the time zero fish ($p < 0.05$) while double asterisks (**) represent highly significant regulation ($p < 0.001$). 109

Figure 4.11. Quantitative RT-PCR analysis of mucin-related transcript expression in gill samples from fish during an early AGD infection stage (7 dpi) (Low AGD; scores 1-2) and untreated fish time point 0h. Statistical differences were determined by a one-way ANOVA and subsequent *post-hoc* Tukey HSD test. Results are normalized expression ratios (mean \pm s.e.m, $n = 5$) of the expression of these genes in relation to untreated fish time point 0h. Asterisk (*) denotes statistically significant regulation in target gene expression relative to the time zero fish ($p < 0.05$) while double asterisks (**) represent highly significant regulation ($p < 0.001$). 110

Figure 4.12. Quantitative RT-PCR analysis of (A) T-cell, (B) B-cell, and (C) Th1/Th17 and Th2 pathway related transcript expression in gill samples from fish during a late AGD infection stage (28 dpi) (High AGD; scores 3-4) and control fish. Statistical differences were determined by a one-way ANOVA and subsequent *post-hoc* Tukey HSD test. Results are normalized expression ratios (mean \pm s.e.m, $n = 5$) of the expression of these genes in relation to untreated fish time point 0h. Asterisk (*) denotes statistically significant regulation in target gene expression relative to the time zero fish ($p < 0.05$) while double asterisks (**) represent highly significant regulation ($p < 0.001$). 111

Figure 4.13. Quantitative RT-PCR analysis of mucin related transcript expression in gill samples from late AGD-infected fish (High AGD; scores 3-4) and control fish. Statistical differences were determined by a one-way ANOVA and subsequent *post-hoc* Tukey HSD test. Results are normalized expression ratios (mean \pm s.e.m, $n = 5$) of the expression of these genes in relation to untreated fish time point 0h. Asterisk (*) denotes statistically significant regulation in target gene expression relative to the time zero fish ($p < 0.05$) while double asterisks (**) represent highly significant regulation ($p < 0.001$). 112

Figure 4.14. Mucous cells semi-quantitative analysis. Graph showing the mucous cell counts across all the time points 0 h, 4 h, 24 h and 14 d. Bars represent mean mucous cell counts \pm s. e. m, $n = 6$, 3 random fields of 10 interlamellar spaces; *post-hoc* Tukey HSD test: $p < 0.001^{**}$). 113

Figure 4.15. Qualitative assesment of mucus production in untreated fish (timepoint 0h) (A & B). Mucus traces can be observed in bright pink between the secondary

lamellae. Methacarn fixed gill sections from control fish were stained with PAS staining..... 115

Figure 4.16. Qualitative assesment of mucus production in 14 dpt fish (A & B). Less mucus traces can be observed in bright pink between the secondary lamellae. Methacarn fixed gill sections from 14 dpt fish were stained with PAS staining..... 116

Figure 4.17. Quantification of the CD3⁺ cell expression on the gills of Atlantic salmon in untreated fish (T0 fish) and 14 dpt fish (T14d fish). Error bars show s.e.m No statistical differences were observed between the two groups ($p > 0.05$). 117

Figure 4.18. Representative images from control gill sections with no CD3⁺ primary antibody added. A. Control slide with the washing buffer and no antibody added. B. Higher magnification of detailed area in Figure 4.18A..... 118

Figure 4.19. Representative images from time 0h fish slides with CD3⁺ primary antibody added. A. Time 0h fish slide with antibody added. Arrows indicate the presence of CD3⁺ cells along the primary and second lamellae. B & C. Higher magnification of detailed area in figure 4.19A. 119

Figure 4.20. Representative images from time 14d fish slides with CD3⁺ primary antibody added. A. Time 14d fish slides with antibody added. Arrows indicate the presence of CD3⁺ cells along the primary and second lamellae. B & C. Higher magnification of detailed area in figure 4.20A. 120

Figure 5.1. Schematic outline of distinctive configurations appearing in Dot Plots; a) one continuous main diagonal shows perfect match for two sequences; b) parallels to the main diagonal indicate repeated regions in the same reading direction on different parts of the sequences (D1, D2: duplications); c) lines perpendicular to the main diagonal indicate palindromic areas; d) partially palindromic sequence; e) bold blocks on the main diagonal indicate repetition of the same symbol in both sequences; f) parallel lines indicate tandem repeats so minisatellite patterns; g) when the diagonal is a discontinuous line this indicates that the sequences T1 and T2 share a common source and the number of interruptions increases with modifications on the text or the time of independent evolution and mutation rate; h) partial deletion in sequence 1 or insertion in sequence 2, so called 'indel' (Source from web article by Jan Schulz (2008), "Introduction to Dot Plots")..... 135

Figure 5.2. RNA quality control virtual gel (Agilent Bioanalyzer) of the cultured *N. perurans* samples. Presenting the ladder, two samples (FG1837_01 and FG1837_02) and a control sample (FG1813_28Ro). Black arrow indicates band

corresponding the 28S and grey arrow corresponds to 18S. Tested samples present both 28S and 18S bands as the control sample..... 136

Figure 5.3. RNA quality control virtual gel (Agilent Bioanalyzer) of the infected AGD gills samples. Presenting the ladder, the two successful samples (FG1904_01 and FG1904_02), the highly degraded sample (FG1904_03) and a control sample (FG1813_28Ro). Black arrow indicates band corresponding the 28S and grey arrow corresponds to 18S. The two first samples present both 28S and 18S bands as the control sample, indicating good RNA quality. 137

Figure 5.4. RNAseq quality control virtual gel (Agilent Bioanalyzer)for the Cultured *N. perurans* samples and the infected gills samples. Presenting the ladder, two samples from the cultured *N. perurans* (D2 and E2) and the infected gills samples (F1 and G1). Black arrow indicates where the amoebal cell mRNA is in the gel.... 138

Figure 5.5. *N. perurans* transcript assessments. A. Length distribution of assembled *N. perurans* transcripts. Clean reads for *N. perurans* were assembled and resulted in 68,447 transcripts. B. BUSCO assessment (Metazoa database) number of BUSCO orthologues equals 978. 139

Figure 5.6. A five-way Venn diagram. The figure shows the unique and overlapped transcripts showing protein sequence similarity with one or more databases (details in Table 5.2). 140

Figure 5.7. Top 15 GO terms associated with transcripts in the cultured amoebae transcriptome. Biological process GO (BP), cellular components GO (CC) and molecular function (MF)..... 141

Figure 5.8. Dot Plot of the TBLASTx alignment of the cultured *N. perurans* transcriptome assembly with the known mRNA sequences. (A) *Trans_g9010_i1* vs. *A. castellanii* transporter, major facilitation subfamily protein (XM_004334424.1). (B) *Trans_g8324_i1* vs. *D. fasciculatum* integrin alpha FG-GAP (XM_004355641.1). (C) *Trans_g1428_i2* vs. *A. castellanii* Papain family cysteine protease (XM_004358251.1). (D) *Trans_g5068_i1* vs. *A.castellanii* Carboxypeptidase Y (XM_004342287.1). Source: Basic local alignment search tool (BLAST) (Altschul *et al.*, 1990). 147

Figure 5.9. Dot Plot of the TBLASTx alignment of the AGD-infected gill transcriptome assembly with the known mRNA sequences. (A) *contig_58495* vs. *D. lacteum* Actin bundling protein (XM_004355841.1). (B) *contig_5081* vs. *A. castellanii*

Reverse transcriptase (XM_004353194.1). Source: Basic local alignment search tool (BLAST) (Altschul *et al.*, 1990)..... 151

Figure 5.10. Dot Plot of the TBLASTX alignment of the cultured *N. perurans* transcriptome assembly with the known mRNA sequences. (A) *Trans_g35334_i1* vs *A. castellani* Encystation-mediating serine proteinase (XM_004355393.1). (B) *Trans_g15171_i1* vs *A. subglobosum* Extracellular matrix protein A (AB743580.1). Source: Basic local alignment search tool (BLAST) (Altschul *et al.*, 1990)..... 155

Chapter 1 : General introduction

1.1. Aquaculture industry: background

Population growth has driven an increase in global seafood production, this standing at ~177.8 million tonnes in 2019 (FAO, 2020). Although wild fisheries still represent 47% of the total, aquaculture now exceeds capture fisheries, being the only of the two sectors that can sustain future growth (FAO, 2020). For this reason, the expansion of world aquaculture production is anticipated to fill the supply–demand gap, avoiding the overexploitation of wild stocks. Within the aquaculture industry, salmonids are one of the most highly esteemed fish for consumption, comprising around 17% of the total value of internationally traded fish. Successful sea cage culture was first developed in the 1960s in Norway to increase Atlantic salmon (*Salmo salar* Linnaeus, 1758) production. This achievement drove the global expansion of salmon culture in different parts of the world such as Scotland, and latterly Ireland, the Faroe Islands, Canada, the north eastern seaboard of the USA, Chile and Australia (Tasmania) followed by a lower production in New Zealand, France, Spain and Russia (Oldham *et al.*, 2016). Nowadays, global farmed Atlantic salmon production has increased by 7% in 2019, to just over 2.6 million tonnes (FAO, 2020).

Scottish salmon production started in the 1970s, increased quickly during the 1980s and 1990s but subsequently plateaued due to production challenges and increased competition for suitable sites with other stakeholders. Scotland's farming contributes over £1.8 billion annually to the Scottish economy. Scottish aquaculture has grown over the years and it's currently dominated by Atlantic salmon making this region the largest producer during the last decade in the EU and the third largest globally, producing 189,707 tonnes during 2017; however, the level of production for 2018 was lower with 156,025 tonnes (-17.8% less) (FAO, 2020).

Industry intensification, often associated with increased stress on fish stocks, has been paralleled by the emergence of numerous infectious diseases, particularly parasitic diseases (Oldham *et al.*, 2016) (**Error! Reference source not found.**) and multifactorial diseases which include parasitic, bacterial and viral pathogens as well as environmental factors (e.g. complex gill disease/disorder (CGD)) (Herrero *et al.*,

2018). Over the years, such diseases have caused large losses within the industry (Shinn *et al.*, 2015). Although some pathogens are intracellular and affect different parts of the fish, gill diseases represent a major challenge to producers and are the cause of high levels of mortality within salmon aquaculture (Rodger, 2007). Due to its direct contact with the environment, the gill constitutes the initial portal of entry through which many bacteria, parasites and viruses enter the host.

Table 1.1. Key parasitic infections affecting Atlantic salmon globally in the aquaculture industry.

| Parasite | Disease | Reference |
|--------------------------------|---------------------------------------|---------------------------------|
| <i>Desmozoon lepeophtherii</i> | Proliferative Gill Inflammation (PGI) | Matthews <i>et al.</i> (2013) |
| <i>Hexamita salmonis</i> | Systemic Granulomatous Disease | Poppe & Mo (1993) |
| <i>Ichthyodo necator</i> | Epidermal Spongiosis | Roubal <i>et al.</i> (1987) |
| <i>Kudoa thyrsites</i> | Post-mortem Muscle Autolysis | St-Hilaire <i>et al.</i> (1997) |
| <i>Myxobolus cerebralis</i> | Salmonid Whirling Disease | Wolf <i>et al.</i> (1986) |
| <i>Neoparamoeba perurans</i> | Amoebic Gill Disease (AGD) | Young <i>et al.</i> (2008) |
| <i>Spironucleus barkhanus</i> | Systemic Spironucleosis | Sterud <i>et al.</i> (1998) |
| <i>Lepeophtheirus salmonis</i> | Sea lice infection | Grimnes & Jakobsen (1996) |

1.2. Amoebic Gill Disease (AGD)

Among all the gill diseases, amoebic gill disease (AGD) has become one of the greatest challenges for marine aquaculture worldwide, since its first reported occurrence in Tasmania, Australia (1984) in Atlantic salmon (Munday, 1986). The aetiological agent was misidentified as *Paramoeba pemaquidensis* (Kent *et al.*, 1988) for several years due to the morphological similarity between different strains and species. However, the actual causative agent was described in the study made by Young *et al.*, (2008) as *Neoparamoeba perurans* using phylogenetic analyses and Koch's postulates were later fulfilled by Crosbie *et al.* (2012).

The repeated emergence of this disease through the years has had a significant health impact in most of the world's salmon producing regions, leading to large economic and growth losses (Nowak *et al.*, 2014; Oldham *et al.*, 2016). An estimation of the AGD-related mortality losses was £9.6 million in Norway (2006) and £61 million in Scotland (2011) (Shinn *et al.*, 2015), two of the European regions with the largest salmon production. In an epidemiological review, Oldham *et al.* (2016) reported that AGD has been found in species such as Coho salmon *Oncorhynchus kisutch* (Walbaum, 1792) in the USA, rainbow trout *Oncorhynchus mykiss*

(Walbaum, 1792) in Australia, brown trout *Salmo trutta* (Linnaeus, 1758) in France, turbot *Scophthalmus maximus* (Linnaeus, 1758) in South Africa and Spain, ayu *Plecoglossus altivelis* (Temminck & Schlegel, 1846) in Japan, ballan wrasse *Labrus bergylta* (Ascanius, 1767) in Norway, Scotland and Ireland, and corkwing wrasse *Symphodus melops* (Linnaeus, 1758) in Norway, among others. Most recently, AGD has been reported in lumpfish *Cyclopterus lumpus* (Linnaeus, 1758) which is used to delouse farmed Atlantic salmon infested with sea lice *Lepeophtheirus salmonis* (Krøyer, 1837) (Haugland *et al.*, 2016).

1.2.1. Biology and taxonomy of *N. perurans*

The morphology of cultured *N. perurans* was observed during a study by Wiik-Nielsen *et al.* (2016). They detected two different morphologies using phase contrast microscopy. The amoebae formed polymorphic (attached and floating trophozoites; **Error! Reference source not found.**1a,b) as well as distinctly rounded morphologies (pseudocyst; **Error! Reference source not found.**1c).

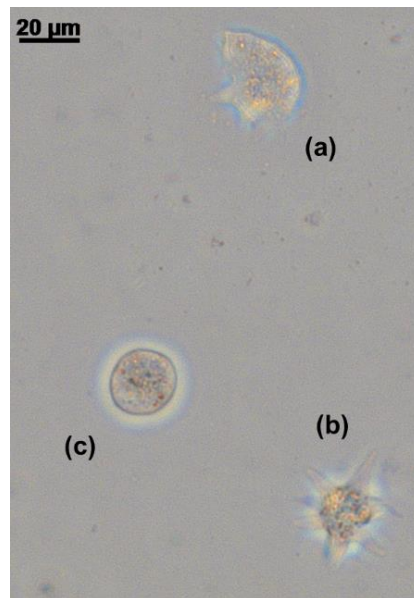


Figure 1.1. Different morphologies observed in the cultured *N. perurans*: attached trophozoites (a), floating trophozoites (b) and pseudocyst/cyst (c). Image taken with light microscope.

Attached and suspended trophozoites present extended pseudopodia. They provide both movement and nutrient's uptake in the marine environment / *in vitro* culture. Additionally, there is a pseudocyst morphology that can be observed during certain times in which the amoebae are challenged (change of temperature, salinity, feeding *etc.*) as a protection (Lima *et al.*, 2017; Collins *et al.*, 2019). This has been previously

described in other species of amoebae such as *Mayorella vespertilioides* (Page, 1983) and *Dictyostelium* spp. (Van Haastert, 2011), allowing specimens to go into latency.

These characteristics make this parasite a facultative organism, permitting its propagation and survival throughout a wide range of temperatures and salinities, as has been observed *in vitro* (Lima *et al.*, 2017; Collins *et al.*, 2019) and as a free-living parasite in the marine environment, found on various structures, sediments on salmon farms and macrofauna (Bridle *et al.*, 2010; Wright *et al.*, 2015). Aside from these traits, one of the most interesting aspects of this parasite's biology is the presence of an endosymbiont which was found to be within the *Paramoeba* species since the 1970s, which originally was thought to be a nucleus-associated parasome (Grell & Benwitz, 1970; Perkins & Castagna, 1971; Page, 1973). Recently Tanifuji *et al.* (2017) investigated the relationship between *P. pemaquidensis* and its endosymbiont. Genomic analysis showed how the endosymbiont *Perkinsella* sp. lost the ability to create a flagellum but maintained the key features of kinetoplastid biology (**Error! Reference source not found.**2). Interdependence and metabolic mosaicism in terms of nutrition between these two organisms was established, but the precise role of this endosymbiont in the pathogenicity of *Paramoeba* species remained unknown. However, a clear co-evolutionary association was observed and considered ancient and also, the kinetoplastid-specific metabolic pathways (e.g. trypanothione biosynthesis) could provide potential therapeutic targets / drugs, which could indirectly kill the host. Further investigations should be performed to confirm if this same relationship is found between *N. perurans* and its endosymbiont.

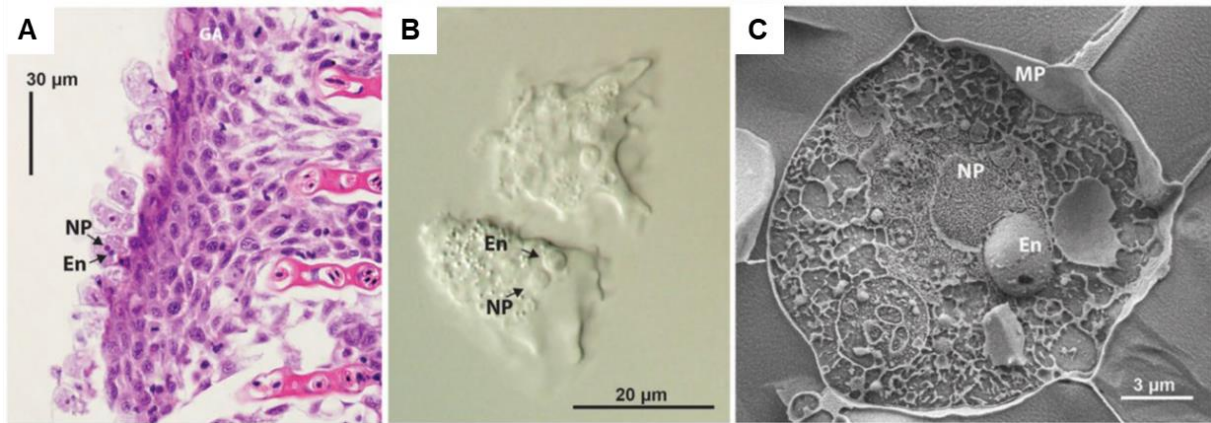


Figure 1.2. Images taken during the study by Tanifuji *et al.* (2017). (A) Atlantic salmon gill infected with *Paramoeba* spp. trophozoites found attached to gill epithelium. Eosin and haematoxylin staining to differentiate NP (nucleus of the host amoeba) from En (*Perkinsela* sp. endosymbiont). (B) Trophozoites of *P. pemaquidensis* with contrast microscopy. (C) Scanning electron microscopy (SEM) of a *P. pemaquidensis* trophozoite with endosymbiont (MP = plasma membrane of *P. pemaquidensis*).

There has been a constant debate amongst authors regarding the name that should be used; however, it is not within the scope of the current study to discuss whether the genus *Paramoeba* or *Neoparamoeba* is the correct taxonomic term, therefore for the purpose of this thesis I will use the latter genus. Although Young *et al.* (2008) determined *N. perurans* as the aetiological agent for AGD, more recent studies investigated through phylogenetic analysis of nuclear SSU rDNA sequences reveal the existence of separate *Paramoeba* and *Neoparamoeba* clades, proposing that *Neoparamoeba* should be considered a junior synonym of *Paramoeba* due to the lack of confirming data regarding their genomic differences (Feehan *et al.*, 2013). Through the comparison of the 18S ribosomal RNA of several pathogenic amoebic species (**Error! Reference source not found.**3) it can be observed that *N. perurans* is closely related to other *Paramoeba* spp. as well as *Neoparamoeba* spp. The next genetically closely-related species is *Acanthamoeba* spp. and the furthest of the analysed amoebae are *Entamoeba* spp. and *Naegleria fowleri*.

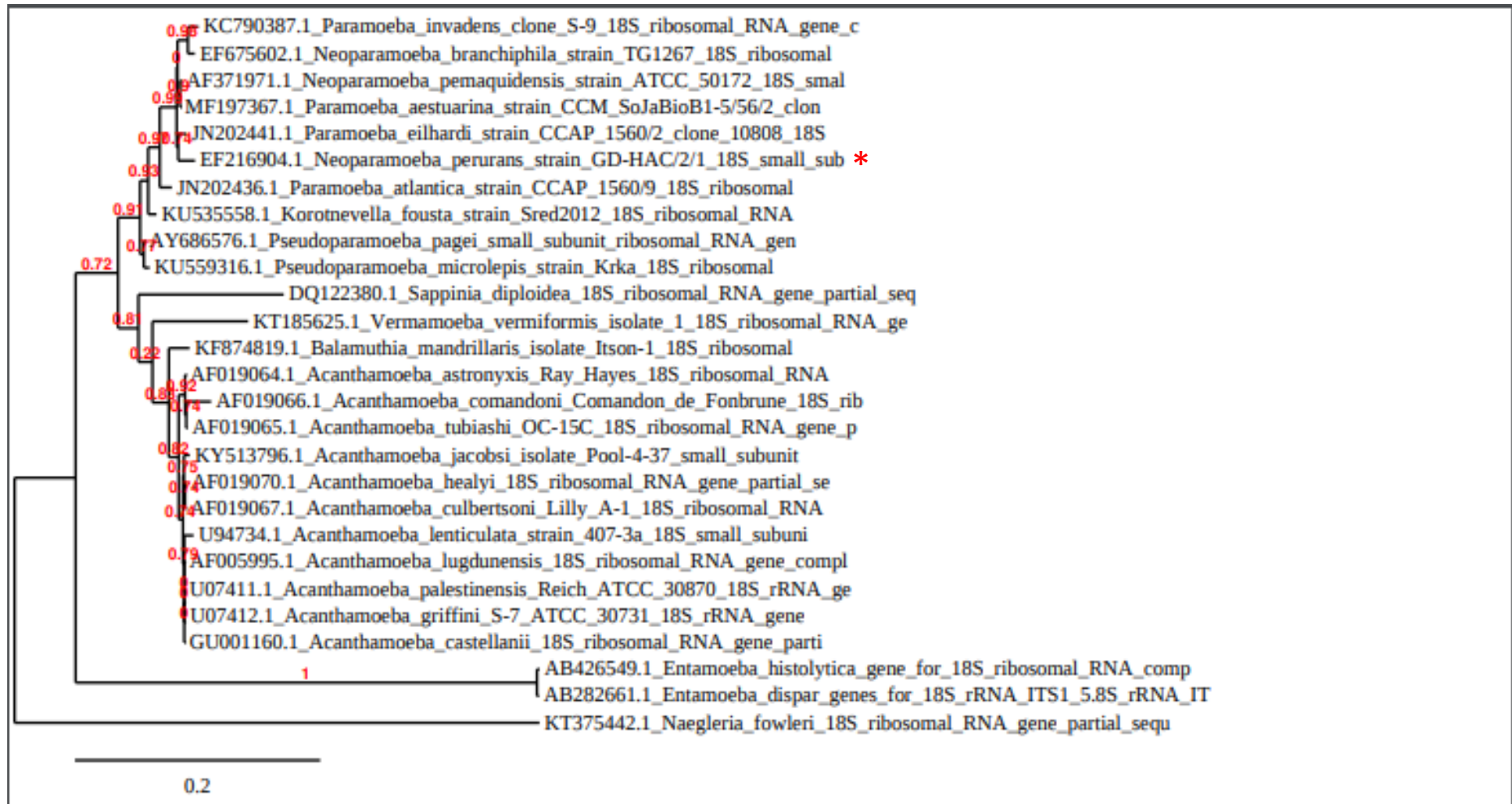


Figure 1.3. Phylogenetic tree of some of the best known parasitic amoebic species using their 18S ribosomal RNA sequences. This was developed through the online tool Phylogeny.fr (Dereeper *et al.*, 2008).

1.2.2. Pathology and clinical signs

It is believed that the principal virulence trait of this amoebic species is the ability to attach to the gill epithelium (Nowak *et al.*, 2014). The preferred area for *N. perurans* to settle is the interstitial region between gill hemibranchs (Adams & Nowak, 2003; Adams & Nowak, 2004). During colonisation, the amoebae causes indentations in the epithelial surface, followed by fenestrations. The penetration of amoebal pseudopodia was shown to be through the affected pavement cells (Wiik-Nielsen *et al.*, 2016) leading to a disruption of the epithelial cells presenting hyperplasia and hypertrophy. Regarding the plasma membrane of the amoebae, when attached to the gill epithelium, an increased membrane density is observed as well as increased cytoplasmic density (Lovy *et al.*, 2008). This was also studied in *in vitro* experiments where a cytopathic effect (CPE) was observed in epithelial cells (Butler & Nowak, 2004; Cano *et al.*, 2019). Amoebal attachment causes white raised lesions, usually beginning at the base of the filaments and scattered along the gill arch (Nowak, 2012).

Excessive mucus secretion is usually observed when routine gill examinations are performed on the infected fish (Nowak & Munday, 1994; Rodger & McArdle, 1996; Taylor *et al.*, 2009; Nowak, 2012). Many studies have covered the pathology associated with AGD infections. Besides the excessive mucus secretion, swollen gill filaments are generally observed in most of AGD cases along with the presence of distal necrosis and oedema of the gill tissue. Same pathological signs have been identified across most of AGD studies regarding the pathology within the infected fish (Nowak & Munday, 1994; Adams & Nowak, 2001; Zilberg & Munday, 2000; Adams & Nowak, 2003; Morrison *et al.*, 2006; Young *et al.*, 2008a). These signs have been described in terms of a local host-tissue response to the parasite through the migration of immunoregulatory cells towards lesion-affected areas. Thus, the deeper study of fish mucosal health could aid the deeper understanding of the pathology / response it's observed during an AGD infection.

1.2.3. Diagnosis

The general approach for diagnosing AGD is through non-destructive tools such as the gill-scoring method developed by Taylor *et al.*, (2009), which runs from clear (0) to heavy (5), to the assessment of gill gross pathology (Munday *et al.*, 1993; Clark &

Nowak, 1999; Adams & Nowak, 2004; Rozas *et al.*, 2011). However, the scoring method is often open to misinterpretation due to its subjective nature. In addition, while the gill condition is assessed, the approach still lacks the ability to identify the aetiological agent. This is relevant because there are other infectious and non-infectious gill diseases that present similar impacts on the gills of salmon (Mitchell & Rodger, 2011; Gjessing *et al.*, 2017; Gunnarsson *et al.*, 2017) and can be mistaken for AGD. To support this method, histology has always been preferred as one of the primary methods for identifying the causative agent. This technique also serves to study the host response to the pathogen (Clark & Nowak, 1999; Adams & Nowak, 2004). Similarly, to the gill scoring method, Mitchel *et al.* (2012) established a histopathological gill scoring method through the examination of changes within the gill health (*e.g.* lamellar oedema/fusion/hyperplasia and cellular anomalies such as necrosis and sloughing)). Depending on the level of gill lesions, a score of 0–3 was assigned. Both scoring methods were compared in a study by Rozas *et al.* (2011), who found a positive correlation between them as well as high sensitivity and specificity.

In recent years, targeted molecular methods have been developed for detecting *N. perurans*. As mentioned before, the aetiological agent was wrongly described as *P. pemaquidensis* for several years (Kent *et al.*, 1988). However, the actual causative agent was first described in the studies by Young *et al.* (2008) as *N. perurans* using phylogenetic analyses and a PCR assay by amplifying a 636-bp region of the 18S rRNA gene. Following these findings, PCR screening started to be used to detect early infections and to estimate efficacy of treatments. During a routine histology, a very early infection could lead to an improper characterisation of the disease due to microscopic lesions and few numbers of amoebae. Thus, several studies have been undertaken to optimise molecular diagnostic techniques through the optimisation of different PCR-assays with gill biopsies (Bridle *et al.*, 2010; Rozas *et al.*, 2011; Fringuelli *et al.*, 2012) and, more recently, a comparison of tissue samples with gill swabs (non-lethal sampling) to test sensitivity and specificity was reported (Downes *et al.*, 2017).

All these studies used the same region of the *N. perurans* 18S rRNA gene. However, different primers were used for its detection and they all proved to be specific and sensitive. Perhaps, the most efficient assay was the duplex quantitative Taqman

real-time PCR by Fringuelli *et al.* (2012) due to allowing the detection of the other two species (*P. pemaquidensis* and *P. branchiphila*). However, the most recent study in regard to the use of non-lethal tools such as swabs for the sampling of gill mucus. Downes *et al.* (2017) compared gill filament biopsies to gill swabs and reported an increase in the sensitivity when swabs were used. Thus, the investigation of these tools further could help determine better ways to quantify amoebae during an AGD infection. Throughout this work, different swab materials would be compared as well as the area of the gill that is sampled to determine if there are differences in the number of amoebae detected.

1.2.4. Current treatments and management

Currently, the **generalised method for** the treatment of AGD involves the use of freshwater or low salinity water bathing (<3 practical salinity unit (PSU) for approx. 3 hours). This treatment has been proven to be less invasive and safer to use at higher temperatures (Powell *et al.*, 2001; Rodger, 2014). However, some areas have very limited access to it (e.g. Tasmania) (Oldham *et al.*, 2016) and also the effort of moving such big quantities of water is highly time-consuming (Rodger, 2014). Thus, in inaccessible areas and where high temperatures are not common, the use of this freshwater bathing has been substituted with the use of hydrogen peroxide. This compound is commonly used against both sea lice (*Lepeophtheirus salmonis*) and AGD, although gill irritation has been observed in treated fish (Kierner *et al.*, 1997; Powell & Clark, 2004). Furthermore, hydrogen peroxide treatment can potentially cause safety problems at higher temperatures (Crosbie *et al.*, 2012; Rodger, 2014) or when treatment is applied to fish that are already compromised by advanced AGD (McCarthy *et al.*, 2015).

The success of freshwater treatment is due to the osmotic shock on amoebae, in addition to the hydration and subsequent reduction of gill mucus viscosity, and facilitated by the water flow, leads to a removal of amoebae (Clark, Powell & Nowak, 2003; Adams & Nowak, 2004). However, a study by Lima *et al.* (2017) observed pseudocyst formation in *N. perurans*. This ability to form a protective state allowed the pathogen to enter a latent stage in which, after 1h of exposure to freshwater, the recovery of the pathogen was very close to 80%. This was also studied *in vivo* by Clark *et al.* (2003) who observed an $86 \pm 9.1\%$ reduction in the number of live amoebae. However, the ones remaining could potentially cause a reinfection within

one week. Following these experiments, the study of the water's properties led to the discovery of beneficial effects when soft freshwater was used. Due to the exposure of the fish to a low cationic medium, mucus from the gills presented a greater hydration and expansion resulting in a low viscosity and thus, reducing the numbers of viable amoebae by 13% overall (Roberts & Powell, 2003).

As mentioned before, hydrogen peroxide is the alternative agent used in many areas where freshwater availability is limited. This agent has been shown to have a high efficacy against several bacterial, protozoan and fungal infections (Bruno & Raynard, 1994; Schreir *et al.*, 1996; Gaikowski *et al.*, 1999). Some regions have had good success rates while using hydrogen peroxide against AGD and sea lice (e.g. Scotland, Chile and Ireland); however, when temperatures rise above 13 °C this chemical becomes dangerous to fish (Gaikowski *et al.*, 1999; Rodger, 2014). In addition, when gills suffer from AGD a decrease in their antioxidant capacity leads to higher susceptibility to hydrogen peroxide (Marcos-Lopez *et al.*, 2018). A further potential control for AGD is the implementation of management practices such as the fallowing of sites and cage rotation, which have been proven to have a positive effect against AGD, with less freshwater baths needed and increased growth rates (Douglas-Helders *et al.*, 2004; Powell *et al.*, 2015).

One of the main objectives in this research field is to improve and develop novel bath and dietary treatments. Experiments involving the use of immunomodulators such as levamisole (Findlay, Zilberg & Munday, 2000), β -glucans (Bridle *et al.*, 2005) and CpGs (Bridle, Butler & Nowak, 2003) have been reported, as well as the use of alternative chemicals / disinfectants such as peracetic acid (Lazado *et al.*, 2019), chloramine-T (Harris *et al.*, 2004) and chlorine dioxide (Powell & Clark, 2004). Also, bithionol, which is a parasiticide, has been tested orally (Florent, Becker & Powell, 2007) and as a bath treatment (Florent, Becker & Powell, 2007a) in Atlantic salmon. However, none of these experiments were successful against this pathogen. Mucolytics (i.e. L-cysteine ethyl ester) were also tested orally in feed, trying to reduce the mucus excess during an AGD infection, however even though early results seemed to point a reduction of AGD in the fish, no further investigations have been carried out since that single study (Roberts & Powell, 2005). Lastly, there was an attempt to test a recombinant protein developed as potential vaccine against AGD after analysing the genome of *N. perurans* (Valdenegro *et al.*, 2014; Valdenegro *et*

al., 2015). Even though there was a humoral immune response reported during this experimental study, there was no protection against the parasite. However, the application of bioinformatics for the study of genome / transcriptome to select vaccine targets is an approach that is being increasingly used in recent years (Adams, 2019). For the effective testing and search of these targets, there is a need for refining the knowledge on fish mucosal and systemic immunology.

1.3. Teleost fish immune system

The immune system of teleost fish has evolved to successfully combat a wide range of pathogens and contaminants that coexist within the aquatic environment. Fish immune system comprise mechanisms for innate and adaptive responses. The innate response contributes to the instant protection of tissues by tackling pathogens entering the host (Uribe *et al.*, 2011). This response acts through three different strategies: (i) epithelial / mucosal barriers, (ii) the humoral and (iii) cellular components. The mucosal barriers (*i.e.* skin, gills and gut) are, therefore, the first immune obstacle that confront environmental challenges, such as contaminants and pathogens (Gomez *et al.*, 2013; Jensen, 2015; Schlenk & Benson, 2001). These immune barriers possess various molecules (*i.e.* lectins, pentraxins, lysozymes, complement proteins, antibacterial peptides (AMPs) and immunoglobulins (Igs) (IgM and IgT)) which are relevant for the inhibition of potential agents / pathogens entering the host (Alexander & Ingram, 1992; Rombout *et al.*, 1993; Aranishi & Nakane, 1997; Boshra *et al.*, 2006; Saurabh & Sahoo, 2008).

If these mucosal barriers are breached by the pathogens, neutrophils and macrophages (*i.e.* phagocytes), which are the two main cell types involved in phagocytosis (Secombes & Fletcher, 1992), act by enveloping and killing the pathogens (Delves *et al.*, 2017). Several actions can be completed by these cells, including the production of reactive oxygen species (ROS), myeloperoxidases, lysozymes and nitric oxide (NO) with the ultimate purpose of eliminating pathogens (Fischer *et al.*, 2006). When phagocytes recognise these pathogens, several pro-inflammatory cytokines (*i.e.* interleukin 1 beta (IL-1 β) and tumour necrosis factor alpha (TNF- α)), as well as chemotactic cytokines called chemokines (*i.e.* interleukin-8 (IL-8)) are produced by phagocytic cells, acting as cellular markers to further promote recruitment of these phagocytes and mount a protective response within the

host (Griffith *et al.*, 2014). After phagocytosis, the digested material is processed by the phagocytes and presented to the adaptive immune system, starting the adaptive response. At this point, co-ordination between innate and adaptive immune systems occurs through cellular and humoral intermediaries (Zou *et al.*, 2016; Thompson, 2017). The mediation within these two systems relies on B-cell and T-cell receptors (BCRs and TCRs), the major histocompatibility complex (MHC I and II) and specific recombination activator genes such as RAG-1 and RAG-2. These mediators will specifically recognise foreign molecules for its further recognition by T-cells and ultimately developing the adaptive response (Zou *et al.*, 2016; Thompson, 2017).

In contrast to the innate immune response, which is activated within minutes, the adaptive immune response is slowly established to ensure high specificity of recognition to the pathogen for subsequent immune memory (Delves *et al.*, 2017). This response is ensured by the involvement of a group of complex and specialised cells, proteins and genes. During the humoral response, B-cells are activated to secrete immunoglobulins (antibodies) which are secreted in different parts of the fish such as skin (Hatten *et al.*, 2001), gill mucus (Davidson *et al.*, 1997), intestine (Rombout *et al.*, 1993), bile (Jenkins *et al.*, 1994) and systemically in the plasma. The antibodies are delivered as a crucial component in the immune response by specifically recognizing and binding to certain antigens and facilitating their destruction (Schroeder & Cavacini, 2010). However, in cell-mediated responses, antigen-specific T-cells are triggered to respond directly against an external antigen that is presented to them on the surface of a host cell. Unlike B-cells, T-cells can only identify an antigen which has been processed and presented by antigen-presenting phagocytic cells via their MHC proteins (Mariuzza *et al.*, 2010). Regarding the humoral response, specific antibodies can be generated in the skin (Cain *et al.*, 2000), intestine (Jones *et al.*, 1999), and gills (Lumsden *et al.*, 1995) without essentially producing a systemic response. Due to their constant contact to the aquatic environment, the immune response of the skin and gills is crucial. The mucosal coat that these organs/tissues have is found deeply linked to the adaptive immune system and consist of mucosal associated lymphoid tissue (MALT) conforming the mucosal immune system. MALT can also be sub-categorized further into four main lymphoid tissues: skin-associated lymphoid tissue (SALT), gill-associated lymphoid tissue (GIALT), gut-associated lymphoid tissue (GALT), and

nasal-associated lymphoid tissue (NALT) (Salinas, 2015). As the work conducted in this thesis will focus on immunity of the gills and its mucosal properties, further review of current literature on mucosal immunity is needed to understand the specific responses within these organs.

1.3.1. Mucosal immunity: gills

In teleosts, the gill is considered to be the largest organ-specific surface interacting continuously with the external environment and is protected by a thin layer of mucus. Due to its constant exposure to the aquatic (freshwater / seawater) environment and its challenges, gill health is nowadays recognised as a major health management issue for farmed salmon, with observed pathologies being recognised to result from a diverse array of pathogens and environmental threats (Bergh *et al.*, 1989; Beck & Peatman, 2015; Lazado *et al.*, 2015). This organ is not only designed for the exchange of respiratory gases, but also for the maintenance of acid-base and mineral balances in addition to the disposal of various waste products of nitrogenous metabolism (Maetz, 1971; Flik *et al.*, 1997; Perry, 1997; Karnaky, 1998; Marshall & Bryson, 1998). Additional functions include osmoregulation, pH regulation and hormone production (Evans *et al.*, 2005). However, one of the most substantial functions of the gill is the protection against several agents (*e.g.* pathogens, contaminants / pollutants) that inflict damage to various tissues: the gill epithelium and the mucus layer (Powell *et al.*, 1994) (**Error! Reference source not found.4**).

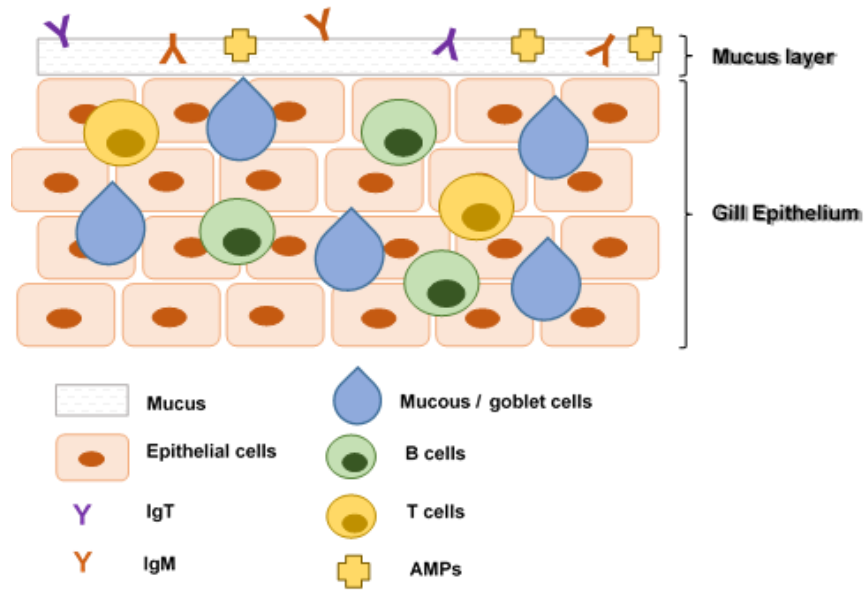


Figure 1.4. Schematic representation of teleost fish gill mucosal surface. The mucus layer is shown containing antibodies (IgM and IgT) along with AMPs (antimicrobial peptides). The gill epithelium comprises epithelial cells along with mucous / goblet cells and B T cells. This diagram is simplified from Gomez *et al.* (2013).

The immediate and most external part of the gill is the mucus layer, which is found intimately related to the gill epithelium. Fish mucus has numerous biological roles including ionic osmoregulation, reproduction, locomotion, protection against various agents/pathogens and, respiration (Shephard, 1994). Regarding its composition, the skin mucus has been studied more successfully due to simpler collection for analysis; however, some studies have effectively analysed gill mucus from Rainbow trout (*Oncorhynchus mykiss* (Walbaum, 1792)) (see Lumsden & Ferguson, 1994). Its amino acid profile was found to be fairly similar to other types of mucus such as the skin mucus from charr (*Salvelinus alpinus* (Linnaeus, 1758)) and eel (*Anguilla japonica* Temminck & Schlegel, 1846) and even mammalian intestinal mucus. More specifically, the amino acid composition was mainly characterised as serine, threonine, alanine and proline, along with carbohydrates (*i.e.* galactose, glucose, fucose, glucosamine, mannose, uronic acid and galactosamine) (Shephard, 1994; Speare & Ferguson, 2006). Additionally, the viscous nature of gill mucous is the result of a high-water content and the presence of high-molecular-weight and gel-forming macromolecules. These predominant gel-forming macromolecules (glycoproteins) are mucins (Asakawa, 1970; Fletcher *et al.*, 1976). Fish mucins appear to be alike mammalian mucins (Alexander & Ingrain, 1992), however, not

only neutral mucins are present within the mucus, but also sialic acid and sulphated monosacchades are present (Pickering & Macey, 1977).

The gill mucosal surface encounters many antigens, as fish live in congruence with commensal microorganisms (*i.e.* microbiota) (Boutin *et al.*, 2013). This indigenous microbiota facilitates the development and maintenance of host immunity (Sellon *et al.*, 1998; Cebra, 1999; Lee & Mazmanian, 2010), provide colonisation resistance through competing for space and nutrients (Balcazar *et al.*, 2006) and recycle and remove waste products (van Kessel *et al.*, 2016). Many factors can affect the balance of this microbiota such as the presence of parasitic species which has an effect on the mucosal gill microbiota as reported in the recent studies (Llewellyn *et al.*, 2017; Birlanga *et al.*, 2020). Along with this microbiota, immunoglobulins (*i.e.* IgM and IgT) are usually found within the mucus layer (Zhang *et al.*, 2010; Xu *et al.*, 2016). Specifically, IgM is known as one of the key components during systemic responses, while IgT specializes in mucosal immunity (Zhang *et al.*, 2010; Xu *et al.*, 2016), which is considered the functional analogue of teleosts to the mammalian IgA. These molecules play an important role in adaptive immunity and are produced by B cells in response to an immunogen (Uribe *et al.*, 2011). Along with these molecules antimicrobial peptides (AMPs) are present. The AMPs include defensins and cathelicidins and contribute to the first line of defence against microbes in the skin and at mucosal surfaces (Boman, 1991) (**Error! Reference source not found.**4). As mentioned before, fish mucus present many substances and macromolecules which also exist in the fish gill mucus and for which presence or absence is influenced by the kind of stress / disease that the fish is experiencing (Harrell *et al.*, 1976; Louis-Comier *et al.*, 1984; Ellis, 2001; Easy & Ross, 2009; Nigam *et al.*, 2012). The innate response initially involves the AMPs which trap and eliminate pathogens posing a threat to the fish's health (Figure 1.5). Furthermore, components such as antimicrobial lectins (Russell *et al.*, 2009) and pro-inflammatory cytokines (Ingerslev *et al.*, 2006) have also been found in the gill epithelium.

However, not all threats are successfully resolved by the activation of this response as many pathogens develop refined evasion mechanisms leading to infection. Thus, epithelial cells interact directly with commensals and pathogens, leading to express pattern recognition receptors (PRRs) for the recognition of pathogen-associated

molecular patterns (PAMPs) or microbe-associated molecular patterns (MAMPs) (Figure 1.5). There are several types of PRRs but, by far, the best described ones in fish are the Toll-like receptors (TLRs). Just like in mammals, most TLRs, upon recognition of these PAMPs / MAMPs in the pathogens, bind adaptor proteins, which ends up activating different pathways leading to the expression of various inflammatory cytokines (e.g. IL-1 β , IL-6) (Rakoff-Nahoum & Medzhitov, 2009). Following this, there is recruitment of several mast cells / eosinophilic granule cells (EGCs) to sites of inflammation (Reite & Evensen, 2006). Also, dendritic cells (DC) have been found in mucosal tissues in teleost fish and are able to directly sample the antigens and progress to antigen presentation through MHC proteins (Lugo-Villarino *et al.*, 2010; Bassity & Clark, 2012). DC present pathogen-specific peptides on the cell surface to T cells acting as messengers between the innate and the adaptive immune systems and cytokines can be detected by B-cells and develop an adaptive response (Fuglem *et al.*, 2010), through antigen presenting proteins (*i.e.* MHC class I and II proteins) (Dijkstra *et al.*, 2003; Koppang *et al.*, 2003) (Figure 1.5).

As mentioned in the previous section, the Igs are one of the components found in the mucosal surfaces as well as key components of humoral adaptive immunity. Only three Ig isotypes have been described in teleosts so far: IgM, IgD and IgT. IgM represents the main Ig in the plasma of teleosts and it is recognised as the main player involved in systemic immune responses. The presence of IgM in mucosal secretions, provides information about its involvement in responses against several pathogens (Salinas *et al.*, 2011). More recently, a study by Tongsri *et al.* (2020) provided more information about the roles of IgM and also IgT against bacterial pathogens in fish gill mucosal and systemic immunity. Their results indicated that there is a mucosal Ig-mediated excretory immune system in the teleost gills in which they are transported directly through mucosal epithelial cells.

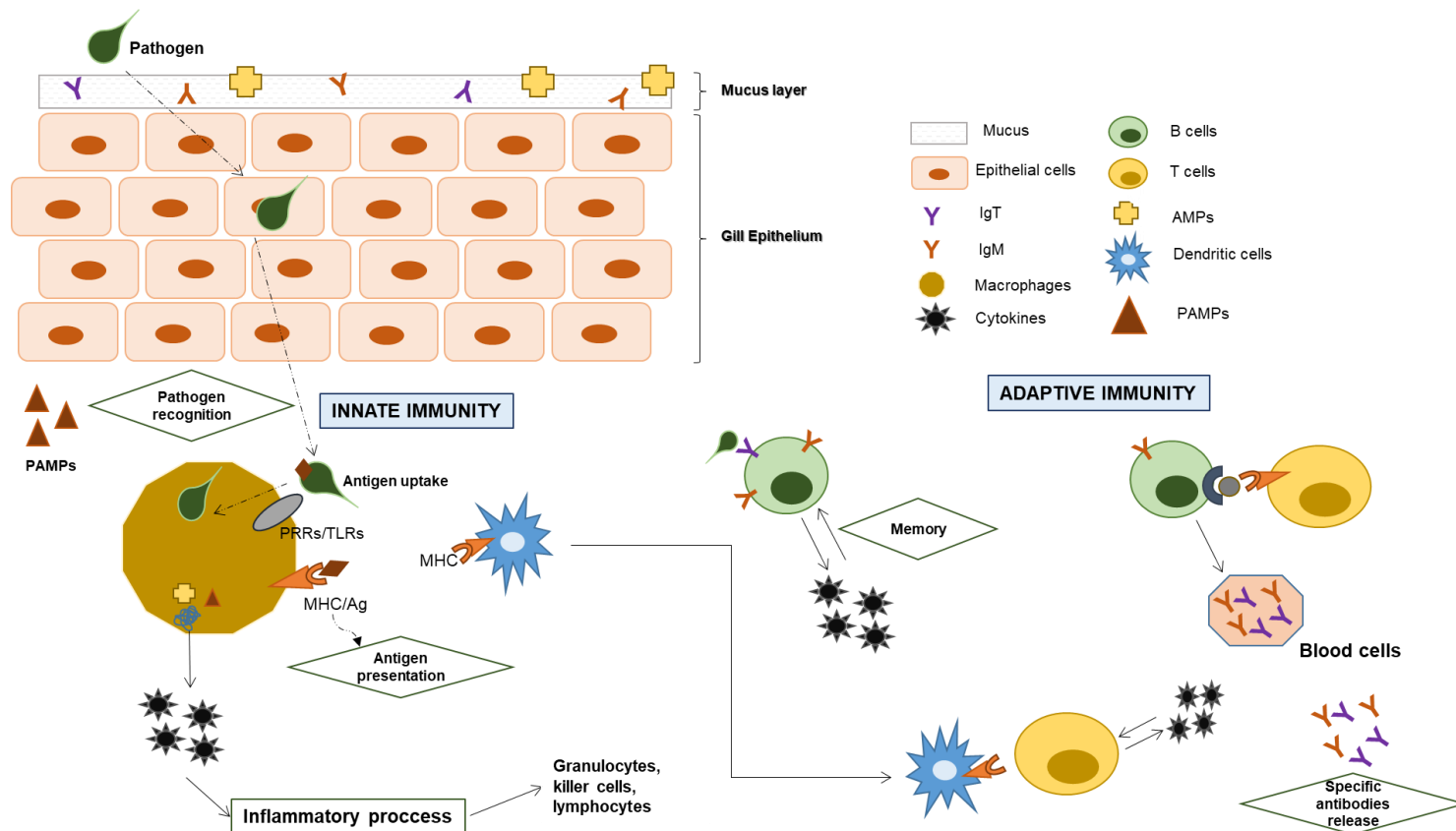


Figure 1.5. Schematic representation of the mucosal immunity of the mucosal surface of the teleost gill. When a pathogen gets through the first barriers (mucus and gill epithelium), the recognition of this pathogen is facilitated by the pathogen-associated molecules (PAMPs) within these organisms. PRRs/TLRs localised on the macrophages recognise them and the antigen presentation takes place. As part of the adaptive immunity, dendritic cells present foreign antigens to T cells that will produce cytokines; B cells also do the same and also activate T cells. Subsequently the release of specific antibodies occurs by B cell produced plasma cells in the blood. This is a simplified version of the schematic representation featured in Beck & Peatman (2015).

1.3.2. Host response to AGD

An extensive literature is available on fish responses to bacterial and viral infections in the gills, whilst knowledge on parasites is very limited. During parasitic infections, the activation of the innate system through the stimulation of the PRRs (Medzhitov, 2007) is a key step for the successful elimination of these pathogens and these PRRs are greatly conserved and respond to PAMPs (Medzhitov & Janeway, 2002; Janeway & Medzhitov, 2002), but the best characterised in teleost fish are TLRs. They are type-I transmembrane proteins with extracellular leucine-rich repeat (LRR) motifs and intracellular Toll/interleukin-1 receptor (TIR) domain. The TLRs have been investigated in many species of teleost fish (e.g. *Carassius auratus*, *Takifugu rubripes*, *Paralichthys olivaceus*, *Oncorhynchus mykiss*, *D. rerio*) (Roach *et al.*, 2005, Purcell *et al.*, 2006). The TLRs of Atlantic salmon (Tsoi *et al.*, 2006) and gilthead seabream (Franch *et al.*, 2006) have also previously been described. In a review by Nie *et al.* (2018), they compiled many of the different TLRs described in fish. Although there are pathogen specific TLRs, some of them are found on phagocytic and epithelial cells recognise several pathogens (Akira *et al.*, 2001; Takeda & Akira, 2001; Alvarez-Pellitero, 2008).

Innate responses have been investigated for various ectoparasitic species; however, two of the most investigated ectoparasites affecting the aquaculture industry are *N. perurans* in marine species and *Ichthyophthirius multifiliis* (Ich) in almost all freshwater species (Shinn *et al.*, 2015). These two parasites have become good models for understanding how innate immune responses play a significant role in the gills of fish. Innate immunity-related cytokines such as IL-1 β , IL-6, IFN- γ , IL-8, TNF- α , TGF β and IL-4/13 have been found up-regulated in the gills of various species of fish when challenged with Ich (De Oliveira *et al.*, 2013; Christoffersen *et al.*, 2017; Xu *et al.*, 2017). All these cellular responses were followed by presence of MHC II+ cells with macrophage morphology, along with CD8 α + cells surrounding Ich parasites in the gills (Olsen *et al.*, 2011). This was confirmed with the up-regulated gene expression of CD8 and CD4 in the gills of rainbow trout during the same study. Similar results were found during investigations involving Atlantic salmon response to AGD, which have been summarised in Table 1.2.

These investigations took different approaches, not only on the level at which the response was measured (i.e. gene expression, proteomics), but also the time points

that were evaluated. In all studies, clear differences were observed when AGD-affected tissue was compared to healthy tissue. A more extensive review on AGD response was already published by Marcos-López & Rodger (2020).

Table 1.2. Summary of the studies that have investigated the host response to AGD in Atlantic salmon (▼ Indicates significant down-regulation, ▲ significant up-regulation).

| Technique | Tissue | Key results | Host responses | References |
|-----------------------|-----------------------------------|---|--|---|
| Microarray and RT-PCR | Gills | ▼p53 tumour suppressor transcripts; ▲asAG-2 transcripts; ▼GADD45β transcripts; ▲PCNA transcripts ▼MHC I and MHC II antigen processing and presentation pathway | Hyperproliferative response through the inhibition of p53 Possible inhibition of acquired immunity through parasite-mediated immune evasion | Morrison <i>et al.</i> (2006) Young <i>et al.</i> (2008b); Morrison <i>et al.</i> (2006a) |
| | Gills, liver and kidney | Generalised down-regulation in apoptosis and antioxidant-related genes | Parasite-mediated gene suppression | Wynne <i>et al.</i> (2008) |
| RT-PCR | Gills, liver, and anterior kidney | ▲ IL-1β transcripts in gills No significant changes in liver and kidney | Inflammation / cellular response in the gills | Bridle <i>et al.</i> (2006) |
| | Gills and head kidney | No significant changes in TNF-α1 and 2, IFN-γ and iNOS transcripts | Modulation of pro-inflammatory cytokines and transcriptional change in directly affected tissue | Morrison <i>et al.</i> (2007) |
| | Gills | ▲ IL-1β transcript; ▼IL-1RI transcripts ▲TCR, IL-1β and CD8 transcripts Similar results when re-infected with <i>N. perurans</i> ▲IL-4/13a and IL-4/13b transcripts (Th2 pathway) ▼Th1 (IFN-γ, TNF-α3) , Th17 (IL-17a/f1b, IL-17d, IL-22) and Treg pathways (TGF-β1b, IL-10a, IL-10b) ▲IL-4/13a and IL-4/13b transcripts (Th2 pathway); ▲ muc5 transcripts | Inflammation / cellular immune response; compensatory mechanism through ▼IL-1RI to compensate chronic IL-1β transcript overexpression Inflammation / cellular immune response; infiltration of T-cells Parasite immune evasion strategy or caused an allergic reaction Mucous cell and epithelial cell hyperplasia, mucus hypersecretion and possible allergic reaction | Morrison, Young & Nowak (2012) Penacchi <i>et al.</i> (2014); Penacchi <i>et al.</i> (2016) Benedicenti <i>et al.</i> (2015) Marcos-López <i>et al.</i> (2018) |

| | | | | |
|-------------------------------|-----------------|---|---|--|
| <i>Comparative proteomics</i> | Gills | <p>▲Prohibitin, cyclophilin A, apolipoprotein A1, ictacalcin, RhoGDP dissociation inhibitor α, components of the heat shock proteins 70 family and histones H3a and H4</p> <p>▼Peroxioredoxin-5 and cofilin</p> | Significant differences in cell cycle regulation, cytoskeletal regulation, oxidative metabolism, and immunity responses | Marcos-López <i>et al.</i> (2017a) |
| | Gills and skin | <p><u>Gill mucus</u>: ▼C-reactive-protein;▲Nattectin precursor;▲Transgelin;▲Apolipoprotein A-I; ▼ Myeloperoxidase (MPO)</p> <p>▼Carbonic anhydrase</p> <p><u>Skin mucus</u>: ▼MPO and carbonic anhydrase</p> <p>▲Alanyl-tRNA synthetase and major vault protein (MVP)</p> <p>▼ C3 and C9 complement factors</p> | Significant differences in the cell to cell signalling, inflammation pathways and IL-1 β expression | Valdenegro <i>et al.</i> (2014b) |
| <i>Immuno-histochemistry</i> | Gills | <p>▲MHC class II+ cells within AGD lesions</p> <p>▲Ag-2+ cells within AGD lesions</p> | <p>Antigen presentation capacity to the development of an antibody response</p> <p>Not clear function in teleost fish</p> | <p>Morrison <i>et al.</i> (2006)</p> <p>Morrison & Nowak (2008)</p> |
| | Gills and serum | <p>▼IgM levels and peroxidase, lysozyme, esterase, and protease activities</p> | Humoral immune response; innate immunity; antimicrobial activity; oxidative stress | Marcos-López <i>et al.</i> (2017) |
| <i>Enzymatic analysis</i> | Gills | <p>▼Hydrophilic antioxidant activity (HAA)</p> <p>No differences in the superoxide dismutase (SOD)</p> <p>▼Catalase (CAT)</p> <p>▲ Glutathione reductase (GR)</p> <p>Basal respiratory burst responses and phorbol myristate acetate-stimulated activity were suppressed</p> | <p>Oxidative stress</p> <p>Lysozyme regulation during AGD</p> | <p>Marcos-López <i>et al.</i> (2018)</p> <p>Gross <i>et al.</i> (2005)</p> |

AGD clinical signs have been described in terms of a local host-tissue response to the parasite through the migration of immunoregulatory cells towards lesion-affected areas. This stress is known to cause host-tissue damage, which leads to cellular hyperplasia, mucus production and the release of Th2 cytokines (Frossi et al., 2003; King et al., 2006; Rada et al., 2011; Vital et al., 2016) and which correlates to the principal pathological elements observed in AGD-infected fish. Additional clinical signs include lethargy, respiratory distress, and an increased rate of opercular movement (Munday et al., 2001).

As described in Table 1.2, these responses have been additionally investigated through gene expression analysis in a wide range of studies. There has been a wide range of hypothesis and results from different investigations through the years. However, the most recent studies suggest that this parasite causes a classical inflammatory response in the gills of AGD-infected fish, and also during their reinfection with *N. perurans* (Penacchi *et al.*, 2014). Paralelally, results from the work by Benedicenti *et al.*, (2015) suggests that there is either an immune evasion strategy, which serves to avoid cell-mediated killing mechanisms, or that there is an allergic reaction caused by the parasite. Most recently, two studies by Marcos-Lopez et al., (2017, 2018), investigated the host-response in the gills of affected salmon with AGD. These studies suggest that oxidative stress could be one of the additional key elements involved in development of the pathology of AGD.

However, eventhough the knowledge on AGD keeps expanding, other factors affect negatively to its spread such as health management in cleaner fish, resistance to treatments currently available and not treating fish in time. There are still knowledge gaps in different areas such as the characterisation of all *N. perurans* virulence factors or the potential role of endosymbionts and intrecellular bacteria in their pathogenicity. Thus, in order to improve the welfare of Atlantic salmon culture, further research is needed in the immune response, nutrition, and genetic selection.

1.4. Vaccine development in the aquaculture industry

The first fish vaccine trial was performed in a laboratory in 1938 by Snieszko *et al.* where carp (*Cyprinus carpio*) were injected with killed-*Aeromonas punctata* providing protective immunity. Following this study, the first oral immunisation described in fish was published by Duff (1942). This investigation showed that feeding a diet containing chloroform-killed *Aeromonas salmonicida* to cutthroat trout (*Oncorhynchus clarkii*) induced protection against furunculosis after challenge by injection or after contact with clinically ill fish. However, with the introduction of antibiotics to the aquaculture industry and due to their strong efficacy against pathogens, the development of vaccines was stopped for most of the 1940s and 1950s. Nevertheless, this hiatus didn't last as there was increasing development of antibiotic resistance across several pathogens, coupled with growing importance of viral diseases and the expression of concern that antibiotic use could be harmful to human and animal health. These factors pushed vaccine investigations to be restored during the 1960s and 1970s (Ross & Klontz, 1965; Klontz & Anderson, 1970). Since then, aquaculture vaccines have evolved from a position in the 1980s in which only 2 commercial vaccines were available to one of 24 currently implemented vaccines (bacterial and viral) (Shefat, 2018; Adams & Subasinghe, 2019).

Although proper fish management, followed by the limiting of fish stress and good hygiene are key factors for the control of fish diseases (Press & Lillehaug, 1995; Lillehaug, 1997; Larsen & Pedersen, 1997), disease prevention through vaccination is by far the most environmental and ethical method for pathogen control currently available within the aquaculture industry due to the limiting use of antibiotics and chemotherapeutants. However, in middle/low income countries, vaccination is still a far-off economical alternative for disease prevention (see review by Sommerset *et al.*, 2005). Therefore, the use of antibiotics continues to be a problem in these regions of the world, where its misuse has been reported (Van Boeckel *et al.*, 2015; Phu *et al.*, 2016; Watts *et al.*, 2017). However, vaccination has dramatically reduced the overuse of antibiotics in high-income countries such as UK and Norway (O'Neil *et al.*, 2005; Norwegian Ministries, 2015). Also, the use of vaccines in aquaculture has overcome the negative effects associated with the use of pharmaceuticals, hormones, antibiotics and their residues in the human food chain (Meeusen *et al.*, 2007; Ringø *et al.*, 2014).

The review by Rodger (2016) summarises all the diseases present within the aquaculture industry, including bacterial, viral and parasitic. Although many vaccines are currently available against these diseases, parasitic infections by ectoparasites such as sea lice, *L. salmonis* (sea lice disease) and *N. perurans* (AGD) currently represent significant threats for the Atlantic salmon industry and no commercial vaccines exist for these; similar to the case of fungi or fungi-like organisms (Adams, 2019).

1.4.1. Reverse vaccinology and the challenges in vaccine development against parasitic infections

Reverse vaccinology (RV) is an *in-silico* approach for identifying and predicting protein antigens using the genomic and transcriptomic data from the pathogen of interest. This approach has been widely described in many studies (Davies & Flower, 2007; Jones, 2012; Donati & Rappuoli, 2013). When the proteins or peptides are selected, they are produced as recombinant proteins, in most of the cases, and they are tested *in vivo*. One of the main advantages of this approach is that vaccine candidates are found in a very rapid and efficient manner in comparison with traditional methods (Rappuoli, 2000). Traditional methods use a high number of animals per experiment in order to assess a critical response to potential vaccines, now with RV those targets are better determined with bioinformatic tools and therefore, less animals are used for this purpose. However, there is a key obstacle found with this method. While conventional vaccinology can find a wide range of biological targets, including polysaccharides, RV only facilitates the targeting of proteins (Rappuoli, 2014; Rappuoli *et al.*, 2014). Along these lines, the general approach, when selecting vaccine candidates *in silico*, is considering the predicted location of the targeted protein in the cell. Typically, antigenic proteins are present on the surface or immediately secreted outside the cell. These targets are going to be the ones recognised by the immune system cells, potentially developing an adaptive immune response (Tu *et al.*, 2014; Vishnu *et al.*, 2017). However, there remains a limitation using current bioinformatics capabilities, which is the lack of specialised programs that determine whether the selected candidates induce a protective immune response in a given host or not (Goodswen *et al.*, 2017), particularly for poorly characterised hosts/immune systems.

Regarding the application of this methodology to parasitic infections, there have already been some studies that have used it to identify potential vaccine candidates in species like the malarial parasite *Plasmodium falciparum* (Pritam *et al.*, 2019), whose genome has been available since 2002 (Gardner *et al.*, 2002). Since then, RV has started to be widely applied as an approach to develop human anti-parasite vaccines including those targeting malaria, leishmaniasis (*Leishmania* spp.) and schistosomiasis (*Schistosoma* spp.) (Ben-Othman *et al.*, 2008, Feng *et al.*, 2007, Kanoi & Egwang, 2007; John *et al.*, 2012). This work has become easier due to the development of specific databases such as MalVac, a database of malarial vaccine candidates (Chaudhuri *et al.*, 2008). This is not the only parasite with dedicated resources including a wide range of 'omic' and EST databases. Additional species databases have also emerged such as those for *Cryptosporidia* (Puiu *et al.*, 2004), *Toxoplasma* (Gajria *et al.*, 2008), *Giardia* and *Trichomonas* (Aurrecoechea *et al.*, 2009) and *Schistosoma* (Zerlotini *et al.*, 2012). It should be noted, however, that despite all the efforts put into vaccine development for these various protistan species, no successful vaccines have yet been developed due to the complex biology of these parasitic species (Vercruysse *et al.*, 2007; Adams, 2019).

To understand why this task is difficult, there is a need to recognise the different characteristics that most parasites present. Perhaps the two most obvious differences from bacteria and viruses are the fact that they are eukaryotic and present a larger body size. This is linked to their complex life cycle which can include sexual and asexual reproduction (Good *et al.*, 2004). Lastly and more specifically, their morphological and antigenic diversity changes in every developmental phase. This paired with a series of evasion mechanisms that have developed against host immunity, such as molecular mimicry and sequestration (Good *et al.*, 2004) makes them extremely difficult targets for vaccine development. In the context of fish diseases, RV has been widely applied to the search for vaccine candidates in bacterial species (Chiang *et al.*, 2015; Andreoni *et al.*, 2016; Li *et al.*, 2016; Mahendran *et al.*, 2016; Kim *et al.*, 2019). Since its development, this method has been also useful for the selection of vaccine candidates for several fish parasites. The most studied parasite model is *Ichthyophthirius multifiliis*, which is an ectoparasite of freshwater teleosts that causes a disease commonly known as fish white spot disease (or Ich) (Matthews, 2005). Several host responses have been

reported from vaccine trials against this parasite (Buchman *et al.*, 2001) with the use of vaccine candidates derived from an RV approach, later turned into recombinant proteins. Additional studies used the same method and had similar responses and protective immunity reported (Dickerson & Findly, 2014; He *et al.*, 1997). Additionally, some other species have been studied through RV to look for vaccine candidates, such as *Lernaea cyprinacea* (Pallavi *et al.*, 2016), *Cryptocaryon irritans* (Mo *et al.*, 2016) and the sea louse *Caligus rogercresseyi* (Christie, 2014), which are ectoparasites that affect several cultivated fish species.

As the work in this thesis is focused on the ectoparasitic amoeba, *N. perurans*, a closer look to studies on other amoebic species seems advisable. In humans, a well-known parasitic disease is amoebiasis. The aetiological agent is *Entamoeba histolytica* and it is transmitted through the fecal–oral route via contaminated water and food or by person-to-person contact (Lozano *et al.*, 2012). The presence of a Gal/GalNAc lectin, which binds to galactose (Gal) and *N*-acetylgalactosamine (GalNAc), was identified as the major surface adhesion molecule of *E. histolytica* essential for the adherence of the parasite to mucins and mucosal epithelial cells of the host (Petri *et al.*, 1987). In addition to this, the presence of mucosal SIgA antibodies to inhibit the attachment of the trophozoites to the mucosal surface were detected suggesting a cell-mediated immunity elicited by mucosal immunization through the detection of interferon gamma (IFN γ) and interleukin 17 (IL-17) produced by CD4+ and CD8+ T cells, respectively (Guo *et al.*, 2011). Thus, these results showed how intestinal SIgA antibodies are protective against *E. histolytica* infection, although cell-mediated immunity may also be essential for the protection. Along these lines, studies have focused over the years on understanding the immune system in fish and applying a variety of approaches to the development of potential vaccines against AGD. These approaches included use of sonicated antigens and live amoebae, as well as DNA vaccines and glycoproteins and, more recently, recombinant proteins (Table 1.3). However, although most of the experiments showed an enhanced antibody response, none of the vaccines conferred any protection of vaccinated fish.

Table 1.3. Different vaccination approaches performed against AGD.

| Host species | Amoebae species | Experiments | Immunological responses | References |
|-------------------------------|---|---|---|--------------------------------------|
| <i>Oncorhynchus mykiss</i> | <i>Paramoeba</i> sp. (PA) | Injection with sonicated cultured PA antigens | Very low antibody levels; no protection detected | Akhlaghi <i>et al.</i> (1996) |
| <i>Salmo salar</i> | <i>Paramoeba</i> sp. (PA) | Injection with formalin killed wild PA + Freund's complete adjuvant (FCA) | Significant antibody level at 6-week post-infection (pi); no protection detected | Akhlaghi <i>et al.</i> (1996) |
| | | Injection with: <ul style="list-style-type: none"> ○ Live PA injection ○ Sonicated PA in PBS (1 and 10 mg) ○ Sonicated PA in FCA (1 and 10 mg) | Wide range of % seropositive among the vaccine fish (38-58%); no protection reported | |
| | | Crude antigen (wild PA and cultured PA) | No serological differences nor developed protection as gross signs were observable post-vaccination | |
| | | Detection of PA antigens by ELISA in gill mucus | Gill mucus antibodies were undetectable through ELISA | |
| | | <ul style="list-style-type: none"> ○ Intraperitoneal (IP) injection with sonicated wild and cultured PA + Montanide adjuvant ○ IP injection of live PA ○ Anal intubation of sonicated PA ○ Anal intubation of live PA | Indirect immunofluorescent-antibody test (IFAT) detected infection with PA in all the vaccinated fish; no protection detected | Zilberg & Munday (2000) |
| <i>N. pemaquidensis</i> | Injected with six-antigen DNA vaccine: pbS-Sfi-P1A2, pbS-Sfi-SC10, pbS-Sfi-SN8, pbS-Sfi-S3A4, pbS-Sfi-S3A5, pbS-Sfi-S3G8 | Gene expression detected in fish tissue; SC10 antigen elicits a significant humoral (antibody) immune response in vaccinated salmon; no protection reported | Cook <i>et al.</i> (2008) | |
| <i>Neoparamoeba</i> spp. (NP) | Injection with <i>high molecular weight antigen (HMWA)</i> from NP | No protection reported and immunisation lead to an immunosuppressive effect | Villavedra <i>et al.</i> (2010) | |
| <i>N. perurans</i> (NPE) | <ul style="list-style-type: none"> ○ Injection with three different DNA vaccines: pbsDNA pDEST26, pCDNA ○ Identification of NPE cell surface lectins and recombinant protein production (22C03) | pCDNA demonstrated lower gill scores in vaccinated fish | Cook <i>et al.</i> (2012) | |
| | Injected with recombinant protein r22C03, a mannose-binding protein-like (MBP-like) | Fish hyperimmunised with recombinant 22C03 developed antibodies but recognised proteins in a crude lysate of NPE | Antibody responses in salmon serum, mucus and gill and skin explants; no protection reported | Valdenegro-Vega <i>et al.</i> (2015) |

In the work described in this thesis, RV approaches will be applied to identify vaccine candidates through transcriptomic analysis of the aetiological agent of AGD, *N. perurans*. Firstly, both the host cells and the parasitic agent should have an optimal environment within the experimental system (Lee *et al.*, 2009; Bury *et al.*, 2014). Consequently, and linked to this, is the assurance of optimal growth conditions for the parasite. This has been a problem within this amoebic species, for which axenic culture has not been properly developed, in contrast with other amoebic species such as *Naegleria* and *Acanthamoeba* which can both be cultured axenically supplemented with antibiotics or on tissue culture cells with bacteria as a main food source (Schuster, 2002). However, if these limitations are taken in consideration during these *in vitro* experimental studies its application could lead to the animal testing reduction, due to the similar immune responses that were observed within these *in vitro* studies and the previous *in vivo* studies (Penacchi *et al.*, 2014; Benedicenti *et al.*, 2015).

1.5. Aims and Objectives

The development of tools for the future understanding and characterisation of host-pathogen interactions between *N. perurans* and Atlantic salmon (*S. salar*) entailed the investigation of several aspects of their relationship in the current study. This involved the development of new methods of detection and analysis, always in the context of mucosal surfaces. The implications of mucosal immunity in terms of the host-response to the ectoparasite presence and to current treatments, such as hydrogen peroxide, was also explored.

The work presented in this thesis therefore addressed the following objectives:

- 1- Investigation and development of an improved non-lethal method for the detection of *N. perurans* in AGD-infected fish through the comparison of different swab materials *in vitro* and *in vivo*.
- 2- Screening a range of aqueous and non-aqueous fixatives for their ability to preserve gill mucus in AGD infected and non-infected fish and thereby assist in the elucidation of host parasite interactions.
- 3- Study of the effect of hydrogen peroxide on the gills of non-infected and AGD-infected Atlantic salmon through the analysis of immune and mucin-related gene expression, supported by immunohistochemistry techniques.
- 4- Application of a reverse vaccinology approach, employing cultured *N. perurans* resources, for the *in-silico* search for potential vaccine candidates.

Chapter 2 : A comparison of different swabbing methods for optimised diagnosis of amoebic gill disease (AGD) in Atlantic salmon (*Salmo salar*)

2.1. Introduction

Amoebic gill disease (AGD), caused by *Neoparamoeba perurans*, is one of the main health challenges for the global Atlantic salmon (*Salmo salar*) farming industry (Rodger, 2014; Oldham *et al.*, 2016). Its presence in a number of other marine fish species (Oldham *et al.*, 2016), including cleaner fish species used for the biological control of sea lice in Atlantic salmon farms (Haugland *et al.*, 2016), has resulted in the emergence of new challenges for the industry especially as pronounced mortality can result if AGD is left untreated (Munday *et al.*, 2001). Current approaches for controlling AGD are resource demanding and labour intensive, involving numerous treatments throughout a production cycle. Freshwater bathing has been established as the standard method for treating the disease in Tasmania but is limited by restricted access to freshwater (Nowak *et al.*, 2014). Another recognised treatment is the use of hydrogen peroxide in cooler production areas. Although this treatment has shown more effective results (Nowak *et al.*, 2014), it has also been described as having a reduced safety margin at higher temperatures (Adams *et al.*, 2012) or where fish are compromised by advanced AGD (McCarthy *et al.*, 2015). Overall, AGD-related mortality is getting higher every year, causing great economic losses in locations such as Norway and Scotland (Shinn *et al.*, 2015).

Early diagnosis of AGD is clearly critical for the timely treatment of AGD-infected fish. Although histopathology remains one of the preferred techniques for the case definition of AGD (Clark & Nowak, 1999; Rodger, 2014), the monitoring of gross gill score (Taylor *et al.*, 2009) is by far the most extensively used and practical method for establishing AGD severity and is used as a key prompt for intervention using available treatments. Both techniques are commonly used together, with microscopic analysis used to confirm the presence of lesion-associated amoebae within the gills. Since the identification of *N. perurans* as the causal agent of AGD (Young *et al.*, 2007; Crosbie *et al.*, 2012) specific DNA based molecular diagnostic assays for the detection of the amoebae have been developed in different studies (Bridle *et al.*, 2010; Fringuelli *et al.*, 2012; Downes *et al.*, 2015).

Even though histopathology enables confirmation of both the presence of the pathogen and the resultant localised host response, it requires destructive sampling, which could mean the sacrifice of valued stock during epidemiological studies (Adams *et al.*, 2004; Douglas-Helders *et al.*, 2001). Therefore, the use of non-destructive tools to confirm the presence of *N. perurans* was studied by Downes *et al.* (2017), and also has been previously carried out by Young *et al.*, (2008) and Bridle *et al.*, (2010). When non-destructive gill swabbing was performed, results showed a great improvement on the sensitivity of *N. perurans* detection in comparison to gill filament biopsies. However, the type and physical structure of swab fibres influence the pick-up of target organisms from the site of swabbing and subsequent release of target organisms from the swab for following extraction of DNA and RT-PCR quantification (Turner *et al.*, 2010). Currently, Isohelix® DNA buccal and cotton wool tipped swabs are the most common tools used commercially. However, it is hypothesised, for the purpose of this study, that calcium alginate fibre-tipped swabs could offer an advantage, as they can be dissolved in most sodium salts to give soluble sodium alginate (**Error! Reference source not found.**). This material has multiple uses in the area of bioengineering: for cell encapsulation, surgical sponges, polymer films or wound dressings (Klöck *et al.*, 1994; Boateng *et al.*, 2008; Kneafsey *et al.*, 1996). This natural polymer therefore presents a simple structure and its highly hydrophilic nature allows the diffusion of biological fluids into the polymer. This can translate into a better recovery and subsequent extraction of target organisms, previously having been used in several studies for the investigation of the presence of microbes in dairy equipment and cleansing utensils (Higgins, 1950; Tredinnick & Tucker, 1951; Cain & Steele, 1953) and also for detecting pathogen presence in diagnostics for bacterial infections in skin and nose (Panpradist *et al.*, 2014). However, this material has never been investigated in the context of the aquaculture industry.

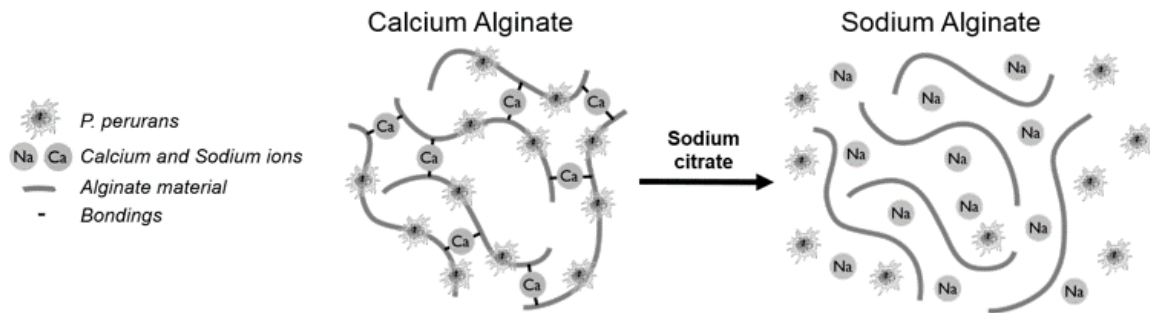


Figure 2.1. Physical changes to the calcium alginate matrix after sodium citrate addition: Following sodium citrate treatment, trapped amoebae would become detached from the material due to matrix disintegration allowing improved access for diagnostic tools. Image modified from www.jchs.edu.

While the type and physical structure of swab fibres is important, the method and area of swabbing is also relevant to the enhanced detection of *N. perurans*. Although the general swabbing method used in research is based on sampling of the second gill arch (Adams & Nowak, 2004a; Young *et al.*, 2008; Taylor *et al.*, 2009; Chalmers *et al.*, 2017), the industry performs swabbing of all the gill arches. The latter increases the swabbing area, and therefore detection of *N. perurans* is more likely to be successful, however, the irritation of the gills is greater.

Therefore, the work undertaken during this chapter was focused in determining if there was a subsequent modification in the detection of amoebae while using different swab types and, also, by swabbing different gill arches (2-4). For this, *in vitro* experiments were first carried out to investigate the characteristics of the different swab materials. Second, these characterised swabs were then applied to sampling in *in vivo* experiments along with the use of molecular tools used in the field for the detection of *N. perurans*.

2.2. Materials and Methods

2.2.1. Clinical swabs

The performance of three different commercially available swabs: CalgiSwab[®], a standard calcium alginate swab (Puritan[®], USA) and two swabs currently used for pathogen detection in the aquaculture industry, comprising Isohelix[®] DNA buccal swabs (Isohelix, UK) and cotton wool tipped swabs (Shintop, UK) were tested (**Error! Reference source not found.**) for efficacy in *N. perurans* detection.

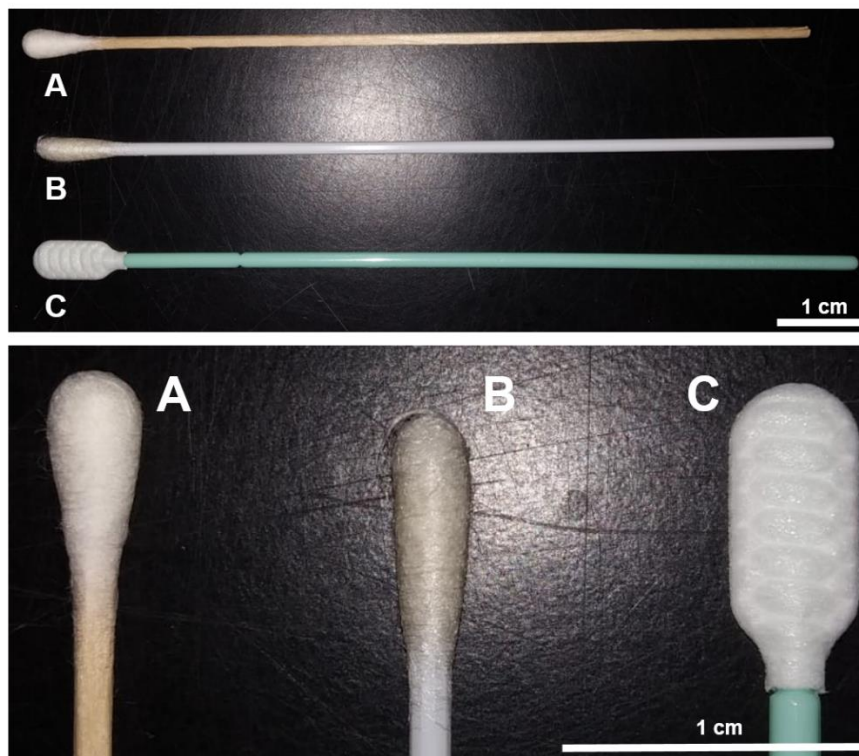


Figure 2.2. Different types of swabs: (A) Cotton wool tipped swabs; (B) CalgiSwab[®]; (C) Isohelix[®] DNA buccal swabs.

2.2.2. Clonal development and culture conditions of *N. perurans*

Amoebae were extracted from AGD-infected fish, which had been previously humanely euthanised using overdose of the anaesthetic MS-222 (100 ppm) and destruction of the brain according to UK Home Office Schedule 1 methods at the Marine Environmental Research Laboratory (MERL), Institute of Aquaculture, Machrihanish, Scotland, UK) under ethical approval reference number AWERB/1617/173/New ASPA. AGD-affected gills were examined for gill scoring according to Taylor et al. (2009). All the gill arches (Figure 2.3) from the left side were excised and placed in 50 mL tubes with 35 ppt filtered sea water (FSW) from

MERL, shaken for 30s and the gills were discarded; the liquid containing potential amoebae was transported to 25 cm² tissue culture flasks (Sarstedt AG & Co. KG, Germany). Monitoring of the flasks was performed daily, and bacterial contamination was limited through several washes with FSW. Isolates were routinely maintained in 75 cm² cell culture flasks containing FSW supplemented with malt yeast broth (MYB; 0.1% yeast (Product number: Y1625; Sigma Aldrich) and 0.1% malt (Product number: 70146; Sigma Aldrich) per litre of FSW) at 15°C.

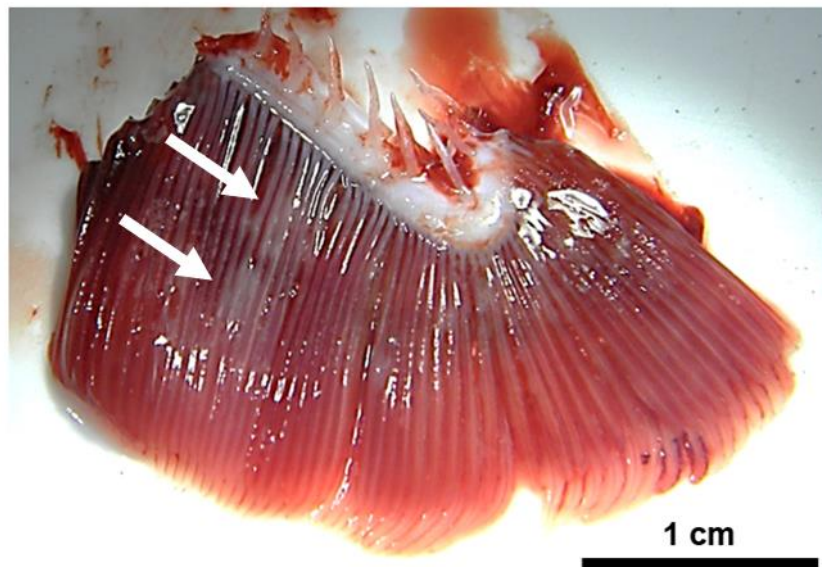


Figure 2.3. Excised AGD-affected gill from Atlantic salmon showing white lesions (white arrows) caused by *N. perurans*.

Amoebae were maintained and observed under the microscope regularly, different morphologies, including the attached, pseudocyst and floating trophozoites being observed (**Error! Reference source not found.**). Sub-culturing was performed every 7-10 days depending on amoeba growth by transferring them from smaller flasks to bigger flasks according to cell growth. To limit bacterial growth, flasks were washed with FSW every two days and supplemented with fresh MYB or FSW depending on bacterial contamination. Flasks were shaken for no longer than 30s and this mechanical disruption culminated in the detachment of the amoeba which were then transferred to 125 cm² cell culture flasks (Sarstedt AG & Co. KG, Germany) for the generation of a high-yield amoeba culture.

For the development of potential clonal cultures, amoebae were isolated through a manual single-picking technique (with a flame-drawn glass pipette) and transferred to 96-well plates (Corning®, US) supplemented with 100 µL of MYB. After

approximately fortnightly (14 days) intervals, amoebae were transferred to 75 cm² cell culture flasks (Sarstedt AG & Co. KG, Germany) supplemented with 10 mL of MYB. Amoebae were observed daily under a compound light microscope (Olympus BX53M) and images taken using an Olympus SC100 camera.

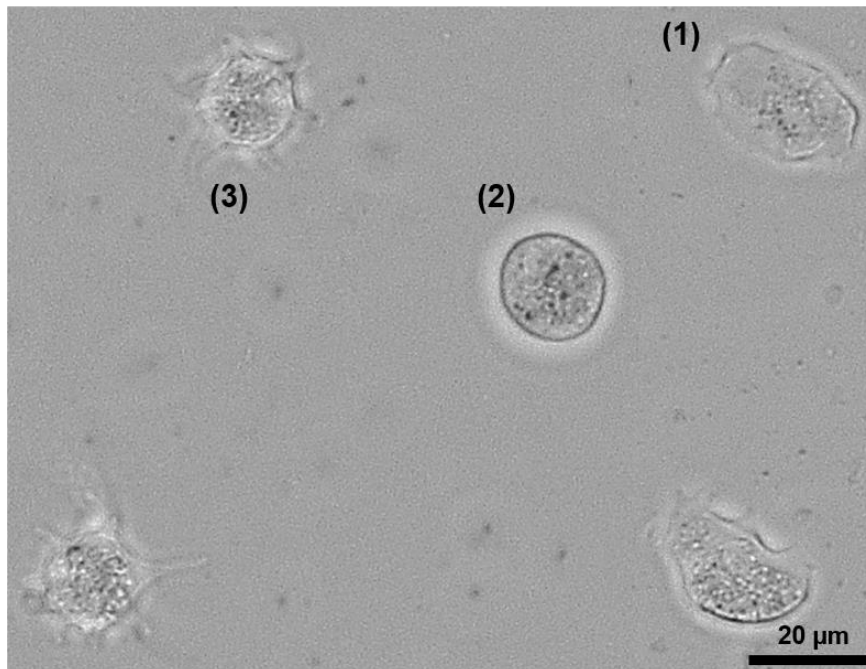


Figure 2.4. Culture of *N. perurans*. Different morphologies including attached (1), the latent stage, pseudocyst (2) and floating trophozoite (3). Observed with an Olympus BX53M microscope and captured using an Olympus SC100 camera.

When a monoclonal culture was developed and grown, cells were then harvested by centrifugation at 800 × g for 10 min. The supernatant was discarded by slowly pipetting it out and the pellet was re-suspended in 2.5 mL of FSW. The number of cells were quantified using a haemocytometer (Neubauer Improved, Marienfeld, Germany). Replicates of five counts were performed in four large squares of the whole grid. Cell density was adjusted to the desired quantity by dilution with FSW.

For confirmation of the presence of *N. perurans*, a DNA extraction was performed with the DNeasy Tissue Kit (Qiagen, Doncaster, Vic., Australia) followed by a diagnostic PCR with specific primers for the 18S rRNA gene used by Young *et al.* (2008). Amplification of the 18S rRNA gene was performed in volumes of 20 µL containing between 10-20 ng of DNA, miTaq polymerase (Bioline, UK), a set of primers (10µM) for 18S rRNA sequences as follows:

N. perurans F: '5-ATCTTGACYGGTTCTTTTCGRGA-3'
R: '5-ATAGGTCTGCTTATCACTYATTCT-3'

P. branchiphila F: '5-GACCCTTTTGGGAAGAGATG-3'
R: '5-CAGCCTTGCGACCATACTC-3'

P. Pemaquidensis F: '5-CTGGTTGATCCTGCCAGTAGTC-3'
R: '5-CAGCCTTGCGACCATACTC-3'

The PCR cycle conditions were 95°C for 5 min; 95°C for 30 s, 58°C for 30 s and 73°C for 2 min, for 35 cycles; and 73°C for 8 min. Full-length 18S rRNA gene of *P. perurans* (637 bp) was used as a positive control and a sample with only ddH₂O as the negative control. The PCR reaction products were subjected to electrophoresis through 1% agarose/tris–borate EDTA buffer and bands were visualized by staining with a final concentration of 0.5 µg mL⁻¹ from a 10 mg mL⁻¹ ethidium bromide stock (usually about 3 µL of solution in a 100 mL gel).

An attempt to cryopreserve stocks / isolates of amoebae was performed during this period, however, the results were not replicable thus further investigations were not undertaken. The description of the methodology and preliminary results from this experiment are described in the Appendices I and II.

2.2.3. Evaluation of the potential inhibition of PCR by sodium citrate

In order to determine whether sodium citrate inhibited subsequent molecular analysis, amoebae were harvested from a one week 75 cm² flask tissue culture and collected in Eppendorf tubes to give a final concentration of 1 x 10³ cells mL⁻¹ and these were resuspended in 1 mL of 0.2 M sodium citrate solution. Samples were stored at 4°C for 7 and 14 days. Following DNA extraction, PCR detection was performed as described in Section 2.2.2.

2.2.4. *In vitro* testing for the swabbing and spiking of the three clinical swabs

In order to investigate the material nature and to provide information about the absorption capacity of the different swabs, two different *in vitro* experiments were developed. Spiking of the swabs with different concentrations of the parasite was performed to help understand the absorption capacity of the tested materials and,

lastly, the swabbing of agar plates with known concentrations of amoebae would aid evaluate the retrieval capacity.

2.2.4.1. Spiking of swabs with *N. perurans*

Swabs were inoculated with a sample volume of 15 μ L, which was less than the fluid capacity for all swabs, as described in Panpradist *et al.* (2014). Each swab type (n=10) was spiked with 15 μ L containing different numbers of amoebae: low (10 amoebae), medium (100 amoebae) and high (1000 amoebae). Calcium alginate tipped swab tips were immersed in a 1.5 mL centrifuge tube with 0.2 M sodium citrate and manually shaken for 30s before being discarded. Isohelix[®] and Cotton swab tips were immersed in 1.5 mL centrifuge tubes with 95% ethanol. Ethanol samples were stored in the freezer at -20°C and sodium citrate samples were stored in the fridge at 4°C until molecular analyses were carried out.

2.2.4.2. Retrieval / recovery of amoebae from agar plates

Each seawater agar plate (SWA; FSW at 35 ppt salinity, filtered through 0.22 μ m, and 10 g agar) (n=10 per group) was spiked with 50 μ L containing different numbers of amoebae: low (10 amoebae), medium (100 amoebae) and high (1000 amoebae) and the volume was made up to 5 mL with FSW. Plates were incubated for 2 h at 15°C in order to allow the attachment of amoebae to the agar surface. The overlay was then removed prior to the immediate standardised swabbing, which consisted in swabbing the entire plate vertically to then rotate the plate 90 degrees to the right and repeating the step once again to cover the whole surface of the plate (**Error! Reference source not found.**).

The treatment of the swab tips for molecular analysis was carried out as described in Section 2.2.4.1.

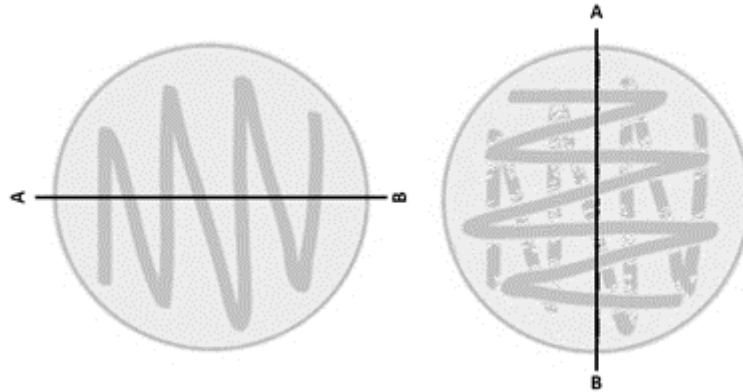


Figure 2.5. Swabbing method: amoebae were swabbed on a seawater agar plate in two perpendicular directions.

2.2.5. *In vivo* testing of the three clinical swabs

2.2.5.1. Experimental fish and swabbing method for the AGD-infected gills

Gill swabbing was carried out at MERL. Swabbing was performed ventrally and dorsally in one direction. A total of 60 fish was sampled over the course of two sampling events (December 2018 and April 2019). The two trials were performed in order to provide more biological samples and to investigate whether different time periods would provide more information about variation on AGD progression due to the different seasons. Fish were infected with AGD by cohabitation challenge as follows.

The cohabitation challenge was undertaken according to methods developed at the Institute of Aquaculture, Stirling, Scotland. Challenge cohabitants were produced using a stock of infected Atlantic salmon held at the MERL facility as part of an *in vivo* amoebae culture. Four of these preinfected fish were added to a separate stock of 40 naïve Atlantic salmon smolts. Gills were grossly assessed until the appropriate gill score for cohabitation infection (approximately 1.5–2 gill score) was achieved. The cohabitants (seeder fish) were adipose fin-clipped, marked with a Panjet (0.0652 g Alcian blue mL⁻¹, Sigma-Aldrich, UK) and added to the appropriate challenge groups (6 cohabitants tank⁻¹). A group of uninfected cohabitants was also produced using the same method, with 4 uninfected Atlantic salmon added to

another stock of 40 naïve smolts. No clinical pathology was observed in uninfected seeders after 2 weeks.

Sampling occurred after 6 weeks post infection, after which the challenge was terminated. At each sampling point, 6 fish per stock per tank were removed from the tanks, sized (24.7 ± 1.9 (s.d.) cm), weighed (181 ± 12 (s.d.) g) and, lastly, culled by lethal anaesthesia (10% Benzocaine, Sigma-Aldrich, UK) before being sampled. Work was conducted under ethics application reference number AWERB/1617/173/New ASPA. AGD-affected gills were examined for gill scoring according to Taylor et al., (2009). Subsequently, second, third and fourth gill arches were sampled as indicated in Table 2.1. The treatment of the swab tips for molecular analysis was carried out as described in previous sections.

The facility was supplied with flow-through seawater (35 ‰), filtered at 100 µm. Fish were maintained under ambient temperatures. Slight differences in temperature between the different trials was reported. During the month of December a min. temperature of 11 °C and a max. temperature of 13 °C were registered. In April a min. temperature of 11.5 °C a max. temperature of 14 °C were registered. Commercial salmon pellets equivalent to 1% of their body weight per day were fed to the fish. Experimental procedures were all approved by the Animal Welfare and Ethical Review Body (AWERB) of the University of Stirling and were conducted under UK Government Home Office project licence 60/4189.

Table 2.1. Method for swabbing the gills of AGD-infected fish: gills were sampled with different swab types (e.g. Cotton 2.1: cotton is the swab type; 2 is the 2nd gill arch; 1 is the replicate number).

| Fish no. | Swab type | | |
|-----------------|------------------|----------------|----------------|
| 1 | Cotton 2.1 | CalgiSwab 3.1 | Isohelix® 4.1 |
| 2 | Cotton 2.2 | CalgiSwab 3.2 | Isohelix® 4.2 |
| 3 | Cotton 2.3 | CalgiSwab 3.3 | Isohelix® 4.3 |
| 4 | Cotton 2.4 | CalgiSwab 3.4 | Isohelix® 4.4 |
| 5 | Cotton 2.5 | CalgiSwab 3.5 | Isohelix® 4.5 |
| 6 | Cotton 2.6 | CalgiSwab 3.6 | Isohelix® 4.6 |
| 7 | Cotton 2.7 | CalgiSwab 3.7 | Isohelix® 4.7 |
| 8 | Cotton 2.8 | CalgiSwab 3.8 | Isohelix® 4.8 |
| 9 | Cotton 2.9 | CalgiSwab 3.9 | Isohelix® 4.9 |
| 10 | Cotton 2.10 | CalgiSwab 3.10 | Isohelix® 4.10 |
| 11 | Isohelix® 2.1 | Cotton 3.1 | CalgiSwab 4.1 |
| 12 | Isohelix® 2.2 | Cotton 3.2 | CalgiSwab 4.2 |
| 13 | Isohelix® 2.3 | Cotton 3.3 | CalgiSwab 4.3 |
| 14 | Isohelix® 2.4 | Cotton 3.4 | CalgiSwab 4.4 |
| 15 | Isohelix® 2.5 | Cotton 3.5 | CalgiSwab 4.5 |
| 16 | Isohelix® 2.6 | Cotton 3.6 | CalgiSwab 4.6 |
| 17 | Isohelix® 2.7 | Cotton 3.7 | CalgiSwab 4.7 |
| 18 | Isohelix® 2.8 | Cotton 3.8 | CalgiSwab 4.8 |
| 19 | Isohelix® 2.9 | Cotton 3.9 | CalgiSwab 4.9 |
| 20 | Isohelix® 2.10 | Cotton 3.10 | CalgiSwab 4.10 |
| 21 | CalgiSwab 2.1 | Isohelix® 3.1 | Cotton 4.1 |
| 22 | CalgiSwab 2.2 | Isohelix® 3.2 | Cotton 4.2 |
| 23 | CalgiSwab 2.3 | Isohelix® 3.3 | Cotton 4.3 |
| 24 | CalgiSwab 2.4 | Isohelix® 3.4 | Cotton 4.4 |
| 25 | CalgiSwab 2.5 | Isohelix® 3.5 | Cotton 4.5 |
| 26 | CalgiSwab 2.6 | Isohelix® 3.6 | Cotton 4.6 |
| 27 | CalgiSwab 2.7 | Isohelix® 3.7 | Cotton 4.7 |
| 28 | CalgiSwab 2.8 | Isohelix® 3.8 | Cotton 4.8 |
| 29 | CalgiSwab 2.9 | Isohelix® 3.9 | Cotton 4.9 |
| 30 | CalgiSwab 2.10 | Isohelix® 3.10 | Cotton 4.10 |

2.2.6. Swab digestion, DNA extraction and qPCR quantification

Prior to the DNA extraction, a pre-treatment of the Ethanol preserved swab tips was first needed. They were removed from storage and vigorous agitation was performed with a Top Mix FB15024 vortexer (Fisher Scientific, UK) for 60s at a maximum

frequency setting and, ultimately, the tip of the swabs was discarded. For the sodium citrate tubes, no swab tip was longer inside the tube, so they were directly centrifuged.

To pellet the amoebae, tubes were centrifuged at 14,000 x g for 10 min. Ethanol was carefully discarded and the remaining liquid was pipetted off. Tubes were left open to dry for up to 1 h in a heat cabinet at 60 °C. The same procedure was followed for the sodium citrate preserved swabs; however no drying step was needed for the alginate swabs.

After centrifugation of the tubes, DNA extraction was then performed following the manufacturer's instructions for the Wizard[®] SV Genomic DNA purification (Promega) with a few variations. A volume of 100 µL of Nuclei lysis buffer, 25 µL EDTA (both included in the DNA extraction kit) and 10 µL of Proteinase K (New England BioLabs, USA) were added to each tube and tubes were incubated for 3 h or overnight in a heat cabinet at 60 °C. Once the incubation was finished, a volume of 250 µL of pre-heated (at 60 °C) SV Buffer was added to the tubes and the contents transferred to the columns. Columns were then centrifuged at 12,000 x g for 1 min. A column wash was performed with 500 µL of the column wash buffer and columns were centrifuged for 3 min at 14,000 x g. Lastly, DNA was eluted in 50 µL of distilled water.

The qPCR quantification was carried out using the qTOWER³ (Analytik Jena, Germany) with a set of primers designed in Mowi Laboratories, Fort William, UK (FW: 5' GTT CTT TCG GGA GCT GGG AG 3': RV: 5' GAA CTA TCG CCG GCA CAA AAG 3') and a probe (FAM) (5' CAA TGC CAT TCT TTT CGG A 3'). Primer and probe concentrations for each well were 0.3 µM and 0.15 µM, respectively. Every reaction volume was set to 20 µL. A volume of 15 µL was set for the primers, probe, and master mix (Luna[®] Universal Probe qPCR Master Mix, New England Labs, USA) and the remaining was the 5 µL of DNA sample.

DNA extracted from cultured amoebae was used as a positive control, whilst milli-Q water was used as a negative control (NTC). All samples were analysed in duplicate. For the development of the qPCR method, a standard curve was performed from a stock solution of Plasmid DNA (PCR2.1-AGD) (provided by Mowi Laboratories, Fort William, UK) at 320 ng µL⁻¹ followed by a set of standard dilutions (from 1 x 10¹ copies to 1 x 10¹⁰). PCR conditions comprised a pre-denaturation step at 95°C for 60 s, followed by 45 cycles of a denaturation step at 95°C for 15 s, an extension step of

56°C for 60 s and a last step of melting curve. This protocol was developed in Mowi Laboratories, Fort William, UK, and afterwards applied to the samples in the Institute of Aquaculture, Stirling, UK.

2.2.7. Statistical analysis

All results obtained from the *in vitro* and *in vivo* testing were exported to IBM SPSS statistical analysis software (v23, IBM Corporation) and were processed and tested to determine significant differences between type of swabs, amoebic loads and gill arches. Shapiro-Wilk test was conducted to verify normality, followed by Levene's, test to determine homogeneity of variance. Two-Way ANOVA was then performed on the data to examine the significance between means followed by *post-hoc* Tukey HSD test to discriminate between experimental groups. *In vivo* challenges were treated as individual sets of data to investigate the potential differences between the two different time periods. A Pearson's correlation test was also performed to assess the correlation (R^2) between *Ct* values and observed gill scores.

2.3. Results

2.3.1. PCR evaluation of the capacity of sodium citrate to preserve *N. perurans* rRNA

After the incubation period, a subsequent PCR of amoeba samples stored for 7 (n=3) and 14 days (n=3) in 0.2 M sodium citrate was carried out. Results showed that sodium citrate did not affect PCR chemistry, demonstrated by the presence of specific bands for *N. perurans* 18S rRNA sequence (637 bp) (**Error! Reference source not found.**). This provided proof of the preservation capacity of sodium citrate; however, more controls should have been provided to use as a comparison (e.g. ethanol) and thereby strengthen these results, as well as the use of qPCR for the proper quantification of the bands.

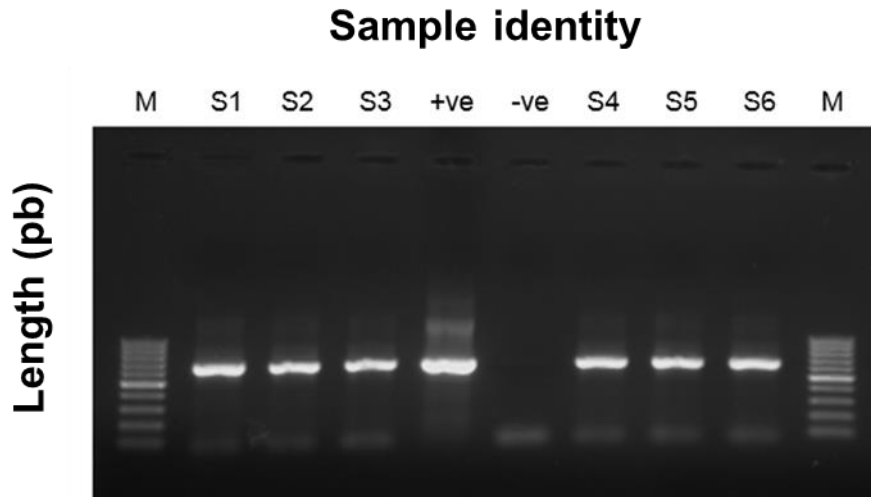


Figure 2.6. PCR results after preservation of amoebae in 0.2 M sodium citrate for 7 days (lanes S1-S3) and 14 days (S4-S6). M: 100 bp DNA ladder. +ve control: *N. perurans* 18S rRNA sequence. -ve control: ddH₂O.

2.3.2. Detection of *N. perurans* from the *in vitro* and *in vivo* testing

NanoDrop results from the spiked samples showed a high variation in DNA yields ranging from 0.54 to 4.90 ng μL^{-1} in the lowest concentration, 5.3 to 35.6 ng μL^{-1} in the medium concentration and 52.1 to 75.6 ng μL^{-1} in the highest concentration. Similar high variation was showed in the plate swabs with a slightly higher range from 0.75 to 8.35 ng μL^{-1} in the lowest concentration, 7.8 to 57.6 ng μL^{-1} in the medium concentration and 71.3 to 102.7 ng μL^{-1} in the highest concentration. From the *in vivo* trials, very high variation in DNA yields was also observed (0.55 to 7.65 ng μL^{-1}). For the detection of the pathogen, a standard volume of DNA solution was used from each sample (5 μL /qPCR reaction). These data on the DNA yields by themselves, showed the differences between swab materials and the variation between the pathogen recovery capacity.

2.3.2.1. *In vitro* testing results

Lower *Ct* values were observed when Isohelix[®] DNA buccal swabs were used for the recovery of *N. perurans* from the swabs. A significant difference was seen between Isohelix[®] DNA buccal swabs and the other two swab types (ANOVA and *post-hoc* Tukey HSD Test; $p < 0.05$) when higher concentrations of amoebae were loaded onto the spiked samples (100 and 1,000) (Fig.2.7).

When swabbing was performed on the agar plates, lower *Ct* values were observed throughout with the use of Isohelix® DNA buccal swabs (Fig. 2.7). However, differences were not significantly different (*post-hoc* Tukey HSD Test; $p > 0.05$) (Error! Reference source not found.).

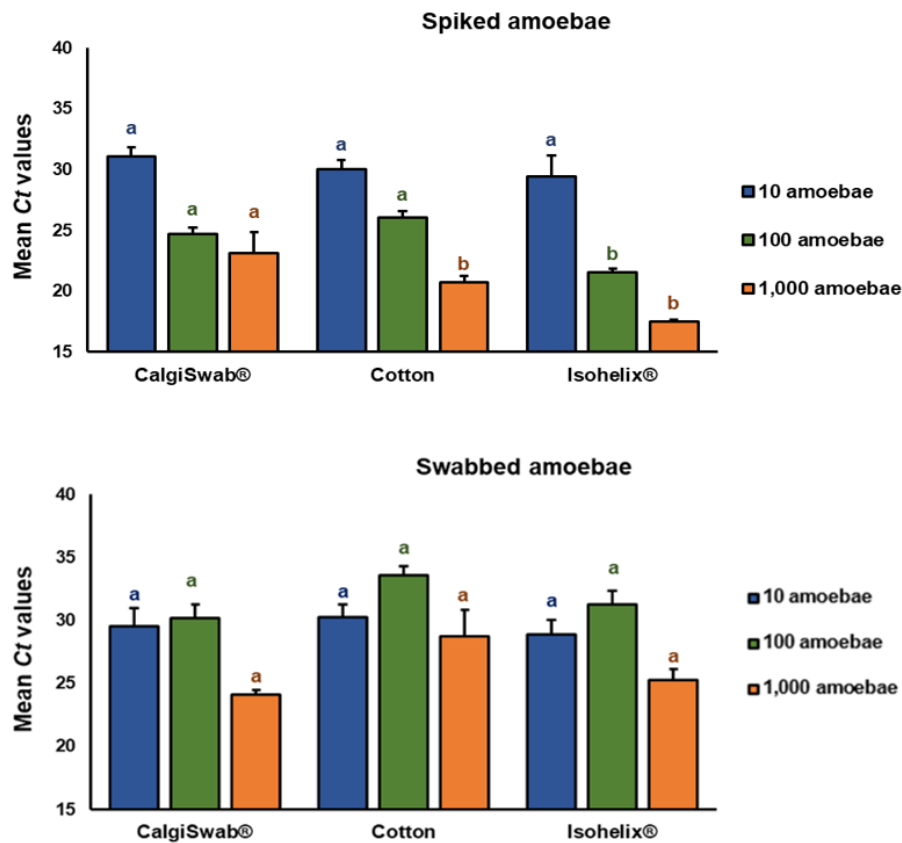


Figure 2.7. Spiked amoebae: qPCR *Ct* values of *N. perurans* for three clinical swab types spiked with different concentrations of amoebae (10, 100 and 1,000/swab). **Swabbed amoebae:** qPCR *Ct* values of *N. perurans* for three clinical swab types used to detect amoebae from MYA plates seeded with different concentrations of amoebae (10, 100 and 1,000/plate). Bars represent the mean *Ct* values ($n = 10$ per concentration) (\pm s.e.m). Different letters represent statistically significant differences between swab types ($p < 0.05$).

Although there were statistically significant differences between swab types and the amoeba load ($p < 0.001$), there was not a statistically significant interaction between the swab type and concentration on the *Ct* values for the spiked samples and for the swabbing of plates ($p > 0.05$) (Table 2.2).

Table 2.2. Results from the two-way ANOVA for the interaction: Swab type vs amoebae load vs *Ct* values for the spiked samples (A) and swabbed samples (B). F: F-test. Sig.: statistical significance.

Bold values represent the significance of interactions ($p < 0.001$), while underlined values represent the non-significant interactions ($p > 0.001$).

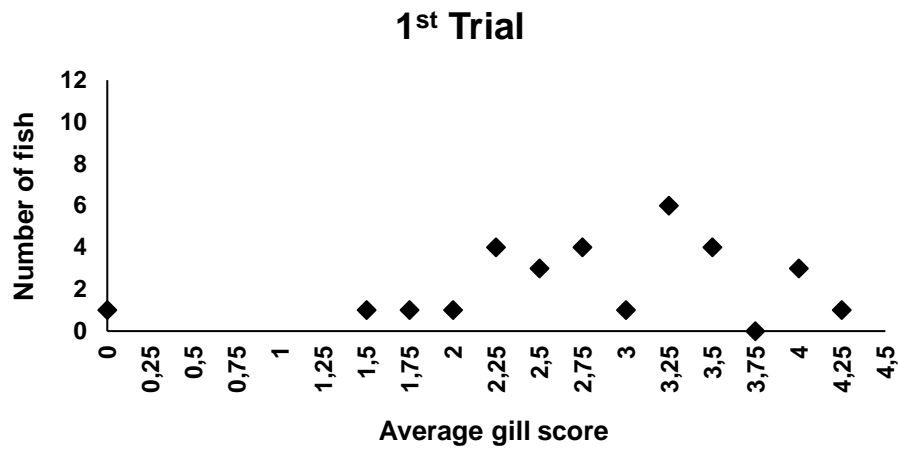
| (A) | Interaction | F | Sig. |
|---------------------------------|--------------------|----------|------------------|
| <i>Swab Type</i> | Ct values spiked | 11.639 | <0.001 |
| <i>Amoebal load</i> | Ct values spiked | 83.390 | <0.001 |
| <i>Swab Type * Amoebal load</i> | Ct values spiked | 2.215 | <u>0.075</u> |

| (B) | Interaction | F | Sig. |
|---------------------------------|--------------------|----------|------------------|
| <i>Swab Type</i> | Ct values swabs | 16.972 | <0.001 |
| <i>Amoebal load</i> | Ct values swabs | 5.080 | 0.008 |
| <i>Swab Type * Amoebal load</i> | Ct values swabs | 0.714 | <u>0.585</u> |

2.3.2.2. *In vivo* testing

During this study, two experiments were performed, with level of AGD scores differing (**Error! Reference source not found.**) possibly due to the different seasons in which these experiments were performed or other factors. During the first trial (**Error! Reference source not found.A**), there were more fish presenting lower scores compared to the later trial (**Error! Reference source not found.B**) where a greater number of fish presented higher scores.

(A)



(B)

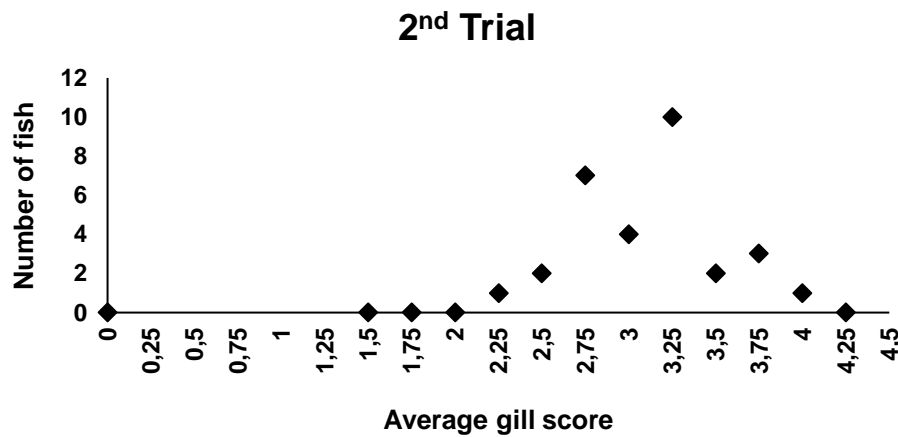


Figure 2.8. Scores and number of fish for the first trial in December 2018 (A) and second trial in April 2019 (B) (n = 30 fish per trial).

During the first trial in December 2018, many negative results were observed for *N. perurans* by PCR within the cotton and CalgiSwab® swabs. In contrast, the second trial during April 2019 showed less negatives and even lower *Ct* values across all swab types (Table 2.3). Although the use of Isohelix® swabs resulted in fewer negative results and more stable results throughout the experiment (Table 2.4.), lower *Ct* values were observed when using the CalgiSwab® swabs.

Table 2.3. Results from the first experiment *in vivo* during December 2018. Scoring of all fish and *Ct* values are described in this table. Negative results are underlined and when no *Ct* value was detected during the qPCR, a value of 37 was assigned as this is the limit value when diagnosing AGD in the industry.

| | Score (mean of left and right gill arch) | CalgiSwab® | <i>Ct</i> value | <i>Isohelix</i>® | <i>Ct</i> value | Cotton | <i>Ct</i> value |
|----------------|---|-------------------|------------------------|-------------------------|------------------------|---------------|------------------------|
| Fish 1 | 3.25 | 3.1 | 25.1 | 4.1 | 31.3 | 2.1 | <u>37</u> |
| Fish 2 | 1.75 | 3.2 | 29.1 | 4.2 | 32.7 | 2.2 | <u>37</u> |
| Fish 3 | 2.25 | 3.3 | 28.5 | 4.3 | 30.6 | 2.3 | <u>37</u> |
| Fish 4 | 3.5 | 3.4 | 34.0 | 4.4 | 28.6 | 2.4 | <u>37</u> |
| Fish 5 | 3.25 | 3.5 | <u>37</u> | 4.5 | 27.8 | 2.5 | <u>37</u> |
| Fish 6 | 2.75 | 3.6 | <u>37</u> | 4.6 | 27.1 | 2.6 | <u>37</u> |
| Fish 7 | 2.75 | 3.7 | <u>37</u> | 4.7 | 30.1 | 2.7 | <u>37</u> |
| Fish 8 | 3.25 | 3.8 | <u>37</u> | 4.8 | 30.2 | 2.8 | <u>37</u> |
| Fish 9 | 4.25 | 3.9 | 21.4 | 4.9 | 30.7 | 2.9 | <u>37</u> |
| Fish 10 | 3.25 | 3.10 | 30.9 | 4.10 | 30.5 | 2.10 | <u>37</u> |
| Fish 11 | 4 | 4.1 | <u>37</u> | 2.1 | 30.2 | 3.1 | <u>37</u> |
| Fish 12 | 3.25 | 4.2 | 24.3 | 2.2 | 34.9 | 3.2 | <u>37</u> |
| Fish 13 | - | 4.3 | 20.0 | 2.3 | 30.0 | 3.3 | 34.9 |
| Fish 14 | 2.25 | 4.4 | 24.7 | 2.4 | 36.8 | 3.4 | 30.7 |
| Fish 15 | 3.25 | 4.5 | 22.5 | 2.5 | 30.7 | 3.5 | 34.2 |
| Fish 16 | 3 | 4.6 | 26.7 | 2.6 | 33.2 | 3.6 | 33.2 |
| Fish 17 | 2.75 | 4.7 | <u>37</u> | 2.7 | <u>37.8</u> | 3.7 | <u>37</u> |
| Fish 18 | 2.5 | 4.8 | 24.6 | 2.8 | 32.6 | 3.8 | <u>37</u> |
| Fish 19 | 2.25 | 4.9 | 24.3 | 2.9 | 32.7 | 3.9 | <u>37</u> |
| Fish 20 | 2.5 | 4.10 | 27.5 | 2.10 | 32.3 | 3.10 | <u>37</u> |
| Fish 21 | 2 | 2.1 | <u>37</u> | 3.1 | 31.8 | 4.1 | 31.4 |
| Fish 22 | 1.5 | 2.2 | 29.5 | 3.2 | 29.5 | 4.2 | 27.2 |
| Fish 23 | 2.25 | 2.3 | 32.1 | 3.3 | 29.5 | 4.3 | 31.9 |
| Fish 24 | 4 | 2.4 | 25.9 | 3.4 | 27.2 | 4.4 | 31.9 |
| Fish 25 | 3.5 | 2.5 | <u>37</u> | 3.5 | 30.1 | 4.5 | 36.6 |
| Fish 26 | 4 | 2.6 | <u>37</u> | 3.6 | 27.1 | 4.6 | 29.4 |
| Fish 27 | 2.5 | 2.7 | <u>37</u> | 3.7 | 29.1 | 4.7 | <u>37</u> |
| Fish 28 | 3.5 | 2.8 | 26.9 | 3.8 | 30.8 | 4.8 | 28.9 |
| Fish 29 | 2.75 | 2.9 | <u>37</u> | 3.9 | 32.5 | 4.9 | 30.6 |

Fish 30 3.5 2.10 **37** 3.10 **33.8** 4.10 **30.1**

Table 2.4. Results from the second *in vivo* experiment during April 2019. Scoring of all fish and Ct values are described in this table. Negative results are underlined and when no Ct value was detected during the qPCR, a value of 37 was assigned as this is the limit value when diagnosing AGD in the industry.

| | Score (mean of left and right gill arch) | CalgiSwab[®] | Ct value | Isohelix[®] | Ct value | Cotton | Ct value |
|----------------|---|------------------------------|------------------|-----------------------------|------------------|---------------|--------------------|
| Fish 1 | 3 | 3.1 | 19.7 | 4.1 | 23.1 | 2.1 | 28.7 |
| Fish 2 | 2.75 | 3.2 | 21.4 | 4.2 | 23.5 | 2.2 | 29.2 |
| Fish 3 | 3.25 | 3.3 | 25.8 | 4.3 | 27.2 | 2.3 | 35.3 |
| Fish 4 | 3.25 | 3.4 | 19.2 | 4.4 | <u>37</u> | 2.4 | <u>37.5</u> |
| Fish 5 | 3.5 | 3.5 | 30.8 | 4.5 | 20.1 | 2.5 | 32.3 |
| Fish 6 | 2.5 | 3.6 | 24.8 | 4.6 | 23.5 | 2.6 | 25.2 |
| Fish 7 | 3.25 | 3.7 | 22.5 | 4.7 | 26.1 | 2.7 | 30.3 |
| Fish 8 | 2.75 | 3.8 | 25.6 | 4.8 | 23.1 | 2.8 | 34.2 |
| Fish 9 | 2.75 | 3.9 | 23.5 | 4.9 | 35.2 | 2.9 | 35.08 |
| Fish 10 | 2.75 | 3.10 | 21.5 | 4.10 | 32.4 | 2.10 | 32.8 |
| Fish 11 | 3.25 | 4.1 | 19.6 | 2.1 | 39.1 | 3.1 | 29.6 |
| Fish 12 | 2.25 | 4.2 | 24.5 | 2.2 | 27.2 | 3.2 | 33.5 |
| Fish 13 | 3.25 | 4.3 | 22.3 | 2.3 | 23.2 | 3.3 | 23.4 |
| Fish 14 | 3.25 | 4.4 | 22.4 | 2.4 | 24.4 | 3.4 | 27.1 |
| Fish 15 | 3.25 | 4.5 | 28.0 | 2.5 | 34.6 | 3.5 | 26.8 |
| Fish 16 | 3.25 | 4.6 | <u>37</u> | 2.6 | 22.3 | 3.6 | 26.4 |
| Fish 17 | 3.25 | 433.7 | 20.4 | 2.7 | 36.7 | 3.7 | 21.2 |
| Fish 18 | 3.75 | 4.8 | 19.8 | 2.8 | 27.9 | 3.8 | 23.2 |
| Fish 19 | 3.75 | 4.9 | 23.2 | 2.9 | 37.9 | 3.9 | 21.9 |
| Fish 20 | 3 | 4.10 | 21.6 | 2.10 | 27.2 | 3.10 | 24.5 |
| Fish 21 | 3.75 | 2.1 | 21.9 | 3.1 | 34.0 | 4.1 | 27.9 |
| Fish 22 | 2.75 | 2.2 | 25.4 | 3.2 | 23.0 | 4.2 | 24.3 |
| Fish 23 | 2.75 | 2.3 | 27.5 | 3.3 | 23.4 | 4.3 | 24.2 |
| Fish 24 | 3.25 | 2.4 | 24.2 | 3.4 | 21.1 | 4.4 | 26.6 |
| Fish 25 | 3 | 2.5 | 25.4 | 3.5 | 23.6 | 4.5 | 24.3 |
| Fish 26 | 4 | 2.6 | 18.9 | 3.6 | 28.0 | 4.6 | 24.3 |
| Fish 27 | 3 | 2.7 | 22.5 | 3.7 | 29.7 | 4.7 | 23.0 |
| Fish 28 | 2.5 | 2.8 | 20.2 | 3.8 | 25.3 | 4.8 | 23.9 |
| Fish 29 | 3.5 | 2.9 | 25.4 | 3.9 | 24.4 | 4.9 | 26.1 |

Table 2.5. shows the percentages of negative and positive results across all swab types during both samplings. A two-way ANOVA was conducted that examined the effect of swab type and gill arch on DNA quantity during both trials (December 2018 and April 2019). For the first trial, there were statistically significant differences between swab types and gill arches (both with $p = <0.001$) (**Error! Reference source not found.**). During the trial that was performed in April 2019, the results indicate similar statistical differences when the two-way ANOVA was conducted (**Error! Reference source not found.**).

Table 2.5. Percentages of positives and negative results by qPCR during both trials: (A) First trial in December. (B) Second trial in April. Isohelix® and CalgiSwab® present higher percentages of positive results throughout the experiment.

| (A) | December trial | | |
|------------------|----------------|-----------|--------|
| | CalgiSwab® | Isohelix® | Cotton |
| Positives | 60% | 96.67% | 56.67% |
| Negatives | 40% | 3.33% | 43.33% |

| (B) | April trial | | |
|------------------|-------------|-----------|--------|
| | CalgiSwab® | Isohelix® | Cotton |
| Positives | 96.67% | 96.67% | 96.67% |
| Negatives | 0% | 3.33% | 3.33% |

Table 2.6. December 2018 trial results from the two-way ANOVA for the interaction: Swab type vs gill arches vs Ct values. F: F-test. Sig.: statistical significance. Bold values represent the significance of interactions ($p < 0.05$), while underlined values represent the non-significant interactions ($p > 0.05$).

| Interaction | F | Sig. |
|------------------------------|--------|------------------|
| <i>Swab type</i> | 11.135 | <0.001 |
| <i>Gill arch</i> | 15.671 | <0.001 |
| <i>Swab type * Gill arch</i> | 1.318 | <u>0.270</u> |

Table 2.7. April 2019 trial results from the two-way ANOVA for the interaction: Swab type vs gill arches vs Ct values. F: F-test. Sig.: statistical significance. Bold values represent the significance of interactions ($p > 0.05$), while underlined values represent the not significant interactions ($p < 0.05$).

| Interaction | F | Sig. |
|------------------------------|-------|--------------|
| <i>Swab type</i> | 2.703 | 0.001 |
| <i>Gill arch</i> | 1.060 | 0.002 |
| <i>Swab type * Gill arch</i> | 0.513 | <u>0.150</u> |

During the first trial in December 2018, when a *post-hoc* Tukey HSD Test was performed to examine the differences between groups, lower *Ct* values were observed with CalgiSwab® swabs (average *Ct* value = 30.73). However, there were no statistical differences between this swab type and the Isohelix® DNA buccal swabs (average *Ct* value = 31.07) ($p = 0.928$). The only statistical differences were found when comparing both swab types to cotton (average *Ct* value = 34.66) ($p = 0.001$) (Figure 2.9). Significant interaction was observed when looking at the gill swabs results alone, or the swab types alone as shown in **Error! Reference source not found.**

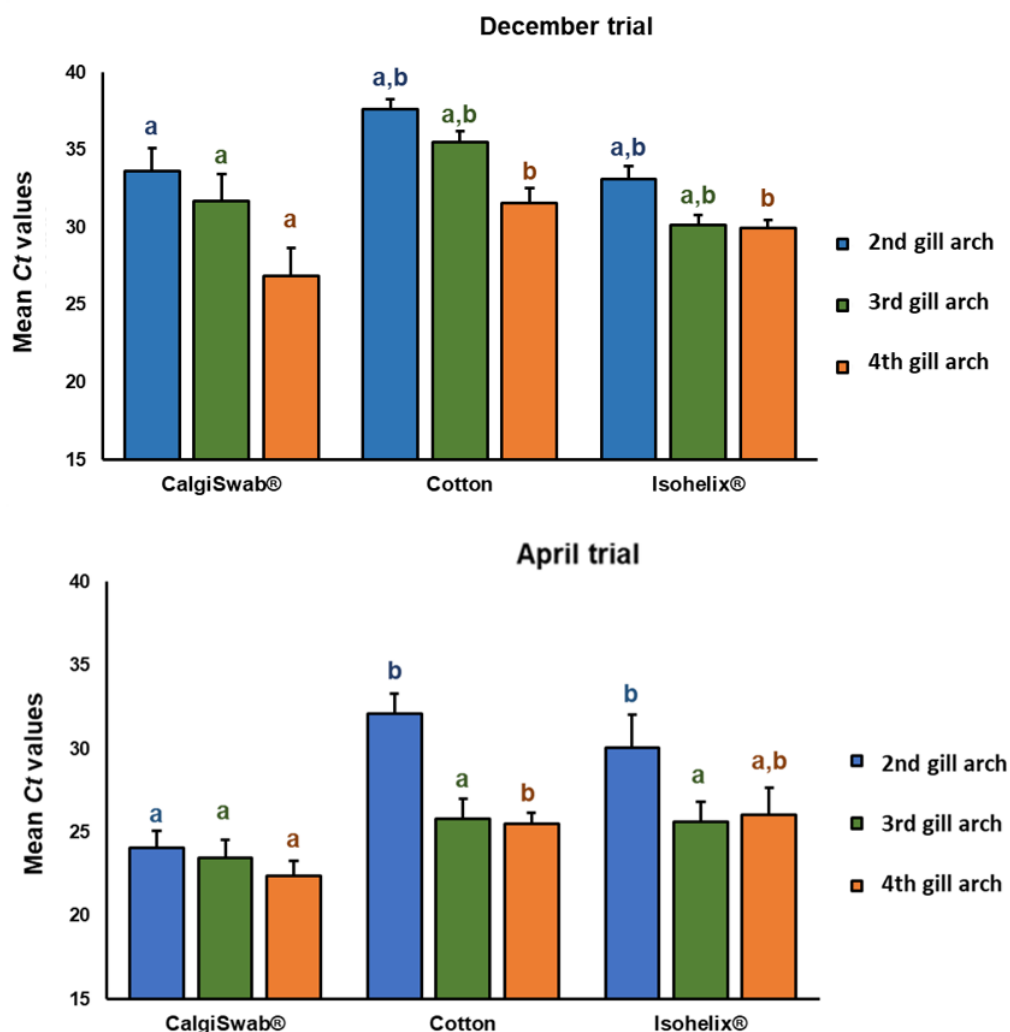


Figure 2.9. Results of the qPCR detection of *N. perurans* 18S rRNA sequences when only gill arches were compared, regardless of the swab type during both trials (December 2018 and April 2019). Bars represent the mean *Ct* values ($n = 30$) (\pm s.e.m). Different letters represent statistically significant differences (*post-hoc* Tukey HSD Test; $p < 0.05$) and same letters mean no statistical differences ($p > 0.05$). Different coloured letters represent statistically significant differences between gill arches ($p < 0.05$).

During the later experiment in April 2019, lower *Ct* values were again found within the CalgiSwab® swabs (Average *Ct* value = 23.80) and statistical differences were found against the other two swab types (Cotton: $p = 0.002$; Isohelix: $p = 0.003$); however, no statistically significant differences between Isohelix® DNA buccal swabs (average *Ct* value = 27.60) and cotton swabs (average *Ct* value = 27.75) ($p = 0.991$) (Figure 2.9).

Although both trials present different results in terms of statistical differences, the tendency across both experiments is that CalgiSwab® *Ct* values were lower than the other two swab types. Thus, this swab material provided the best retrieval and detection of amoebal DNA. Of all the swab types, the least successful was the cotton swab.

Regarding the gill arches sampled, results from both trials showed a tendency of lower *Ct* values across the 3rd and 4th gill arches. During the first trial in December 2018, it was demonstrated that the 4th gill arch presented the lowest *Ct* values (average *Ct* value = 29.44) and statistical differences were found (*post-hoc* Tukey HSD Test; 2nd gill arch vs 4th gill arch: $p < 0.001$; 3rd gill arch vs 4th gill arch: $p = 0.005$; 2nd gill arch vs 3rd gill arch = 0.059). Although the later trial in April 2019 showed no statistical differences between the 3rd and 4th gill arches (*post-hoc* Tukey HSD Test; $p = 0.890$), there were statistical differences when these were compared to the 2nd gill arch (*post-hoc* Tukey HSD Test; 2nd gill arch vs 4th gill arch: $p = 0.014$; 2nd gill arch vs 3rd gill arch: $p = 0.004$). In addition, lower *Ct* values were observed through the 3rd (average *Ct* value = 24.96) and 4th (average *Ct* value = 25.47) gill arches (Figure 2.10).

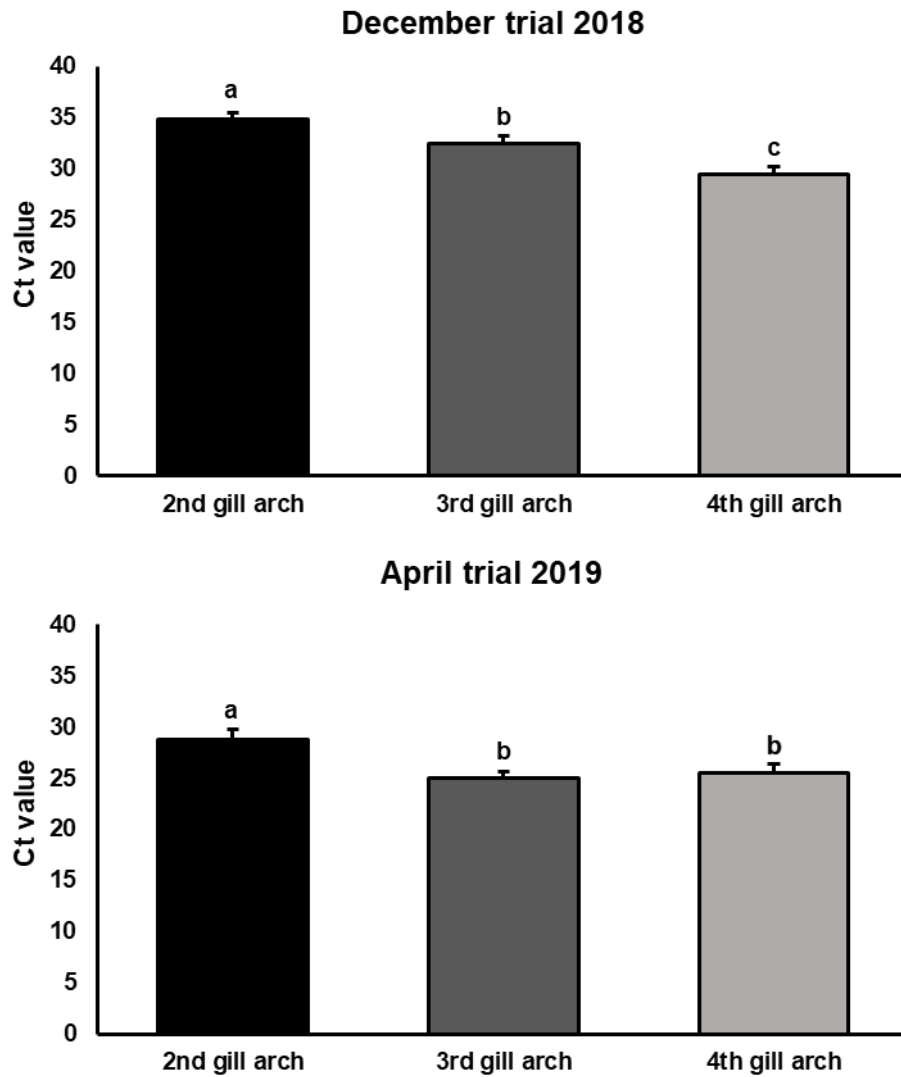


Figure 2.10. Results of the qPCR detection of *N. perurans* 18S rRNA sequences when only gill arches were compared, regardless of the swab type during both trials (December 2018 and April 2019). Bars represent the average Ct values (n= 30) (± s.e.m). Different letters represent statistically significant differences (*post-hoc* Tukey HSD Test; $p < 0.05$) and same letters mean no statistical differences ($p > 0.05$).

Estimates of the statistical correlation between gill score and *Ct* value for different swab types examined for both trials.

As observed in **Error! Reference source not found.**, weak correlation coefficient ($R^2 \leq 0.7$) is observed throughout the use of the different swabs. Trend lines suggest that higher gill score implied the presence of higher amoebic load and therefore lower *Ct* values. However, there is a high variation between both trials. The first trial suggests that this correlation between gill score and *Ct* values is stronger when Isohelix® swabs are used, which corresponds to the trend line indicating that higher gill scores lead to lower *Ct* values. Nevertheless, different results are found in the trial performed in April. Stronger correlation coefficients are present in both Isohelix® and cotton swabs while trend lines do not correlate. Besides these results, a greater number of lower *Ct* values were found when CalgiSwab® swabs were used suggesting them to be capable of enhancing amoeba detection.

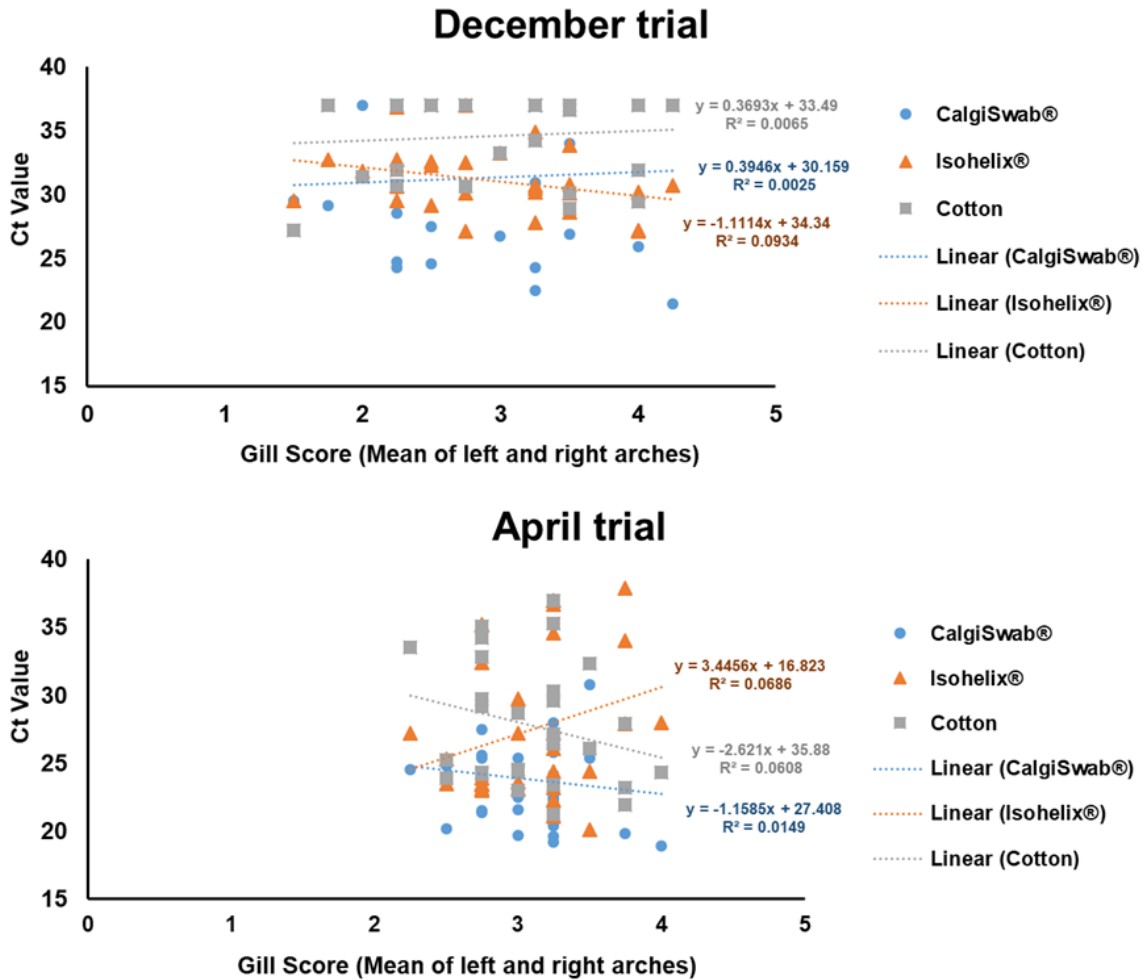


Figure 2.11. Scatterplot showing the relationship between the gill score (mean of left and right arches), measured during both trials in December and April, and the Ct values quantified through qPCR. Different trend line equations show the correspondent correlation coefficient (R^2); n= 30 per swab type.

2.4. Discussion

During this study, the different properties of two swab types used globally in aquaculture (Isohelix® DNA buccal and classic cotton swabs) were compared against CalgiSwab®, a calcium alginate swab used for specialist medical diagnostics. The potential utility of the latter lies in the fact that calcium alginate is wholly soluble in a solution of sodium citrate. The aims of this study were to assess the efficiency of the different swabs for the detection of the amoebic pathogen, *N. perurans*. First, swabs were characterised through *in vitro* testing (spiking and plate swabbing) and second, *in vivo* testing of AGD infected Atlantic salmon was performed. Additionally, gill arches were separately swabbed with the different swabs to determine which of the tested gill arches could potentially demonstrate a higher amoebic load during testing. Whilst previous studies have focused on comparing different PCR techniques for the development of better pathogen quantification using non-lethal sampling methods (Bergmann & Kempter, 2011; Monaghan *et al.*, 2015; Downes *et al.*, 2017), this study focused on the type of swabbing material and location of the gill swabbing. Results showed how CalgiSwab® swabs presented lower *Ct* values during the *in vivo* trials, which suggests that higher quantities of DNA were retrieved using this approach. In addition, depending on the specific gill arch that was swabbed during the sampling of amoebae, differential amoeba loads were detected. These results suggest a significant tendency for higher amoebic load from the 3rd and 4th gill arches in comparison to the 2nd gill arch. Although the sampling of the gills was not assessed over time, higher numbers of amoebae in 3rd and 4th gill arches may suggest that these arches might provide enhanced detection. Therefore, the swab material and swabbed gill had a significant impact in the retrieval of amoebae.

Following method development, prior *in vitro* testing proved that sodium citrate solution did not degrade amoebic DNA or affect the PCR reaction. This solution already showed an advantage in comparison to ethanol, which is flammable for transport and storage. However, this step should have been complemented with the addition of a few more controls (*e.g.* ethanol) and also performing qPCR to fully assess the use of sodium citrate. By testing with conventional PCR and testing across two different time points, only the preservation capacity of this solution was

studied. During the *in vitro* testing, different amoeba concentrations were spiked onto the different swabs. This resulted in both CalgiSwab[®] and cotton swabs presenting an instant water-absorbing capacity which has been studied before in cotton swabs (Thomas *et al.*, 2013). During this study, the recovery efficiency of *Bacillus* spores was suggested to be higher among the cotton swabs due to their major hydrophilicity index. In regard to the other swab material, other studies have investigated the use of calcium alginate dressings on blood coagulation, showing an improvement in the absorbance of blood and other fluids (Kneafsey *et al.*, 1996; Segal, Hunt & Gilding 1998). In contrast, Isohelix[®] swabs were observed to absorb spiked drops containing amoebae more slowly than other swabs. Therefore, Isohelix[®] swabs could perhaps possess a less absorbent surface suggesting that the sample might be more promptly released into the ethanol, resulting in a higher recovery of the amoebae. In contrast, the hydrophilic material of the CalgiSwab[®] and cotton swabs, may have led to a fuller absorption of the low concentration amoeba sample, causing the sample to saturate the swab interior resulting in poorer recovery during agitation as observed in past experiments involving bacteria (Turner *et al.*, 2010). However, further investigation on the properties of this material and the interaction with parasitic species should be conducted in the future to validate this hypothesis. The greatest differences were observed when higher numbers of amoebae were spiked. As expected, higher numbers of spiked amoebae led to lower *Ct* values. The detection of amoebae *in vitro* at lower concentrations from spiked samples was not improved with any of the tested swabs.

The subsequent *in vitro* experiment, in which swabs were used on agar plates containing different amoebic loads, enables clarification of the capacity of the different swabs to successfully collect the sample from agar plates mimicking the *in vivo* testing on the gill. This experiment showed significant differences between the swabs. When the agar plates containing higher numbers of amoebae were swabbed, lower *Ct* values were obtained, as expected. Even though there were no significant differences between the CalgiSwab[®] and Isohelix[®] swabs, both swabs presented lower *Ct* values than the cotton swabs, suggesting an enhanced collection of the amoebae from the substrate. During method development, first trials involved the use of larger volumes of sodium citrate (20 mL) which led to the creation of a mesh of the swab's material and captured cell fragments, leading to a poorer DNA

quantification. Therefore, swabs were introduced into a smaller volume of sodium citrate and manually agitated for a standardised time for all samples. Using this approach, the swab was not fully dissolved, only the outer layer, to which the amoebae were nominally attached, was dissolved. In future experiments, a wider range of amoeba concentrations would provide a better understanding of the potential enhanced sensitivity of the alginate swabs in comparison to the other tested swabs.

Whilst helpful in refining methodology, these *in vitro* models, were not, however, realistic. During field sampling, biological fluids are commonly found within clinical samples. In the case of *N. perurans*, due to the high mucus secretion following an AGD infection (Roberts & Powell, 2003; Vincent, Morrison & Nowak, 2006; Valdenegro-Vega *et al.*, 2014), these complex matrices can interact with the physical or chemical properties of the swab materials. Specifically, mucins have been considered to reduce non-specific binding of protein and can deter negatively charged molecules, like DNA (Hollingsworth & Swanson, 2004). During this study, a tendency for lower *Ct* values was found with the CalgiSwab[®] swabs, but it was not always significant. However, the swabbing of different gill arches showed an interesting trend. The second gill arch presented higher *Ct* values in both experiments and with the use of the different swabs meaning that a lower number of amoebae are presumably present in the second gill arch. In contrast, the third and fourth gill arches offered a better detection of amoebae, presumably due to the higher numbers of parasites in these gill arches.

The common practice of examining the 2nd gill arch when sampling for pathogens follows from the frequent observation that this arch is the preferred site for many gill-inhabiting parasites *e.g.* the copepod *Ergasilus sarsi* (Kilian & Avenant-Oldewage, 2013). One of the principal determining factors for this is the water current over the gill surfaces which influences the available attachment surface, level of oxygenation and potential for dispersion of disseminules (Suydam, 1971; Hanek & Fernando, 1978; Turgut, Shinn & Wootten, 2006; Kilian & Avenant-Oldewage, 2013, Crafford, Luus-Powell & Avenant-Oldewage, 2014). Hence many gill pathogens tend to colonise the areas of the gill where there is more water-flow (*e.g.*, first and second gill arches) (Llewellyn, 1956; Davey, 1980; Dzika, 1999; Chapman *et al.*, 2000; Matejusová *et al.*, 2003). These factors may not, however, hold true for *N. perurans*,

which, in addition to gaining protection within the host mucus layer, has been suggested to have wide environmental tolerances (Crosbie *et al.* 2012), including conditions found in marine sediments, that may allow it to thrive under conditions of lower oxygen and flow.

In the context of the aquaculture industry, the findings of the presented research can potentially improve methods employed for routine sampling. While visiting fish farms for this experimental study, the general sampling regime consisted of the gill swabbing of all the gill arches. However, by sampling only third or fourth gill arches, lower relative *Ct* values within this area were found. Therefore, the sampling of a smaller region of the gills could reduce its irritation. When looking at the correlation between gill score and *Ct* values, although correlations were not strong, trend lines suggested that higher gill scores lead to lower *Ct* values detected through qPCR. The fact that these correlations are not higher, however, provides a wider caveat, supporting previous suggestions that the number of amoebae present does not directly reflect the visible pathology (Adams & Nowak, 2001). In part, this may result from the fact that pathology may reflect historical events, *e.g.* tissue scarring, not the current location / activity of amoebae. Some studies have even reported the presence of *N. perurans* where gross pathology was not detected (Zilberg & Munday, 2000; Dyková & Novoa, 2001; Adams & Nowak, 2004a) and have also demonstrated less amoebae in sampled areas with higher visible pathology. The weak correlation between higher gill scores and lower *Ct* scores observed in this study warrant further investigation, as they clearly have a bearing on diagnostic outcomes, sensitivity and interpretation.

Conclusions

In conclusion, although this experimental chapter did not show consistently significant differences between different swab materials, there is a trend showing a higher sensitivity with the use of CalgiSwab® and Isohelix®, implicating an effect of the swab material in the recovery of amoebae. Cotton consistently proved the least effective swab material for the detection of amoebae across all experiments. However, further work needs to be performed in order to study this material in depth. Regarding the gill arch swabbing, it can be concluded that the gill or gill area that is chosen for swabbing during sampling, has an impact on the success of detecting

parasites. This makes the third and fourth gill arches more appropriate tissue regions for detecting *N. perurans* and therefore swabbing of this region. Ultimately, the further study of this calcium alginate material and consideration of the swabbing of less gill surface could potentially translate to a timely diagnosis of AGD and could potentially lead to more successful treatment outcomes. Additionally, restricting the number of gills sampled during non-lethal sampling could reduce gill irritation, minimising the exposure of fish to parallel infections or environmental antigens. However, the comparison with the sampling of all gill arches and only the fourth gill arch should be approached in the future to really consider an enhanced detection of amoebae.

Chapter 3 : Methacarn preserves mucus integrity and improves visualisation of amoebae in gills of Atlantic salmon (*Salmo salar* L.)

3.1. Introduction

Amoebic gill disease (AGD) is a major threat that has had significant economic impact on the Atlantic salmon (*Salmo salar* L.) aquaculture industry. In the context of gill surface mucus, gross signs of the disease include raised, multifocal white mucoid patches on the gills (Adams & Nowak, 2003). Investigations into the pathogenesis of AGD, particularly in the early stages of the disease, can be hampered by loss of the mucous coat and its pathogen load during fixation and therefore the work described here seeks to improve preservation and visualisation of these features.

Fish mucus provides a protective barrier between the organism and the external environment (Shephard, 1994). Components of the gill mucus are similar to those found in skin mucus such as antimicrobial peptides (Cole *et al.*, 2000), enzymes *i.e.* lysozyme (Murray & Fletcher, 1976; Costa *et al.*, 2011), antibodies (both IgM and IgT) (Xu *et al.*, 2013), mucins (neutral, acid and basic) and other glycoproteins such as glycosaminoglycans (Murray & Fletcher, 1976). It can serve as a barrier that restricts access of microorganisms to the host, a protective matrix for microorganisms and a rich feeding substrate for a range of obligate, facultative and opportunistic pathogens. Therefore, mucus plays a key part in mediating the interaction between potential pathogens and the host and can thus play an important role in disease development.

When choosing the different fixatives, two different types were considered, Davidson's solution and Methacarn solution. Both fixatives present different advantages. The first fixative belongs to the category of conventional aqueous fixatives, which, whilst providing excellent cytological preservation, often remove the overlying mucus layers (Mays *et al.*, 1984; Leist *et al.*, 1986; Lee *et al.*, 1995). In the context of AGD, Davidson's solution was firstly used in Cadoret *et al.* (2013) for the examination of *N. perurans* providing a good preservation of the tissue. Later on, Chalmers *et al.* (2017) also used this aqueous based fixative for the examination of mucous cells on the gill epithelium. However, these fixatives failed to preserve the

mucus layer. Using non-aqueous or other specialised fixatives, can therefore offer significant advantages in increasing understanding of target tissue's structure and function and its relationship with its mucous surface. The search for improved preservation of mucus layers by a variety of techniques using solvent-based fixatives when compared with aqueous based fixatives has been well described in mammals e.g. an improved retention of mucus has been demonstrated in bovine and rat trachea using light and electron microscopy (Sims *et al.*, 1991). Also, in rat trachea and various mucosal surfaces in pig (Allan-Wojtas *et al.*, 1997). However, there is a paucity of work focusing on the adaptation of these methods, previously developed for mammalian tissue, for use in observing adherent mucus on fixed mucosal tissues in fish. In the past, Methacarn solution had been investigated for mucus visualisation (Johansson *et al.*, 2012; Wlodarska *et al.*, 2015) as well as conserving mucus thickness. The chemical fixation through this solution provided less loss of mucus thickness. Additionally, it has been recently used in the study by Röhe *et al.*, (2018) to study the mucus layer on the pig's intestine epithelium. Even though the mucus was preserved in patches and not showing a clear thin layer across the pig's epithelium, the nature of this fixative was interesting enough to explore its use in fish.

Combined with the above techniques, some studies implemented the addition of Alcian blue 0.5% (w/v) in different fixatives, *i.e.* aqueous buffered glutaraldehyde (Sims *et al.*, 1997) for the characterisation of the composition and thickness of tracheal mucus in rats. In fish, Alcian blue has also been used as an addition to routine fixatives for both light and electron microscopy in the gills of rainbow trout (Powell *et al.*, 1992). Other non-fish studies have used Alcian blue as a colorimetric assay for mucous glycoproteins (Hall *et al.*, 1980) or for the characterisation of sialylated, sulphated and mixed mucins (Meyerholz *et al.*, 2009).

It has already been established that a simple, rapid and inexpensive technique for the preservation of the mucus layer for routine histology of gills would be useful for disease diagnostic use in fish (Powell *et al.*, 1992). A number of studies have attempted to optimise mucus stabilisation in teleost tissue for microscopy e.g. oesophageal epithelium in the eel (*Anguilla anguilla*) (Humbert *et al.*, 1984) through scanning electron microscopy (SEM) finding different densities in the layers of the anterior and posterior oesophageal epithelium and, similarly to that study, the intestinal tract of the goldfish (*Carassius auratus* (Linnaeus, 1758)) was also

investigated to characterise elements of the intestinal epithelium (Caceci, 1984) using the same technique. Other studies have investigated different fixatives in order to assess the biofilms and surface-associated pathogens often embedded within the skin mucus of Rainbow trout (*Onchorynchus mykiss*) (Speare & Mirsalimi, 1992; Sanchez *et al.*, 1997) and the gill mucus of Rainbow trout (Handy & Eddy, 1991; Powell *et al.* 1992; Powell *et al.*, 1994).

In this chapter, research undertaken to optimise fixation methods is described, particularly in the context of investigating mucus stabilisation for gills. A number of different fixatives are compared to standard fixation approaches, with the aim of enhancing our understanding of parasite interactions with gill mucus during an AGD infection. It is envisaged that the development of practical techniques for mucus preservation that are also amenable to standard histopathological staining, visualisation and interpretation, would also be of benefit not just to studies of AGD pathogenesis and amoeba-host interaction, but also serve more generally for observing surface associated pathogens in fish. In particular, such an approach might help to elucidate relationships affecting mucus secretion in other gill-associated conditions, where details of boundary layer / surface interactions are often obscured due to a loss of mucus coating using generic fixation and processing techniques.

3.2. Materials and Methods

3.2.1. Fish and sampling

All sampling for the present study was carried out at the MERL under ethics application reference number AWERB/1617/173/New ASPA between May and July 2017. The facility was supplied with flow-through seawater (35 ‰), filtered at 100 µm. Fish were maintained under ambient temperature (min: 11 °C, max 13 °C) and fed with commercial salmon pellets (Inicio Plus, BioMar, UK) equivalent to 1% of their body weight per day.

In order to compare the effect of different fixatives on mucus preservation in the gill, samples were taken from six Atlantic salmon (167.7 ± 21.4 (s.d.) g and 25.6 ± 1.6 (s.d.) cm body weight and fork length, respectively), taken from a population of stock fish

held in a 13000 L tank. For sampling, fish were euthanised by lethal anaesthesia using MS-222 (100 mg/L) (Sigma Aldrich, UK) followed by destruction of the brain, according to Home Office Schedule 1 procedures. Gill pathology was visually assessed and scored for gill lesion severity according to Taylor *et al.* (2009). Examined fish were found to have a mean gill score of 0.5-1. The third and fourth left gill arches were carefully excised, briefly rinsed in PBS, cut into equal sized parts and fixed in each of the five fixatives described above.

In order to examine the relationship between amoebae and mucus during an AGD infection, a further five fish (324.2 ± 35.6 g and 30.5 ± 12.2 cm body weight and fork length, respectively) were sampled from a 1 m diameter tank (400 L) at the termination of an AGD co-habitation challenge experiment (previously described in Chapter 2, Section 2.2.5.1). Sampling was also carried out at MERL under ethics application reference number AWERB/1718/038/New ASPA between October 2017 and April 2018, part of a project carried out by Dr. Sophie Fridman. Fish were euthanised by Schedule 1 methods as described above and gills similarly visually assessed and scored for gill lesion severity. Gills from that study were found to have a mean gill score range of 2-3.5. For these fish, the entire second gill arch was removed and fixed in MS, which had proven to be the best fixative for the preservation of gill mucus (see results).

Experimental procedures were all approved by the Animal Welfare and Ethical Review Body (AWERB) of the University of Stirling and were conducted under UK Government Home Office project licence 60/4189.

3.2.2. Histology processing

Whole third and fourth left gill arches were dissected out, cut into five pieces and each piece fixed in 1:10 tissue fixative in one of the following: 10% Neutral buffered formalin (NBF), Modified Davidson's solution (MDS), methacarn solution (MS), Modified Davidson's supplemented with 2% (w/v) Alcian Blue (MDAB), and methacarn solution supplemented with 2% (w/v) Alcian Blue (MSAB) all prepared as described in **Error! Reference source not found.**, for histopathological analysis. All fixatives were freshly prepared immediately before use.

Fixation of all the samples was followed by blocking the gill tissues in cassettes. Samples fixed in NBF and Davidson's were placed in a Shandon Citadel 2000

automated tissue processor (Thermo Scientific, Epsom, Surrey, UK) in order to accomplish the dehydration through a graded alcohol series (30%, 50%, 70%, 90% and 100% ethanol) followed by clearing over seven baths of xylene and finally infiltration with paraffin wax at 60 °C (Histowax, Sweden). Alternatively, tissues fixed in methacarn were processed manually as follows: 2 x 30 min in 100% methanol and 2 x 20 min in 100% ethanol baths; clearing was performed for 2 x 15 min in xylene baths. Last, all tissues were impregnated with paraffin wax with the Leica EG1160 Histoembedder (Leica Biosystems, Milton Keynes, UK) at 60°C.

For slide preparation, trimming was undertaken using the Thermo Shandon Finesse E Microtome (Leica Biosystems, Milton Keynes, UK) to a thickness of 20 µm until a uniform layer of tissue was exposed; followed by decalcification. Trimmed blocks for all fixatives were left to soak for 1 h in distilled water. All blocks were then dried and chilled face down on a cold plate (5 min) prior to 5 µm sectioning using the Thermo Shandon Finesse E Microtome (Leica Biosystems, Milton Keynes, UK) and disposable metal blades. Sections were spread using a water bath (37°C), placed, 12 to a slide, on glass microscope slides and dried overnight in a drying cabinet (60°C).

Table 3.1. Preparation and maintenance of the distinct fixatives. RT: room temperature.

| Fixative | Preparation | Maintenance |
|--|---|---|
| 10% NBF | One part of formaldehyde ¹ (37-40% stock) and nine parts distilled water | RT |
| Modified Davidson's solution | One part of glacial acetic acid ² , two parts of formaldehyde ¹ (37-40% stock), three parts of 95% ethanol ³ , and three parts of PBS | RT; Tissue transferred to 70% ethanol after 24h |
| Methacarn solution | 60% Absolute methanol ⁴ , 30% chloroform ⁵ , and 10% glacial acetic acid ² | RT |
| Modified Davidson's solution + 2% (w/v) Alcian blue | One part of glacial acetic acid ² , two parts of formaldehyde ¹ (37-40% stock), three parts of 95% ethanol ³ and three parts of PBS + 2% (w/v) Alcian blue | RT; Tissue transferred to 70% ethanol after 24h |
| Methacarn solution + 2% (w/v) Alcian blue | 60% Absolute methanol ⁴ , 30% chloroform ⁵ , and 10% glacial acetic acid ² + 2% (w/v) Alcian blue | RT |

¹Formaldehyde (Product number: 10160052; Fisher Scientific); ²Glacial acetic acid (Product number: 10394970; Fisher Scientific); ³ Absolute ethanol (Product number: 10437341; Fisher Scientific); ⁴Methanol (Product number 10675112; Fisher Scientific); ⁵Chloroform (Product number: 10102190; Fisher Scientific); ⁶Alcian Blue 8GX (Product number: A5268; Sigma Aldrich).

3.2.3. Staining for mucus layer evaluation

All sections taken from NBF, MDS and MS fixed samples were stained using three types of stain. First, a haematoxylin and eosin staining protocol were performed as a control staining. Initially, samples were de-waxed through a 2-step xylene bath lasting 3 min and 2 min respectively, after which they were subsequently immersed in absolute alcohol for 2 min, methylated spirit for 1 ½ min and rinsed in running tap water for 30 s to 1 min. Sections were then immersed in Mayer's Haematoxylin (2 g Haematoxylin, 2 g Citric Acid, 0.4 g Sodium Iodate, 100 g Chloral hydrate, 100 g Potassium alum dissolved in 2 L of ddH₂O) for 5 min, followed by another rinse in running tap water for 30 s to 1 min. Sections were then quickly dipped three times in 1% acid alcohol (1% hydrochloric acid (HCl 37%) in ethanol (70%)) and rinsed in running tap water for 30 s to 1 min. Samples were then placed in eosin (eosin Y 1 g dissolved in 1 L of 70% Ethanol and 5 mL of Glacial acetic acid) for 5 min and quickly washed in running tap water. Then, sections were briefly immersed for 30 s in methylated spirit. Dehydration was performed through a 2-step absolute alcohol bath, 2 min and 1 ½ min respectively.

Second, for the gill tissues that already contained 2% Alcian blue, Periodic Acid Schiff stain (PAS) protocol was performed as a further staining step. The same steps were followed as described above until the first wash in running tap water. After this, sections were oxidised in 1% periodic acid solution (1 g periodic acid in 100 mL of ddH₂O) for 5 min, then washed in running tap water for 2 min and placed for 20 min in Schiff's reagent (Product number: J62171.AP, VWR International) at room temperature. Sections were then washed again in running tap water for 1 min, counterstained in Mayer's Haematoxylin for 5 min, washed again in tap water for 1 min and then incubated for an additional minute in Scott's tap water substitute (sodium bicarbonate 3.5 g, magnesium sulphate 20 g, dissolved in 1 L of tap water) and finally washed for 1 min in running tap water. Sections were then dehydrated in 2 steps of absolute ethanol (by quickly dipping). Lastly, clearing was carried out for both protocols in a xylene bath for 5 min followed by mounting of the slides using Pertex. Slides were then left overnight to allow xylene to evaporate.

Finally, all gill tissues whose fixatives did not contain 2% Alcian blue were stained using a combined Alcian blue-PAS technique (Mowry, 1956; Chalmers *et al.*, 2017). Briefly, sections were de-waxed and rehydrated as previously described and immersed in Alcian blue solution (pH 2.5) for 5 min. The residual stain was then removed by washing in water and sections were then oxidized in 1% (aq) periodic acid (5 min), washed (5 min) and immersed in Schiff's reagent (20 min). Slides were then processed further as described above following Schiff's exposure.

3.2.4. Comparison of the different fixatives for semi-quantitative analysis of mucus and mucous cells

Tangentially embedded and sectioned gills were assessed in order to quantify the presence of mucous cells and inter-lamellar mucus. As the mucus did not present as a uniform layer over the lamellae and inter-lamellar area (see **Error! Reference source not found.A&B**), the semi-quantification of mucus was achieved through microscopic image acquisition of areas (~1 mm²) of well-preserved gill sections, counting the number of times mucus traces were not evident (**Error! Reference source not found.A**) or evident (**Error! Reference source not found.B**). Twelve randomised fields of view of twenty inter-secondary lamellar spaces in the mid-section of the primary lamella (n=6 control fish) were assessed, using one section

per fish. Only one section was used per fish due to the small size of the gill samples, therefore more randomised fields were counted in order to assess inter variation within different fish rather than intra variation within different sections of the fish. Counts and measurements were carried out on filaments which had equal length lamellae on both sides and cartilage in the centre, to ensure comparability of sections.

For the quantification of mucous cells, as above, twelve randomised fields of view of twenty inter-secondary lamellar spaces in the mid-section of the primary lamella (n=6 control fish) were assessed, one section per fish. The total number of mucous cells were counted. However, only gills that had been fixed in NBF, modified Davidson's solution and methacarn were assessed, since the addition of Alcian blue in the fixatives presented an overall blue colouration, making it difficult to specifically differentiate mucous cells.

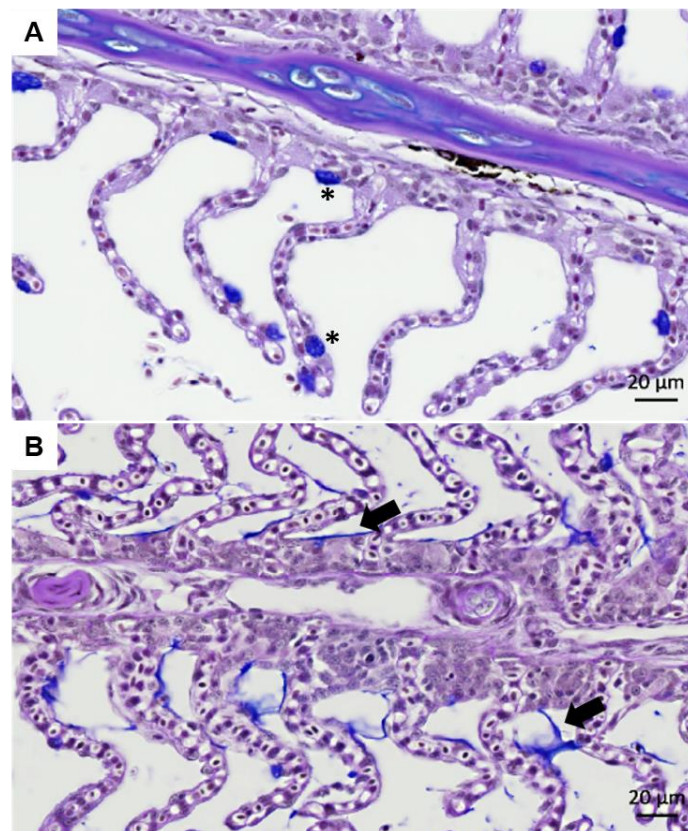


Figure 3.1. Method of semi-quantitative analysis for mucus and mucous cell quantification. Mucus was quantified by counting the absence (A) or presence (B, arrows) of mucus traces (blue) in twenty inter-lamellar spaces from twelve random mid-sections of the primary lamellae. This method was used for all the fixation and staining techniques (e.g. A. NBF fixation with AB/PAS staining. B. Methacarn fixation with AB/PAS staining). For the mucous cell counts, the same method was

performed by counting the presence (asterisk) of mucous cells in twenty inter-lamellar spaces from twelve random mid-sections of the primary lamellae. Images taken by slide scanner, Axio Scan.Z1 (ZEISS, Cambridge, UK).

3.2.5. Confirmation of mucus presence with fluorescent lectin labelling

Samples fixed with methacarn were prepared following the haematoxylin and eosin stain protocol described in Section 3.2.3. Slides were kept overnight in the 55°C oven. Prior to the labelling, lectin wash buffer (LWB; 50 mM Tris, 150mM NaCl, 2mM MgCl₂, CaCl₂) was prepared in 1 L of dH₂O and full dissolution of the reagents achieved through stirring for 15-20 min with a magnetic stirrer. This buffer was used as a control (lectin free). Slides were taken from 55°C oven and were de-waxed manually into two changes of xylene for 3 min each and a following dehydration step was performed by immersing sections in 100% and 70% ethanol for 2 min each step. A final wash in dH₂O was performed for 1 min, keeping them immersed until labelled by lectins. Prior to the labelling, a circle was drawn around each section using an ImmEdge hydrophobic pen (Vector labs, p/n H-4000) to keep the lectin/buffer in place. They were then labelled with two types of rhodamine-labelled lectin conjugates from the rhodamine lectin kit I (Vector Laboratories, Burlingame, CA, U.S.A) (Table 3.2) diluted with LWB to a final concentration of 30 µg mL⁻¹, using a slightly higher concentration than that usually recommended (5-20 µg mL⁻¹) (Hsu & Mahal, 2006) according to previous in-house experience. A volume of 200 µL of lectin solution was pipetted on to the sections and incubated in a dark chamber at RT for 2 h. Final washing of the sections was performed three times after incubation with LWB for 5 min each time. One control slide was treated the same but only LWB was applied, instead of lectin dilutions. For the counterstaining, slides were firstly washed with PBS and then a 300nM amount of DAPI solution was added to the slides, incubated for 3 min in the dark and then finally mounted in VECTASHIELD® (mounting medium for fluorescence with DAPI from Vector Laboratories, Burlingame, CA, U.S.A), coverslipped, and sealed with nail polish for long-term storage. Prior to the viewing of the slides, they were maintained in the dark for 2 h at 4°C. Slides were examined using an Arcturus XT Laser Capture Microdissection System (Applied Biosystems, Life technologies, USA) or a TCS SP2 AOBS Laser Scanning Confocal Microscope (Leica Microsystems, Wetzlar, Germany).

Table 3.2. Lectins used and their specificity to glycoproteins present in gill mucus.

| Lectin | Specificity | Reference |
|--|---|-----------------------------|
| WGA (<i>Triticum vulgare</i> (wheat germ)) | N-acetylglucosamine; Acetylneuraminic acid | Díaz <i>et al.</i> , (2010) |
| DBA (<i>Dolichos biflorus</i> agglutinin) | N-acetylgalactosamine | |

3.2.6. Statistical analysis

All the results obtained from the semi-quantitative analysis were exported to IBM SPSS statistical analysis software (v23, IBM Corporation) and were processed and tested to determine significant differences of mucus and mucous cell counts in the variety of fixatives. A Shapiro-Wilk test was performed on the data in order to verify normality, followed by Levene's test to determine homogeneity of variance. Subsequently a one-way ANOVA (analysis of variance) was performed on the data, in order to examine the significance of differences between mean mucous / mucus cell values for different fixatives, and *post-hoc* Tukey HSD test (honestly significance difference) was carried out to assess if the groups were significantly different from each other.

3.3. Results

3.3.1. Evaluation of different fixatives for the conservation of gill mucus

Overall both the aqueous and the solvent-based fixatives resulted in good maintenance of gill architecture (**Error! Reference source not found.**). The presence of a mucous coating or mucus secretions from mucous cells was not evident in the branchial tissue fixed in neutral buffered formalin (NBF) (Figure 3.2A&B), although the mucous cells were visible due to the PAS/AB staining. There was, however, some evidence of patchy/diffuse and weakly stained interlamellar mucus in gills fixed with modified Davidson's solution (Figure 3.2C–F), this being slightly more extensive in tissues fixed with modified Davidson's solution with 2% (w/v) Alcian blue, where some apparent secretions from the mucous cells were preserved (Figure 3.2E&F).

With the non-aqueous based fixative an improved stabilisation/preservation of mucus was clearly evident. Branchial tissue fixed in methacarn solution displayed mucus as a thin attached layer on both interlamellar spaces and on secondary lamellae with mucus extending from mucous cells to form a 'mesh' between the secondary lamellae (**Error! Reference source not found.2G&H**) which can also be seen in transverse sections (**Error! Reference source not found.A&B**). Fixation in methacarn solution with 2% (w/v) Alcian blue did not improve preservation of mucus, and the mucous layer was patchy and seemed to lift from the underlying tissue, forming more compact streaks of dark blue stained mucus between the secondary lamellae (**Error! Reference source not found.2I&J**). Images taken by slide scanner, Axio Scan.Z1 (ZEISS, Cambridge, UK).

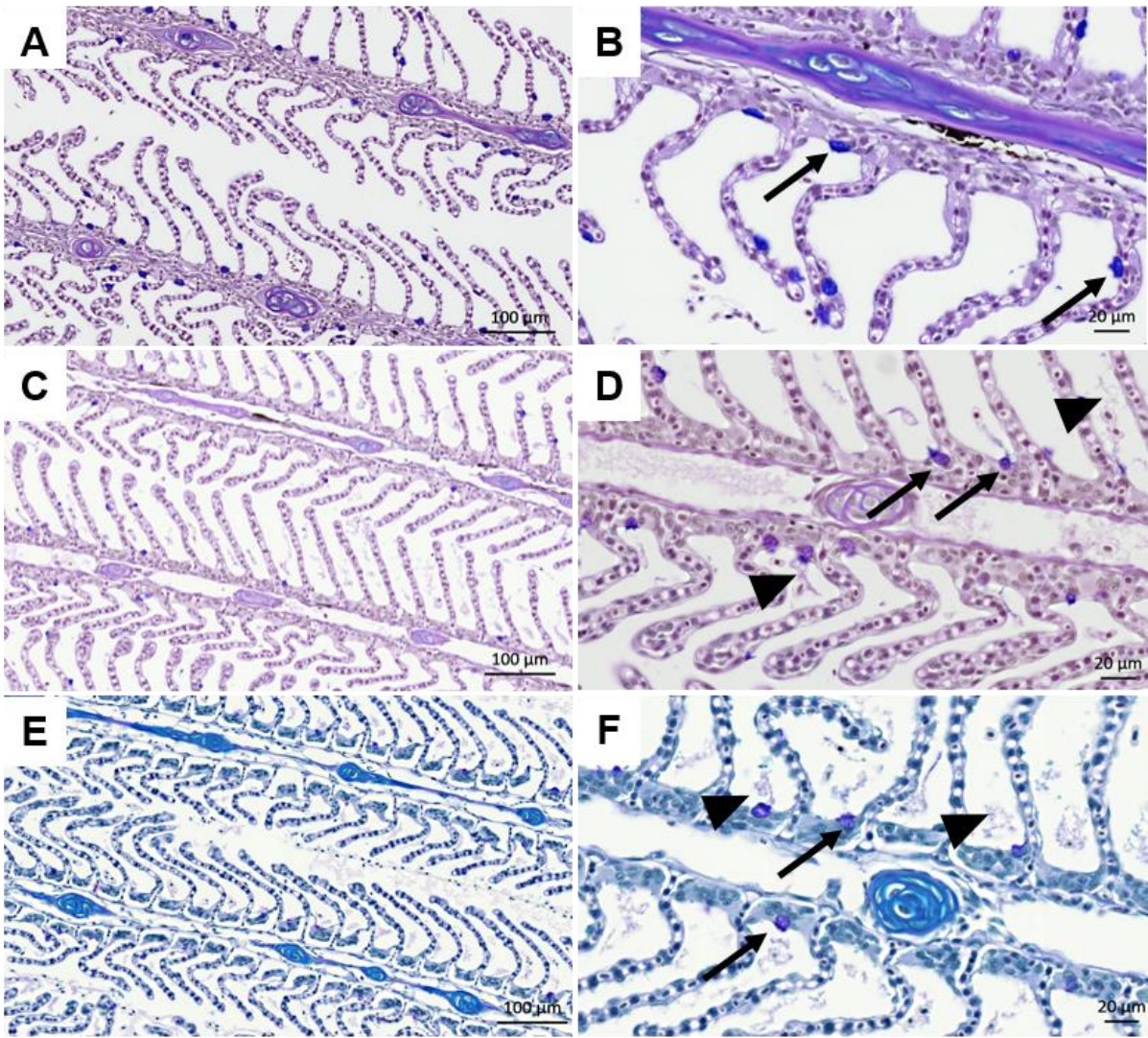


Figure 3.2. Evaluation of aqueous-based and solvent-based fixatives to preserve mucus layer in Atlantic salmon gills. A) Lower magnification and B) higher magnification of gill sample fixed with 10% neutral buffered formalin (10% NBF) stained with Alcian blue and Periodic acid-Schiff's reagent (AB/PAS). Note that there is no evidence of overlying mucus on epithelial layers or associated secretions from mucous cells (black arrow); C) lower magnification and D) higher magnification of gill sample fixed with modified Davidson's solution, stained with AB/PAS. There is some evidence of patchy preservation of mucus between the secondary lamellae (arrow heads) with some mucus secretions from mucous cells (black arrows); E) lower magnification and F) higher magnification of gill sample fixed with modified Davidson's and 2% Alcian blue (AB) solution stained with PAS. Note increased amount of mucus evident between lamellae (arrow heads) and some mucus secretions from mucous cells (black arrows).

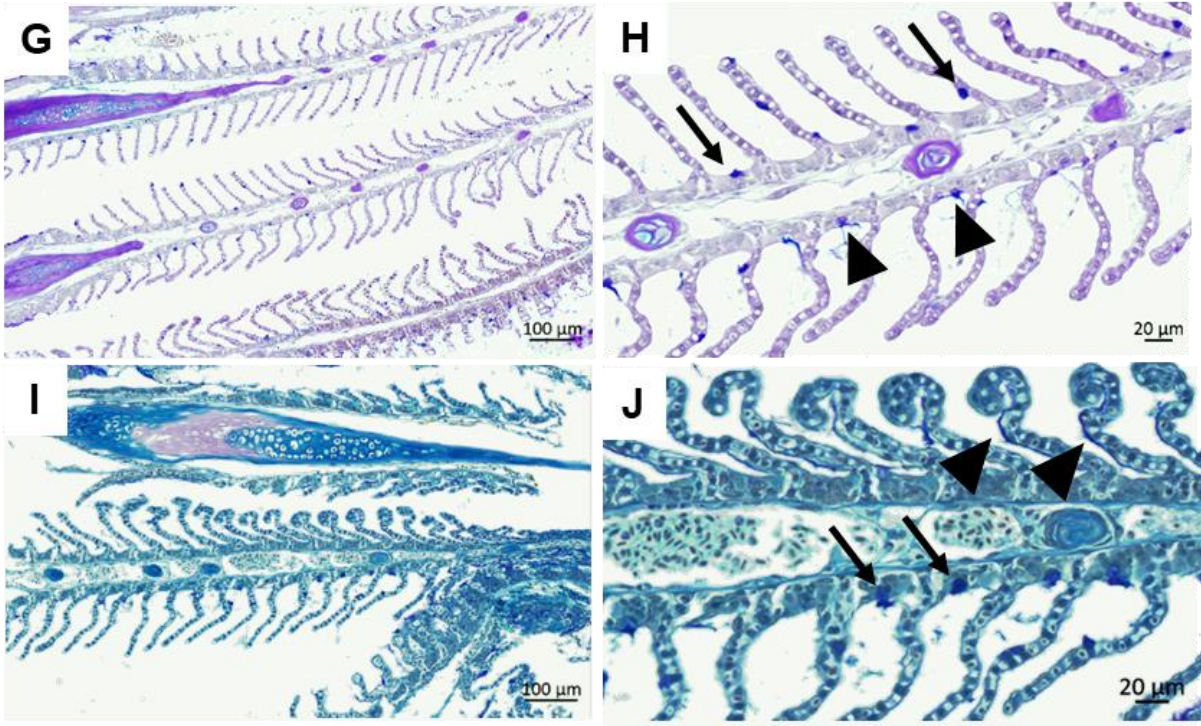


Figure 3.2. (cont.) Evaluation of aqueous-based and solvent-based fixatives to preserve mucus layer in Atlantic salmon gills. G) lower magnification and H) higher magnification of gill sample fixed with Methacarn solution stained with 2% AB, stained with PAS showing presence of mucus as a thin attached layer on both interlamellar spaces and mucus being secreted from mucous cells (arrow heads) and on secondary lamellae (black arrows), I) lower magnification and J) higher magnification of gill sample fixed with Methacarn solution and 2% AB, stained with Periodic acid-Schiff's reagent (PAS). Evidence of mucus as a thin attached layer on interlamellar spaces (arrow heads) and also presence of mucous cells (black arrows).

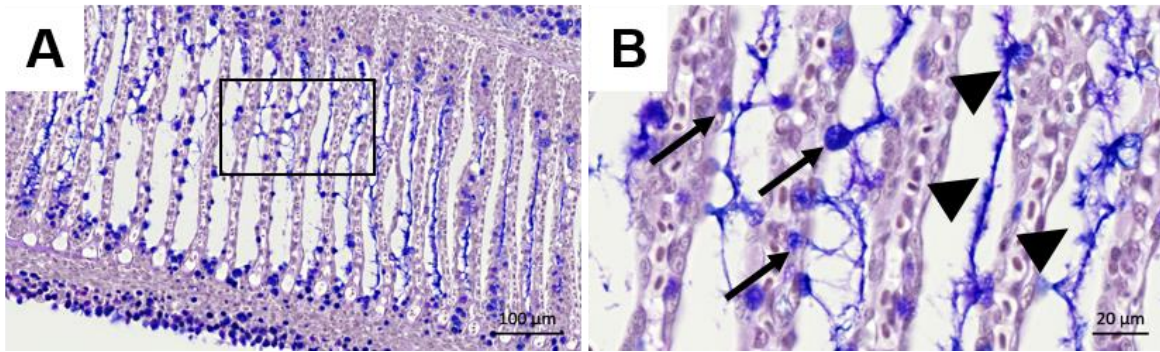


Figure 3.3. Transverse sections of methacarn fixed Atlantic salmon gills stained with Alcian blue and Periodic acid-Schiff reagent (AB/PAS). A) Transverse section of gill from Atlantic salmon showing interlamellar mucus) and B) higher magnification of boxed area from A) with mucous cells (black arrows) and mucus layer (arrowheads).

3.3.2. Semi-quantitative analysis study for mucus and mucous cells

Semi-quantitative analysis of the presence of mucus traces in the interlamellar regions demonstrated that there was a significant difference in the preservation of the mucus between the different fixatives. Methacarn and methacarn with 2% Alcian blue showed a significantly higher incidence of mucus traces (one-way ANOVA and subsequent post-hoc Tukey HSD test; $p=0.0010053$) when compared to the aqueous fixatives (**Error! Reference source not found.A**). The fixatives containing Alcian blue did not enable mucous cells to be distinguished due to the overall blue coloration of the tissue. No significant differences ($p>0.05$) were found in the apparent mucous cell numbers between the examined fixatives (**Error! Reference source not found.B**). Mucus results were presented as proportions of the interlamellar spaces containing mucus.

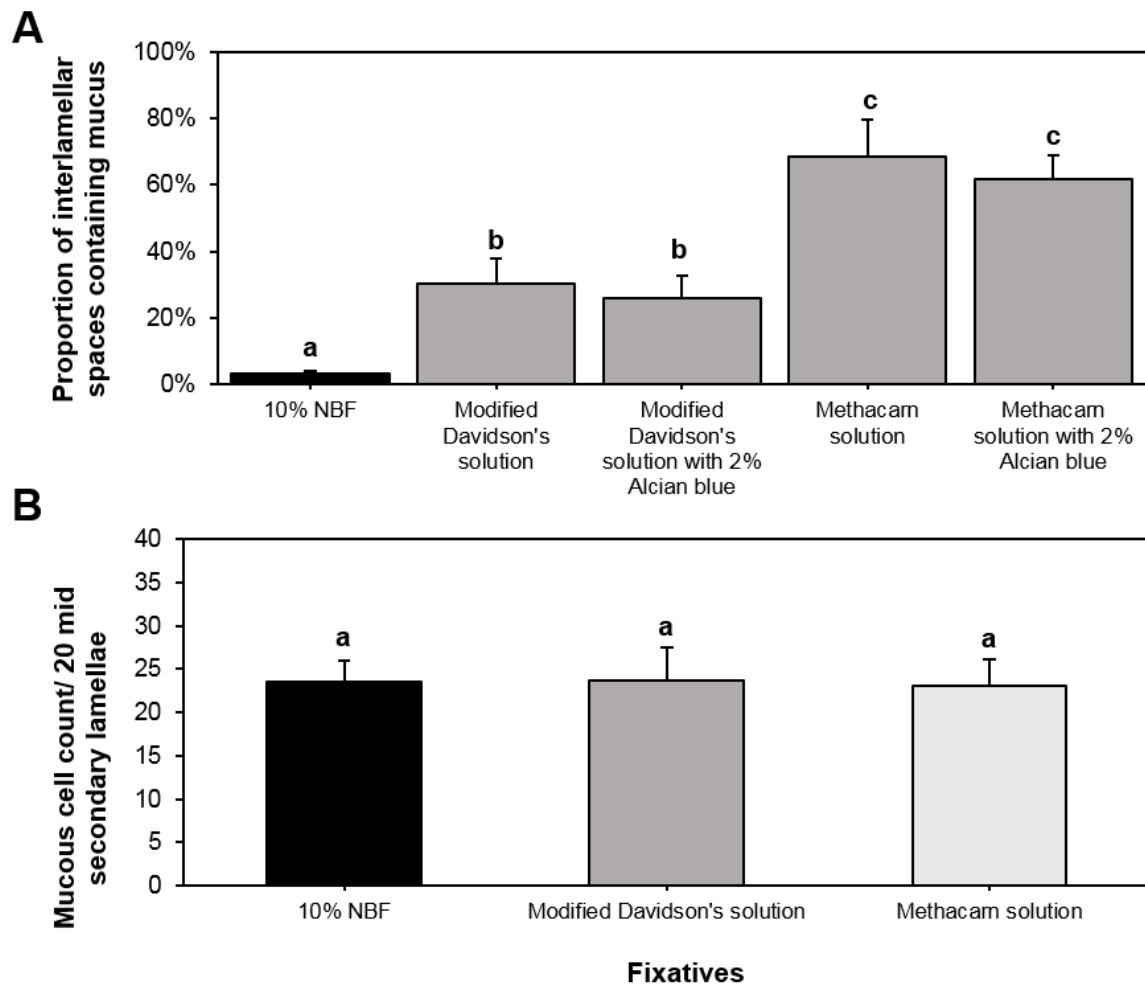


Figure 3.4. Effects of different fixation methods on presence of mucus and mucous cells on Atlantic salmon gills. A) Graph showing the proportion of examined interlamellar spaces showing mucus traces and B) graph showing number of mucous cells in gill fixed with 10% NBF, modified Davidson's solution and methacarn solution. Different superscript letters indicate significant differences between fixatives (mean \pm s.e.m, $n = 6$ control fish, 12 random fields of 20 interlamellar spaces; ANOVA test: $p < 0.05$).

3.3.3. Examination of the relationship between amoebae and mucus during an AGD infection

Sections of gills from AGD-infected Atlantic salmon that had been fixed in methacarn were stained with H&E (Figure 3.5. A&C) and AB/PAS (Figure 3.5. B&D). The AB/PAS stain aided differentiation between acid and neutral polysaccharides (Figure 3.5. B&D), highlighted amoebae with Alcian blue inclusions, and allowed observation of the preserved mucus (Figure 3.5. B&D). Hyperplastic lesions were visible with both stains, in addition to evident lamellar fusion that led to lacuna formation (lac) (Fig. 3.5A&B). These formations have been studied in different studies in which Atlantic salmon was infected with AGD (Rodger *et al.*, 2011; Chalmers *et al.*, 2017). Images taken by slide scanner, Axio Scan.Z1 (ZEISS, Cambridge, UK).

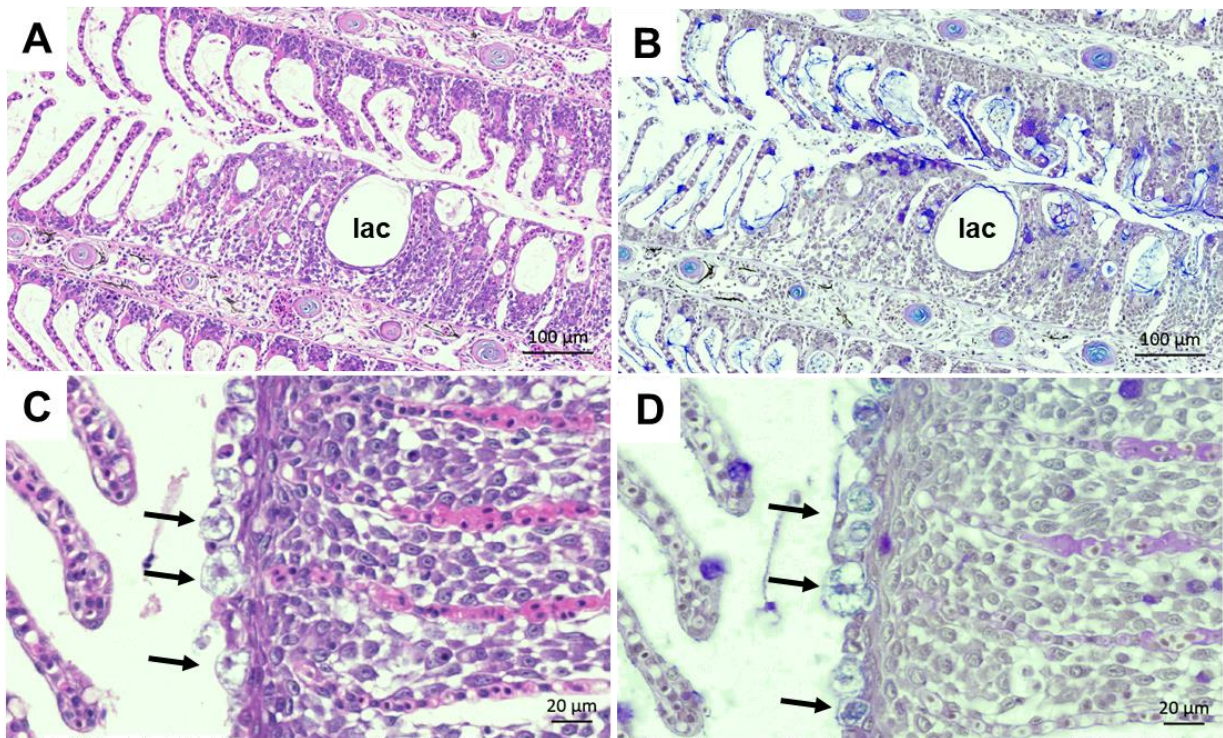


Figure 3.5. Comparison of histological stains of methacarn fixed Atlantic salmon gill infected with AGD (gill score 2.5) with H&E and AB/PAS staining. A) & B) Epithelial hyperplastic lesions with lacuna formation (lac) from AGD-infected gill stained with A) H&E stain and B) Alcian blue and Periodic acid-Schiff reagent (AB/PAS); C) & D) advanced hyperplastic lesions with associated amoeba trophozoites (arrows) stained with C) routine H&E stain and D) Alcian blue and Periodic acid-Schiff reagent (AB/PAS). Amoebae trophozoites (arrows) between lacuna formation (lac) in a hyperplastic lamella.

Amoebae were visible at the periphery of the hyperplastic tissue (**Error! Reference source not found.A–C**) often embedded within the mucus layer (Figure 3.6A) and in close association with mucous cells (**Error! Reference source not found.C**). **Error! Reference source not found.D** shows the presence of a single trophozoite between a lacuna formation.

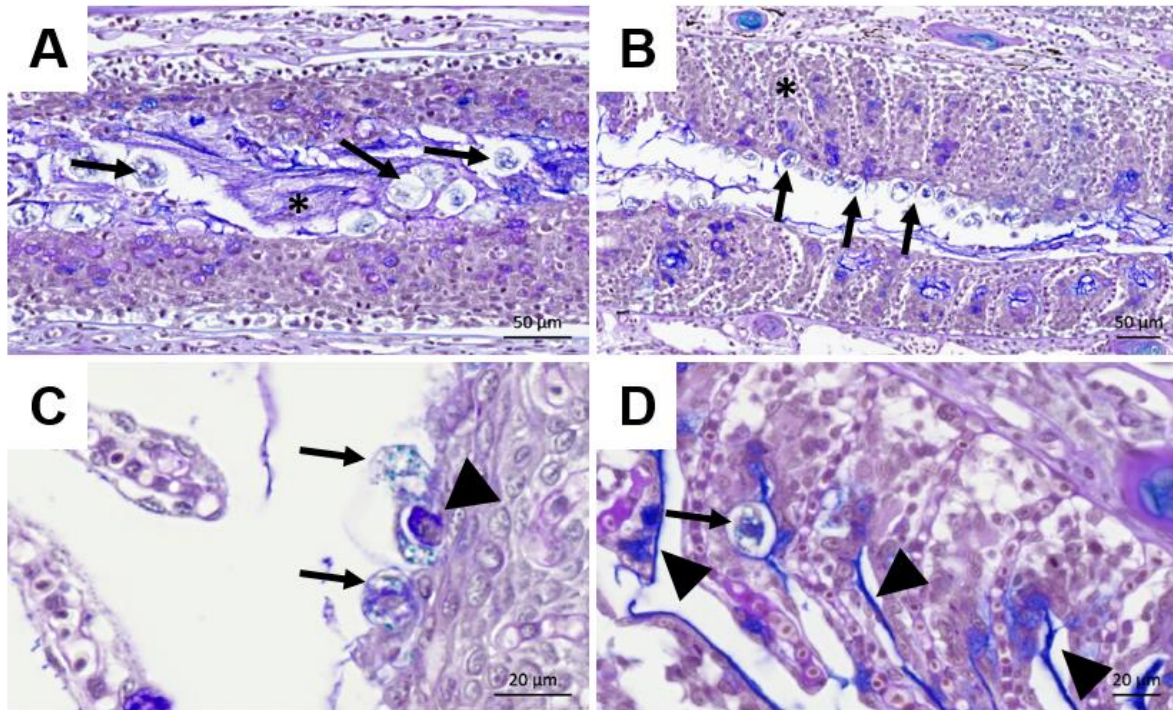


Figure 3.6. Gills of Atlantic salmon infected with AGD fixed in methacarn and stained with AB/PAS. A) & B) Hyperplastic gill epithelial tissue with mucous cells and mucus throughout (asterisks), in addition to numerous amoeba trophozoites (black arrows) associated with the periphery of the lesion surface and showing close interaction with overlaying mucus (asterisk); C) trophozoites are found attached to the gill epithelium (black arrows) and a mucous cell (arrow head) and D) trophozoite found between a lacuna formation (black arrow) surrounded by mucus and mucous cells (arrow heads).

Hyperplastic epithelial lesions associated with amoebic gill disease were clearly visible, with lamellar fusion causing additional lacunae formations in which amoebae was found between (**Error! Reference source not found.A–C**). A transverse section of the gill shows another lacuna formation and the presence of mucus with embedded amoebae (**Error! Reference source not found.D**).

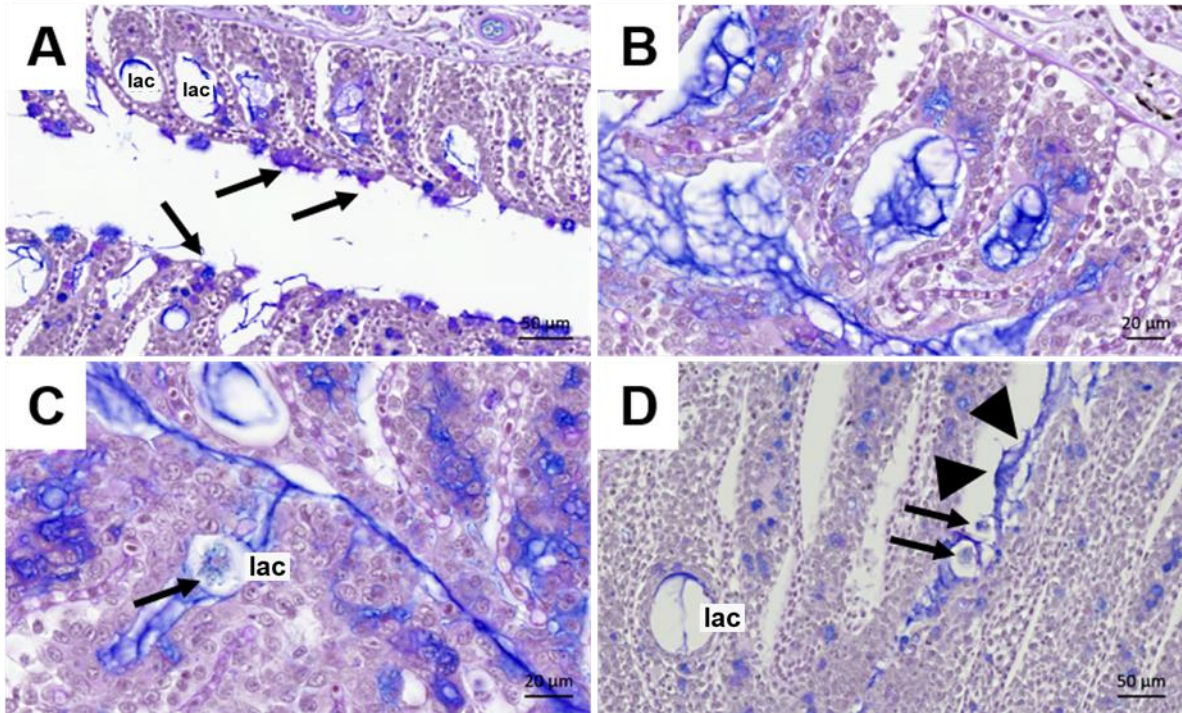


Figure 3.7. Gills of Atlantic salmon infected with AGD fixed in methacarn and stained with AB/PAS. A) Lacunae formations (lac) across the hyperplastic epithelial tissue with mucous cells (arrows) and amoebae trophozoites (asterisks); B) more lacunae formations (lac) with additional mucus; C) trophozoite (arrow) between a lacuna formation (lac) in hyperplastic gill tissue and D) transverse section of gill with lacunae formations (lac) and amoebae attached to the epithelium (arrows) surrounded by a mucus layer (arrow heads).

All these images provide valuable information about the importance of preserving the mucus layer in gill samples as numerous trophozoites seem to be closely linked to the presence of mucus, therefore in the context of gill diseases and mucosal responses this technique can be helpful in highlighting the relationship between pathogen and mucus. This methodology can therefore provide a platform for the study of whether the amoebae are drawn to the mucus or whether the amoebae become embedded in the mucus following overproduction during an AGD infection.

3.3.4. Confirmation of mucus preservation using lectin histochemistry

Wheat germ agglutinin (WGA) lectin labelling was employed to check the preservation of mucus on AGD-infected Atlantic salmon gills (Figures **Error! Reference source not found.** & 3.9). A negative control confirmed that the lectin buffer without the lectin did not stain the mucous cells and mucous overlay, showing a faint auto fluorescence of the mucus traces (Figure 3.8A). Gills fixed in 10% neutral buffer formalin (NBF) showed only faint traces of mucus streaks visible in inter-lamellar spaces (Figure 3.9B), whereas gills fixed in methacarn displayed clearly visible mucous cells and overlay of mucus (Figure 3.8C&D). Images taken with Arcturus (XT) laser capture microdissection instrument (Applied Biosystems, UK) using a blue band fluorescence filter.

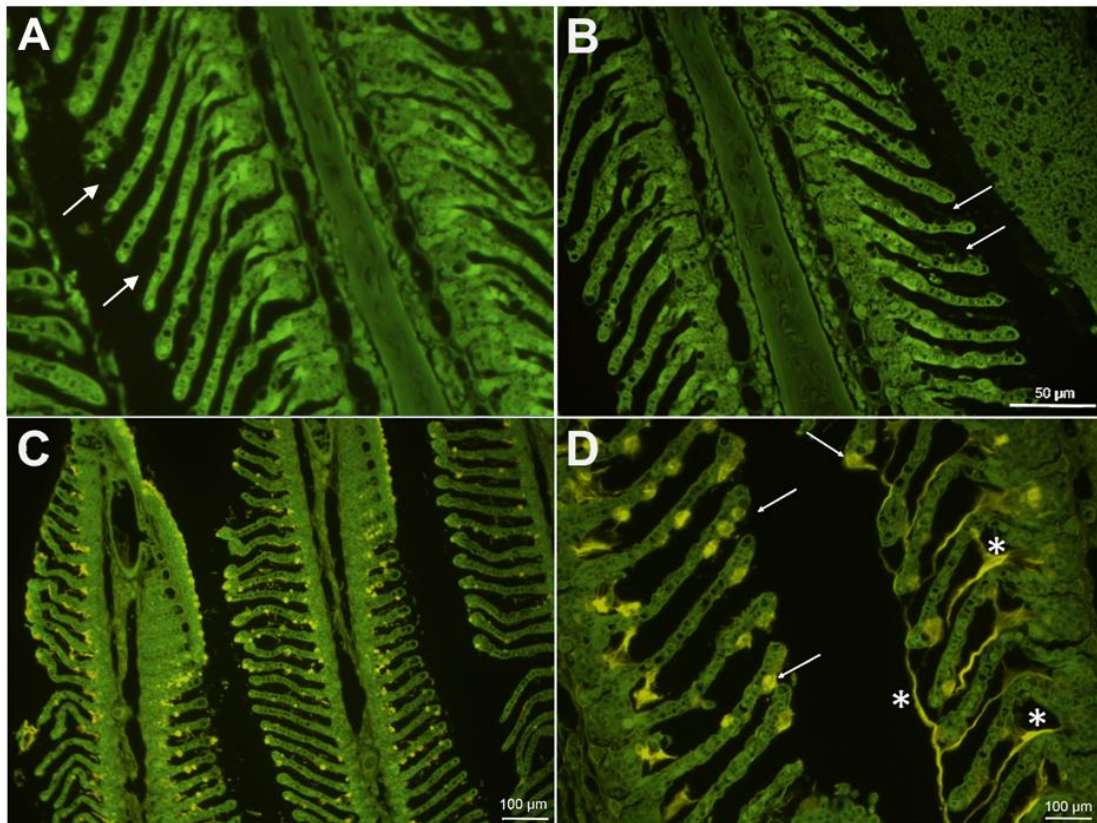


Figure 3.8. Lectin labelling of Atlantic salmon gills. A) Section of gill fixed in methacarn; negative control using lectin wash buffer. *Note* very faint presence of mucus or mucous cells (arrows); B) section of gill fixed in 10% neutral buffered formalin (NBF) labelled with wheat germ agglutinin (WGA); faint traces of mucus visible in inter-lamellar spaces (arrows); C) lower magnification and D) higher magnification of section of gills fixed in methacarn and labelled with wheat germ agglutinin (WGA); visible mucous cells (arrows) and overlay of mucus (asterisks).

Gill tissue displaying AGD-associated hyperplastic lesions with lectin labelling showed well-preserved mucus (**Error! Reference source not found.A–D**) and inter-lamellar vesicles were visible both with (**Error! Reference source not found.A**) and without (**Error! Reference source not found.D**) an entrapped trophozoite. Images taken with Arcturus (XT) laser capture microdissection instrument (Applied Biosystems, UK) using a triple band fluorescence filter.

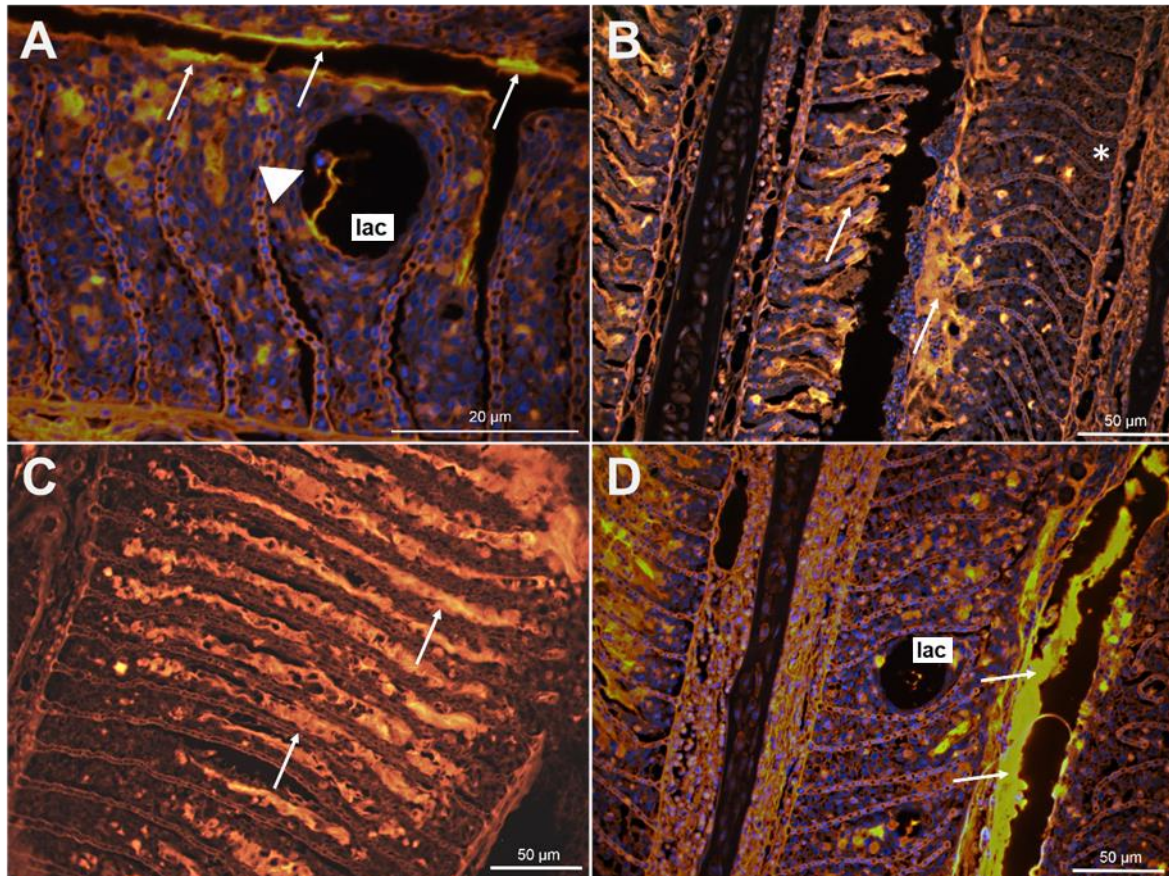


Figure 3.9. Lectin histochemistry using wheat germ agglutinin (WGA) on AGD-infected Atlantic salmon gills. A) Section of gill showing an amoeba trophozoite found between a lacuna formation (lac) (white arrowhead); visible mucus layer (arrows) and counterstaining with DAPI highlighting host and parasite nuclei in blue; B) section of gill showing thick mucus layer in inter-lamellar spaces (arrows) and overlying hyperplastic tissue (asterisk); C) transverse section of gill showing interlamellar mucus (arrows) and D) section of gill showing lacuna formation within hyperplastic tissue and thick mucus layer (arrows).

Additionally, scanning laser confocal microscopy was employed to provide images of greater resolution of the lectin-labelling for the methacarn-fixed samples (**Error! Reference source not found.A**) and for the control samples (NBF fixation) (**Error! Reference source not found.B**). Samples were observed with a TCS SP2 AOBS

Laser Scanning Confocal Microscope (Leica Microsystems, Wetzlar, Germany). Faint auto fluorescence of the mucus traces is observed when sections were stained with H&E for methacarn fixation (**Error! Reference source not found.A**) and no lectin was added. However, in the NBF fixated sample (**Error! Reference source not found.B**), no traces of mucus are observed confirming the lack of capacity of this fixation method for mucus preservation. When lectin-labelling was performed on the methacarn samples (**Error! Reference source not found.C&D**), gills displayed clearly visible mucous cells and overlay of mucus. Samples were observed and constructed with a TCS SP2 AOBS Laser Scanning Confocal Microscope (Leica Microsystems, Wetzlar, Germany).

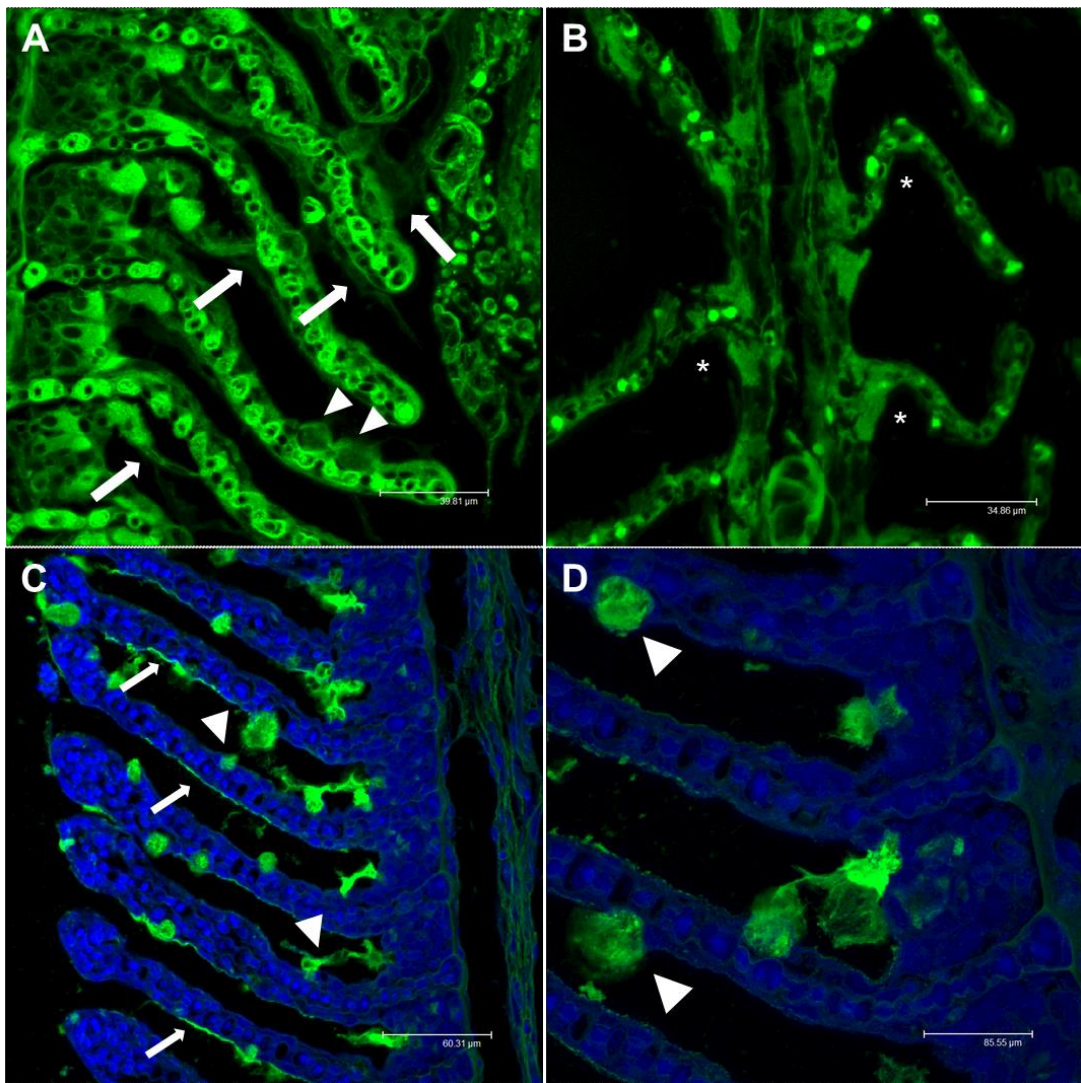


Figure 3.10. Confocal microscopy images of the lectin labelling of non-AGD infected Atlantic salmon gills. A) Section of gill fixed in methacarn; negative control using lectin wash buffer; faint traces are observed (arrows); B) section of gill fixed in 10% neutral buffered formalin (NBF) labelled with wheat

germ agglutinin (WGA); no mucus visible (asterisk); C) and D) gills fixed in methacarn and labelled with wheat germ agglutinin (WGA); visible mucous cells (arrowheads) and overlay of mucus (arrows).

Furthermore, this same technique was used to observe high AGD-infected gills. High level of hyperplasia is clear (**Error! Reference source not found.A&B**) with greater level of mucus presence in the inter-lamellar space (**Error! Reference source not found.A**). In addition, large accumulation of mucous cells is noted in the gill epithelium exterior (**Error! Reference source not found.B**).

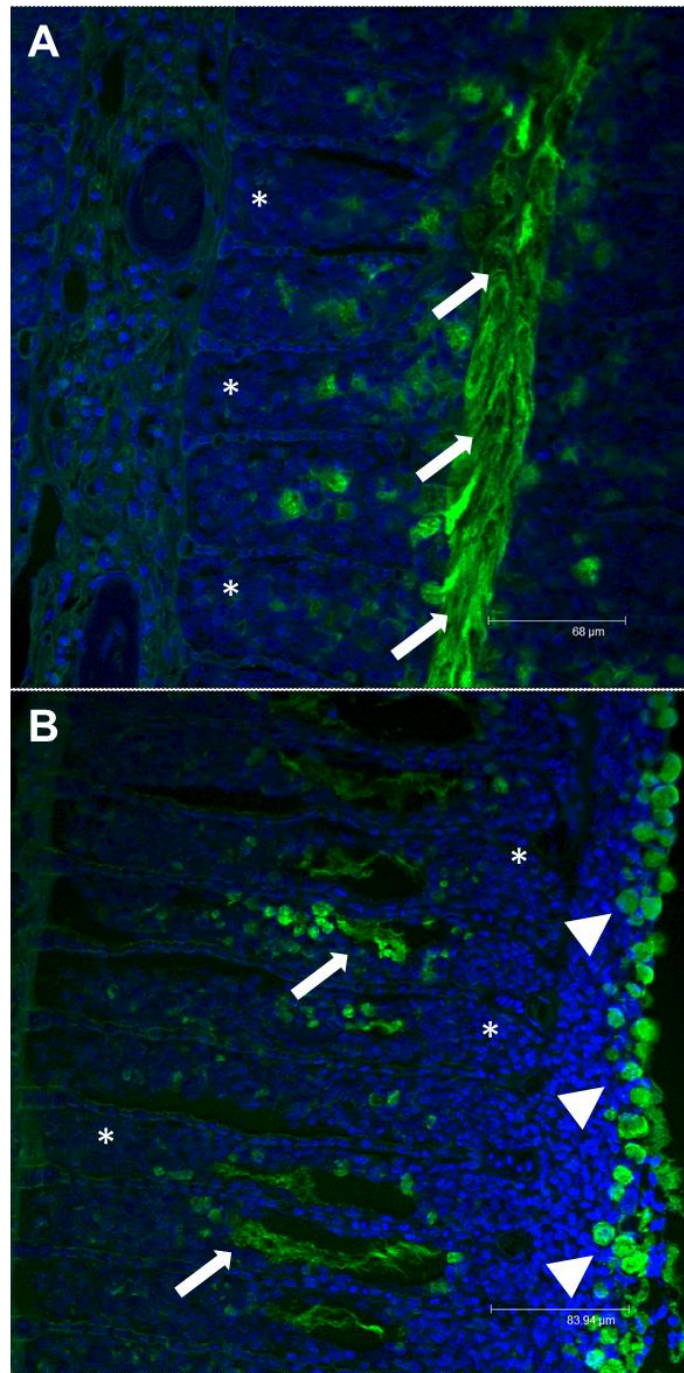


Figure 3.11. Confocal microscopy images of the lectin labelling of high AGD-infected Atlantic salmon gills. A) and B) sections of high hyperplastic gills fixed with methacarn solution and labelled with wheat germ agglutinin (WGA); high level of mucus traces visible in inter-lamellar spaces (arrows) along with high numbers of mucous cells (arrowheads).

3.4. Discussion

In the current study it was found that aqueous fixatives provided good cytological preservation but that mucus overlying the gill epithelium was lost following fixation. This was presumed to be due to the loss of most of the proteoglycan content, as reported by Toledo *et al.* (1996). The non-aqueous, solvent-based fixatives, however, demonstrated a significant improvement in the preservation of mucus traces in the studied gill samples. Despite this, no preservation method employed in the current study gave rise to the appearance of a clear and uniform mucous layer as previously observed for rat gut (Sims *et al.*, 1997) or rat colon (Bollard *et al.*, 1986), pig intestine (Allan-Wojtas *et al.*, 1997), and, more recently, human intestine (Swidsinski *et al.*, 2005). This suggests either that the mucus covering of the gills of Atlantic salmon is less uniformly structured or pronounced than that of mammalian gastric mucosae or that aspects of the sampling and fixation process still need to be optimised.

Davidson's solution has been previously used for demonstration of *N. perurans* presence in infected gills (Cadoret *et al.*, 2013), as well as for other tissues and species (Black *et al.*, 1991; Latendresse *et al.*, 2002). Although the modified Davidson's fixative used in the current study was useful for assessing the number of mucous cells, it was found to be less successful in preserving the mucous coat of the epithelium. Although some patchy mucus could be observed associated with the interlamellar epithelium, the aqueous nature of this fixative allowed most of the mucus to be washed away during the sampling process.

The use of the methacarn solutions in the present study proved to be significantly more successful in stabilising the structure of the mucous layer during fixation and retaining it during subsequent processing, as has been seen in previous investigations involving gut and intestinal tissue in mammals (Johansson *et al.*, 2008; Johansson & Hansson, 2012). In particular, this fixation method has previously given positive results for the immunofluorescent imaging of mucins in pig gut (Earle *et al.*,

2015) showing that there is a greater conservation of the mucous layer structure compared to traditional formaldehyde-based fixatives in which the mucus collapses.

In terms of logistics and sampling, methacarn presents a disadvantage due to its chemical nature. Tissues had to be placed in glass tubes instead of the plastic ones, that are typically used in this kind of procedures, and it's also more dangerous to handle compared to the other two fixatives used during this work. In addition, as the tissues were processed right after they were sampled, there is no actual knowledge about the effects in a long-term storage of the tissue in this fixative. This aspect should then be studied further. Apart from these facts, methacarn solution has provided a good histological maintenance as it has been previously reported in a study by Howat & Wilson (2014) in which different kind of fixatives were compared. They reported no key differences between the fixatives and, also, an enhanced quality while performing molecular techniques such as immunohistochemistry and DNA/RNA analysis.

Overall, the present results conclude that both methacarn solution and methacarn solution with 2% (w/v) Alcian blue enhanced preservation of mucus. One challenge that was encountered when quantifying the mucus was that it was not present as a uniform layer over the gill epithelium; therefore, the presence of mucus was determined by the enumeration of mucus traces that were still in contact with the originating mucous cells or were fixed *in situ* across the gill epithelium. This clearly underlines the necessity of an improved mucus quantification method. Perhaps a more automated technique should be developed in order to provide a better quantification of mucus.

The lectin-binding study confirmed the fixation results, indicating that the apparent mucus observed using basic histological techniques was indeed mucus or mucin-like glycoproteins. This was achieved using a WGA (*Triticum vulgare* (wheat germ)) lectin, which is one of the best studied plant lectins and specifically targets glycoproteins (GlcNAc (N-Acetylglucosamine), its β -(1, 4)-oligomers, and N-acetylneuraminic acid). Its specificity for GlcNAc-carrying ligands has been investigated through fluorescence methods which were applied to study the interactions of carbohydrate-binding lectins with glycopolymers, where clustering glycopolymers were shown to induce a much-enhanced binding affinity compared to the

corresponding mono- and oligosaccharides (Nishimura *et al.*, 1994). Therefore, some investigations (Fischer *et al.*, 1984; Madrid *et al.*, 1989; Ferri & Liquori, 1992; Coet-Zee *et al.*, 1995) hypothesised the possibility of this lectin binding to mucopolysaccharides found within the mucus and mucosal cells. They described lectin-binding in goblet cells of both the small and large intestines of animals belonging to at least five different classes of vertebrates studied, *i.e.* sea bream, frog, tortoise, chicken, rat, hamster, elephant, monkey and human. Regarding fish, the WGA lectin has been used in several studies, including examination of bony fish olfactory epithelium mucus (Wolfe *et al.*, 1998; Ferrando *et al.*, 2006), skin mucus (Guardiola *et al.*, 2014) and GlcNAc and acetylneuraminic acid residues in the gill epithelium of Argentinian silverside *Odontesthes bonariensis* (Valenciennes, 1835) (*Teleostei, Atherinopsidae*) (Diaz *et al.*, 2010).

Unsurprisingly, observation of AGD-affected gills in this study demonstrated the presence of amoebae closely associated with the gill epithelium. However, using the mucus-targeted fixation approaches explored and optimised in this study, amoebae were also observed within the retained mucous layers that would normally be lost during standard fixation. Observed pathology was characterized by hyperplasia and hypertrophy of the epithelial cells, inducing lamellar fusion and the consequent emergence of apparent lacunae or vesicles in the gill lamellae with associated amoebae, as previously observed by other authors (Munday *et al.*, 2001; Adams & Nowak, 2001; Chalmers *et al.*, 2017). Along with these formations, amoebae are found embedded within the mucus which acts as an essential first host barrier against them and prevents, to some degree, pathogen invasion and subsequent infection. The ability to observe mucus presence and distribution provides considerable scope for improving the understanding of the relationship between amoebae and the former. Preservation and labelling of mucus in histological sections also allows direct observation/confirmation of levels of mucus production and of adherence of mucus to gills, which may also reflect changes in mucus composition and function.

Teleost mucus plays a protective role by inhibiting pathogen binding, but also by acting as a vehicle for mucins and humoral immune factors (Dash *et al.*, 2018). Mucus contains high molecular weight glycoproteins that can potentially trap pathogens, acting as a physical barrier (Johansson & Hansson, 2016). Many studies

have verified this statement by researching the relationship between pathogens, mucus and mucins. A study by Nagashima *et al.* (2003) indicated that some pathogenic bacteria could be found attached to the mucous layer and developed biofilms to protect themselves against the host mucosal immunity. Similar observations were made in other studies in which they investigated the interactions of mucosal surfaces and pathogens such as bacteria affecting the respiratory organs (Zanin *et al.*, 2016), the pathogen interactions with the mucus in the gastrointestinal tract of farmed animals (Quintana-Hayashi *et al.*, 2018) and also bacteriophages, whose adherence to host mucus has been shown to provide a preventive protection against other pathogenic bacteria (Almeida *et al.*, 2019).

Other studies have pointed out that pathogenic microorganisms, such as some *Vibrio* strains, are capable of utilising mucus as a carbon source, helping the colonisation of these pathogens and eventually supporting the initiation of infection in fish (Bordas *et al.*, 1996). More recently, study of immunological responses within the gill has highlighted the potential role of secreted IgT, which is involved in B cell recruitment and humoral response, in part delivered through mucus, as well as gene expression reflecting production of other defensins carried in mucus and acting against gill pathogens (Xu *et al.*, 2016; Brinchmann, 2016) and their correlated pathology (Hishida *et al.*, 1997; Benhamed *et al.*, 2014). Additionally, mucins have been investigated as reliable markers of prognostic and diagnostic value of fish intestinal health (Estensoro *et al.*, 2013; Marcos-López *et al.*, 2018). There is, therefore, a need to maintain the mucous coat in order to identify the pathogens embedded in it and potentially study their relationship to the mucus secretions.

While the maintenance of the mucous coat has been improved through the techniques employed in this chapter, the precise composition of the gill mucus was not investigated. In the past, the relationship between AGD presence and the gill ionoregulatory response was investigated by Roberts & Powell (2005) defining the negative effect of this disease on ion transport. Additional studies have also determined differences between the viscosity and glycoprotein biochemistry of salmonid mucus within salmonids species and disease presence, like AGD (Roberts & Powell, 2005). Also in the context of AGD infection and response to treatment, the decreased activities of peroxidase, esterase, lysozyme, protease, and IgM levels in the gill mucus were well defined in the study by Marcos-López *et al.* (2017). Although

the full composition of gill mucus is not investigated throughout this thesis, the following chapter will effectively investigate one aspect, looking at mucin expression and its variability within hydrogen peroxide treated fish and AGD-infected fish, in addition to those of other genes involved in gill mucosal immunity.

Conclusions

In conclusion, the work presented in this chapter has explored several mucus fixation approaches in the context of studying AGD in Atlantic salmon and has identified an optimal protocol involving methacarn fixation. The study demonstrated the utility of taking deliberate steps to preserve mucus integrity and provides evidence that retention of mucus, particularly in the context of gill diseases, such as AGD or complex gill disease, can provide useful data that would be lost under normal fixation and processing procedures.

Chapter 4 : H₂O₂ treatment impacts on the T-cell response in Atlantic salmon gills and causes similar mucin disruption to fish during a late stage AGD-infection

4.1. Introduction

Gill diseases have become a consistent problem in salmonid aquaculture worldwide through the actions of infectious and non-infectious agents (Mitchell & Rodger, 2011; Gjessing *et al.*, 2017; Gunnarsson *et al.*, 2017). One of the most important challenges at present is amoebic gill disease (AGD), caused by the marine ectoparasite *Neoparamoeba perurans* (Young *et al.*, 2008). Due to an expansion of its geographic distribution and its host range, this disease has had a great impact on the Atlantic salmon industry (Rodger, 2014; Shinn *et al.*, 2015; Oldham *et al.*, 2016). Hyperplasia and fusion of the lamellar epithelium are the most obvious outcomes during the course of infection in fish (Munday *et al.*, 1990; Adams & Nowak, 2001, 2003, 2004a,b; Adams *et al.*, 2004; Powell *et al.*, 2008). In addition, an increased number of mucous cells and mucus secretion have also been described in AGD-infected fish (Nowak & Munday, 1994; Zilberg & Munday, 2000; Adams & Nowak, 2003; Roberts & Powell, 2003; Chalmers *et al.*, 2017).

For treatment, two different approaches are generally employed within the salmon industry. Freshwater baths are used where freshwater is readily available (Parsons *et al.*, 2001; Powell *et al.*, 2015). This treatment creates an osmotic shock for the amoebae and a subsequent reduction of gill mucus viscosity (Adams & Novak, 2004; Roberts & Powell, 2008). However, when not easily accessible, hydrogen peroxide (H₂O₂) is used as an alternative treatment due to its amoebicidal efficacy (Adams *et al.*, 2012). At present, the general H₂O₂ concentration ranges and timings that are used within the industry range between 800-1300 ppm for 12-20 minutes for AGD (Rodger, 2014). Even though, this treatment has shown success when used on sea lice (*Lepeophtheirus salmonis*) and *N. perurans*, secondary effects have been observed such as gill irritation (Powell & Clark, 2014) and, also, higher water temperatures (>13.5°C) at the time of treatment have been found to be an added risk (Rodger, 2014). In a more recent study, different temperatures were tested during a treatment with hydrogen peroxide on AGD-infected salmon and it was found that the

lower the temperature (8°C), the more effective the treatment was (Martinsen *et al.*, 2018).

In addition, secondary effects of H₂O₂ have also been investigated in other fish species. A study by Avendaño-Herrera *et al.* (2006) demonstrated that treating with this chemical, provoked intense signs of respiratory distress and accelerated mortality of the affected turbot (*Scophthalmus maximus* (Linnaeus, 1758)) when high concentrations of this chemical were used. The same acute effects were observed on kingfish (*Seriola lalandi* Valenciennes, 1833) health, although implications for the health of the fish were much less than that caused by chronic infection with the pathogen that was being targeted by treatment, the monogean *Zeuxapta seriolae* (Meserve, 1938) (see Mansell *et al.*, 2005). Most recently, another study revealed that increasing the concentration of H₂O₂ for treatment against sea lice on Atlantic salmon did not improve delousing and instead, increased mortalities (Overton *et al.*, 2018). Another species of fish, olive flounder *Paralichthys olivaceus*, was investigated after its treatment with hydrogen peroxide. They found some secondary effects on mucous cells and lysozyme in gill tissue, showing an increase in the number of mucous cells as well as an up-regulation of lysozyme, which was linked to an innate immune response modulation when a concentration of 500 mg L⁻¹ was used (Hwang *et al.*, 2014). These impacts on the fish are potentially due to the strong oxidising nature of H₂O₂ which causes peroxidation of lipid and cellular membranes, inhibition of DNA replication and inactivation of enzymes (Sies *et al.*, 2017). Also, in the study mentioned before by Martinsen *et al.*, (2018) all the Atlantic salmon were susceptible to re-infection due to the high level of AGD fish had prior to the treatment. This showed that conditions prior treatment might also have an impact in its success.

On a molecular level, different studies have evaluated the effects on the immune and mucin response of fish gills subject to AGD infection (Young *et al.*, 2008; Pennacchi *et al.*, 2014; Benedicenti *et al.*, 2015; Marcos-López *et al.*, 2017, 2018). However, there are observable differences between the different stages of the infection. These studies have found many different results making the characterisation of the host-response a challenging task. Young *et al.* (2008) was the first to show that there was a downregulation of the major histocompatibility complex I (MHC-I) pathway related genes at the later stages of infection, as well as in AGD lesions. Therefore, the

differences in cell type and the non-affected areas caused different responses. Also, different outcomes were observed through the studies by Benedicenti *et al.* (2015) and Pennacchi *et al.* (2014), which presented differences in time dose, infectious dose and sampling times, as well as for different fish sizes and seawater temperatures. Both of these studies studied the role of T helper cells during the development of the immune response, specifically through the analysis of gene expression profiles of cytokines produced by this T helper subsets (Th1, Th2, Th17 and Treg). Each pathway assumes a different function. While Th1 cells activate macrophages and permit phagocytosis to destroy intracellular pathogens, Th17 cells secrete interleukins which recruit neutrophils to the site of infection and Th2 cells regulate humoral immunity. Lastly, Treg cell subsets produce molecules such as TGF- β and IL-10 which modulates immune responses, regulating the overall immune response (Castro *et al.*, 2011). In the study by Benedicenti *et al.* (2015), gill tissue from the last stage of the disease (21 dpi) showed a downregulation across different markers from the Th1, Th17 and Treg cell subsets, while Th2 pathway was found to be upregulated. The authors therefore proposed that either an immune evasion strategy or an allergic reaction was caused by the amoebae. In the most recent AGD study, whilst a number of Th1 cytokines and pro-apoptotic genes were down-regulated, up-regulation of Th2 cytokine IL4/13 was reported in addition to several genes related to mucin secretion and cell proliferation (Marcos-López *et al.*, 2018). These results support the findings of Benedicenti *et al.* (2015). The correlation between these two pathways has been studied in humans, where the over stimulation of Th2 cytokines induces hyperplasia in goblet cells making mucins (Muc5ac/Muc5B) which show up-regulation (Yu *et al.*, 2010; Zeng *et al.*, 2011).

Mucus is recognised as playing a very significant role during the course of infection. Mucus is composed of mucins, which are known to play a key role in innate immunity, accommodating the natural commensal flora overlying mucosal tissue and restraining infectious disease (Linden *et al.*, 2008). Most of the databases include predicted mucin sequences based on homology with other species; however, the detection of mucin expression in mucosal tissue (i.e. skin, pyloric caecae, gills and intestine) has been largely carried out through gene expression analysis (Sveen *et al.*, 2017). During the study by Marcos-López *et al.* (2018), mucins muc5 (secreted and gel-forming) and muc18 (membrane-bound) were consistently detected in gills of

Atlantic salmon. Whilst muc5 was significantly up-regulated in fish with AGD lesions, muc18 was significantly down-regulated at 21 days post-infection (dpi). It is understood that muc5-type mucins are the principal components of the distinctive mucus patches observed during an AGD infection (Marcos-López *et al.*, 2018), making them a potential biomarker for this disease. Previous studies investigating mucous cells during an AGD infection (Munday *et al.*, 2001), observed an increase in numbers containing neutral and carboxylated mucins, although subsequent studies showed lower numbers (Roberts & Powell, 2008). This could imply different mucus expression due to their different glycoprotein compositions making them more acidic or neutral; however, this aspect of the mucin-mucus relationship hasn't been investigated in detail.

Although many studies have investigated mucin and immune responses to AGD, the effects of treatment with H₂O₂ on mucins have not been evaluated in salmon. Aspects of H₂O₂ impacts on Atlantic salmon health have however been studied including the response of various stress markers (*e.g.* glucose, lactate, cortisol *gpx1*, *cat*, *Mn-sod* and *hsp70*) which increased as a result of sublethal toxic effects in Atlantic salmon (Vera & Migaud, 2016). Therefore, in this Chapter, an investigation of the potential effects of H₂O₂ on the gills of non AGD-infected Atlantic salmon was carried out by evaluating three different types of mucins (muc5ac, muc1 and muc17), in addition to eleven genes related to T-cell (CD4- α , Cd8 α , TCR α chain and CD3 $\gamma\delta$ B), B-cell (IgT and mIgM), and Th1/Th17 and Th2 (TNF- α 2, IFN- γ , IL-3/13 β 2, IL-22, IL-10) pathways. Additional early (7 days dpi; 1-2 scores) and late AGD-infected fish (28 dpi; 3-4 scores) were also subjected to the same analysis.

4.2. Material and Methods

4.2.1. Experimental fish

For the H₂O₂ treatment experiment, Atlantic salmon were randomly allocated into 8 x 250 L tanks (n=6 fish per tank; 48 in total) at MERL. One group of 24 fish were previously challenged with AGD by cohabitation with infected adult Atlantic salmon over a period of 6 weeks prior to the start of H₂O₂ treatment and sampling (AGD challenged groups); the remaining group of 24 fish were not challenged with AGD and were used as control fish (Non-AGD challenged groups) (Table 4.1).

Table 4.1. Table representing means \pm s.e.m of the weight (kg), fork length (length; cm) of each fish used for the H₂O₂ treatment experiment (n= 48 fish). The Table shows data from the non-AGD challenged group. Time 0 sub-groups are H₂O₂ untreated Atlantic salmon, whilst time 4 h, 24 h and 14 d are the post-H₂O₂ treatment sub-groups named after the time point at which they were sampled.

| Group | Fish (n) | Weight (kg) | Length (cm) | AGD score |
|------------------------------------|----------|-------------------|------------------|-----------|
| Time 0 Non-AGD challenged group | 6 | 0.177 \pm 0.014 | 23.3 \pm 2.1 | 0 \pm 0 |
| Time 4 h Non-AGD challenged group | 6 | 0.155 \pm 0.011 | 25.3 \pm 0.677 | 0 \pm 0 |
| Time 24 h Non-AGD challenged group | 6 | 0.166 \pm 0.011 | 26.16 \pm 0.54 | 0 \pm 0 |
| Time 14 d Non-AGD challenged group | 6 | 0.190 \pm 0.008 | 26.8 \pm 0.360 | 0 \pm 0 |

The cohabitation challenge was undertaken as described in Chapter 2, Section 2.2.5.1. All groups were held at a temperature of 11 \pm 1°C, in full-strength seawater taken from pipes opening 50 m from the shore (ca. 35 ‰), and at a concentration of dissolved oxygen (DO) equal to 8.6-8.8 ppm. Fish were fed daily with commercial salmon pellets (Inicio Plus, BioMar, UK) at 1% of their body weight.

As the AGD challenge failed and qPCR analysis did not detect the presence of *N. perurans* amoeba DNA in nominally AGD-infected gills, samples from a previous cohabitation challenge undertaken using the same experimental parameters (Chalmers *et al.*, 2017) were used to investigate transcript expression. In that study, five fish (0.176 \pm 0.007 kg; 24.73 \pm 0.754 cm) were sampled 7 dpi to characterise the immune and mucin expression during an early stage of AGD infection and the same analysis was conducted for an additional five fish (0.168 \pm 0.010 kg; 24.63 \pm 0.823 cm) sampled at 28 dpi during a later stage of AGD infection. Gill scores from

the early AGD-infected fish were low (1-2) and the ones concerning the late AGD-infected fish were high (3-4).

4.2.2. Sampling collection and hydrogen peroxide treatment

Fish belonging to AGD challenged groups and Non-AGD challenged groups were treated with H₂O₂. For the treatment, tank volume was decreased to 200 L and the treatment was administered at a concentration of 1250 mg L⁻¹ for 15 min, same concentration used in the study by Adams, Crosbie & Nowak (2012). Water chemistry parameters such as oxygen concentration (7.4 ± 0.5 mg L⁻¹) and pH (7.1 ± 0.2) were monitored and logged every 3 min during the entire duration of the H₂O₂ treatment. As mentioned before, water temperature was monitored to keep at 11±1°C. In addition, samples of water were taken at 1, 8- and 15-min post-treatment to determine H₂O₂ concentration by the cerium sulphate titration method (Reichert *et al.* 1939). In brief, for this titration, 5 mL of 5N sulphuric acid and 7.5 mL of cerium IV sulphate were mixed in a conical flask. A burette was filled with 50 mL of the water sample and was slowly added to the mixture. Once the solution turned completely transparent, the amount of water added was read and H₂O₂ concentration was calculated according to the formula described in **Error! Reference source not found.** At the end of the treatment period, the tanks were flushed, and water replaced.

$$H_2O_2 \text{ concentration} = \frac{(7.5 \times 0.1 \times 1000 \times 34)}{2} \times \text{water added}$$

Figure 4.1. Formula for the calculation of H₂O₂ concentration prior to the treatment.

A total of eight groups of six fish were sampled at 0 h (left untreated), 4 h, 24 h and 14 days post treatment (dpt), in AGD-challenged and control groups (total n=48). Fish were subject to anaesthetic overdose using MS-222 (100 mg L⁻¹) and destruction of the brain according to UK Home Office Schedule 1 methods and each individual gill arch was scored in accordance to Taylor *et al.* (2009). When subjecting the fish to anaesthetic they were taken two by two and instantly sampled. Swabbing of the right gill arches was performed following lethal anaesthesia to collect mucus for downstream qPCR quantification of amoeba load. Cotton swabs were preserved in 95% ethanol.

For tissue collection, samples were taken from the second left gill arch for further processing. One eighth was preserved in RNAlater (0.45 M ammonium sulphate, 2

mM EDTA, and 25 mM sodium citrate, pH 5.2) for RNA extraction and subsequent qPCR analysis for assessing gene expression. An additional one eighth of tissue was placed in 95% ethanol for DNA extraction and qPCR analysis for assessing *N. perurans* load. A record of the fish fork lengths and weights was taken immediately following euthanasia.

4.2.3. TaqMan RT-qPCR analysis for *N. perurans* quantification

4.2.3.1. DNA extraction

All the samples from both groups, non-AGD challenged and AGD-challenged, were preserved in 95% ethanol and processed for DNA extraction using a DNeasy Blood & Tissue Kit (QIAGEN, Manchester, UK). The tissue was transferred to 1.5 mL Eppendorf tubes; 180 μ L of Buffer ATL and 20 μ L of proteinase K were added. Samples were quickly vortexed and incubated at 56°C until complete lysis of the tissue was achieved. Samples were vortexed again, incubated at 56°C for 10 min, and 200 μ L of 100% ethanol was added to each sample. This solution was then pipetted into a DNeasy Mini spin column and placed within a 2 mL collection tube and centrifuged at 600 x g for 1 min. After centrifugation, the flow-through was discarded, and the spin column was placed into a new 2 mL collection tube; 500 μ L of Buffer AW1 was added to each tube. Samples were then centrifuged at 20,000 x g for 3 min. Again, the flow through was discarded and spin columns were transferred to 1.5 mL Eppendorf tubes. Next 20 μ L of Buffer AE was added to the spin column membrane to elute the DNA.

The final DNA concentration and purity were measured using a NanoDrop 1000 Spectrophotometer. DNA concentration was standardised to 50 ng μ L⁻¹ using Ambion® RT-PCR grade water and then samples were stored at 4°C. All samples were sent to the Marine Institute Fish Health Unit (Galway, Ireland) for analysis of *N. perurans* amoeba loads. Analysis by RT-qPCR was carried out in triplicate according to Downes *et al.* (2015).

4.2.4. SYBR® green RT-qPCR analysis for gene expression on gill tissue

4.2.4.1. RNA extraction from gill tissue and cDNA synthesis

RNA later preserved gill tissues from every time point (0 h, 4 h, 24 h and 14 dpt) and control groups were processed for RNA extraction and subsequent cDNA synthesis. First, tissue was cut into small pieces and 1 mL of TRI Reagent was added (approx. per 100 mg of tissue (maximum of 1.5 mL in screw cap tubes)). Samples were incubated on ice for 60 min.

Homogenised samples were incubated at RT for 5 min. Following centrifugation at 12,000 × *g* for 10 min at 4°C, supernatant was transferred to a 1.5 mL fresh Eppendorf tube. A volume of 100 µL 1-Bromo-3-chloropropane (BCP) (per 1 mL TRI Reagent used) was added to the tube and shaken vigorously by hand for 15 s. Tubes were incubated at RT for 15 min, followed by centrifugation at 20,000 × *g* for 15 min at 4°C. The aqueous (upper) phase was tipped slowly from the top and transferred to a new 1.5 mL Eppendorf tube.

For precipitation of the RNA, RNA precipitation solution (1M NaCl, 1M C₆H₆Na₂O₇) and isopropanol were added at 50% volume (per aqueous phase volume) of the final sample solution. Then, the samples were gently inverted 4-6 times and incubated for 10 min at RT. Samples were centrifuged at 20,000 × *g* for 10 min at 4°C. RNA precipitate formed a gel like pellet on the side/bottom of the tube.

For the RNA wash, the supernatant was removed by pipetting and the pellet washed for 15 min at RT with 1 mL of 75% ethanol. The pellet was re-suspended by flicking the bottom of the tube and inverting it a few times so that the entire surface of the pellet and tube were washed. Centrifugation at 20,000×*g* for 5 min at RT was performed, followed by removal of most of the supernatant. Samples were pulsed (2 s) and all remaining ethanol was removed, before air drying the RNA pellets at RT for 3-5 min, until all visible traces of ethanol were gone. Finally, the pellet was re-suspended in 100 µL of RNase free water. The samples were incubated at RT for 30-60 min with gentle flicking of the tubes every 10 min to aid resuspension. RNA concentration was measured using a NanoDrop 1000 Spectrophotometer. Dilutions

of the RNA samples (1:10) were made for a final total RNA concentration of 2 µg in 10 µL. The remainder of RNA samples were stored at -70°C.

DNase treatment of the samples was performed prior to cDNA synthesis with Ambion® DNA-free™ DNase Treatment and Removal Reagents. Volumes of 0.1 µL 10X DNase I Buffer and 1 µL rDNase I were added to the RNA and mixed gently. Samples were incubated for 20 min at 37°C in the LightCycler 480 thermocycler (Roche, UK). Following this, 2 µL of resuspended DNase Inactivation Reagent were added and mixed well, followed by an incubation of 2 min at RT, mixing occasionally. A final centrifugation at 10,000 × g for 1.5 min was performed and total treated RNA was transferred to a fresh tube.

cDNA synthesis was performed using the High Capacity cDNA Reverse Transcription Kits (Applied Biosystems, Cheshire, UK). Master Mix (10× RT Buffer, 100 mM 25× dNTP Mix, 10× RT Random Primers, Oligo dT primers (5' TTTT TTTTTT VN 3'), MultiScribe™ Reverse Transcriptase (R.T.), and Nuclease-free water) was prepared following manufacturer's protocol. A volume of 10 µL of 2× RT master mix was pipetted into each individual tube, already containing 10 µL of diluted RNA (2 µg/10 µL). Finally, all samples were reverse transcribed in a thermocycler under the conditions described in Table 4.2. Thermocycler conditions for cDNA synthesis of the RNA samples.

Table 4.2. Thermocycler conditions for cDNA synthesis of the RNA samples.

| | Step 1 | Step 2 | Step 3 | Step 4 |
|------------------|--------|--------|--------|--------|
| Temperature (°C) | 25 | 37 | 85 | 4 |
| Time (min) | 10 | 120 | 5 | ∞ |

RNA samples were stored at -70°C. cDNA samples were diluted by pipetting 10 µL from the stock solution to a volume of 90 µL of ddH₂O (1:10 dilution). Dilutions and stock cDNA samples were stored at -20°C. RNA samples were visualised via electrophoresis through 1% agarose/tris–borate EDTA buffer and bands were visualized by staining with a final concentration of 0.5 µg mL⁻¹ from a 10 mg mL⁻¹ ethidium bromide stock. After cDNA synthesis was performed, conventional PCR was performed with the samples with housekeeping transcript ELF-1α primers (FW: 5' CTGCCCTCCAGGACGTTTACAA 3' and RV: 5' CACCGGGCATAGCCGATTCC

3'; NCBI accession number: AF321836) to assess Atlantic salmon cDNA quality. These primers were designed and validated by laboratory technicians prior this experimental work, in the Molecular laboratory at the Institute of Aquaculture (Scotland, UK). Cycle conditions were 95°C for 5 min; 95°C for 30 s, 58°C for 30 s and 73°C for 2 min, for 35 cycles; and 73°C for 8 min. The PCR reaction products were subjected to electrophoresis through 1% agarose/tris–borate EDTA buffer and bands were visualized by staining with a final concentration of 0.5 µg mL⁻¹ from a 10 mg mL⁻¹ ethidium bromide stock.

4.2.4.2. Quantitative RT-qPCR and data analysis

Quantitative RT-PCR was performed on a qTOWER³ (Analytik Jena, Germany) using SYBR green chemistry to measure the differential expression of the target genes and primer sequences listed in Table 4.3. Each PCR reaction consisted of 15 µL of the SYBR® master mix (Thermo Scientific, Epsom, Surrey, UK) along with the forward and reverse primers (final concentration 0.2 µM each) and 5 µL cDNA template in molecular grade water to a final volume of 20 µL. Samples were assayed in duplicates and cycling conditions consisted of an initial activation of DNA polymerase at 95°C for 3 min, followed by 40 cycles of 5 s at 95°C, 10 s at 60°C, and 10 s at 72°C. The mRNA transcripts / gene expression was calculated relative to the geometric mean of three reference genes ELF1-α, β-actin and β-tubulin which were previously described as valid reference genes in Atlantic salmon (Ingerslev *et al.*, 2006a). All the primers described in Table 4.3 were designed and validated in-house prior to the initiation of this work. Primers were designed over splice sites to ensure no amplification of contaminating DNA and the efficiency of the qPCR was always checked by performing a standard curve with every pair of primers each time a target was investigated.

Table 4.3. List of primers (5' → 3') used for the immune and mucin gene expression analysis in control fish treated with hydrogen peroxide and fish infected with AGD.

| Gene target name | LOC ID (NCBI) | Accession number (NCBI) | Oligonucleotides (5' → 3') | Product size (bp) | Tm (°C) | Efficiency (%) |
|------------------------|---------------|-------------------------|---|-------------------|----------|----------------|
| Housekeeping | | | | | | |
| ELF-1 α | LOC100136525 | AF321836 | FW: CTGCCCTCCAGGACGTTTACAA RV: CACCGGGCATAGCCGATTCC | 176 | 60 60 | 97.57 |
| β -actin | LOC100136352 | XM_014194537 | FW: CCCATCTACGAGGGTTACGC RV: TGAAACTGTAACCGCGCTCT | 112 | 60 61 | 86.21 |
| β -tubulin | LOC100136483 | DQ367888.1 | FW: CCGTGCTTGTGGACTTGGAG RV: CAGCGCCCTCTGTGTAGTGC | 144 | 60 62 | 91.92 |
| Immune response | | | | | | |
| CD3 $\gamma\delta$ -B | LOC100137057 | NM_001123721 | FW: CCGCAAGAAAACATCTACCAA RV: GCTGATAGTGGCCAATGGGG | 81 | 59 61 | 98.15 |
| CD4-2 α | LOC100169853 | XM_014163618 | FW: GCCCTGAAGTCCAACGA RV: AGGCTTCTCTCACTGCGTCC | 79 | 61 63 | 88.58 |
| CD8 α | LOC100136450 | XM_014167443 | FW: ACTTGCTGGGCCAGCC RV: CACGACTTGGCAGTT | 96 | 62 58 | 81.76 |
| IL-4/13 β 2 | HG794525 | HG794525.1 | FW: GCATCATCTACTGAGGAGGATCATGAT RV: GCAGTTGCAAGGGTGAAGCATATTGT | 63 | 60 63 | 95.07 |
| IL-10 | LOC106594794 | XM_014186180 | FW: GGGTGTACGCTATGGACAG RV: TGTTTCGGATGGAGTCGATG | 118 | 61 57 | 80.17 |
| IL-22 | HQ664669 | HQ664669.1 | FW: CCAGACATCGATACTAAAAAGAACCACA RV: TGTGGTGGTGGTCAGTGTAGTGT | 110 | 59 63 | 99.24 |
| IFN- γ | LOC100329178 | NM_001171804 | FW: TCTCCCTCTAACGGTGAAGGT RV: TGGCCAGTTGAGGCATTTTGT | 148 | 60 62 | 99.7 |

| | | | | | | |
|-----------------------|--------------|--------------|--|-----|----------|-------|
| IgT | ACX50291 | ACX50291.1 | FW: CAACACTGACTGGAACAACAAGGT RV: CGTCAGCGGTTCTGTTTTGGA | 121 | 60 61 | 99.8 |
| m IgM | AAB24064 | AAB24064.1 | FW: TGCCTGTAGATCACTTGAA RV: ATGGTGTGCTGCATGGACA | 134 | 59 60 | 86.21 |
| TCR α | LOC106569062 | XM_014140002 | FW: AACTGGTATTTTGACACAGATGC RV: ATCAGCAGGTTGAAAACGAT | 146 | 56 54 | 88.89 |
| TNF- α 2 | LOC100136458 | NM_001123590 | FW: ACTGGCAACGATGCAGGATGG RV: GCGGTAAGATTAGGATTGTATTCACCCTCT | 144 | 64 62 | 98.25 |
| Mucin response | | | | | | |
| Muc1 | LOC106580087 | XM_014160723 | FW: TCACGTCCAGAAACCAGGAAG RV: GTCGCAGGCTGAGAAAACCT | 101 | 60 61 | 82.52 |
| Muc17 | LOC106585310 | XM_014171406 | FW: TTTCCGACTTCCCAGTTTCC RV: CTGGCATCTTGATTAACCGCTG | 163 | 60 59 | 89.16 |
| Muc5ac | LOC106597903 | XM_014189016 | FW: TTTTCTCAGTTGCCGCTTTT RV: AGTCGGAGCCATAAGACGT | 92 | 58 61 | 82.37 |

4.2.5. Mucous cell semi-quantitative analysis

For this analysis, only the non-AGD challenged group was used, with fish sampled from the different timepoints (0 h -untreated-, 4 h, 24 h and 14 dpt). Slides obtained from samples fixed in Davidson's (prepared as explained in Chapter 3, Section 3.2.1 and 3.2.3), were analysed to quantify the presence of mucous cells. All sections were scanned for any signs of histopathological events. Davidson's fixed tissue sections were all scanned using a 10x objective, selecting an area with at least 3 whole primary lamellae, and an image of $\sim 1\text{mm}^2$ was acquired from each sample. On each of the 3 primary lamellae present in the micrograph, one mid-section comprising 10 inter-secondary lamellar spaces on each side of the primary lamellae was chosen and used for standardised mucous cell counts. Slides were observed under a compound microscope (Olympus BX53M) and images were taken with an Olympus SC100 camera.

Selected fields of primary lamellae were limited to only primary lamellae that appeared to be equally transversally sectioned with limited cutting or folding secondary lamellar artefacts. The 3 resulting counts from each section were then exported to Microsoft Excel and a mean count for each sample was obtained. In addition, a mean was also calculated for each sampling group.

4.2.6. Immunohistochemistry (IHC) for evaluation of CD3+ cells expression and localisation in sampled gill tissue

The same fish described in the previous section (4.2.5) were employed for the following work. Sections obtained from samples fixed in Methacarn (prepared as explained in Chapter 3, Section 3.2.1 and 3.2.3), with the modification of using SuperFrost Plus™ Adhesion slides (Fisher scientific, UK) were dewaxed in 2 steps of xylene for 5 min each, then in 100% ethanol for 5 min and 70% ethanol for 3 min. After dewaxing, sections were rinsed in TBS (2.42 g L⁻¹ Tris Base (10 mM), 24.24 g L⁻¹ NaCl (0.5 mM), pH 7.5 in distilled water). A wax circle was drawn around the tissue with a PAP pen (Merck, UK) and sections were transferred to a humidifying chamber. DAKO Peroxidase block (DAKO EnVision System kit, Agilent, US) was added, just enough to cover the tissue, and slides were incubated for 5 min. After incubation, a rinse was performed for 5 min with TBST (same as TBS recipe but adding 0.5 mL/ L Tween-20). Following this, sections were processed for antigen

retrieval; this procedure was carried out by immersing the slides in 500 mL of tri-sodium citrate solution (2.94 g L⁻¹ Tri-sodium citrate, pH 6) and heating twice at 900W in a microwave for 2 min, with a cooling step of 5 min in between.

Non-specific antibody blocking was performed by covering the tissue with 2% bovine serum albumin (BSA) in TBST. Sections were incubated for 30 min at RT in a humidifying chamber. After this, the BSA-TBST blocker was dabbed off and sections were covered with 10% goat serum diluted in the TBST. Another 30 min of incubation followed at RT in the same chamber. Primary antibodies (previously developed in-house by a scientific colleague) and negative control (TBS and Koi herpesvirus; KHV – isotype control) were prepared by preparing 1/5 dilutions of antibodies in 1% BSA in TBS. Without washing the slides, the primary antibodies and controls were added to the sections by covering the tissue. An overnight incubation was followed at 4°C in the humidifying chamber.

The following day, sections were washed in TBST three times for 3 min. DAKO Labelled polymer HRP Anti-mouse (DAKO EnVision System kit, Agilent, US) was added to the sections in sufficient volume to cover the tissue and incubated for 30 min at RT in the chamber. Sections were then washed in TBST three time for 3 min. After this, DAKO AEC+ Substrate chromogen (DAKO EnVision System kit, Agilent, US) was added the same way as before and sections were incubated between 5-30 min until a signal was evident in the positive control without any background in the negative controls. The reaction was stopped by dipping of the slides in distilled water.

Slides were then counterstained by immersing in haematoxylin for 3-4 min. Excess stain was washed away by submerging in a running tap water bath for 10 min. Sections were coverslipped and left to dry for 1h or overnight.

4.2.7. Image analysis for CD3+ cell expression quantification

Quantification of the expression of CD3+ cells in the gill tissue was undertaken using ImageJ 1.8v software. Twelve randomised fields of view of 10 inter-secondary lamellar spaces in the mid-section of the primary lamella (n=6 control fish and n = 6 14 dpt fish) were assessed, one section per fish and six different images taken within the section. Fields of view were chosen by moving the slide randomly across the areas of interest. Control slides (**Error! Reference source not found.A**) show no

red colouration due to the use of buffer instead of CD3 antibodies. The method followed the splitting of the colour channels of the original images. Blue channel was selected because it provided best highlighting of the CD3⁺ marked cells (**Error! Reference source not found.C**). This image was then adjusted to a threshold of 0 – 121 (**Error! Reference source not found.D**). The same parameters were used for all images. The threshold adjustment masked labelled cells which belonged to the CD3⁺ cell population (**Error! Reference source not found.D**; asterisks). After this, the analysis feature was used to measure the area of the image that was stained with colour red. The expression ratio was calculated following the equation shown in **Error! Reference source not found.** Slides were observed under the microscope Olympus BX53M and images were taken with Olympus SC100 camera. Image analysis was performed using ImageJ 1.8v software.

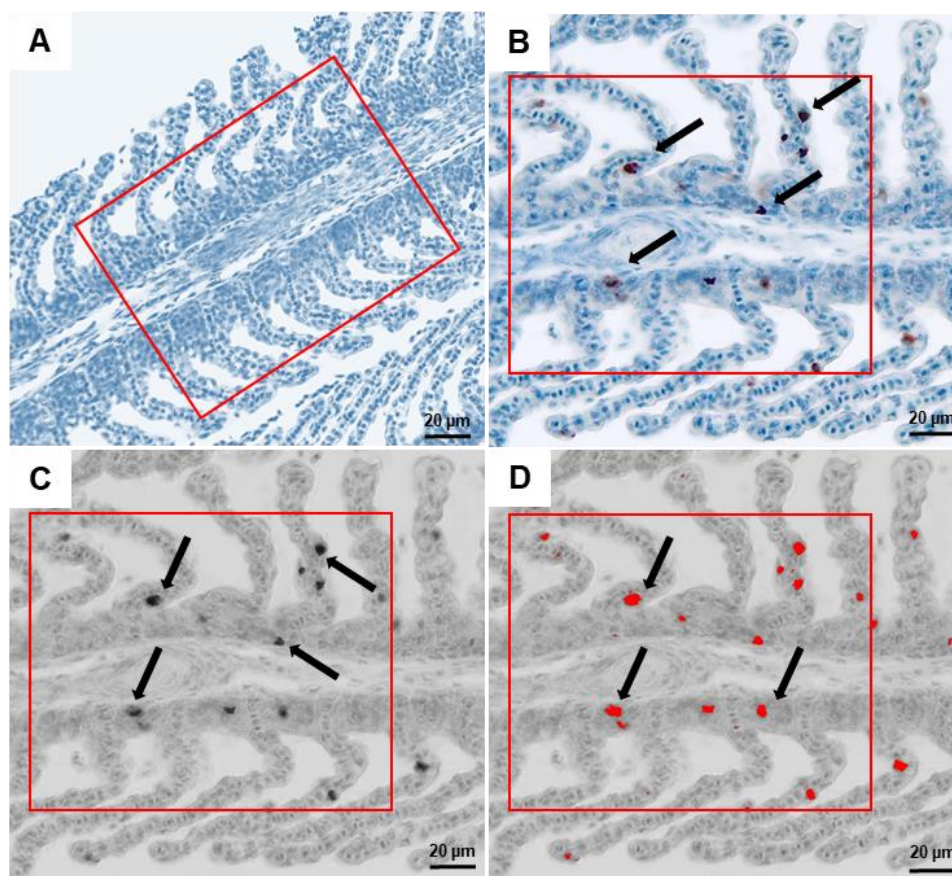


Figure 4.2. Image analysis for the semi-quantitative analysis of CD3⁺ cells expression in control and 14 dpt *A. salmon* gills. A) Control slide without CD3 antibodies. Note no red coloured cells were observed within the selected 10 lamellae inside the red rectangle. B) Antibody labelled slide showing CD3 antibody labelling (red coloured cells) within the selected 10 lamellae described inside the red rectangle (arrows). C) Selection of the blue channel image after separation of the image into different

channels for image analysis. Arrows show the intense black coloured cells (positive for CD3 antibodies). D) Resulting image after applying a 0 – 120 threshold range, masking the CD3⁺ cells in red (arrows).

$$CD3 + \text{ cell expression ratio} = \frac{\% \text{ experimental time points area stained}}{\% \text{ control slides area stained}}$$

Figure 4.3. Equation used for the calculation of the CD3⁺ cell expression.

4.2.8. Statistical analysis

All the results obtained from the semi-quantitative analysis and image analysis for CD3⁺ cell expression quantification were exported to IBM SPSS statistical analysis software (v23, IBM Corporation) and were all processed and tested to determine significant differences between mucous cell counts and cell expression within the different time points and fish. Kolmogorov-Smirnov test was first performed on the data, in order to verify normality. As a result of non-normalised data, a Kruskal-Wallis was performed on the data, in order to examine the significance between medians (time-point after treatment vs semi-quantification of mucous cells; time 0 fish vs time 14d fish for the CD3⁺ cell expression quantification). Mann Whitney test was performed between the two sets of data from time 0 fish and 14d fish to investigate significant differences between fish.

Regarding the qPCR results, Kolmogorov-Smirnov test was performed on the data, in order to verify normality again. Data were then subjected to a one-way ANOVA to examine the significance between means (untreated fish (0 h) vs different time points post-treatment; untreated fish (0 h) vs high and low AGD-fish) for the gene expression. A further *post-hoc* Tukey HSD test was conducted to confirm the differences between groups.

4.3. Results

4.3.1. Macroscopic analysis of gill pathology

No signs of gross pathology were observed in AGD-challenged fish. Likewise, the macroscopic examination of the gills of the 24 h control groups, showed no signs of pathology associated with *N. perurans* colonisation. According to the modified AGD grading criteria of Taylor *et al.* (2009) no fish proved to have scores higher than 0.5.

Slides were observed under the microscope Olympus BX53M and images were taken with Olympus SC100 camera. Control fish presented no pathological signs (Figure 4.4.). The H₂O₂ treated fish were screened (at 4 h, 24 h and 14 d after treatment). All these fish revealed similar signs of pathology: most of them showed focal epithelial lifting, with signs of light to more pronounced areas of interstitial oedema (Figures **Error! Reference source not found.**, Figure 4.6. & **Error! Reference source not found.**). The samples taken 4 h post-treatment also revealed the occasional presence of aneurism of the secondary lamellae tips (**Error! Reference source not found.**). No trophozoites of *N. perurans* were found in any of the tissue sections.

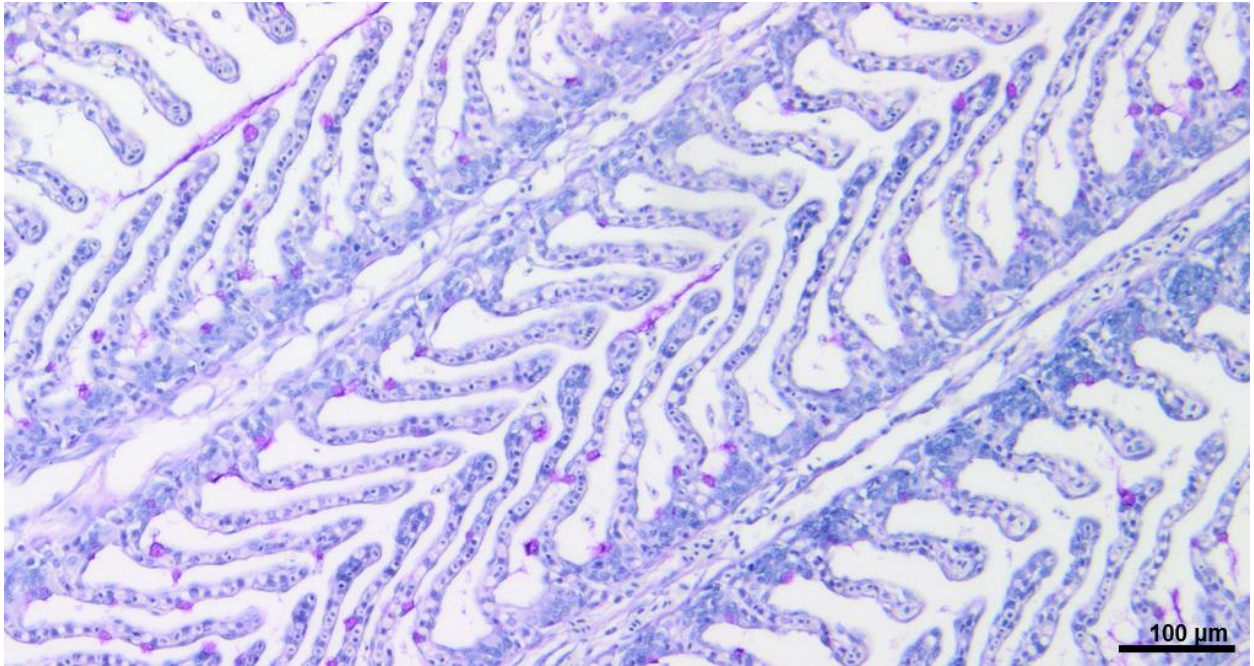


Figure 4.4. Light micrograph of PAS staining of Davidson's fixed gills. Control (0h) non-AGD-challenged fish presenting no signs of pathology.

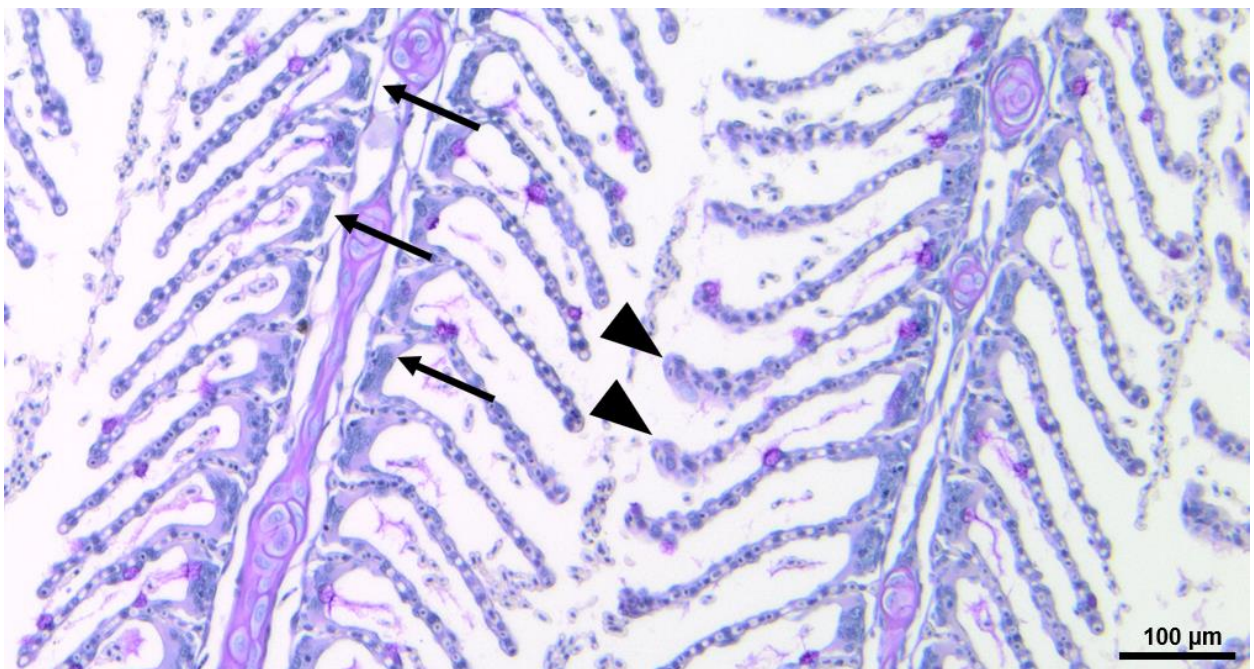


Figure 4.5. Light micrograph of PAS staining of Davidson's fixed gills. H₂O₂ treated fish from the non-AGD- challenged group 4 h post-treatment presenting some epithelial lifting and oedema (arrows) and some aneurism in secondary lamellae tips (arrow heads).

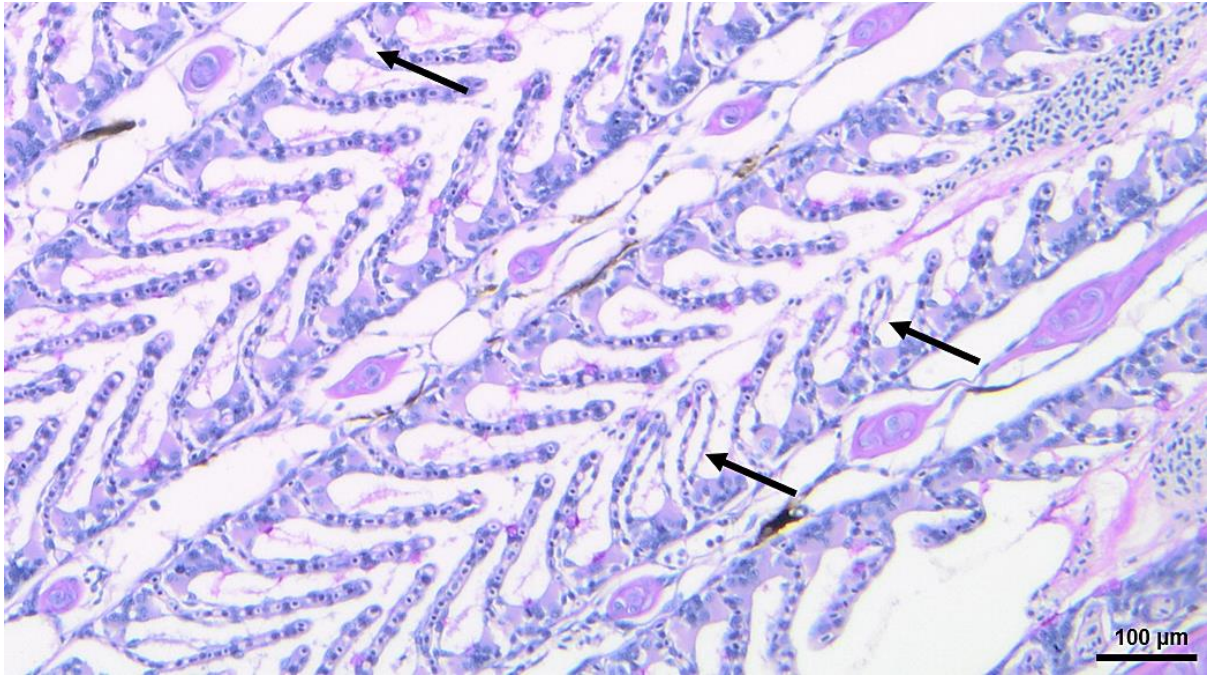


Figure 4.6. Light micrograph of PAS staining of Davidson's fixed gills. H₂O₂ treated fish from the non-AGD- challenged group 24 h post-treatment presenting some epithelial lifting and oedema (arrows).

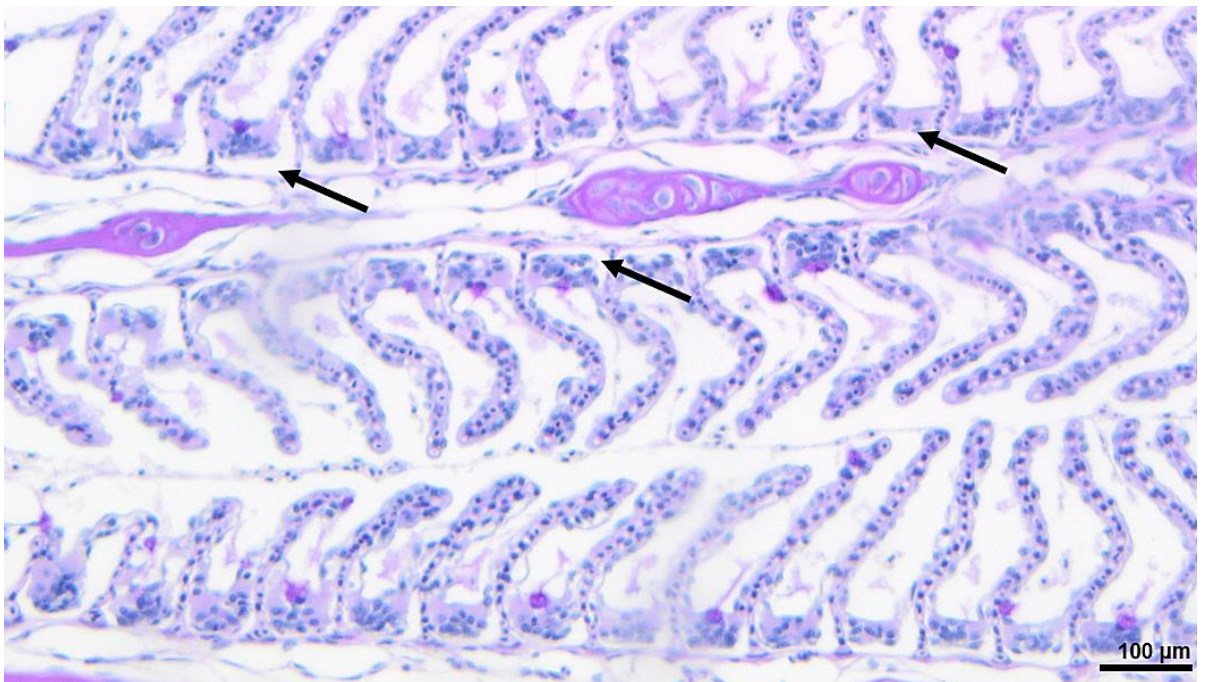


Figure 4.7. Light micrograph of PAS staining of Davidson's fixed gills. H₂O₂ treated fish from the non-AGD- challenged group 14 dpt presenting some epithelial lifting and oedema (arrows).

4.3.2. TaqMan RT-qPCR: *N. perurans* load quantification

The results from the RT-qPCR performed on the DNA samples were negative and/or inconclusive. Therefore, RT-qPCR provided no evidence that AGD was present during the treatment of the fish.

4.3.3. Gill gene expression

Gene expression was quantified in relation to the geometric mean of the three reference genes EF1- α , β -actin and β -tubulin. This was performed using the untreated fish (timepoint 0 h) as a control group against the non-AGD challenged fish after hydrogen peroxide treatment and the additional AGD-affected fish (fish with low (scores 1-2) and high grade AGD (scores 3-4)). The C_t values of the reference genes were tested for differences between time points (4h, 24h, 14d). This was performed to confirm that the treatment had no effect on their constitutive expression levels, and that they were suitable for standardising the expression of the genes of interest.

4.3.3.1. Expression in non-AGD challenged fish after hydrogen peroxide treatment

Quantitative RT-PCR results showed that T-cell activity appeared significantly up-regulated 14 d post-H₂O₂ treatment, in TCR α chain ($p < 0.001$, $n = 5$), CD8 α ($p < 0.001$, $n = 5$) and CD3 $\gamma\delta$ -B ($p < 0.05$, $n = 5$) transcripts. Up-regulation of the IL-4/13 β 2 cytokine was also observed after 14 d post-treatment ($p < 0.05$, $n = 5$) (Figure 4.8. A&C). This was supported by the lack of changes observed in TNF- α 2 ($p > 0.05$; $n = 5$) response (Figure 4.8. C). No significant B-cell response was observed at any of the timepoints (Figure 4.8. B).

Significant down-regulation was, however, observed in IL-22 ($p < 0.001$, $n = 5$) across all time points. (Figure 4.8. C) and in the three mucin genes after 14 d post-treatment ($p < 0.001$, $n = 5$) (Figure 4.9.).

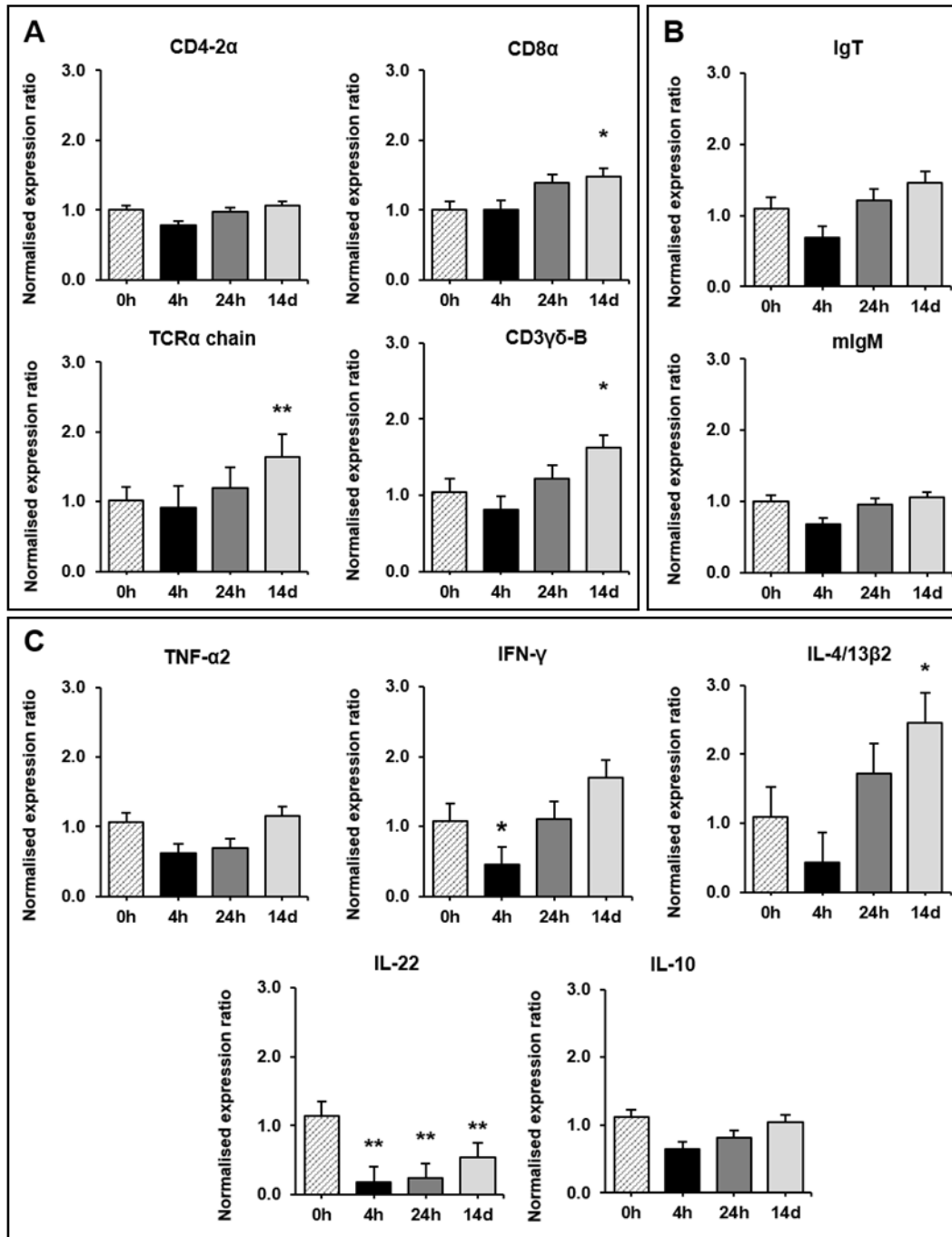


Figure 4.8. Quantitative RT-PCR analysis of (A) T-cell, (B) B-cell, and (C) Th1/Th17 and Th2 pathway-related transcript expression in gill samples from non-AGD-infected Atlantic salmon after hydrogen peroxide treatment at different time points (0h, 4h, 24h and 14 d). Statistical differences were determined by a one-way ANOVA and subsequent *post-hoc* Tukey HSD test. Results are normalized expression ratios (mean \pm s.e.m, $n = 5$) of the expression of these transcripts in relation to untreated fish time point 0h. Asterisk (*) denotes statistically significant regulation in target transcript expression relative to the time zero fish ($p < 0.05$) while double asterisks (**) represent highly significant regulation ($p < 0.001$).

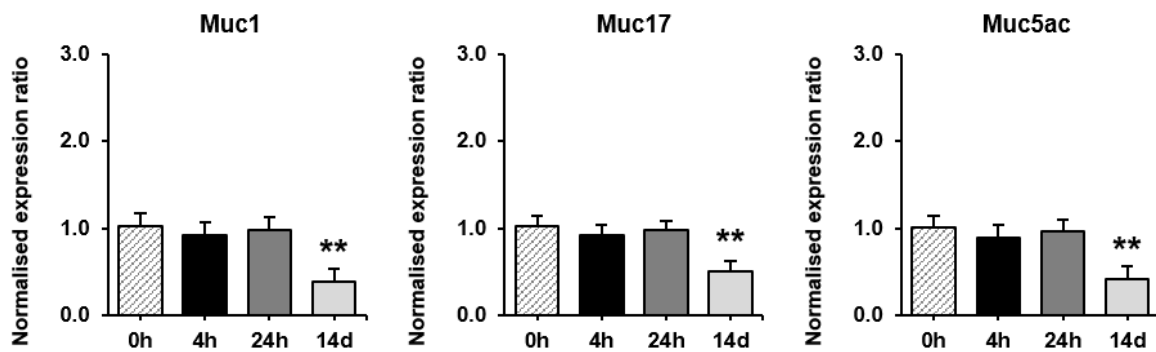


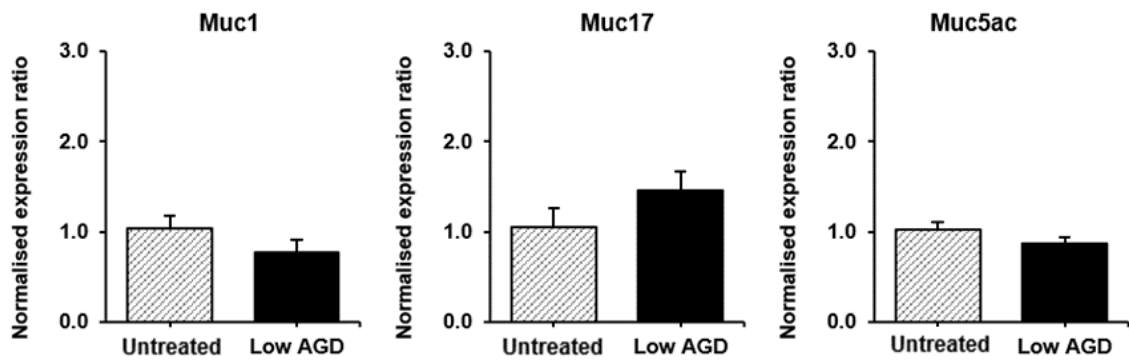
Figure 4.9. Quantitative RT-PCR analysis of mucin-related transcript expression in gill samples from non-AGD-infected Atlantic salmon after hydrogen peroxide treatment within different time points (0h, 4h, 24h and 14 d). Statistical differences were determined by a one-way ANOVA and subsequent *post-hoc* Tukey HSD test. Results are normalized expression ratios (mean \pm s.e.m, n = 5) of the expression of these transcripts in relation to untreated fish time point 0h. Asterisk (*) denotes statistically significant regulation in target transcript expression relative to the time zero fish ($p < 0.05$) while double asterisks (**) represent highly significant regulation ($p < 0.001$).

4.3.3.2. Expression in AGD-challenged fish

Additional AGD-affected fish from an experimental challenge in a previous trial (Chalmers *et al.*, 2017) were used. Five fish were sampled after 7 dpi presenting low scores (1-2) and additional five fish were sampled after 28 dpi which presented high scores (3-4). This was performed to assess the immune and mucin response during an early (Low AGD) and late stage (High AGD) of an AGD-infection. To compare the transcript expression, the AGD fish were compared to the untreated fish (timepoint 0 h) from the H₂O₂ trial.

There were no changes observed for nearly all tested immune-related transcript expression after 7 dpi, during the early stage of the disease. Only IL-10 was significantly up-regulated ($p < 0.001$, n = 5). Some T-cell activity was observed through elevated levels of transcripts of CD8 α and TCR α chain transcripts, but this was not significant ($p > 0.001$; n = 5) (**Error! Reference source not found.A**). Additionally, decreased levels of CD3 $\gamma\delta$ -B and IL-4/13 β 2 transcript mRNA was observed but again was not significant ($p > 0.001$; n = 5) (**Error! Reference source**

not found.A&C). Finally, no significant mucin expression changes were observed (



).

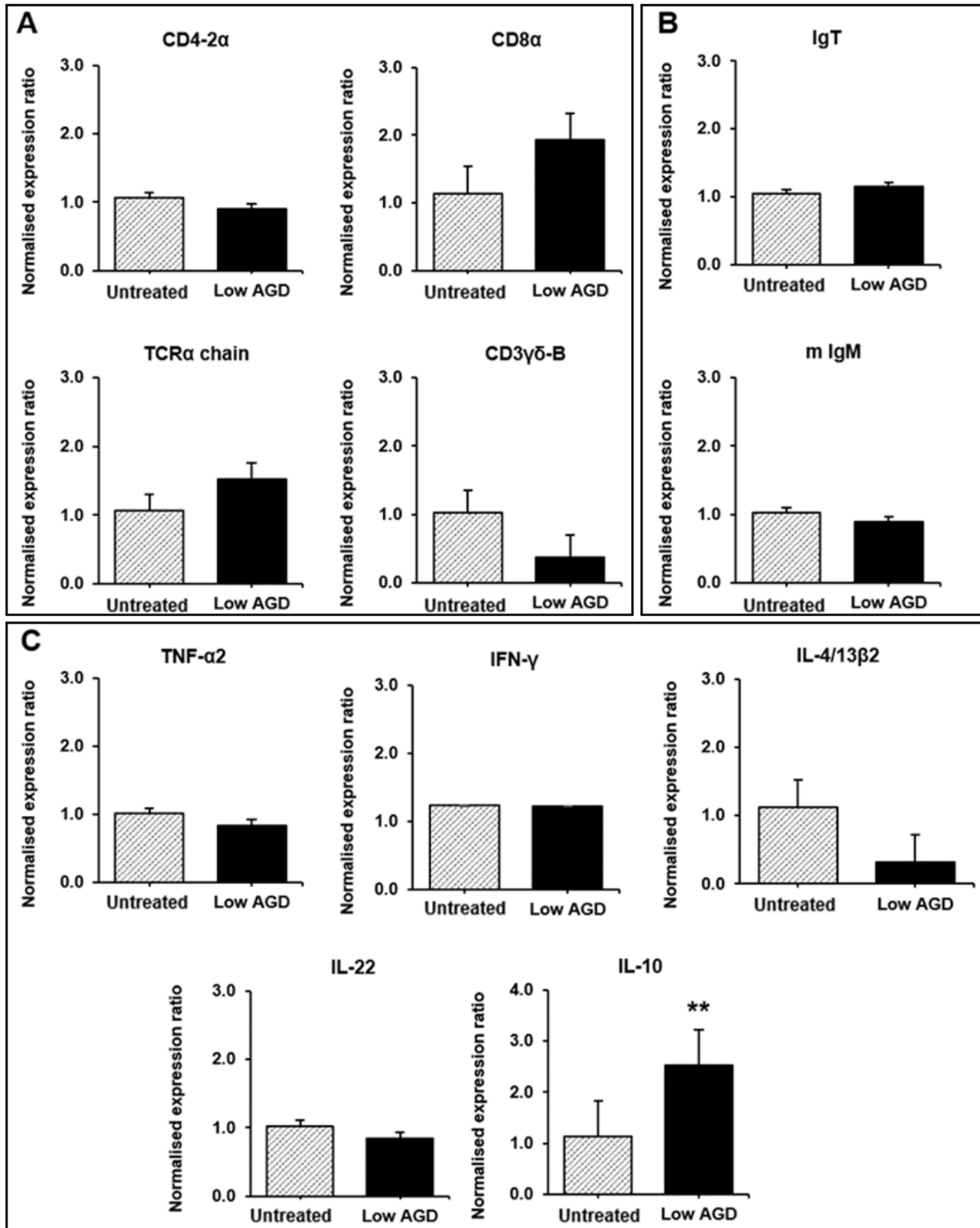


Figure 4.10. Quantitative RT-PCR analysis of (A) T-cell, (B) B-cell, and (C) Th1/Th17 and Th2 pathway related transcript expression in gill samples from fish during an early AGD infection stage (7 dpi) (Low AGD; scores 1-2) and control fish. Statistical differences were determined by a one-way ANOVA and subsequent *post-hoc* Tukey HSD test. Results are normalized expression ratios (mean \pm s.e.m, n = 5) of the expression of these genes in relation to untreated fish time point 0h. Asterisk (*) denotes statistically significant regulation in target gene expression relative to the time zero fish ($p < 0.05$) while double asterisks (**) represent highly significant regulation ($p < 0.001$).

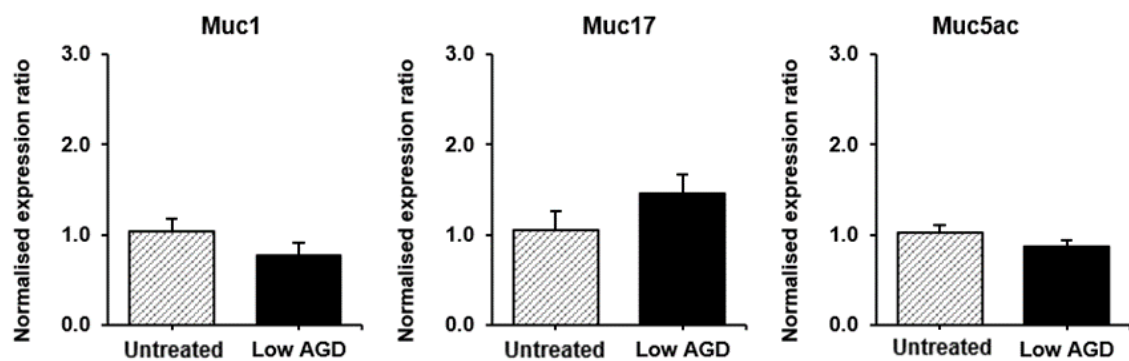


Figure 4.11. Quantitative RT-PCR analysis of mucin-related transcript expression in gill samples from fish during an early AGD infection stage (7 dpi) (Low AGD; scores 1-2) and untreated fish time point 0h. Statistical differences were determined by a one-way ANOVA and subsequent *post-hoc* Tukey HSD test. Results are normalized expression ratios (mean \pm s.e.m, n = 5) of the expression of these genes in relation to untreated fish time point 0h. Asterisk (*) denotes statistically significant regulation in target gene expression relative to the time zero fish ($p < 0.05$) while double asterisks (**) represent highly significant regulation ($p < 0.001$).

Unlike the analysed fish during the early stage of AGD infection, fish from the 28 dpi time point exhibited significant expression changes within the studied immune genes. This could be potentially due to the level of progression of the disease after 28 dpi, in comparison to the 7 dpi time point, during which no general response is detected. T-cell activity was down-regulated, CD4-2 α ($p < 0.001$, n = 5), TCR- $\alpha 2$, CD8 α and CD3 $\gamma\delta$ -B ($p < 0.05$, n = 5) (**Error! Reference source not found.A**). Regarding the B-cell response, m IgM appeared down regulated ($p < 0.01$, n = 5). Additionally, genes associated with both inflammatory and anti-inflammatory responses showed a general down-regulation in IFN- γ ($p < 0.001$, n = 5), IL-4/13 $\beta 2$ ($p < 0.05$, n = 5), IL-22 ($p < 0.001$, n = 5) and IL-10 ($p < 0.05$, n = 5) (**Error! Reference source not found.B&C**). Elevated levels of TNF- $\alpha 2$ transcripts were apparent but not significantly differently ($p > 0.001$; n = 5) (**Error! Reference source not found.C**). The mucin response was down-regulated as noted for all three mucins analysed ($p < 0.001$, n = 5) (**Error! Reference source not found.**).

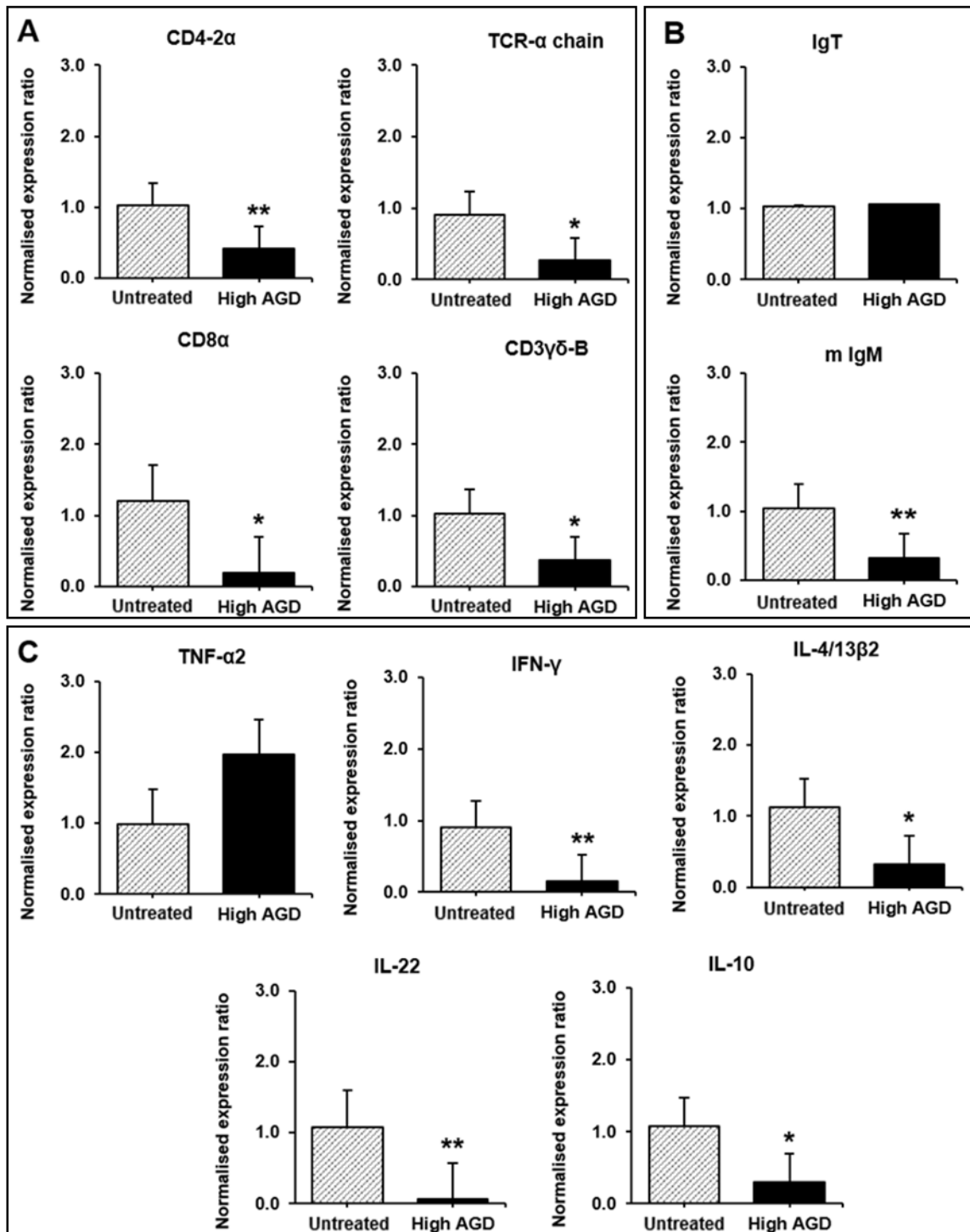


Figure 4.12. Quantitative RT-PCR analysis of (A) T-cell, (B) B-cell, and (C) Th1/Th17 and Th2 pathway related transcript expression in gill samples from fish during a late AGD infection stage (28 dpi) (High AGD; scores 3-4) and control fish. Statistical differences were determined by a one-way ANOVA and subsequent *post-hoc* Tukey HSD test. Results are normalized expression ratios (mean \pm s.e.m, n = 5) of the expression of these genes in relation to untreated fish time point 0h. Asterisk (*) denotes statistically significant regulation in target gene expression relative to the time zero fish ($p < 0.05$) while double asterisks (**) represent highly significant regulation ($p < 0.001$).

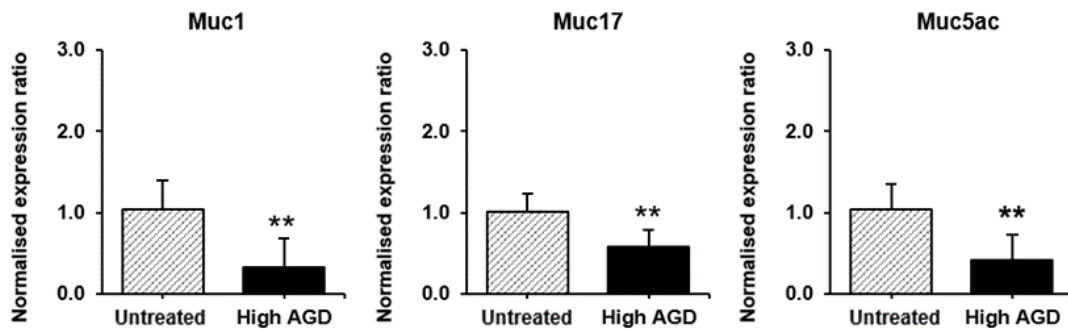


Figure 4.13. Quantitative RT-PCR analysis of mucin related transcript expression in gill samples from late AGD-infected fish (High AGD; scores 3-4) and control fish. Statistical differences were determined by a one-way ANOVA and subsequent *post-hoc* Tukey HSD test. Results are normalized expression ratios (mean \pm s.e.m, n = 5) of the expression of these genes in relation to untreated fish time point 0h. Asterisk (*) denotes statistically significant regulation in target gene expression relative to the time zero fish ($p < 0.05$) while double asterisks (**) represent highly significant regulation ($p < 0.001$).

4.3.4. Mucous cells semi-quantitative analysis and qualitative assessment of mucus production

Fish treated with H₂O₂ were used for this analysis looking at the differences in mucous cell numbers in all the time points (0h -untreated-, 4h, 24h and 14 dpt). Different distributions were observed when an ANOVA test was performed on the data ($p < 0.05$). Results for the semi-quantification of the mucous cells showed a significant decrease in mucous cell number 14 dpt compared to the untreated fish (0h) (*post-hoc* Tukey HSD test; $p < 0.001$; $n = 6$) (Figure 4.14.).

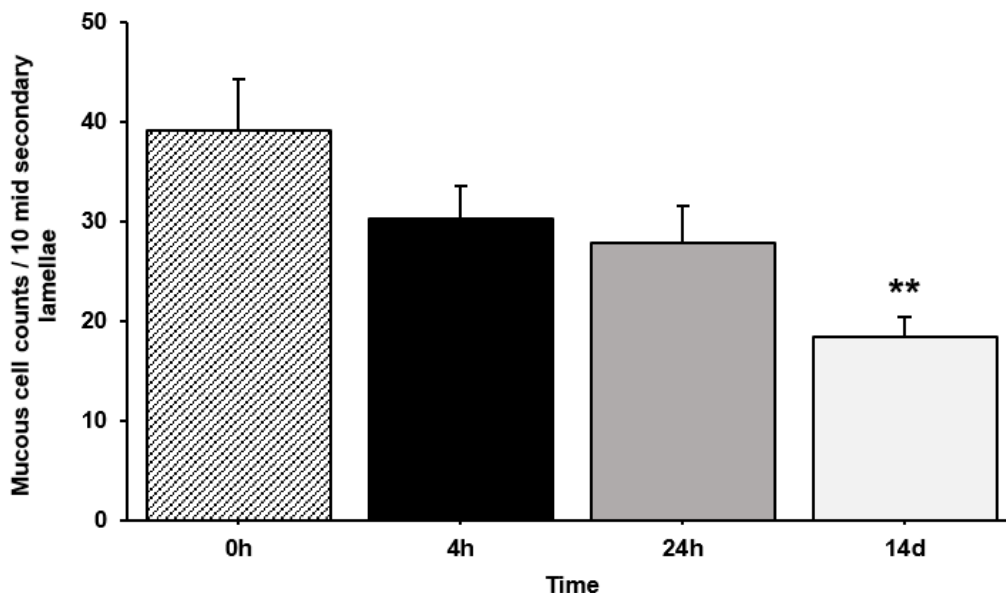


Figure 4.14. Mucous cells semi-quantitative analysis. Graph showing the mucous cell counts across all the time points 0 h, 4 h, 24 h and 14 d. Bars represent mean mucous cell counts \pm s. e. m, $n = 6$, 3 random fields of 10 interlamellar spaces; *post-hoc* Tukey HSD test: $p < 0.001^{**}$).

Mucous cell counts for AGD-challenged fish were performed during the investigation described in Chalmers *et al.* (2017). Fish showed higher numbers of mucous cells in the 28 dpi fish (343.0 ± 2.0) in comparison to the 7 dpi fish (288.0 ± 38.0), although with no statistically significant change (Chalmers *et al.*, 2017).

In addition to this semi-quantitative analysis some representative images from the H₂O₂ trial fish treated with hydrogen peroxide control (0h) and 14 dpt fish were captured to assess the differences in mucus production. As we can observe in Figures 4.15 and 4.16 **Error! Reference source not found.**, higher mucus traces

are seen in the control fish in comparison to the 14 dpt fish where less presence of mucus traces can be perceived. Due to the size of the tissue sample and the intense use of the histological blocks, no mucus quantification could be assessed, hence use of representative images of the slides. Tissue sections presented also mucous cells (empty and full of mucus), apart from the presence of additional mucus traces; however a higher number of mucous cells were observed in the gills from time point 0h as the graph from Figure 4.14 shows.

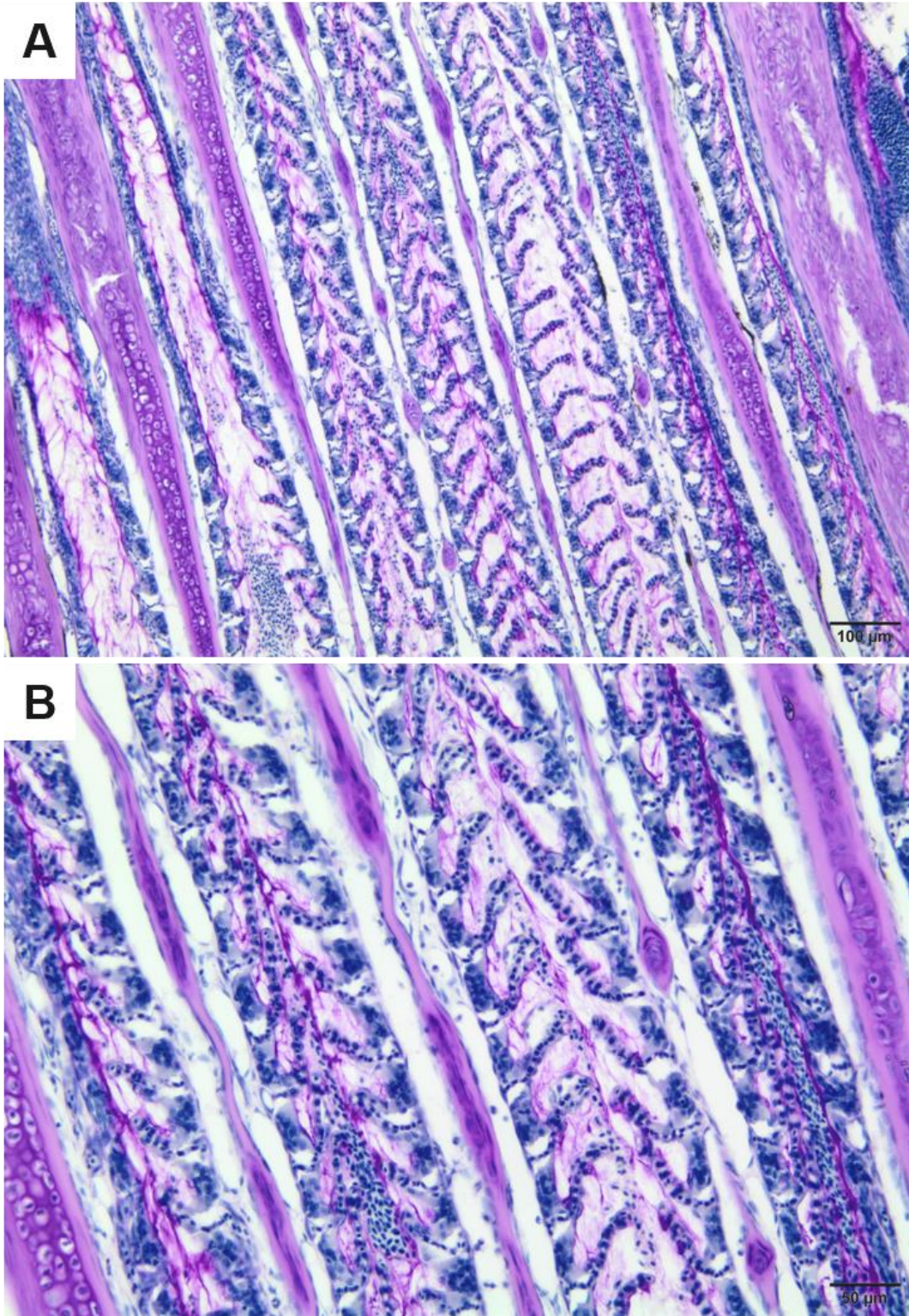


Figure 4.15. Qualitative assesment of mucus production in untreated fish (timepoint 0 h) (A & B). Mucus traces can be observed in bright pink between the secondary lamellae. Methacarn fixed gill sections from control fish were stained with PAS staining.

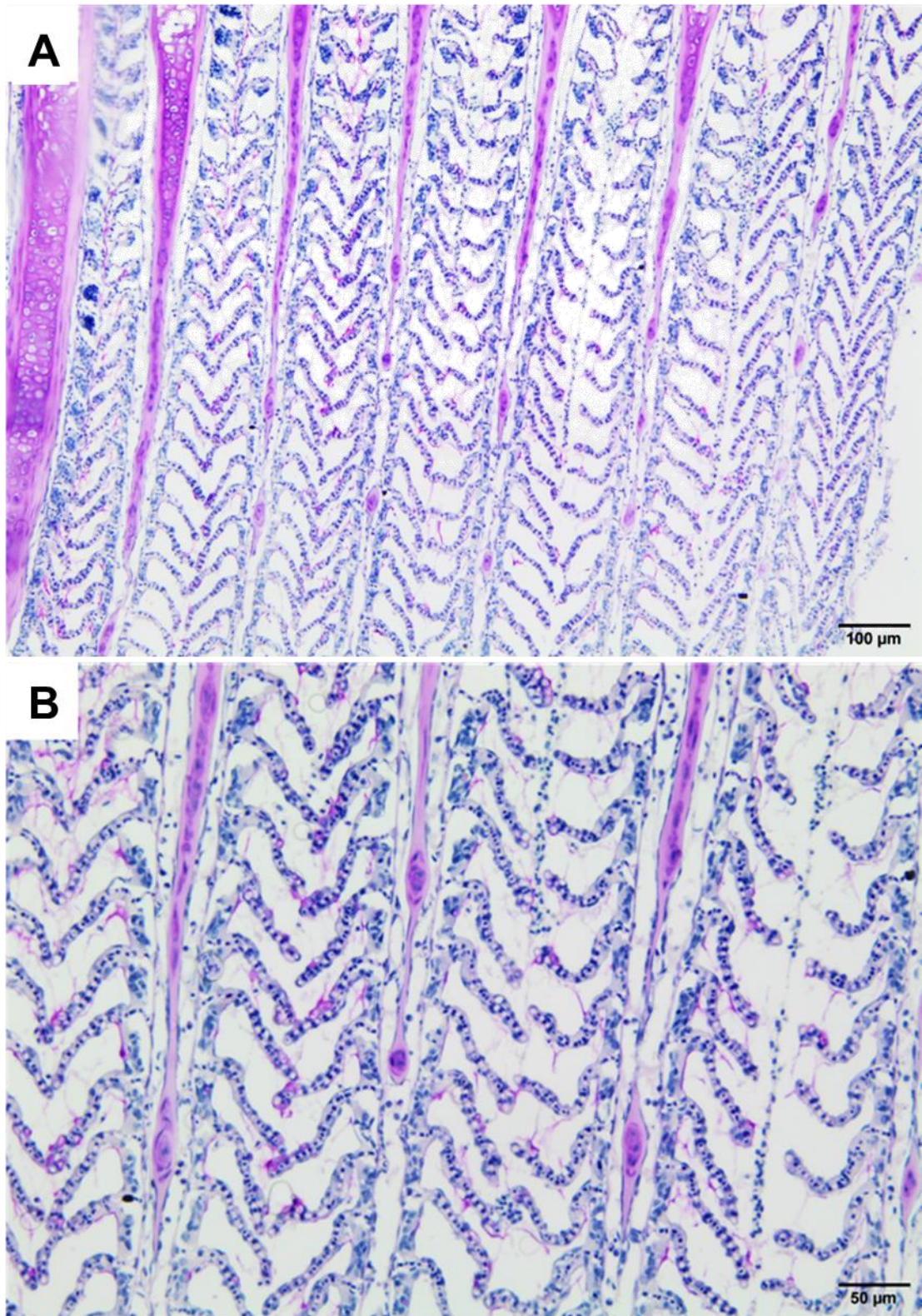


Figure 4.16. Qualitative assesment of mucus production in 14 dpt fish (A & B). Less mucus traces can be observed in bright pink between the secondary lamellae. Methacarn fixed gill sections from 14 dpt fish were stained with PAS staining.

4.3.5. Immunohistochemistry for CD3⁺ cell expression quantification

Expression of CD3⁺ cells was found to be higher in the group of fish 14 dpt (**Error! Reference source not found.**), although this was not statistically significant ($p = 0.1203256$) when compared to the untreated fish (T0 fish) (Figure 4.17). This was likely due to the high variation between individual fish.

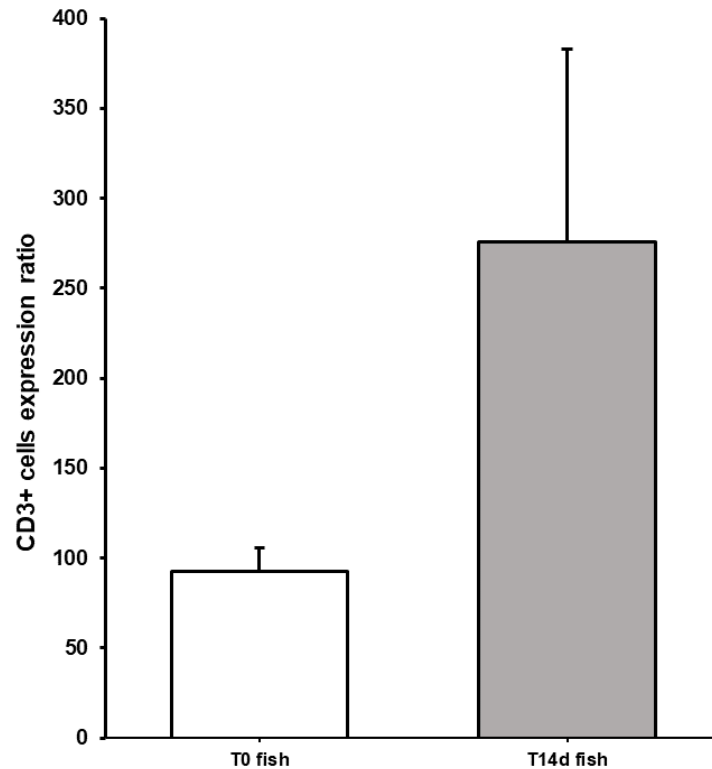


Figure 4.17. Quantification of the CD3⁺ cell expression on the gills of Atlantic salmon in untreated fish (T0 fish) and 14 dpt fish (T14d fish). Error bars show s.e.m. No statistical differences were observed between the two groups ($p > 0.05$).

Slides were observed under a compound microscope (Olympus BX53M) and representative images from this immunohistochemistry experiment were taken using an Olympus SC100 camera. Control slides with no CD3 antibody can be observed in **Error! Reference source not found.**, where no red colouration is observed. For the time 0h fish, red coloured cells can be observed (**Error! Reference source not found.**) but in less quantity than in the 14d fish (Figure 4.20.). However, not all fish showed the very obvious colouration, there was a lot of variation between slides and fish. This could be due to the different responses to the treatment between fish. Also,

different cell distributions along the primary and secondary lamellae could be the reason for high variability.

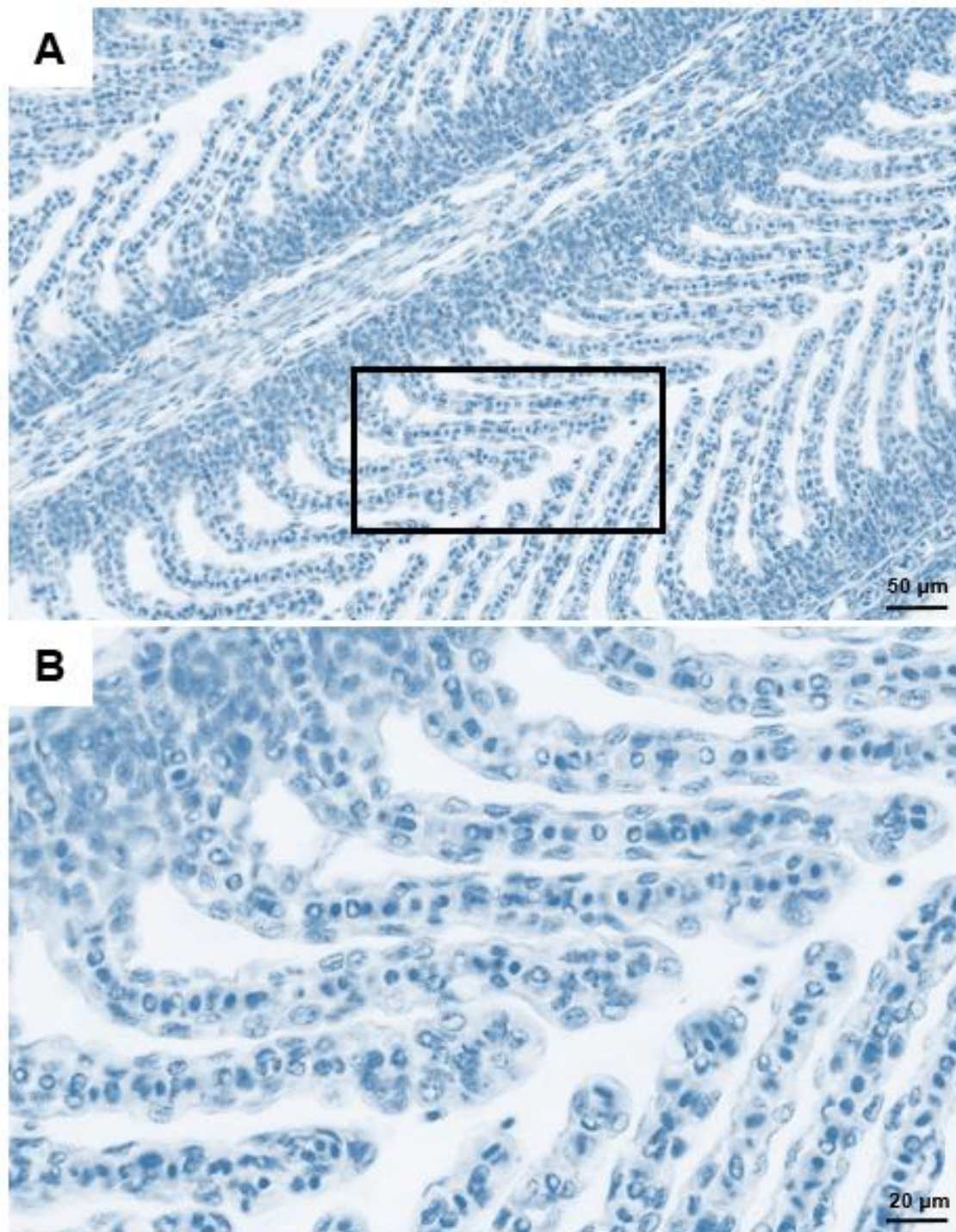


Figure 4.18. Representative images from control gill sections with no CD3+ primary antibody added. A. Control slide with the washing buffer and no antibody added. B. Higher magnification of detailed area in Figure 4.18A.

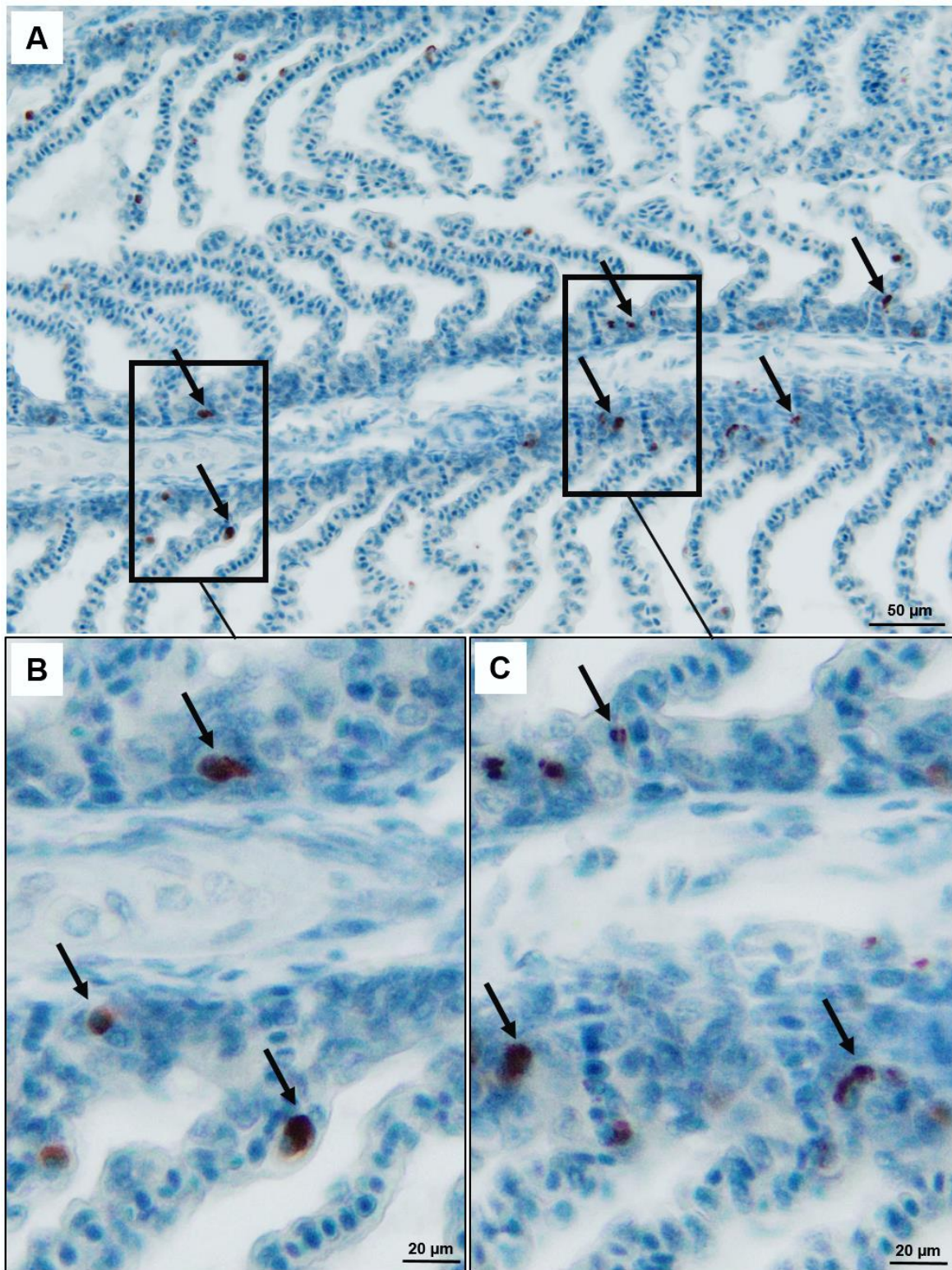


Figure 4.19. Representative images from time 0h fish slides with CD3+ primary antibody added. A. Time 0h fish slide with antibody added. Arrows indicate the presence of CD3+ cells along the primary and second lamellae. B & C. Higher magnification of detailed area in figure 4.19A.

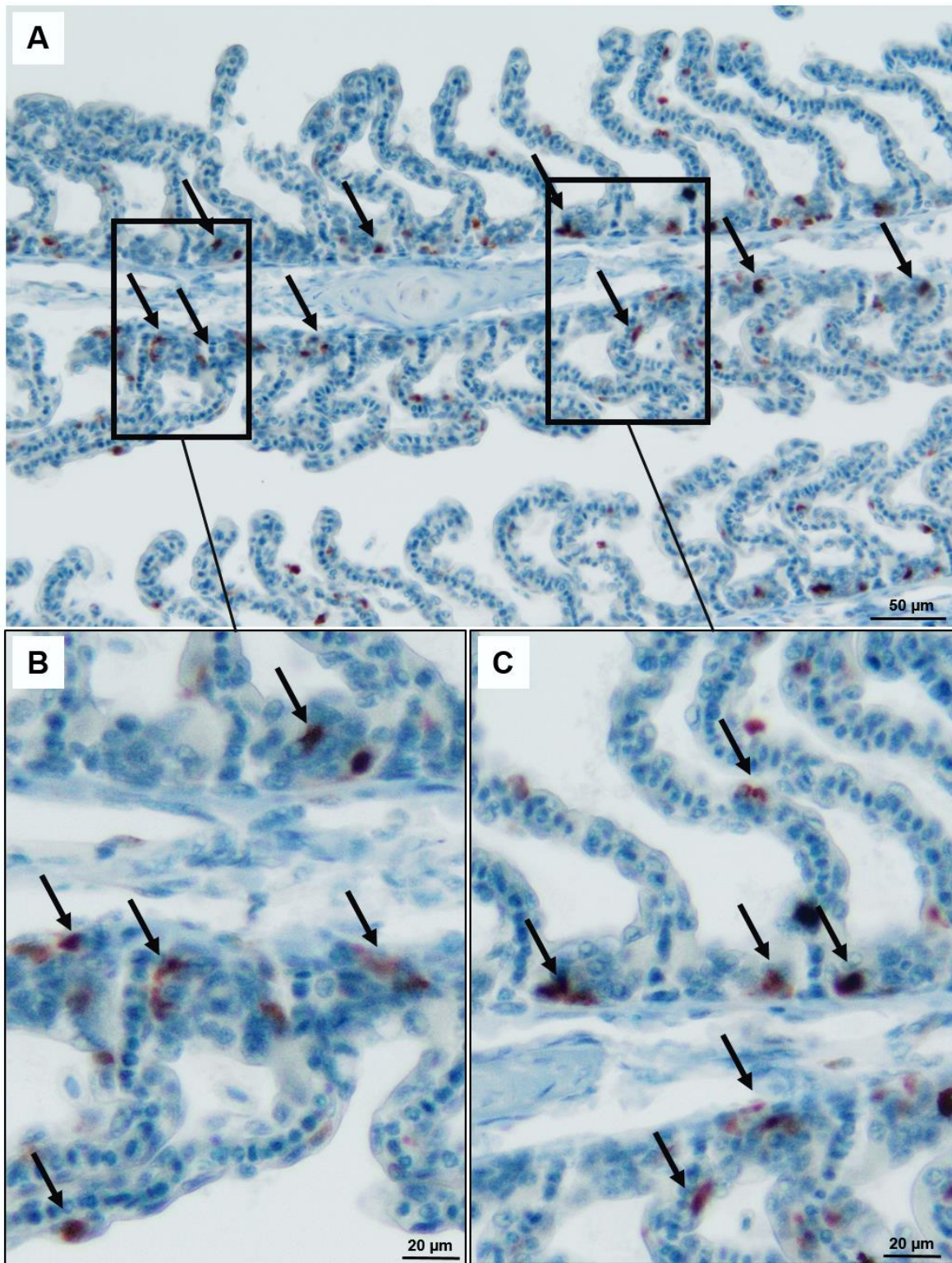


Figure 4.20. Representative images from time 14d fish slides with CD3+ primary antibody added. A. Time 14d fish slides with antibody added. Arrows indicate the presence of CD3+ cells along the primary and second lamellae. B & C. Higher magnification of detailed area in figure 4.20A.

4.4. Discussion

In this experimental chapter, the impact of the commonly used treatment H_2O_2 on the salmon gill was investigated to determine if its use would have implications for the fish immune and mucin response. During the current study, the use of H_2O_2 as a treatment for AGD caused several changes in the fish gills throughout the course of the treatment. Even though dramatic changes in the gills were not observed histologically at the time points examined (*i.e.* 0 h, 4 h, 24 h and 14 dpt), mild clinical signs were observed. Overall, mostly epithelial lifting was observed throughout the different time points, with no obvious signs of pathology within the control fish. This light damage to the gill tissue corresponded to some degree to the pathology observed in previous studies. The effect of longer exposures (over 20 min) and high temperatures ($14^\circ C$) on the gills was investigated by Kierner & Black (1997) proving that these factors caused gill damage and indeed mortality. During another study by Speare & Arsenault (1997), an assessment of the gills was performed after a treatment with hydrogen peroxide. The first sampling point was performed at 7 dpt, followed by 14 dpt. At 14 dpt, greater pathological effects (*i.e.* lamellar fusion, epithelial layer destruction) were reported, which differs to our experiment where only light evidence of epithelial lifting were observed. These differences might have been due to the different sizes of the fish used in the trials, and/or the species investigated (in our case Atlantic salmon instead of Rainbow trout (*Onchoryncus mykiss*)) as well as the different environmental conditions (*e.g.* seawater instead of freshwater, different temperatures *etc.*). All these factors are known to result in different outcomes when using hydrogen peroxide as a treatment (Rach *et al.* 1997). Other studies also evaluated the potentially harmful effects of different doses of H_2O_2 . For example, fish held at a 1500 mg L^{-1} concentration for 20 min and temperatures between the optimal range ($9\text{-}11^\circ C$) lead to the fish gills exhibiting different degrees of necrosis and epithelial lifting depending on the sampling point (Johnson *et al.* 1993; Bowers *et al.* 2002). Such a high concentration of H_2O_2 was not used in the current study (1250 mg L^{-1}), therefore the differences in severity of gill pathology might be due to the use of this lower dose as well as a shorter exposure to the chemical (15 min). In addition, temperature plays an important role in the course of hydrogen peroxide treatment. This has been investigated in different studies in which they determined that lower temperatures ($8\text{-}12^\circ C$) tends to lead to a

higher level of treatment success (Powell *et al.*, 2005; Hytterød *et al.* 2017; Martinsen *et al.*, 2018). However, treatments at higher temperatures, particularly in excess of 15°C have major impacts for fish, particularly if gills are already compromised. Therefore, the temperature used during this trial was always between the range of 10-12°C which has been stated to be optimal for this kind of treatment.

In addition to studying the histopathological effect of H₂O₂ treatment, a semi-quantitative analysis of mucous cells was performed throughout the different time points. Results indicated a slow decrease in the number of mucous cells, with the lowest number of cells observed at 14 dpt. This correlates with the reduced expression of mucins that was observed during gene expression analysis. Thus, it could be speculated that H₂O₂ had an impact on the gill's ability to regenerate mucous cells and mucus production, as has been previously shown in olive flounder *Paralichthys olivaceus* in the study by Hwang, *et al.* (2014). That study investigated the effect of low and high doses of hydrogen peroxide on gill mucus and lysozyme activity. The results showed a decrease of mucous cell numbers when the highest dose was used (500 mg L⁻¹) at 12 dpt with H₂O₂. Previous to these studies, a study by Fast *et al.*, 2002 showed that the variation in mucus lysozyme activity could be related to epidermal thickness and mucus lysosome activities, thus the use of hydrogen peroxide on salmon gills could have critical impact on these activities affecting the mucus production and composition.

The decrease of mucus production and mucous cell numbers translates into the loss of the mucosal coat and therefore, impaired protective covering of the gill epithelium leaving the fish more exposed to the external environment, including invading organisms and antigen exposure (Linden *et al.*, 2008). A consequence of this would be stimulation of immune responsiveness in the gills and may explain the induction of immune gene expression observed using qPCR analysis in this study. Whilst studying transcript markers of the different B, T, Th1/Th17 and Th2 cellular subsets, significant up-regulation of T-cell markers (*i.e.* CD8 α , TCR α chain and CD3 $\gamma\delta$ -B) was observed at 14 dpt, providing strong evidence for the infiltration and involvement of a cellular response (Nakanishi *et al.*, 2011) to potential antigens that the fish gills might have been exposed to due to the loss of the protective mucosal coat. In the work by Takizawa *et al.* (2011), a high number of CD8 α ⁺ cells was observed in mucosal tissues such as intestine and gills. This was investigated in another study

and they described how, in order to provide an efficient gas exchange with the aqueous environment, gill epithelia and the protecting mucus layer are relatively thin. Therefore, the risk of pathogen entry is higher and this is probably the reason for the high abundance of T lymphocytes in the teleost gill (Jiang *et al.*, 2009). Closely related to CD8 α transcript, there are TCR α chain, CD3 $\gamma\delta$ -B and IFN- γ . The latter target does not show a significant up-regulation, however, there is a tendency for increase, just like the other closely-related targets. Ultimately, all these complexes can functionally interact with MHC molecules on antigen presenting cells culminating in T cell activation. The same up-regulation of the CD8 gene was also observed in a study by Henriksen *et al.* (2015) in which gills from rainbow trout were exposed to H₂O₂. The difference between this study and the one described in this chapter is the fact that treatment and infection were studied together, therefore they could determine if the treatment affected the immune response to the pathogen. The present work could only conclude there are evident differences in response which could be attributed to the physical effect of H₂O₂ on the gills, related to stress or maybe both.

An additional up-regulation of the Th2 cytokine IL-4/13 β 2, which is known to have an anti-inflammatory capacity (Fallon *et al.*, 2002), may be induced to prevent extensive inflammatory responses that may occur beyond pathogen/agent clearance. This will avoid further damage to healthy gill tissue by chronic inflammation, causing down-regulation of the immune response till homeostasis is reached (Vigano *et al.*, 2012; Wang *et al.* 2016). In addition to this cytokine, a down regulation was observed in the IL-22 cytokine, which has been studied and characterised as having a role in activating antimicrobial peptide genes and antibacterial immunity (Liang *et al.*, 2006; Aujla *et al.*, 2007; Aujla *et al.*, 2008; Sang & Blecha, 2008; Khader *et al.*, 2009; Monte *et al.*, 2011; Qi *et al.*, 2015). Hence, its down-regulation may have implications for the presence of bacterial pathogens in the gill and the ability of salmon to resist a potential pathogen/agent such as *N. perurans*.

In addition to the gene expression analysis, immunohistochemical analyses were performed to support immune transcript expression observations. T-cells are found to be distributed in many tissues of the fish, however, accumulations of these cells are greater in the thymus, spleen and, have more recently been reported gill in tissue, where lymphoid structures were characterised (Jiang *et al.*, 2009; Koppang *et*

al., 2010). As the development of the CD3 antibody applied for IHC in the current study was not undertaken till after this trial, and the targeted T cell analysis was only decided following qPCR analysis (which revealed T cell activity), sampling of the interbranchial lymphoid tissue was not initially undertaken for the gills. Therefore, the distribution of the CD3⁺ cells were only assessed along the primary and secondary lamellae through image analysis (ImageJ software). This kind of pathological analysis remains, however, a time-consuming and somewhat subjective procedure. Usually, antibody staining is manually conducted and therefore the scoring decision is directly influenced by visual bias. This manner encouraged us to develop a simple method of automated IHC image analysis technique to provide a minimally biased, quantitative assessment of antibody staining intensity in tissue sections. As explained before, a higher expression of CD3- $\gamma\delta$ gene was observed in the fish at 14 dpt in comparison to the control fish (0h). Although the gene expression analysed the regulation of a CD3 variant, the immunohistochemistry revealed a higher expression of CD3⁺ cells within the 14 dpt group of fish. However, fish had to be looked at individually due to the high variation between individuals. This variation was therefore not statistically significant, but this could be due to the small number of replicates counted on only the 3rd gill arch. Therefore, increasing the replicates on different gill arches could reveal whether the trend observed is statistically significant. Perhaps, future work could also focus on investigating these differences specifically within the ILT of the gill. However, there was a high expression of CD3 cells in a few of the positive fish, indicating an obvious effect on these cells 14 dpt.

In contrast to the response to H₂O₂, AGD-infected fish showed different outcomes in terms of immune and mucin response. During the study by Chalmers *et al.* (2017), Atlantic salmon gills showed no apparent signs of inflammation nor parasite presence at 7 dpi (scores 1-2); however, at 28 dpi (scores 3-4), although a high degree of hyperplasia and hypertrophy of the gill epithelial cells was observed. In addition to histopathological assessment Chalmers *et al.* (2017) also performed a quantification of the mucous cells. Although the method used here was different to that implemented in the Chalmers *et al.* study, the number of mucous cells were significantly higher in the long-term infection high score (3-4) AGD-infected gills in comparison to the shorter infection low score (1-2) AGD-infected individuals. In the present study, a differential mucin response was absent when fish from the early

stage of AGD infection were compared to the control fish. Nevertheless, a trend was observed in Muc17 showing a slight up regulation. This differs to the response found within the fish from the late stage of AGD infection, whereby all mucins were down regulated. Our results differ from those described in the study by Marcos-Lopez *et al.* (2018), where Muc5ac was found to be highly up regulated in the gills of AGD-infected fish. However, our results could be explained through different assumptions. When the histopathology of gills from the high AGD-infected fish were assessed, high levels of hyperplasia and hypertrophy were reported. Although the total number of mucous cells was higher in the gill tissue, the number of gill epithelial cells also proliferated. Thus, the ratio of epithelial cells and mucous cells could have had an impact on tissue sampling and subsequent RNA extraction. Therefore, the hyperplasia of these cells in the infected tissue could have affected the ratio of mucin transcripts thus diluting the total number of mucin-specific RNA transcripts resulting in a decrease in their expression profile. Therefore, the level of gill damage could potentially be playing a key role in the context of gene/transcript expression profiles.

With respect to the cytokine TNF- α 2, although its up-regulation was not statistically significant, its expression was higher than in the untreated fish. In humans, TNF- α 2 has been observed to induce necrosis, among other processes such as cell survival and apoptosis (Chu, 2013). Although the variation was not significant, an elevated TNF- α 2 expression profile could be interpreted as a response to developing necrotic tissue due to the high amoebic load and the immunosuppression of the high AGD-infected tissue, although further work would be needed to confirm this. However, the TNF- α 2 isoform has been previously studied in rainbow trout during an *Ichthyophthirius multifiliis* infection and vaccination trial (Akbari *et al.*, 2017). They showed how this isoform was present in gills, however its homologue TNF- α 1 was more highly expressed in the gills. This pro-inflammatory cytokine has already been investigated in the context of AGD (Benedicenti *et al.*, 2015; Marcos-Lopez *et al.*, 2018), thus, it may be playing a role in the recruitment and maintenance of inflammatory cells in the gills.

Along with these results, the immune response differed significantly between the fish from the early and late stage AGD infection. Shorter infection low score (1-2) AGD-infected individuals did not exhibit a stimulated cellular immune response (*i.e.* no significant up-regulation of TCR α chain and CD8 α). This correlates with the

histopathological assessment of the sections which presented no clinical changes. Notably, there was an up-regulation of the Th2 cytokine IL-10, which is known to be anti-inflammatory, playing critical inhibitory roles in a wide range of immune responses including production of cytokines and chemokines, pathogen resistance and immune cell activation. Even though the work was carried out *in vitro*, Cano *et al.* (2019) also described an up-regulation of this IL-10 during early stages of infection of RT gill cells with *N. perurans*. Prior to this, in a study by Gorgoglione *et al.*, 2013, this cytokine was found to have a specific response to the parasite *Tetracapsuloides bryosalmonae* in rainbow trout during a natural outbreak of proliferative kidney disease (PKD). Therefore, it may be an immunomodulatory response which can be exploited by some pathogens, leading to a decrease in antigen-specific and proinflammatory responses that are generally essential to control or end infection as investigated in several studies (Nieuwenhuizen *et al.*, 2006; Forlenza *et al.*, 2008; Saraiva & O'Garra, 2010; Buchmann, 2012). Last, the general response observed within the high AGD-infected fish was a down-regulation in all the markers related to cellular immune responses and B-cell markers (m IgM) and in addition, all the genes related to these Th1/Th17 pathways were found down-regulated (*i.e.* IL-4/13 β 2, IL-22, IFN- γ and IL-10). This response may imply a possible immunosuppression mechanism being performed by the ectoparasite on the host's immune system, similar to what has been previously reported in the study by Steinel & Bolnick (2018) in the stickleback (*Gasterosteus aculeatus*) by its parasitic helminth, *Schistocephalus solidus*. An additional study also investigated this phenomenon in *Trypanosoma cruzi* during a certain phase of Chagas' infection (Ouaisi, *et al.*, 2001). These authors proved the presence of immunosuppressive protein (*Tc52*) through a gene targeting approach, to further explore the biological function, which elicited a complex series of cellular interactions, resulting in specific immune responses, or suppression.

Conclusions

In conclusion, results suggest that H₂O₂ activates a T-cell response in the gills of treated fish due to the decrease of mucous cell numbers at 14 dpt, translating into loss of the protective mucosal coat normally found in healthy fish. These findings underline the importance of preservation of the mucosal surface, which represents a barrier against different agents and pathogens potentially capable of affecting gill

health. These results were supported by the CD3⁺ cell IHC assessment, which although highly variable, presents generally higher numbers in the fish gills at 14 dpt. Contrasting results were found in the AGD-infected fish during different stages of the disease.

Fish with low scores after 7 dpi presented no significant T-cell response, perhaps due to the low level of infection. However, a novel response against a *N. perurans* infection was identified. A specific IL-10 response, possibly parasite specific, was detected causing potential host immunomodulation, *i.e.* a response combating the emerging amoebal infection. Although no significant difference was observed in mucin response, an increasing trend of Muc17 was observed in response to the developing infection.

In contrast, fish showing higher scores after 28 dpi presented a general down-regulation of most T cell associated transcripts, Th1, Th17, Th2 and B cell markers with an increased trend of TNF- α 2 transcripts that although not significant, may be associated with the advanced severity of pathology, potentially reflecting development of necrotic tissue and immunosuppression in heavily-infected gills. In terms of mucin response, down regulation was observed. High levels of hyperplastic infected tissue presenting higher number of epithelial cells could be potentially led to a lower detection of mucin transcripts.

Ultimately, this study suggests that H₂O₂ treatment does not immunocompromise Atlantic salmon but does disrupt the mucus covering of the gills, which may have implications for fish susceptibility to AGD and other pathogens and for responses to a range of other environmental factors. This provides a platform for future research focusing on the mucosal health in salmon.

Chapter 5 : Characterisation of *N. perurans* transcriptome for the *in-silico* prediction of potential vaccine candidates

5.1. Introduction

There remains an urgent need for alternative treatments against amoebic gill disease (AGD). It is considered one of the most threatening diseases in world aquaculture due to high mortality, broad host range, and abundant distribution (Oldham *et al.*, 2016). Recently, the development of effective vaccines to prevent this ectoparasitic disease has been one of the key approaches that aquaculture research has been interested in. This alternative would potentially aid in restricting the use of chemical treatments (*e.g.* hydrogen peroxide) in fish farming, subsequently reducing environmental impact and economic losses within the aquaculture industry. As the repeated use of chemotherapeutants can lead to the development of resistance against them (Burrige *et al.*, 2010), use of vaccines can also prolong the lifetime of chemotherapeutants. In addition, the use of some treatments *e.g.* hydrogen peroxide has a potentially long-lasting impact on the treated fish, as demonstrated in Chapter 4. The development of a vaccine could reduce the impact of chemotherapeutant stress on fish, leading to a more effective long-term solution.

The use of effective vaccines has proven to be one of the key factors aiding the success when culturing salmonids (Brudeseth *et al.*, 2013). Approaches such as the injection of antigens with oil adjuvants have been the most effective ones in the past (Brudeseth *et al.*, 2013). However, the strategies against fish parasites have remained unsuccessful (Crampton & Vanniasinkam, 2007) with no available vaccine, only viral and bacterial vaccines remain licensed (Ma *et al.*, 2019). These licensed fish vaccines have mostly comprised inactivated organisms formulated with adjuvants and delivered via immersion / injection (Ulmer *et al.*, 2012). However, there are more methods used such as modified live vaccines, where pathogens are attenuated/low virulence (Desmettre & Martinod, 1997). This approach is generally more successful due to the greater ability of the host to proliferate an effective immune response, both innate and adaptive (Levine & Sztein, 2004). More recently, vaccine development has been focused on the targeting of specific pathogen components and virulence factors (Hansson, Nygren & Ståhl, 2000). Even though is

not as successful as the other approaches, due to weaker immune responses, the production of a subunit vaccine through the development of recombinant proteins presents potential advantages for pathogens that are difficult to cultivate (Alvarez-Pellitero, 2008).

For the production of subunit vaccines, a more novel tool has been recently adopted. The implementation of a reverse vaccinology / computational approach involves the use of genome information for the *in-silico* discovery of potential antigens/targets within the pathogen (Del Tordello *et al.*, 2017). In addition to genome analysis, transcriptomic and proteomic tools have provided further information about host-pathogen interactions in fish, helping with the identification of potential virulence factors, conserved antigens within a heterogeneous pathogen population and also, antigens that are unique to pathogenic isolates but not present in commensal strains (Duchaud *et al.*, 2007; Want *et al.*, 2009; Morita *et al.*, 2011; Touchon *et al.*, 2011; Nho *et al.*, 2011; Naka *et al.*, 2011; Jiang *et al.*, 2013; Bohle *et al.*, 2014). The results of these investigations have helped to build lists of candidate antigens that could potentially be tested in animal models, reducing the costs and time of downstream analyses (Andreoni *et al.*, 2013; Chiang *et al.*, 2015; Andreoni *et al.*, 2016).

A platform for future studies in vaccines against AGD was set during the study by Findlay *et al.* (1995) in which consecutive infections with *Paramoeba* spp. developed antibody responses in serum samples. In the following years, multiple studies would apply different vaccine methods such as the use of live amoebae, sonicated antigens, glycoproteins and DNA vaccines (Akhlaghi *et al.*, 2001; Zilberg & Munday, 2001; Villavedra *et al.*, 2010; Cook *et al.*, 2008; Cook *et al.*, 2012). However, there were no successful results and some of these studies did not even target the actual causative agent, *Neoparamoeba perurans*. More recently, a recombinant attachment protein (r22C03) was produced by Valdenegro *et al.* (2014a) which was identified using transcriptomics data from *N. perurans*. Investigators observed an induction of both, systemic and mucosal antibodies capable of binding to the surface of the parasite. Thus, by blocking this putative attachment factor using functional antibodies present in the mucosal surfaces it would potentially reduce AGD severity. However, previous studies (Valdenegro *et al.*, 2014a) showed no IgM antibodies and IgT involvement couldn't be assessed neither. Following these results, another and last study on AGD vaccine development was performed by using this recombinant

protein, and even though there was a very strong antibody response in serum and mucosal surfaces, there was no protection to the subsequent challenge with the parasite (Valdenegro *et al.*, 2015). The fact that this target provoked an antibody response and was pulled out of the transcriptome from *N. perurans* and was produced as a recombinant protein, opens the possibility for *in-silico* searching to provide a good tool to yield a list of vaccine candidates from genome / transcriptome data without the need of grow large numbers of the pathogen.

In order to select the proper vaccine targets, it is important to know as much as possible about the virulence characteristics within the pathogen. In the case of *N. perurans*, (Young *et al.*, 2007; Crosbie *et al.*, 2012) although often free-living, it can colonise the gills of a wide range of species causing the appearance of white, multifocal lesions on the gill surface. At the histopathological level, the effects of AGD are critical to the gill epithelium, causing hyperplasia and, generally, an increase of size and numbers of mucous cells. These clinical signs are often found along with attached amoebae and lamellar fusion (Adams *et al.*, 2004). It is believed that one of the virulence factors of this species is associated with its capacity to attach to the gill epithelium (Adams & Nowak, 2004) and it can subsequently cause cytopathic effect (CPE) through production of cytolytic products (Butler & Nowak, 2004). Other studies have investigated a range of other pathogenic amoebic species, proving the presence of additional virulence factors such as proteases in *Entamoeba histolytica* (Serrano *et al.*, 2013), extracellular vesicles (EVs) in *Acanthamoeba castellanii* (Gonçalves *et al.*, 2019) and N-acetyl-D-galactosamine (GalNac) in *E. histolytica* (Ravdin *et al.*, 1985; Connaris & Greenwell, 1997; Moncada *et al.*, 2005). Recently, studies have also pointed out the pathogenic role of the GalNac and other mucin associated products in *E. histolytica* and *Naegleria fowleri* infections in relation to the protective mucus layer. In the former species, GalNac was found strongly binding to mucins within the mucus layer of mice intestines. This binding was achieved through the Gal/GalNac-lectin, which has high affinity for galactose and N-acetyl-D-galactosamine glycans present on the O-linked sugar side chains of the MUC2 molecule (Leon-Coria *et al.*, 2019). The latter species was also investigated and produced secretory products that played an important role in mucus and mucin degradation (MUC5AC) during the invasion (Martínez-Castillo *et al.*, 2017).

In addition, not only is the function important while choosing these targets, but there should not, ideally, be any homology between the selected sequences and the host, in this case Atlantic salmon. This avoids generation of a potential autoimmune response (Bertholet *et al.*, 2014). In addition, the location of these proteins in the cell is relevant. Extracellular/secreted or cell membrane proteins are considered good vaccine candidates due to their accessibility to the immune system (Chaudhuri *et al.*, 2014; Bertholet *et al.*, 2014). These characteristics, in addition to these proteins presenting antigenic and adhesion properties, would increase the probabilities of developing protection within the host. The quality of the sample also plays an important role when the different targets are being pulled out of the transcriptome / genome data. During this work, this was a constant problem as no axenic culture was developed in the end and there was a lot of contamination from bacteria or salmon tissue.

Transcriptomes of cultured *N. perurans* and AGD-infected gills were, nevertheless, sequenced, and resultant assemblies analysed to provide a final list of potential vaccine candidates. Transcriptome assemblies were studied individually and also previously described vaccine candidates in various other protistan species were searched *in silico* using a range of bioinformatics tools to select additional candidates. Only extracellular/secreted proteins and cell surface proteins were considered throughout our search and characteristics such as adhesion, protease activity and mucin degradation were taken into consideration when examining the transcriptome analysis. The final list of vaccine candidates provides a rational starting point for the construction of recombinant proteins for *in vivo* testing and will ultimately assist the process of vaccine development against AGD.

5.2. Materials and Methods

5.2.1. Preparation of *N. perurans* cultures for transcriptomic analysis

Two monoclonal cultures of *N. perurans* were developed as explained in Section 2.2.2 of Chapter 2. These monoclonal cultures were less than six months old, in order to preserve the virulence. Prior to the preparation of cell pellets for RNA extraction, several FSW washes were performed in order to reduce the high bacterial contamination. Harvest of the cells was executed as explained in Section 2.2.2 of Chapter 2. Small volumes were centrifuged at 1,000 x *g* and pellets were snap-frozen on dry ice. Approximately 2.5 million cells were harvested and stored at –80°C. Lastly, samples were sent to Future Genomics Technologies B.V. (Leiden, Netherlands) where transcriptomic library preparation, sequencing and initial quality analyses were carried out.

5.2.2. Sampling of high infected AGD fish for transcriptomic analysis

All gills were excised and kept in 95% ethanol from three AGD-infected fish (gill scores of 2.5) (following cohabitation challenge as described in Chapter 2, Section 2.2.5.1), which had been previously humanely euthanised by overdose of the anaesthetic MS-222 (100 ppm) and subsequent destruction of the brain, at MERL (Institute of Aquaculture, Machrihanish, Scotland, UK). Work was conducted under the same regulations already specified in Chapter 2, Section 2.2.5.1.

5.2.3. RNA extraction and quality control

RNA was isolated from homogenized and snap-frozen *N. perurans* samples (TissueRuptor, Qiagen, Venlo, Netherlands), as well as from the gill tissue of the AGD-infected fish, using the miRNeasy mini kit (Qiagen). Quality and integrity of the isolated RNA were checked on an Agilent Bioanalyzer 2100 total RNA Nano series II chip (Agilent, Amstelveen, Netherlands).

5.2.4. RNAseq libraries preparation, sequencing data processing and *de novo* assembly

For both, cultured *N. perurans* and AGD-infected gills, Illumina multiplexed RNAseq libraries were prepared from 0.5 µg total RNA using the Illumina TruSeq stranded mRNA LT Kit according to the manufacturer's instructions (Illumina Inc.). RNAseq libraries were sequenced on an Illumina NovaSeq6000 sequencer as 2 × 150 nucleotides paired-end (PE2x150) reads according to the manufacturer's protocol. Image analysis and base calling were done by the Illumina pipeline.

In the case of cultured *N. perurans*, reads of low quality (*i.e.*, with an average quality score less than 20), those having ambiguous bases, those that were too short or those comprising PCR duplicates were discarded using PRINSEQ v0.20.4 (Schmieder & Edwards, 2011), and adaptors were clipped using Trimmomatic v0.38 (Bolger, Lohse & Usadel, 2014) as standard pre-processing methods. Reads aligning to *N. perurans*' symbiont genome *Perkinsela* sp. (NCBI assembly GCA_001235845.1) or any bacterial genomes were also removed using BWA v0.7.17 (Li & Durbin, 2009). Ribosomal RNA was further removed using SortMeRNA v3.0.2 (Kopylova *et al.*, 2012) against the Silva version 119 rRNA databases (Quast *et al.*, 2012). The remaining reads were assembled using Trinity v2.8.4 (Grabherr *et al.*, 2011). The raw assembly was filtered for a minimum transcript length of 300 nucleotides and a detectable CDS with TransDecoder v5.5.0 (<https://transdecoder.github.io/>). Completeness of the assembly was assessed using BUSCO v3.1.0 (Waterhouse *et al.*, 2017) using the Metazoa dataset.

Regarding the transcriptome from the AGD-infected gills, different approaches were performed. For quality control and trimming of the sequencing reads the bbmap/bbduk suite program was employed (Bushnell, 2017). Then, raw reads were aligned back to the assembled contigs using Bowtie2 (Langmead & Salzberg, 2012) against the Atlantic salmon reference transcriptome (GCF_000233375.1_ICSASG_v2_rna_from_genomic.fna). For the collection of the unaligned read Samtools was used (Ramirez-Gonzalez *et al.*, 2012). CLC assembly cell v4.4.1 (<http://www.clcbio.com/products/clc-assembly-cell/>) was used at multiple settings for *de novo* contig assembly from the unaligned reads.

5.2.5. Annotation and functional classification

5.2.5.1. Cultured *N. perurans* transcriptome

The resulting *de novo* transcriptome was annotated using InterProscan v5.33-72.0 (Jones *et al.*, 2014; Mitchell *et al.*, 2018), Swiss-Prot release 2018_11 and Pfam release 32.0 database (El-Gebali *et al.*, 2018). For classification, the transcripts were handled as queries using BLAST+/BLASTP v2.8.1 (Altschul *et al.*, 1990), E-value threshold of 10^{-5} , against Kyoto Encyclopedia of Genes and Genomes (KEGG) release 89.0 (Kanehisa *et al.*, 2019). Gene Ontology (GO) (Ashburner *et al.*, 2000) were recovered from InterPro, KEGG and SwissProt annotations. Subsequently, classification was performed using R v3.5.1 (R Team, 2018). Protein subcellular localisation predictions were produced using DeepLoc v1.0 (Almagro *et al.*, 2017).

5.2.5.2. AGD-infected gill transcriptome

In this case, Diamond-BLASTX alignment (Buchfink *et al.*, 2015) was performed against NCBI-NR (Non-redundant RefSeq proteins) and then the same alignment was performed against NCBI-Taxon_554915 (Amoebozoa).

5.2.6. Selection of potential vaccine candidates through *in-silico* search

Transcripts for proteins found to contain domains related to cell membrane location or secretion / extracellular domains were identified using the online tool WoLF PSORT (Protein Subcellular Localization Prediction) (<https://wolfpsort.hgc.jp/>). All transcripts that matched by homology those identified as extracellular/secreted and cell membrane proteins, were ranked by E-values. When E-values were $\leq 10^{-40}$, the contig ID was used to find the correct sequence using BioEdit v7.0.5 software and the sequence was subjected to TBLASTX against all Eukaryota in NCBI. From this latter homology search, only proteins presenting low E-values ($\leq 10^{-40}$) from organisms genetically closer to amoebic species (Amoebozoa (taxid:554915)) were selected as potential candidates. This E-value was set to 10^{-40} due to most studies in transcriptomics setting values to at most 10^{-20} to avoid strong homologies with other sequences (Song *et al.*, 2017; Yue *et al.*, 2018).

Additionally, Signal-P v5.0 web tool (Almagro-Armenteros *et al.*, 2019) was used to check for the presence of signal peptides (SPs) in the protein sequences and

VaxiJen v2.0 web tool (Doytchinova & Flower, 2008) was applied to check for antigenicity with a threshold of 0.5 as used in previous studies (Pallavi *et al.*, 2016). Also, Dot Plots from the Basic local alignment search tool (BLAST) (Altschul *et al.*, 1990) of the mRNA sequences alignments were used to interpret homology visually (Figure 5.1.). Additional alignments of all the sequences were also performed with BioEdit Sequence Alignment Editor (Hall, 1999) (Appendix III).

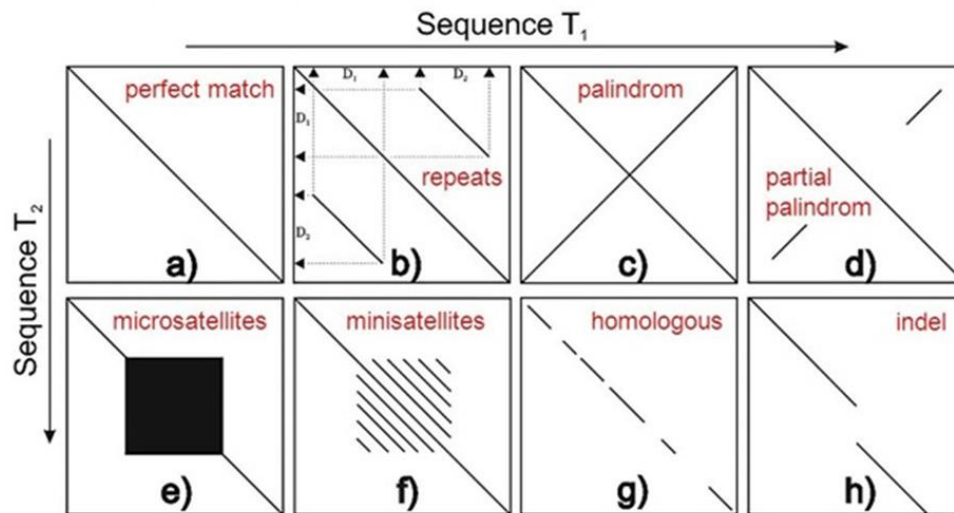


Figure 5.1. Schematic outline of distinctive configurations appearing in Dot Plots; a) one continuous main diagonal shows perfect match for two sequences; b) parallels to the main diagonal indicate repeated regions in the same reading direction on different parts of the sequences (D1, D2: duplications); c) lines perpendicular to the main diagonal indicate palindromic areas; d) partially palindromic sequence; e) bold blocks on the main diagonal indicate repetition of the same symbol in both sequences; f) parallel lines indicate tandem repeats so minisatellite patterns; g) when the diagonal is a discontinuous line this indicates that the sequences T1 and T2 share a common source and the number of interruptions increases with modifications on the text or the time of independent evolution and mutation rate; h) partial deletion in sequence 1 or insertion in sequence 2, so called 'indel' (Source from web article by Jan Schulz (2008), "Introduction to Dot Plots").

Additional sequences, relating to other better characterised protistan pathogens described in previous studies, were blasted against both new *N. perurans* transcriptome assemblies to investigate if homologues to formerly identified vaccine candidates/virulence factors could be discovered. As described in previous chapters, some aspects of the mucosal immunity and mucus-pathogen interactions were investigated. Therefore, we decided to look for previously described and characterised proteins involved in these processes, in addition to some proteins involved in epithelial attachment and immunomodulation

5.3. Results

5.3.1. RNA isolation and quality control

In vitro cultured *N. perurans*

Two tubes (FG1837_01 and FG1837_02) containing approximately 2.5 million cultured *N. perurans* cells were processed and quality control showed reasonable RNA quality for both samples although some degradation of RNA could be seen; this was observed in a corresponding RNA gel (Figure 5.2.).

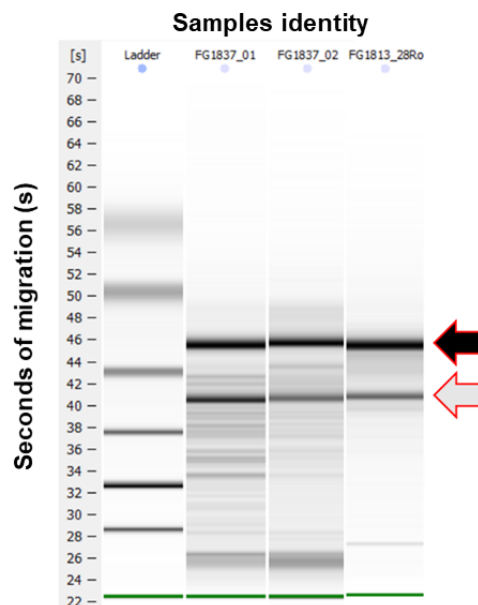


Figure 5.2. RNA quality control virtual gel (Agilent Bioanalyzer) of the cultured *N. perurans* samples. Presenting the ladder, two samples (FG1837_01 and FG1837_02) and a control sample (FG1813_28Ro). Black arrow indicates band corresponding the 28S and grey arrow corresponds to 18S. Tested samples present both 28S and 18S bands as the control sample.

In vivo host-infecting *N. perurans*

Three tubes with highly AGD-infected gill tissue (FG1904_01, FG1904_02 and FG1904_03) were also processed and quality control showed reasonable RNA quality for two of the samples (FG1904_01 and FG1904_02) although some degradation of RNA could be seen; this was observed in a corresponding RNA gel (**Error! Reference source not found.**). The third sample FG1904_03 was seen to be highly degraded (**Error! Reference source not found.**).

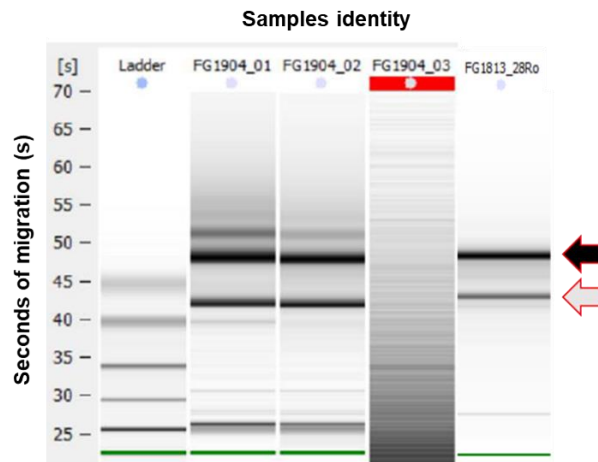


Figure 5.3. RNA quality control virtual gel (Agilent Bioanalyzer) of the infected AGD gills samples. Presenting the ladder, the two successful samples (FG1904_01 and FG1904_02), the highly degraded sample (FG1904_03) and a control sample (FG1813_28Ro). Black arrow indicates band corresponding the 28S and grey arrow corresponds to 18S. The two first samples present both 28S and 18S bands as the control sample, indicating good RNA quality.

5.3.2. RNAseq libraries preparation

RNAseq library quality control indicated all samples to be of acceptable quality (**Error! Reference source not found.**). This is demonstrated by the lack of degradation of the intact mRNA that can be observed in the gel (black arrow). During RNAseq library preparation, mRNA is fragmented to a certain size, in this case is between 300-400 bp as shown in the gel. A heavily degraded mRNA sample would present numerous bands across the gel.

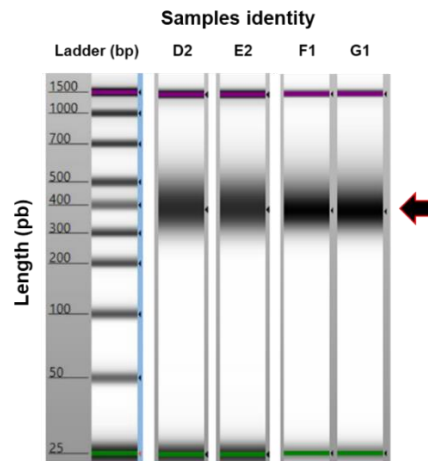


Figure 5.4. RNAseq quality control virtual gel (Agilent Bioanalyzer) for the Cultured *N. perurans* samples and the infected gills samples. Presenting the ladder, two samples from the cultured *N. perurans* (D2 and E2) and the infected gills samples (F1 and G1). Black arrow indicates where the amoebal cell mRNA is in the gel.

5.3.3. Illumina sequencing and *de novo* assembly of the cultured *N. perurans* transcriptome

The Illumina sequencing of the sample generated 62,178,179 raw paired-end reads. A total of 40,526,555 paired-end reads (65.2%) passed the pre-processing filters; and a final 38,157,716 (61.3%) passed the mRNA cleaning (i.e. bacterial genomes) and *Perkinsela sp.* genome removal step and were used during the *de novo* assembly process (**Error! Reference source not found.**).

The final assembly reconstructed a total of 103,385 transcripts with an average length of 976.46 nt and an N₅₀ length of 1,213 nt (Figure 5.5. A). A recall of the filtered reads mapped 94.66% of the reads to the transcriptome.

A BUSCO completeness assessment recovered 80.6% of near-universal single-copy orthologues selected from the Metazoa database (Figure 5.5. B). The clustering of the transcripts generated 75,558 unigenes with a mean length of 913.06 nt and an N₅₀ length of 1129 nt (**Error! Reference source not found.**).

Table 5.1. Summary statistics of sequencing and assembly of cultured *N. perurans* transcriptome.
*based of the longest transcript for each unigene.

| Category | Number/length |
|---|---------------|
| Total number of raw PE reads | 62,178,179 |
| Maximum read length (nt) | 150 |
| Pre-process PE reads | 40,526,555 |
| Filtering out rRNA reads | 39,346,872 |
| Filtering out <i>Perkinsela sp.</i> sequences | 38,157,716 |
| Clean bases | 5.7 Gb |
| Transcripts generated (raw) | 128,817 |
| Percentage of read assembled | 94.74% |
| Transcripts (filtered) | 68,447 |
| GC content | 50.28% |
| Maximum transcript length | 13,585 |
| Minimum transcript length | 300 |
| Transcripts > 500 bp | 50,807 |
| Transcripts > 1 Kb | 24,200 |
| Transcripts > 10 Kb | 18 |
| N ₅₀ length (bp) | 1213 |
| Mean length (bp) | 976.46 |
| Unigenes | 50,461 |
| N ₅₀ length (bp) | 1,129* |
| Mean length (bp) | 913.06* |

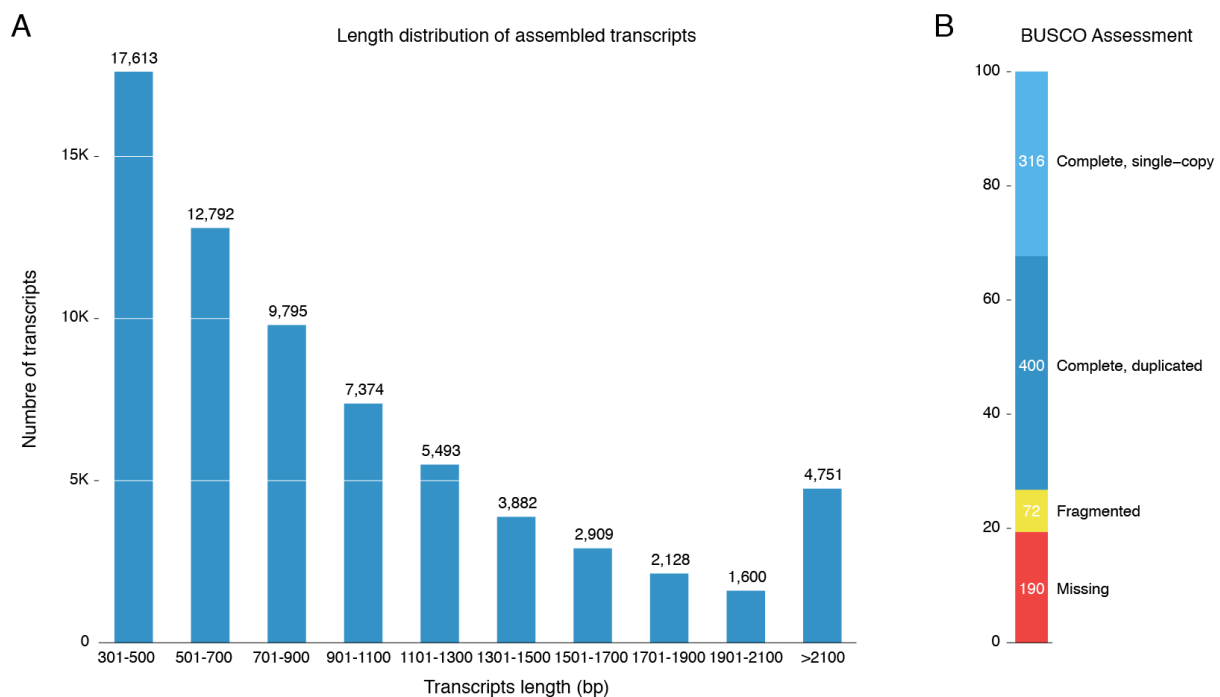


Figure 5.5. *N. perurans* transcript assessments. A. Length distribution of assembled *N. perurans* transcripts. Clean reads for *N. perurans* were assembled and resulted in 68,447 transcripts. B. BUSCO assessment (Metazoa database) number of BUSCO orthologues equals 978.

5.3.4. Annotation and functional characterisation of the cultured *N. perurans* transcriptome

The reconstructed transcripts were subjected to BLASTP similarity searches against SwissProt, Pfam, InterPro, KEGG and GO databases. Of the total of 103,385 transcripts, 67,999 (99.3%) were annotated by at least one database, and 26,062 (38.1%) were annotated in all five databases (Table 5.2. ; **Error! Reference source not found.**).

Table 5.2. Statistics of annotation results for *N. perurans* unigenes. *Interpro covers 12 databases (CATH-Gene3D, CDD, HAMAP, PANTHER, PIRSF, PRINTS, ProDom, PROSITE (patterns and profiles), SFLD, SMART, SUPERFAMILY, TIGRFAMs).

| Database | Number annotated |
|-----------|------------------|
| PfamA | 54,965 |
| Interpro* | 41,562 |
| SwissProt | 59,209 |
| KEGG | 59,209 |
| GO | 38,311 |
| All | 26,062 |
| Total | 67,999 |

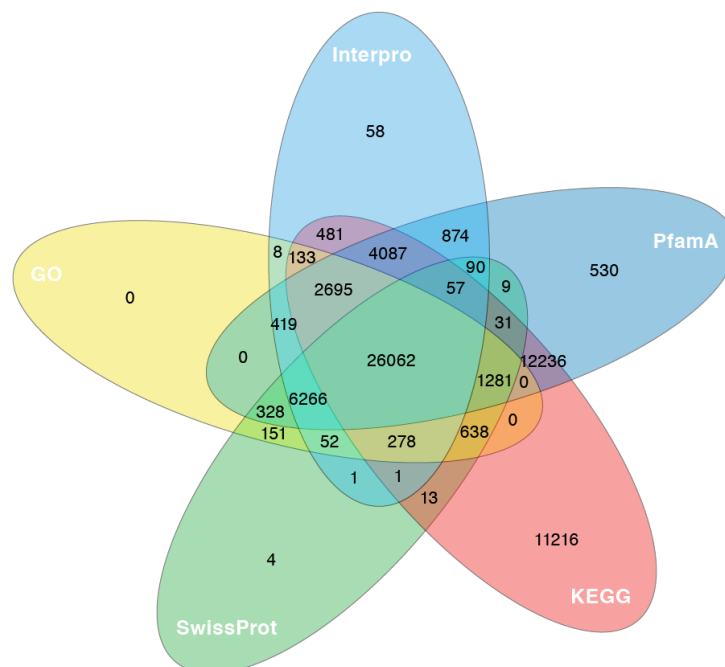


Figure 5.6. A five-way Venn diagram. The figure shows the unique and overlapped transcripts showing protein sequence similarity with one or more databases (details in Table 5.2).

Additionally, GO analysis (gene ontology analysis) of biological process, cellular component and molecular function were performed for the assembled transcriptome of the cultured amoebae, with the top 15 GO terms for each category shown in Figure 5.7. . In regards to the biological process (Figure 5.7. ; BP), GO analysis revealed higher proportions within proteins related to signal transduction, protein phosphorylation and the oxidation-reduction processes. When observing the cellular components (Figure 5.7. ; CC), higher proportion of transcripts relate to proteins found within the plasma membrane, nucleus, membrane, intermembrane and cytoplasm. More specifically, in terms of molecular function, the GO analysis shown a very high proportion of protein binding function in comparison to the rest of transcripts (Figure 5.7. ; MF).

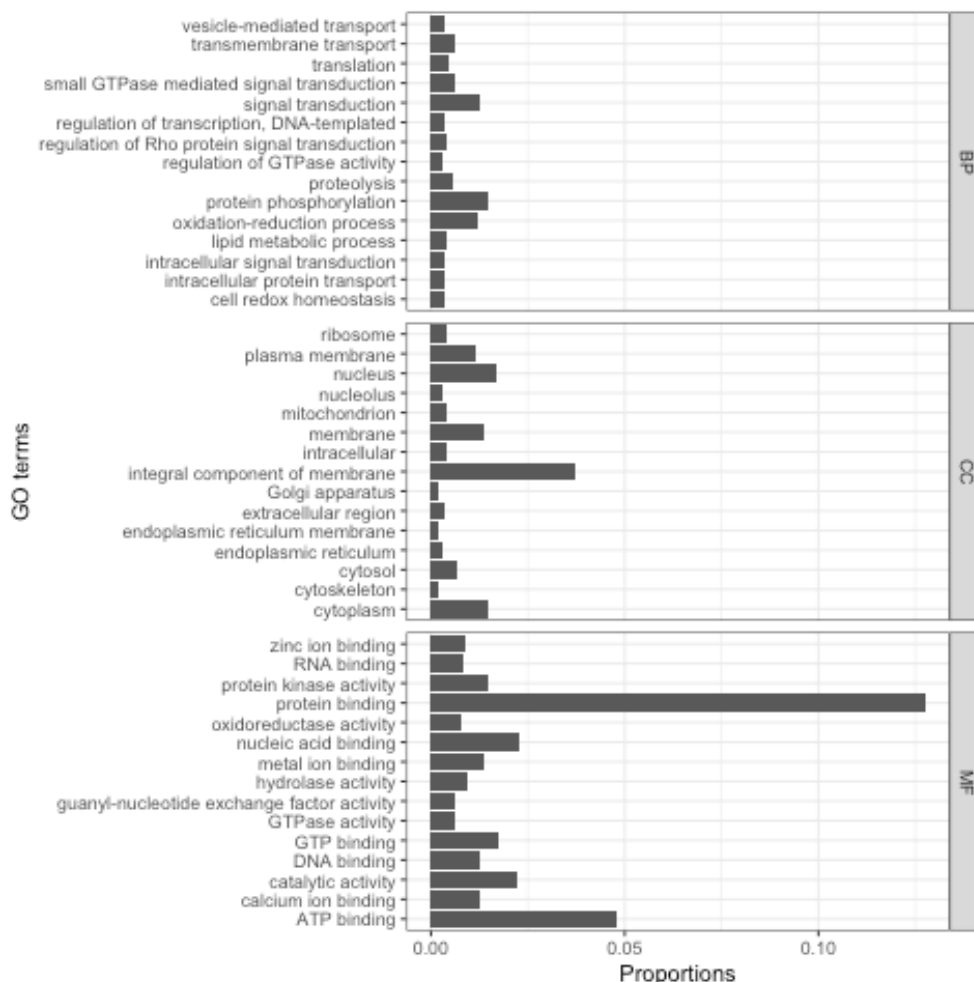


Figure 5.7. Top 15 GO terms associated with transcripts in the cultured amoeba transcriptome. Biological process GO (BP), cellular components GO (CC) and molecular function (MF).

5.3.5. Illumina sequencing and de novo assembly of the AGD-

| Cell Localisation | Transcript ID | Matched organism | Protein name | E-value ^a |
|-------------------|---------------|------------------|--------------|----------------------|
|-------------------|---------------|------------------|--------------|----------------------|

infected gill transcriptome

The Illumina sequencing of the sample generated approximately 21 Gb of Illumina RNAseq data. In total, about 86% of the raw data was derived from salmon and the remaining RNAseq data (~3 Gb) was used for *de novo* cDNA contig assembly. This resulted in 108,188 contigs with an N₅₀ of 429 pb and a total assembly length of 45.59 Mb (Table 5.3.). Diamond-BLASTX alignment of the 108,188 contigs against NCBI-NR (Non-redundant RefSeq proteins) reference database resulted in 8,055 hits (E-value < 0.00001). Of those hits, 42 were hits to Amoebozoan species (taxon ID = 554915).

A total of 8,055 contigs (~7.5%) had a BLASTX hit in the NCBI-NR (Non-redundant RefSeq proteins) reference database, 42 of which were Amoebozoan sequences (taxon ID = 554915). Additional Diamond-BLASTX alignment of the total of contigs against NCBI-Taxon_554915 (Amoebozoa) resulted in 614 hits (E-value < 0.00001).

Table 5.3. Summary statistics of sequencing and assembly of AGD-infected gill transcriptome

| Category | Number/length |
|-----------------------------|---------------|
| #Contigs | 108,188 |
| N ₅₀ length (bp) | 429 pb |
| Assembly length | 45.59 Mb |
| Max contig length | 6,946 bp |
| Min contig length | 200 |

5.3.6. Selection of potential vaccine candidates from the cultured *N. perurans*

The *in-silico* search resulted in a total of 823 transcripts previously described as extracellular/secreted proteins and a total of 543 transcripts previously described as cell membrane proteins in other organisms. To select the best matching proteins, E-values were assessed as well as the coverage of the sequence. The cut-off values for the E-value were set at < 10⁻⁴⁰ and coverage at > 70 %. From this assessment, only 73 transcripts from cellular membrane proteins were selected (best ten shown in

| | Transcript ID | Matched organism | Protein name | E-value |
|------------------------|-----------------|----------------------------------|--|---------|
| | Trans_g13033_i1 | <i>Dictyostelium purpureum</i> | Hypothetical protein | <1e-200 |
| Cell Localisation | Trans_g16976_i3 | <i>Entamoeba invadens</i> | Myosin I | 1e-200 |
| | Trans_g9352_i1 | <i>Polysphondylium</i> | PN500 P-type ATPase | 1e-167 |
| Membrane | Trans_g13033_i1 | <i>Dictyostelium pallidum</i> | Hypothetical protein | <1e-200 |
| | Trans_g9529_i1 | <i>Acanthamoeba purpureum</i> | P-type ATPase family protein | 3e-105 |
| | Trans_g16976_i3 | <i>Entamoeba invadens</i> | Myosin I | <1e-200 |
| | Trans_g9010_i1 | <i>A. castellanii</i> | Transporter, major facilitator subfamily | 2e-111 |
| | Trans_g9352_i1 | <i>Polysphondylium</i> | PN500 P-type ATPase protein | 1e-167 |
| | Trans_g8324_i1 | <i>Dictyostelium pallidum</i> | Putative integrin alpha FG-GAP repeat | 1e-97 |
| | Trans_g9529_i1 | <i>Acanthamoeba fasciculatum</i> | P-type ATPase family protein containing protein | 3e-105 |
| Membrane | Trans_g8073_i1 | <i>D. purpureum</i> | Guanine nucleotide binding protein | 1e-87 |
| | Trans_g9010_i1 | <i>A. castellanii</i> | Transporter, major facilitator subfamily | 2e-111 |
| | Trans_g13993_i2 | <i>Monosiga brevicollis</i> | ABC transporter protein | 4e-82 |
| | Trans_g6724_i1 | <i>Trypanosoma conorhini</i> | Cystinosin | 5e-75 |
| | Trans_g1674_i2 | <i>A. castellanii</i> | Solute carrier family 35, member E3, putative | 8e-54 |
| Extracellular/secreted | Trans_g8925_i1 | <i>P. pallidum</i> | PN500 ubiquinone oxidoreductase | <1e-200 |
| | Trans_g4530_i1 | <i>D. purpureum</i> | Homogentisate 1,2-dioxygenase | 1e-174 |
| | Trans_g15791_i1 | <i>A. castellanii</i> | Phosphoglucomutase | 2e-143 |
| | Trans_g1428_i2 | <i>A. castellanii</i> | Papain family cysteine protease | 1e-123 |
| | Trans_g16658_i1 | <i>A. castellanii</i> | Prokumamolisin, activation domain containing protein | 9e-115 |
| | Trans_g5068_i1 | <i>A. castellanii</i> | Carboxypeptidase | 2e-97 |
| | Trans_g4459_i1 | <i>D. fasciculatum</i> | Carboxylic ester hydrolase | 2e-93 |
| | Trans_g7829_i1 | <i>A. castellanii</i> | Prokumamolisin, activation domain containing protein | 5e-89 |
| | Trans_g8922_i1 | <i>D. purpureum</i> | Hypothetical protein | 2e-86 |
| | Trans_g542_i1 | <i>A. castellanii</i> | Deoxyribonuclease II, putative | 2e-81 |

Table 5.4. List of the best twenty selected proteins from the in-silico search of the cultured *N. perurans* transcriptome from low to high E-values.

Table 5.5. Summary of the best vaccine candidates from the *in-silico* search of the cultured *N. perurans* transcriptome. These candidates were selected after blasting the sequences against the host's transcriptome, *S. salar*; the remaining four proteins presented no homology with the host and the rest described in Appendix II) and from the extracellular/secreted proteins, a total of 62 transcripts were chosen (best ten shown in

| | | | | |
|----------------------------|------------------------|-----------------------------------|--|---------|
| | <i>Trans_g8324_i1</i> | <i>Dictyostelium fasciculatum</i> | Putative integrin alpha FG-GAP repeat-containing protein | 1e-97 |
| | <i>Trans_g8073_i1</i> | <i>D. purpureum</i> | Guanine nucleotide-binding protein | 1e-87 |
| | <i>Trans_g13993_i2</i> | <i>Monosiga brevicollis</i> | ABC transporter protein | 4e-82 |
| | <i>Trans_g6724_i1</i> | <i>Trypanosoma conorhini</i> | Cystinosin | 5e-75 |
| | <i>Trans_g1674_i2</i> | <i>A. castellanii</i> | Solute carrier family 35, member E3, putative | 8e-54 |
| Extracellular/ secreted | <i>Trans_g8925_i1</i> | <i>P. pallidum</i> | PN500 ubiquinone oxidoreductase | <1e-200 |
| | <i>Trans_g4530_i1</i> | <i>D. purpureum</i> | Homogentisate 1,2-dioxygenase | 1e-174 |
| | <i>Trans_g15791_i1</i> | <i>A. castellanii</i> | Phosphoglucomutase | 2e-143 |
| | <i>Trans_g1428_i2</i> | <i>A. castellanii</i> | Papain family cysteine protease | 1e-123 |
| | <i>Trans_g16658_i1</i> | <i>A. castellanii</i> | Prokumamolisin, activation domain containing protein | 9e-115 |
| | <i>Trans_g5068_i1</i> | <i>A. castellanii</i> | Carboxypeptidase | 2e-97 |
| | <i>Trans_g4459_i1</i> | <i>D. fasciculatum</i> | Carboxylic ester hydrolase | 2e-93 |
| | <i>Trans_g7829_i1</i> | <i>A. castellanii</i> | Prokumamolisin, activation domain containing protein | 5e-89 |
| | <i>Trans_g8922_i1</i> | <i>D. purpureum</i> | Hypothetical protein | 2e-86 |
| | <i>Trans_g542_i1</i> | <i>A. castellanii</i> | Deoxyribonuclease II, putative | 2e-81 |

Table 5.4. List of the best twenty selected proteins from the in-silico search of the cultured *N. perurans* transcriptome from low to high E-values.

Table 5.5. Summary of the best vaccine candidates from the *in-silico* search of the cultured *N. perurans* transcriptome. These candidates were selected after blasting the sequences against the host's transcriptome, *S. salar*; the remaining four proteins presented no homology with the host and the rest described in Appendix II).

A more rigorous assessment was followed by setting the cut off E-values even lower ($\leq 10^{-80}$) and blasting the selected transcripts against Eukaryote transcripts from the NCBI database through the BLASTx tool. Four sequences from the cell membrane proteins and seven sequences for the extracellular/secreted proteins provided very good levels of homology (E-values: $\leq 10^{-80}$). However, when these sequences were blasted against the host transcriptome (*S. salar*) only two sequences from the cell membrane proteins and two sequences from the extracellular/secreted proteins presented sufficiently low homology to *S. salar* sequences to provide feasible candidates (cut off values: E-values $\geq 10^{-50}$; Coverage < 50%) (Table 5.5).

Table 5.4. List of the best twenty selected proteins from the in-silico search of the cultured *N. perurans* transcriptome from low to high E-values.

| Cell Localisation | Transcript ID | Matched organism | Protein name | E-value ^a | Protein ID (UniProt) | mRNA sequence AN (NCBI) |
|----------------------------|------------------------|-----------------------------------|--|----------------------|----------------------|-------------------------|
| Membrane | <i>Trans_g13033_i1</i> | <i>Dictyostelium purpureum</i> | Hypothetical protein | <1e-200 | F0ZR69 | XM_003289861.1 |
| | <i>Trans_g16976_i3</i> | <i>Entamoeba invadens</i> | Myosin I | <1e-200 | A0A0A1UGM3 | XM_004259540.1 |
| | <i>Trans_g9352_i1</i> | <i>Polysphondylium pallidum</i> | PN500 P-type ATPase | 1e-167 | D3B4A2 | XM_020573502.1 |
| | <i>Trans_g9529_i1</i> | <i>Acanthamoeba castellanii</i> | P-type ATPase family protein | 3e-105 | L8GVH2 | XM_004338036.1 |
| | <i>Trans_g9010_i1</i> | <i>A. castellanii</i> | Transporter, major facilitator subfamily protein | 2e-111 | L8GHX2 | XM_004334424.1 |
| | <i>Trans_g8324_i1</i> | <i>Dictyostelium fasciculatum</i> | Putative integrin alpha FG-GAP repeat-containing protein | 1e-97 | F4Q5F1 | XM_004355641.1 |
| | <i>Trans_g8073_i1</i> | <i>D. purpureum</i> | Guanine nucleotide-binding protein | 1e-87 | F0ZF11 | XM_003285972.1 |
| | <i>Trans_g13993_i2</i> | <i>Monosiga brevicollis</i> | ABC transporter protein | 4e-82 | A9VCE9 | XM_001750336.1 |
| | <i>Trans_g6724_i1</i> | <i>Trypanosoma conorhini</i> | Cystinosin | 5e-75 | A0A3R7JRY5 | XM_029376667.1 |
| | <i>Trans_g1674_i2</i> | <i>A. castellanii</i> | Solute carrier family 35, member E3, putative | 8e-54 | L8GU22 | XM_004338639.1 |
| Extracellular/ secreted | <i>Trans_g8925_i1</i> | <i>P. pallidum</i> | PN500 ubiquinone oxidoreductase | <1e-200 | D3BLC0 | XM_020580149.1 |
| | <i>Trans_g4530_i1</i> | <i>D. purpureum</i> | Homogentisate 1,2-dioxygenase | 1e-174 | F1A3P0 | XM_003294234.1 |
| | <i>Trans_g15791_i1</i> | <i>A. castellanii</i> | Phosphoglucomutase | 2e-143 | L8GKT1 | XM_004335635.1 |
| | <i>Trans_g1428_i2</i> | <i>A. castellanii</i> | Papain family cysteine protease | 1e-123 | L8HJH5 | XM_004358251.1 |
| | <i>Trans_g16658_i1</i> | <i>A. castellanii</i> | Prokumamolisin, activation domain containing protein | 9e-115 | L8H2I7 | XM_004341758.1 |
| | <i>Trans_g5068_i1</i> | <i>A. castellanii</i> | Carboxypeptidase | 2e-97 | L8H6Y6 | XM_004342287.1 |
| | <i>Trans_g4459_i1</i> | <i>D. fasciculatum</i> | Carboxylic ester hydrolase | 2e-93 | F4PJY9 | XM_004361707.1 |
| | <i>Trans_g7829_i1</i> | <i>A. castellanii</i> | Prokumamolisin, activation domain containing protein | 5e-89 | L8H2I7 | XM_004341758.1 |
| | <i>Trans_g8922_i1</i> | <i>D. purpureum</i> | Hypothetical protein | 2e-86 | F0ZSA3 | XM_003290254.1 |
| | <i>Trans_g542_i1</i> | <i>A. castellanii</i> | Deoxyribonuclease II, putative | 2e-81 | L8GV23 | XM_004338820.1 |

Table 5.5. Summary of the best vaccine candidates from the *in-silico* search of the cultured *N. perurans* transcriptome. These candidates were selected after blasting the sequences against the host's transcriptome, *S. salar*; the remaining four proteins presented no homology with the host

| Cell Localisation | Transcript ID | Matched organism | Protein name | E-value ^a | Protein ID (UniProt) | mRNA sequence AN (NCBI) |
|------------------------|-----------------------|------------------------|--|----------------------|----------------------|-------------------------|
| Membrane | <i>Trans_g9010_i1</i> | <i>A. castellanii</i> | Transporter, major facilitator subfamily protein | 2e-111 | L8GHX2 | XM_004334424.1 |
| | <i>Trans_g8324_i1</i> | <i>D. fasciculatum</i> | Putative integrin alpha FG-GAP repeat-containing protein | 1e-97 | F4Q5F1 | XM_004355641.1 |
| Extracellular/secreted | <i>Trans_g1428_i2</i> | <i>A. castellanii</i> | Papain family cysteine protease | 1e-123 | L8HJH5 | XM_004358251.1 |
| | <i>Trans_g5068_i1</i> | <i>A. castellanii</i> | Carboxypeptidase Y | 2e-97 | L8H6Y6 | XM_004342287.1 |

^a*E-value* is the number of distinct alignments, with a score equivalent to or better than bit-score *S*, that are expected to occur in a database search by chance. The lower the *E-value*, the more significant the score is.

Only four transcripts from the annotated transcriptome presented good hits, therefore showing a good level of homology (E-values: $\leq 10^{-80}$; homology additionally shown with Dot Plots in Figure 5.8 with previously characterised proteins from two different amoebic species: *Acanthamoeba castellanii* and *Dictyostelium fasciculatum*. Also, no homology was found for these targets when sequences were blasted against *S. salar* transcripts. As explained in the material and methods, the presence of signal peptide and the potential antigenicity were investigated and annotated in Table 5.6.

Table 5.6. Summary of the remaining proteins from the cultured *N. perurans* transcriptome with the details of signal peptide presence and antigenicity.

| Cell Localisation | Matched organism | Protein name | Signal Peptide presence (≥ 0.5) | Antigenicity (≥ 0.5) |
|------------------------|------------------------|--|--|-----------------------------|
| Membrane | <i>A. castellanii</i> | Transporter, major facilitator subfamily protein | No (0.0077) | Yes (0.58) |
| | <i>D. fasciculatum</i> | Putative integrin alpha FG-GAP repeat-containing protein | No (0.1479) | Yes (0.6) |
| Extracellular/secreted | <i>A. castellanii</i> | Papain-family cysteine protease | Yes (0.9937) | Yes (0.51) |
| | <i>A. castellanii</i> | Carboxypeptidase Y | Yes (0.9675) | No (0.48) |

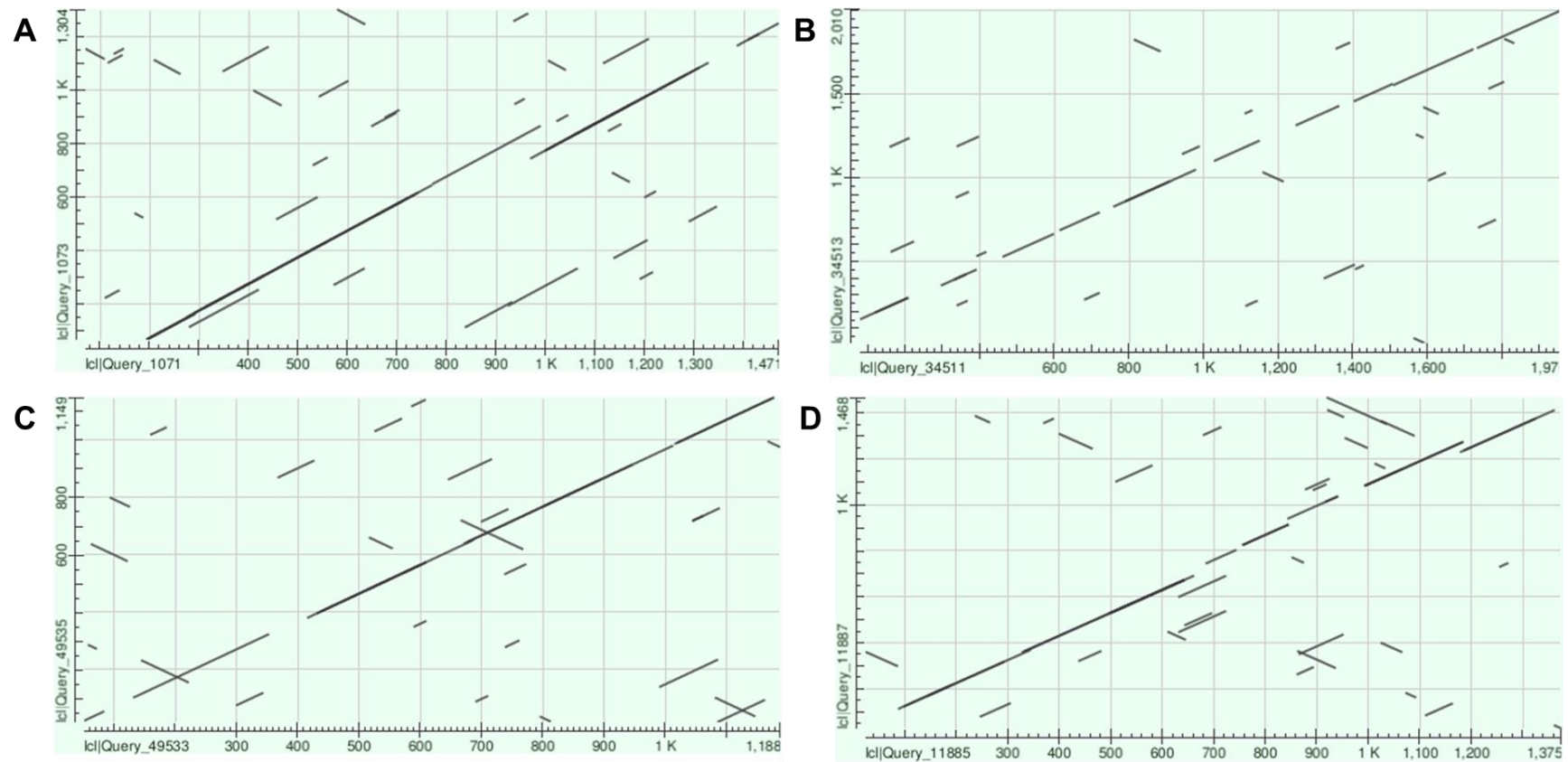


Figure 5.8. Dot Plot of the TBLASTx alignment of the cultured *N. perurans* transcriptome assembly with the known mRNA sequences. (A) *Trans_g9010_i1* vs. *A. castellanii* transporter, major facilitation subfamily protein (XM_004334424.1). (B) *Trans_g8324_i1* vs. *D. fasciculatum* integrin alpha FG-GAP (XM_004355641.1). (C) *Trans_g1428_i2* vs. *A. castellanii* Papain family cysteine protease (XM_004358251.1). (D) *Trans_g5068_i1* vs. *A. castellanii* Carboxypeptidase Y (XM_004342287.1). Source: Basic local alignment search tool (BLAST) (Altschul *et al.*, 1990).

5.3.7. Selection of the potential vaccine candidates from the salmon AGD- infected gills

Due to the high quantity of salmon RNA, the *in-silico* search resulted only in a total of 614 transcripts that matched with the taxon Amoebozoa. After looking at the E-values ($< 10^{-40}$) for this list of transcripts, 60 transcripts were selected (top ten proteins described in Table 5.7. However, when these transcripts were blasted against the host transcriptome (*S. salar*) only two of them presented very low homology to *S. salar* sequences (*contig_58495* and *contig_5081*) (E-values: $< 10^{-50}$; Coverage: $< 50\%$) (Table 5.8.). Visual representation of homology (E-values: $\leq 10^{-80}$) shown with Dot Plots in **Error! Reference source not found..**

Table 5.7. List of the best ten proteins from the *in-silico* search of the AGD-infected gill transcriptome from low to high E-values.

| Cell Localisation | Transcript ID | Matched organism | Protein name | E-value ^a | Protein ID (UniProt) | mRNA sequence AN (NCBI) |
|------------------------|---------------------|---|--|----------------------|----------------------|-------------------------|
| Extracellular/secreted | <i>contig_2104</i> | <i>Paramoeba pemaquidensis</i> | Elongation factor 1 α | 2.6e-145 | C1K9W2 | KF772980.1 |
| Mitochondria | <i>contig_28</i> | <i>Phalansterium sp. PJK-2012</i> | Apocytochrome b (mitochondrion) | 4.7e-103 | T1QDX4 | --- |
| Membrane | <i>contig_58495</i> | <i>Tieghemostelium lacteum</i> (syn. <i>Dictyostelium lacteum</i>) | Actin bundling protein | 1.2e-97 | A0A152A7V9 | XM_004355841.1 |
| Extracellular/secreted | <i>contig_5081</i> | <i>Acanthamoeba castellanii</i> | Reverse transcriptase | 1.8e-48 | L8HG65 | XM_004353194.1 |
| Cytoplasm | <i>contig_27790</i> | <i>Acanthamoeba castellanii</i> | Ribosomal proteins l2, RNA binding domain containing protein | 3.8e-97 | L8H292 | XM_004341389.1 |
| Extracellular/secreted | <i>contig_4134</i> | <i>Entamoeba nuttalli</i> | MiaB family tRNA modifying enzyme, archaeal-type protein | 9.1e-92 | K2H631 | XM_008857531.1 |
| Cytoplasm | <i>contig_28521</i> | <i>T. lacteum</i> (syn. <i>Dictyostelium lacteum</i>) | Ribosomal protein L10 | 5.7e-81 | A0A151ZG94 | --- |
| Mitochondria | <i>contig_98</i> | <i>P. pemaquidensis</i> | NADH dehydrogenase subunit 5 (mitochondrion) | 5.2e-80 | A0A1D8D5F2 | --- |
| Cytoplasm | <i>contig_51944</i> | <i>Planoprotostelium fungivorum</i> | Ribosomal protein S3a, component of cytosolic 80S ribosome and 40S small subunit | 8.2e-78 | A0A2P6NHG3 | --- |
| Cytoplasm | <i>contig_14689</i> | <i>Acytostelium subglobosum</i> | Hypothetical protein SAMD00019534_1258 20, partial | 1.2e-76 | UPI000644D7C7 | XM_012892195.1 |

Table 5.8. Summary of the best vaccine candidates from the *in-silico* search of the AGD-infected gill transcriptome. These candidates were selected after blasting the sequences against the host's transcriptome *S. salar*; the remaining two proteins presented no homology with the host.

| Cell Localisation | Transcript ID | Matched organism | Protein name | E-value ^a | Protein ID (UniProt) | mRNA sequence AN (NCBI) |
|------------------------|---------------------|--|------------------------|----------------------|----------------------|-------------------------|
| Membrane | <i>contig_58495</i> | <i>T. lacteum</i> (syn. <i>Dictyostelium lacteum</i>) | Actin bundling protein | 1.2e-97 | A0A152A7V9 | XM_004355841.1 |
| Extracellular/secreted | <i>contig_5081</i> | <i>A. castellanii</i> | Reverse transcriptase | 1.8e-48 | L8HG65 | XM_004353194.1 |

^a*E-value* is the number of distinct alignments, with a score equivalent to or better than bit-score S, that are expected to occur in a database search by chance. The lower the E-value, the more significant the score is.

Table 5.9. Summary of the remaining proteins from the AGD-infected gill transcriptome with the details of signal peptide presence and antigenicity.

| Cell Localisation | Matched organism | Protein name | Signal Peptide presence (≥ 0.5) | Antigenicity (≥ 0.5) |
|-------------------------|--|------------------------|--|-----------------------------|
| Membrane | <i>T. lacteum</i> (syn. <i>Dictyostelium lacteum</i>) | Actin bundling protein | No (0.0011) | Yes (0.63) |
| Extracellular /secreted | <i>A. castellanii</i> | Reverse transcriptase | No (0.2304) | Yes (0.55) |

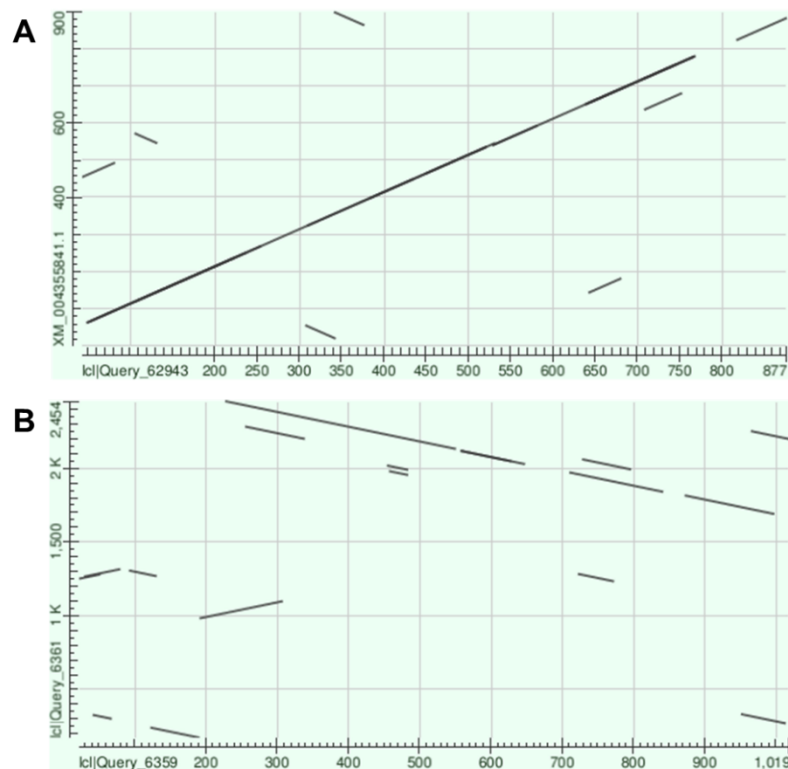


Figure 5.9. Dot Plot of the TBLASTx alignment of the AGD-infected gill transcriptome assembly with the known mRNA sequences. (A) *contig_58495* vs. *D. lacteum* Actin bundling protein (XM_004355841.1). (B) *contig_5081* vs. *A. castellanii* Reverse transcriptase (XM_004353194.1). Source: Basic local alignment search tool (BLAST) (Altschul *et al.*, 1990).

5.3.8. Selection of potential vaccine candidates from literature survey

Sequences of previous amoebic proteins were retrieved from the UniProt Database and blasted against both transcriptome assemblies. Subsequently, only the sequences which presented no homologies with the host were selected (Table 5.11.).

Table 5.10. List of proteins investigated within both transcriptome assemblies (cultured *N. perurans* and AGD-infected gills)

| Organism | Proteins/Enzymes | Biological process | Ref. |
|---|--|--|--|
| <i>E. histolytica</i> | Cysteine proteinases | Mucin degradation | Moncada, Keller & Chadee (2000, 2003 & 2005); Que & Reed (2000) |
| <i>Naegleria fowleri</i> <i>Trichomonas foetus</i> <i>T. vaginalis</i> <i>Giardia lamblia</i> <i>E. histolytica</i> <i>Leishmania donovani</i> <i>Trypanosoma brucei</i> <i>T. cruzi</i> | Glycosidases | Mucin degradation | Connaris & Greenwell (1997); Cervantes-Sandoval <i>et al.</i> , (2008); Martínez-Castillo <i>et al.</i> (2017) |
| <i>E. histolytica</i> <i>N. fowleri</i> <i>Acanthamoeba spp.</i> | Adhesins Proteases Amoebapores Prostaglandin Occludin-like proteins Proteinases | Epithelial attachment Host tissue destruction Pathogenesis Digestion of phagocytosed food | Moon <i>et al.</i> (2008); Betanzos <i>et al.</i> (2019) |
| <i>Plasmodium berghei</i> NK65 | Histamine releasing factor (HRF) Elongation factor 1 α (EF-1 α) | Immunomodulation functions | Demarta-Gatsi <i>et al.</i> (2019) |

Table 5.11. Summary of the best vaccine candidates from the *in-silico* search of the cultured *N. perurans* and AGD-infected gill transcriptome assemblies. These candidates were selected after blasting the sequences against the host's transcriptome, *S. salar*.

| Cell Localisation | Transcript ID | Matched organism | Protein name | E-value ^a | Protein ID (UniProt) | mRNA sequence AN (NCBI) | Ref. |
|------------------------|---|-----------------------------------|---|----------------------|----------------------|-------------------------|--|
| Membrane | <i>Trans_g22727_i2</i> | <i>D. discoideum</i> | GlcNAc transferase | 1e-130 | Q54QB2 | XM_633740.1 | Eichinger <i>et al.</i> (2005); Whitney <i>et al.</i> (2010) |
| | <i>Trans_g1976_i1</i> | | Autocrine proliferation repressor protein A | 2e-92 | Q5XM24 | XM_635474.1 | Tang <i>et al.</i> (2018) |
| Cytoplasm | <i>Trans_g42616_i1</i> | <i>Perkinsela sp. CCAP 1560/4</i> | IgE-dependent histamine-releasing factor | 2e-085 | A0A0L1KJC5 | LFNC01000427.1 | David <i>et al.</i> (2015) |
| | <i>Trans_g18920_i1</i> (cultured amoebae) > <i>contig_2104</i> (AGD-infected gills) | <i>Paramoeba pemaquidensis</i> | Elongation factor 1 alpha | <1e-200 1e-148 | C1K9W2 | KF772980.1 | Lima <i>et al.</i> (2014) |
| Extracellular/secreted | <i>Trans_g35334_i1</i> | <i>A. castellani</i> | Encystation-mediating serine proteinase | 1e-62 | B0FYM2 | XM_004355393.1 | Moon <i>et al.</i> (2008) |
| | <i>Trans_g15171_i1</i> | <i>Acytostelium subglobosum</i> | Extracellular matrix protein A | <1e-200 | R4X5L8 | AB743580.1 | Urushihara <i>et al.</i> (2015) |

^aE-value is the number of distinct alignments, with a score equivalent to or better than bit-score S, that are expected to occur in a database search by chance.

The lower the E-value, the more significant the score is.

Table 5.12. Summary of the remaining proteins from both transcriptome assemblies (cultured amoebae and AGD-infected gills) with the details of signal peptide presence and antigenicity.

| Cell Localisation | Matched organism | Protein name | Signal Peptide presence (≥ 0.5) | Antigenicity (≥ 0.5) |
|------------------------|-----------------------------------|---|--|-----------------------------|
| Membrane | <i>D. discoideum</i> | GlcNAc transferase | No (0.0023) | No (0.44) |
| | | Autocrine proliferation repressor protein A | Yes (0.99) | Yes (0.53) |
| Cytoplasm | <i>Perkinsela sp. CCAP 1560/4</i> | IgE-dependent histamine-releasing factor | No (0.004) | Yes (0.56) |
| | <i>Paramoeba pemaquidensis</i> | Elongation factor 1 alpha | No (0.0008) | No (0.4) |
| Extracellular/secreted | <i>A. castellani</i> | Encystation-mediating serine proteinase | Yes (0.99) | Yes (0.59) |
| | <i>Acytostelium subglobosum</i> | Extracellular matrix protein A | Yes (0.99) | Yes (1.02) |

Visual representation of homology (E-values: $\leq 10^{-80}$) shown with Dot Plots in Figure 5.10.

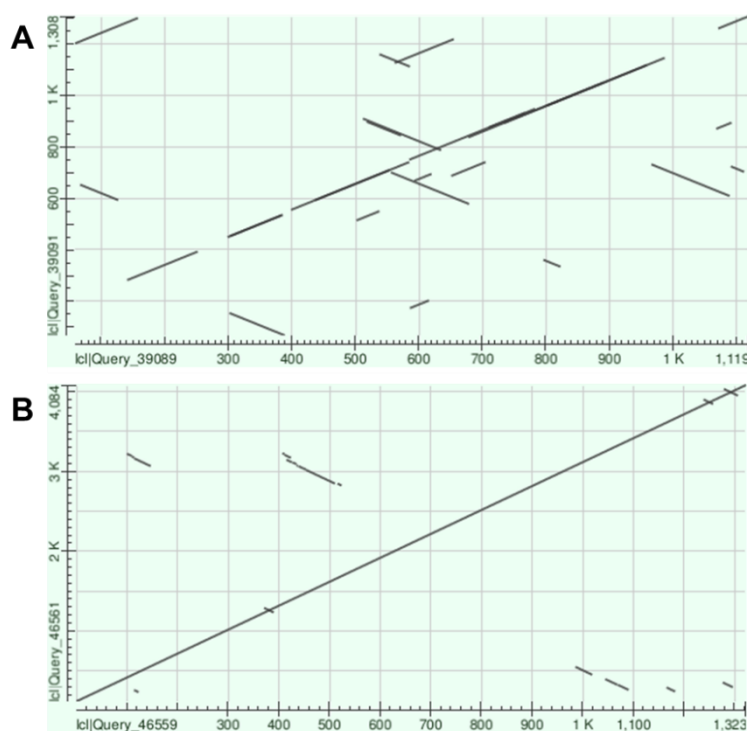


Figure 5.10. Dot Plot of the TBLASTX alignment of the cultured *N. perurans* transcriptome assembly with the known mRNA sequences. (A) *Trans_g35334_i1* vs *A. castellani* Encystation-mediating serine proteinase (XM_004355393.1). (B) *Trans_g15171_i1* vs *A. subglobosum* Extracellular matrix protein A (AB743580.1). Source: Basic local alignment search tool (BLAST) (Altschul *et al.*, 1990).

The ranking of all the proteins is summarised in **Error! Reference source not found.** The selection was performed by taking into consideration the homology to known proteins, level of antigenicity, signal peptide presence and proposed function of the proteins.

Table 5.13. Summary of the six best vaccine candidates identified in this experimental chapter according to their homology to known proteins, antigenicity, presence of signal peptide and proposed

| Rank | Protein | Protein ID (Uniprot) |
|------|--|----------------------|
| 1 | Extracellular matrix protein A (EMPA) | R4X5L8 |
| 2 | Actin bundling protein (ABP) | A0A152A7V9 |
| 3 | Papain-family cysteine protease | L8HJH5 |
| 4 | Carboxypeptidase Y | L8H6Y6 |
| 5 | Autocrine proliferation repressor protein A (APRP-A) | Q5XM24 |
| 6 | Putative integrin alpha FG-GAP repeat-containing protein | F4Q5F1 |

function.

5.4. Discussion

Reverse vaccinology (RV) has proven to be a very efficient tool for identifying potential vaccine candidates within different fish pathogens (Chiang *et al.*, 2015; Andreoni *et al.*, 2016; Liu *et al.*, 2017; Liu *et al.*, 2017a; Baliga *et al.*, 2018). The greatest benefit from this technology is the ability to find vaccine targets rapidly and efficiently, whereas traditional methods might take longer as they require a better understanding of host-pathogen interactions and immunity, as *in vivo* and *in vitro* have to be performed in order to characterise different immune responses and the interactions between the pathogen and the host (Rappuoli & Aderem, 2011). In contrast to more traditional methods, RV allows the identification of new vaccine candidates and their subsequent testing in considerably less time, employing recombinant antigen or DNA-vaccine strategies to allow more rapid test antigen production. In the context of bacterial diseases, the use of antibiotics has given rise to some concerns among the aquaculture industry, due to the continuing appearance of more and more antibiotic-resistant bacterial strains (Vincent *et al.*, 2019). However, a difference is observed from the parasitic disease perspective. Even though antibiotics are not being applied when treating parasitic diseases, chemicals/therapeutants are used and increasing risks to the environment and consumers can be associated. Therefore, the need for alternative treatments for parasitic diseases is increasing sharply within this industry. This experimental chapter attempts the application of this RV technology by characterising the genome / transcriptome of *N. perurans* and using the acquired knowledge to screen for and identify potential vaccine candidates.

This is not the first attempt to perform transcriptomic analysis on a *N. perurans* close-related species. The work by Tanifuji *et al.* (2017) revealed that there is cell biological and biochemical obligate relationship between *N. pemaquidensis* and its endosymbiont *Perkinsela* spp. However, the work undertaken during this thesis counts as the first attempt at elucidating the transcriptome of *N. perurans*. This

investigation has provided some information about potential functions and virulence traits. As explained briefly in the results section, some of the proteins found matching the *N. perurans* transcriptome qualified as potential targets for drug testing. However, the ultimate goal of this experimental chapter was to identify potential vaccine candidates, thus the successful selection of a final list of six best competent proteins according to its potential antigenicity and the presence of signal peptide (section 5.3.8; Table 5.12).

First in the final list, the extracellular protein (Extracellular matrix protein A) was identified in the study of the the social amoeba *Acytostelium subglobosum* by Urushihara *et al.* (2015) as performing a key role during slug formation. This could be a relevant vaccine candidate as it could be actively expressing in *N. perurans* during its trophozoite stage while attaching to the gill epithelia during extension of the pseudopodia. Moreover, it presented the highest antigenicity score of all the proteins that were investigated, and its extracellular nature also makes it very accessible and therefore, an ideal vaccine candidate. Next, actin bundling proteins have been previously characterised in studies involving *Dictyostelium discoideum* in which it was shown that these proteins are regulated by signal transduction during chemotaxis (Okazaki & Yumura, 1995). They have additionally been described in *Acanthamoeba* spp. (Alafag *et al.*, 2006) and genomic and cDNA actin sequences were also found within the virulent strain of *E. histolytica* (Edman *et al.*, 1987; López-Camarillo *et al.*, 2009). The fact that this protein was upregulated during a high AGD infection, suggests it as a potential virulence factor as it has been described in bacterial strains of *Vibrio parahaemolyticus* (Hiyoshi *et al.*, 2011) in which these proteins caused cytotoxicity and enterotoxicity in the infected human cells.

The next two proteins of the list also presented good E-values ($\leq 10^{-80}$) when the transcriptome assembly was blasted and they have been previously characterised as extracellular or secreted products (Papain family cysteine protease and Carboxypeptidase Y) in *A. castellanii* (Clarke *et al.*, 2013). Papain-like cysteine proteases have been described from a wide range of organisms such as virus, bacteria, yeast, plants, animals and, more specifically, protozoa (Rawlings *et al.*,

1992, 2010; Enenkel & Wolf, 1993; Kantyka *et al.*, 2011; Novinec & Lenarcic, 2013). Apart from the catabolic functions that these proteins present, this family of proteases may also play a key role in parasite immunoevasion, excystment/encystment, exsheathing and cell and tissue invasion (Sajid & McKerrow, 2002). For these characteristics, this specific protein could be a useful potential vaccine target as described in previous studies (Engel *et al.*, 1998; Caffrey *et al.*, 2000; Mottram *et al.*, 2004). The second protein which matched the transcriptome of *N. perurans* was a Carboxypeptidase, which has been previously described not only in the genome of *A. castellani* (Clarke *et al.*, 2013) but in various species of protozoan parasites such as *Trypanosoma cruzi* (Hemerly *et al.*, 2003; Parussini *et al.*, 2003; Niemirowicz *et al.*, 2008) and *Leishmania* spp. (Judice *et al.*, 2004; Isaza *et al.*, 2008). This protein presents serine-type carboxypeptidase activity, which catalyses the hydrolysis of a peptide bond from the C-terminus. These studies suggest that these activities present a specific role in these pathogenic protozoa, making them suitable targets for vaccine development or immunotherapy.

The last two proteins of the final vaccine candidate list have been identified in the cell membrane of *Dictyostelium* spp. The most recent characterised protein within this species was the Autocrine proliferation repressor protein A (AprA) as an inhibitor for cell density sensing and chemorepulsion limiting slug formation (Brock & Gomer, 2005; Bakthavatsalam *et al.*, 2008). It was observed that *D. discoideum* cells were able to sense this AprA protein using G proteins, therefore the existence of a G protein-coupled AprA receptor was postulated. Thus, this protein could be a good vaccine candidate against AGD as it could be presenting a similar growth-limiting function in *N. perurans*, therefore the exposure of this protein to the salmon immune system could potentially stimulate an immune response. The second protein, Putative integrin alpha FG-GAP repeat-containing protein, has been characterised not only in *D. fasciculatum* but in *P. pallidum*, another parasitic species. This protein has been found to be in the plasma membrane and mediates cell-to-cell adhesions and also adhesions to particles (Heidel *et al.*, 2011). Due to its adhesin nature, this protein may also be considered as a potential vaccine candidate.

In addition to this list of potential vaccine candidates, another two interesting proteins matched our assembled transcriptome. Elongation factor 1 alpha and IgE-dependent histamine-releasing factor (IgE-HRF) presented very low E-values but are located in the cytoplasm. Cytoplasmic proteins are normally used as drug targets, whereas extracellular and membrane bound proteins are appropriate for vaccine targets due to greater accessibility to the immune system (Butt *et al.*, 2012; Sudha *et al.*, 2019). Although these proteins may not represent good vaccine candidates, they are still interesting to investigate when taking into consideration their potential role during an immune response. As is well-known, the Elongation factor 1 alpha gene (*elfa1*) has been established as a housekeeping gene for use in the normalisation of relative reverse transcription real-time-PCR (RT-PCR) data in salmon (Ingerslev *et al.*, 2006). The protein form acts as a cytoplasmic translation factor and it is implicated in the nuclear export of tRNA species in lower eukaryotes; however, it has been demonstrated that these proteins play an essential role in nuclear export of proteins in mammalian cells (Khacho *et al.*, 2008). However, in the context of parasitic diseases, a recent study by Demarta-Gatsi *et al.* (2019) discovered a potential new function of ELF-1 α during an infection of mice with malaria parasites (*Plasmodium berghei*). During the infection, these parasites produce extracellular vesicles (EVs) to facilitate their survival and chronic infection (Feng *et al.*, 2013; Ramakrishnaiah *et al.*, 2013) and they are known to contain a wide range of molecules, including proteins (Simpson *et al.*, 2009; Torrecilhas *et al.*, 2012), which can be delivered to target host cells. These proteins have been shown to modulate immune responses in some pathogenic protozoan parasites (Schorey & Harding, 2016; Szempruch *et al.*, 2016; Ofir-Birin *et al.*, 2018). During the experiment by Demarta-Gatsi *et al.* (2019), they found that HRF and EF-1 α proteins were localised in *P. berghei* parasites and potentially interacted with each other leading to the inhibition of T cell activation due to the EVs and the presence of these two proteins, acting either independently or together. To verify these findings, the authors performed an immunisation trial with derived EVs to protect the mice against the infection and they acquired a long-lasting antiparasite immune memory.

Within our transcriptome, both assemblies of cultured amoebae and AGD-infected gills presented the ELF-1 α transcript for this protein, but in addition an IgE-HRF homology sequence from endosymbiont (*Perkinsela* spp.) that the amoeba contains. This protein was first characterised in atopic children, where lymphocytes produced this IgE-HRF in response to histamine release. Through the development of recombinant proteins with this specific immunoglobulin, results showed that they caused histamine release from the human basophils and this release was dependent on the presence of IgE (MacDonald *et al.*, 1995). A More recent study determined that some parasitic pathogens like *T. cruzi* present this IgE-HRF and induce histamine production by the host basophils or mast cells, facilitating a successful infection (Menna-Barreto *et al.*, 2010). However, only IgM, IgD, and IgT/Z have been identified in teleost fish (Rombout *et al.*, 2014). Perhaps IgM and IgT, which are known to be linked to AGD infections (Penacchi *et al.*, 2014), act as substitutes for the absent IgE in teleost fish, although neither IgM nor IgT have been reported to be associated with allergic immunity to date.

However, one of the main problems that was encountered during the assembly was the quality of the samples. This was due to the difficult task of growing axenic cultures of *N. perurans*. First, this species' high demands in terms of its culture conditions (*e.g.* temperature and salinity) led to a very slow growth rate which limited the bulking up of the cultures for the ultimate DNA/RNA extraction. In addition, the development of an axenic culture (*i.e.* lacking any bacterial associates or any other metabolising cells) was impossible to accomplish (as it has been for other groups), as this amoebic species was only successfully grown at sufficient numbers when live bacteria were present as a nutrient source. Consequently, due to the high bacterial contamination and the very low DNA yields, the genome characterisation of this parasitic species was not successfully achieved, and the main focus was therefore placed on transcriptome assembly instead. The annotation of the transcriptome was less challenging due to the possibility of filtering out the bacterial transcripts from the parasitic transcripts regarding the presence of shorter poly (A) tails in prokaryote mRNA compared to the ones found in eukaryotic mRNA (Sarkar, 1997). These poly (A) tails are added to the mRNA sequences during a process defined as

polyadenylation culminating in the maturation of the mRNA (Proudfoot *et al.*, 2002; Régnier & Narujo, 2013). However, this transcriptome assembly produced a high number of transcripts (approx. 103,400) in comparison to the transcriptome assembly from the AGD-infected gills which comprised ~90% of raw data from salmon RNA, leaving roughly 8,000 contigs which matched species other than salmon. Thus, the results from the AGD-infected gills did not deliver abundant information about the expression of potential virulence genes during an intense AGD infection. This should have been expected as RNA extraction was performed with a high quantity of gill tissue from salmon, thus a more efficient method should have been explored to achieve a better sample for transcriptomic analysis. Even though the amoebae cultures provided better results and higher number of transcripts, the virulence of this amoebae should have been tested prior to proceeding with posterior RNA extraction and transcriptome assembly. However, during the development of this work experiments with fish were very restricted and, therefore, only cultured amoebae was available to work with. Virulence was not checked but it was supposed to still present virulence as they were less than six months old, which is the time limit that has been described in the past (Bridle *et al.*, 2015). Also, in future work, the endosymbiont present in *N. perurans* should not be pulled out from the genomic data and perhaps better methods and approaches should be taken place such as the work described in Tanifuji *et al.* (2017). During this work, an evident relationship was observed between *N. permaquidensis* and *Perkinsela* spp. with close-linked metabolic pathways. Thus, a deeper investigation when applying RV to these two organisms together, could help understand more about their common biological and biochemical pathways.

Conclusions

In summary, the work described in this chapter has proven that the use of RV for successful *in-silico* screening and identification of potential vaccine candidates is possible. Although there were many difficulties encountered during the assembly of the *N. perurans* transcriptome, the results from this first attempt has delivered some valuable data about, not only novel vaccine candidates, but also potential virulence

traits such as the possible immunomodulation of the host's protective response or the presence of specific enzymes potentially targeting mucins. Ultimately, the investigation of these proteins during *in vivo* challenges might provide a hope of providing protection against *N. perurans*, confirming the level of *in silico* antigenicity that was described when selecting vaccine candidates.

Chapter 6 : Discussion

Aquaculture is a growing industry that is providing solutions to difficulties such as overfishing, by reducing the pressure on wild stocks, which remain under pressure (Anderson, 1985; Frankic & Hershner, 2003; Valderrama & Anderson, 2010), but also plays a key role in food security and provides a source of income and social improvement in developing countries (FAO, 2018). By 2013 approximately 90% of global fisheries were considered to be fished to maximum capacity (FAO, 2018) and with the global demand for food increasing every year due to growing populations (York & Gossard, 2004; Garcia & Rosenberg, 2010; Béné *et al.*, 2015) this is leading to an expansion of the aquaculture industry. Aquaculture has now outgrown fisheries production (FAO, 2018), with salmonids being one of the most valued cultured fish groups, contributing 17% of total global exports by worth to the aquaculture sector. In addition, farmed Atlantic salmon production already exceeds 2 million tonnes per year compared to the 700,000 tonnes obtained from the wild (FAO, 2018). The continuous growth and intensification of this industry can, however, provide conditions that suit the emergence and spread of infectious disease, causing substantial economic losses (Lafferty *et al.*, 2015), linked to negative effects on animal welfare (Folkledal *et al.*, 2016). In this context, gill diseases comprise one of the main problems affecting fish farms and, more specifically, amoebic gill disease (AGD) represents one of the most important challenges for marine fish farms worldwide, affecting not only salmon farming but also a wide range of other fish species (Oldham *et al.*, 2016). Gills represent an easy target for the ectoparasitic agent of this disease, *Neoparamoeba perurans*, due to the gills being in continuous contact with the environment (Rodger, 2007). A compromised gill translates to decreased growth performance and affects gas exchange; this potentially being followed by direct mortalities and the high cost of treating this threat incurs indirect economic losses (Rozas-Serri, 2019). Therefore, there is a clear need for better understanding of the immune systems of fish, more particularly mucosal health, in the context of gill diseases.

Timely treatment of AGD can offer the opportunity to decrease mortalities, and this may be achieved in part through investigation of new methods for molecular detection coupled with the implementation of non-destructive methodologies (Downes *et al.*, 2017). One of the most commonly used treatments against AGD is hydrogen peroxide (H₂O₂), which has been used since the preliminary success demonstrated in a study by Adams *et al.*, 2012. In parallel, when available, freshwater bathing remains a highly effective treatment against this disease (Parsons *et al.*, 2001). However, both treatments have been proven to have some negative effects on salmon. Regarding the freshwater baths, fish showed physiological effects with reduced gill enzyme activity, more specifically Na⁺/K⁺ ATPase and succinic dehydrogenase (SDH) (Powell *et al.*, 2001). Additionally, treatment with H₂O₂ induced stress and a detoxification response in infected salmon (Vera & Migaud, 2016). Therefore, the search for alternative treatments for AGD is one of the main objectives within the industry. Vaccines could provide an ideal solution and are considered to be environmentally friendly (Lieke *et al.*, 2019). Reverse vaccinology (RV), which is a genome/transcriptome-based approach, has been used extensively to identify potential vaccine candidates for other pathogens, facilitating development of protein subunit vaccines and allowing a faster vaccine design process, which reduces animal testing (Rashid *et al.*, 2019). This approach hence appears a highly applicable approach for targeting the causative pathogen for AGD.

During this work, the development of improved methods for handling, culture, visualisation and measurement of amoebae from the fish were approached. However, one of the most challenging aspects of this work has been the culture of *N. perurans*, due to its very slow growth and high maintenance requirements. Thus, *in vitro* work was regularly very limited leading to many experiments having to be discontinued. Also, while optimising the amoebal culture, numerous additional experiments were performed (not reported here but described briefly in Appendix I) with a focus on the cryopreservation of this parasite. The loss of virulence during *in vitro* culture has been previously reported (Bridle *et al.*, 2015); therefore, the ability to cryopreserve stocks / isolates at different points in culture was considered to be

important. Previous studies have already accomplished the successful cryopreservation of several species of amoeba (e.g. *Acanthamoeba* spp. and *Naegleria* spp.), however the survival rates generally did not reach numbers higher than ~40% in most experiments (Kilvington & White, 1991; Seo *et al.* 1992; John & John, 2006). Similar methods were tested on *N. perurans* throughout this study and although there were some initially positive results, they were impossible to replicate hence this work was not further developed. Notably, the strain *Neoparamoeba pemaquidensis* (ATCC® 30735™) which is being held in the ATCC (American Type Culture Collection) has a successful method developed for its cryopreservation and has already been tested providing good results. However, no researchers have been able to replicate this success for *N. perurans*, suggesting fundamental differences in physiology / cryotolerance. Nonetheless, *N. perurans* presents a pseudocyst form that provides short-term survival under salinity and temperature variations (Lima *et al.*, 2017; Collins *et al.*, 2019). These properties provide a possible basis for future research regarding its cryopreservation. Thus, even though the results during this study were not replicable, there is still optimism for this parasite being cryopreserved.

This definitely affected the *in vitro* work, as high numbers of amoebae could not be produced for the experiments with the different swab materials and transcriptomic analysis. Although It did help us to understand the characteristics of the materials such as capacity of retrieval and absorption of the different swab materials, the quality of the cultured amoebae for the characterisation of the amoebae transcriptome was not optimal, as an axenic culture was never achieved. This also limited genomic analysis, which was never performed due to the low numbers of amoebae. Another issue that was not explored prior to this analysis was the possibility of loss of virulence in these cultures, which has been reported in the past (Bridle *et al.*, 2015). To compensate for this, the following work focused on producing some transcriptome data from AGD-infected gills with high scores (2.5) to investigate the potential amoebal transcripts that could be down- or up-regulated during a high level of infection. However, the separation of tissue and amoebae could not be performed, leading to samples with high salmon RNA yields. Different approaches,

potentially with the tools developed through this study, should be explored for the proper characterisation of the transcriptome of amoebae during the course of infection. As explored in one of the experimental chapters, the relevance of mucus preservation is a key step forward because mucus plays an important role during AGD infections due to its increased secretion from the parallel increase of mucous cells (Nowak & Munday, 1994; Zilberg & Munday, 2000; Adams & Nowak, 2003; Roberts & Powell, 2003; Chalmers *et al.*, 2017). The methacarn fixation proved to be an enhanced method for the preservation of mucus. It did also allow the observation of amoebae trophozoites, that were found in close contact with the mucus coating the gill epithelium. Thus, future work could be focus on the development of a method for the recovery of these parasites for transcriptomic analysis that are strongly related to mucus. Mucus extraction methods like the one described in the study by Hellio *et al.* (2002) could provide enough biological material such as mucus and the pathogens that might be present within. The method follows the scraping with a scalp of the fish's skin mucus and the posterior treatment for RNA / DNA extraction. This would limit the presence of salmon during the genomic / transcriptomic analysis.

Thus, the knowledge of fish mucosal immunity is key to understand host-pathogen interactions. The gill mucosal surface encounters many antigens as fish live in congruence with commensal microorganisms (*i.e.* microbiota) (Boutin *et al.*, 2013). Regarding the mucosal immune response, immunoglobulins (*i.e.* IgM and IgT) are usually found within the mucus layer. These molecules play an important role in adaptive immunity and are produced by B cells in response to an immunogen (Uribe *et al.*, 2011). Along with these molecules antimicrobial peptides (AMPs) are present. The AMPs include defensins and cathelicidins and contribute to the first line of defence against microbes in the skin and at mucosal surfaces (Boman, 1991). Fish mucus present many substances and macromolecules which also exist in the fish gill mucus and for which presence or absence is influenced by the kind of stress / disease that the fish is experiencing (Harrell *et al.*, 1976; Louis-Comier *et al.*, 1984; Ellis, 2001; Easy & Ross, 2009; Nigam *et al.*, 2012). The innate response initially involves the AMPs which trap and eliminate pathogens posing a threat to the fish's health. Furthermore, components such as antimicrobial lectins (Russell *et al.*, 2009)

and pro-inflammatory cytokines (Ingerslev *et al.*, 2006) have also been found in the gill epithelium. Therefore, the preservation of the mucus through the developed techniques in this work, in addition to the application of transcriptomic / genomic analysis could enlighten some of the specific immunity of the fish to *N. perurans* if gill mucus is extracted in a more efficient way so the high numbers of transcripts from the host do not diminish the amount of sequenced amoeba transcripts. Nevertheless, Chapter 5 aided in characterising the host-pathogen interactions in the context of mucosal health through the identification of some interesting proteins. Peptidases such as the Papain-family cysteine protease and Carboxypeptidase Y have been previously described in other parasitic infections (Engel *et al.*, 1998; Caffrey *et al.*, 2000; Mottram *et al.*, 2004; Hemerly *et al.*, 2003; Parussini *et al.*, 2003; Judice *et al.*, 2004; Isaza *et al.*, 2008; Niemirowicz *et al.*, 2008). Apart from their potential role in mucus degradation, other virulence traits such as parasite immunoevasion and cell and tissue invasion (Sajid & McKerrow, 2002), qualify them as good vaccine candidates. Additional proteins were identified and have also been investigated in other studies. Different specific functions were presented such as movement and chemotaxis (Actin bundling protein) (Okazaki & Yumura, 1995), attachment (Extracellular matrix protein A) (Urushihara *et al.*, 2015), chemorepulsion (Autocrine proliferation repressor protein A) (Bakthavatsalam *et al.*, 2008) and mediation of cell-to-cell adhesions (Putative integrin alpha FG-GAP repeat-containing protein) (Heidel *et al.*, 2011).

While trying to understand the host-pathogen interactions and the response to treatment, the examination of some of these immune and mucin transcripts was performed through qPCR and the validation of these results was also achieved through the use of immunohistochemistry. H₂O₂ is widely used for the removal of this excess mucus and although several studies have covered the possible effects of this on fish at a histopathological level (Martinsen, 2018), and in terms of oxidative stress (Vera & Migaud, 2016), the potential effect on the mucosal health of salmon has not been directly explored. Thus, in Chapter 4, a study was performed with the main objective of focusing on the effect of this oxidative agent on the gills of AGD-infected and non AGD-infected fish through a limited targeted aspect of the immune

response to treatment in salmon. To achieve this, the analysis was focused in particular on gene transcripts associated with immunity and mucin production in the gills. Further work should consider targeting a wider range of targets, instead of limiting the study to the ones already published in other scientific papers during AGD infections (Penacchi *et al.*, 2014; Benedicenti *et al.*, 2015).

However, the challenge did not result in a successful AGD infection, thus only non AGD-challenged fish were subjected to the analysis, to study the effect of treatment alone. Additionally, samples and data from fish at early (7 dpi) and late (28 dpi) AGD-infection stages, used in the previously published work of Chalmers *et al.*, (2017), were employed to compare the responses found to those seen in an AGD infection challenge conducted under near-identical conditions. Although the same location and conditions were established during both trials, the fact that fish were derived from two separate experiments means that the results described warrant repeated investigation. In terms of the results, there was a potentially long-term effect of weeks on gill mucus production. This could possibly have led to the observed infiltration and involvement of a cellular response at 14 dpt, which was also confirmed with the semi-quantification of CD3⁺ cells. In addition, visual assessment of the methacarn-fixed gill sections provided data about the lower presence of mucus in the 14 dpt fish. Loss of the mucus layer potentially exposes the gills to several environmentally sourced / potentially pathogenic antigens (Linden *et al.*, 2008), culminating in the detected immune response. However, it is worth mentioning that due to the small gill size during the sampling, higher numbers of sections could not be examined, and this might explain the greater variation between individuals.

Due to the AGD-trial failing during this experiment, the actual effect of both treatment and infection was not accomplished, thus future work should certainly look into this aspect. As it has been previously stated in the introduction of this thesis, there has been a wide range of studies that focused on investigating the effects of AGD on fish, but also cases of reinfection with amoebae. However, not many studies on the effect of treatment of the fish, in a genetic / immunological level, has been previously performed in Atlantic salmon. Eventhough there are novel results in this thesis

regarding the effects of hydrogen peroxide on fish, is obvious that further work should be focus on the improvement of experimental design (i.e. the lack of more control groups during the experiments postulated in the thesis). Many factors affect the reinfection of the fish with AGD, lack or excess of mucus production and the immune response. Nevertheless, the results in this chapter do indicate an effect on the mucus production, mucous cell numbers, and an obvious immune response. Thus, when fish are routinely treated in the field, different levels of AGD are present and perhaps fish with lower levels of infection or suffering poor health could be losing most of the mucosal coat affecting the innate immune response and, culminating in compromised gills contributing to other secondary infections.

In addition, AGD-infected fish were studied as a comparison. However, these fish were not subjected to the same number of analyses. Only transcript expression was performed due to only having access to RNA samples and gill tissue that was already preserved in 10% NBF, thus no methacarn-fixed gills were available to study the mucous cells and mucus production. However, as described in the work by Chalmers *et al.* (2017) no differential changes were observed within the sections of fish presenting an early AGD-infection in contrast to the high level of hyperplastic tissue observed in the fish at a later AGD-infection phase. Higher numbers of mucous cells were also observed in the fish with later AGD-infection. Thus, although the results from this current study suggested a generalised down-regulation of all the markers related to cellular immune responses and B-cell markers, it was postulated that perhaps the uneven ratio of epithelial cells and mucous cells could have had an influence on tissue sampling and consequent RNA extraction. This potentially translated into a diminution of the mucin-transcript expression profile. Similar results were reported in the study by Marcos-Lopez *et al.* (2018) when looking at the gene expression profile of specific gill lesions, where lower levels of mucin expression were detected, along with higher expression of TNF- α 3. This work implies that the level of gill damage could hypothetically be playing a key role in the context of gene / transcript expression profiles and has not been taken into consideration in previous studies.

During the characterisation of the amoebae's transcriptome, two further reported proteins did not qualify as good potential vaccine candidates. However, their presence offers a platform for the future research on how a possible immune modulation/allergic response is occurring within the fish as a response to the parasite's IgE-HRF and ELF-1 α proteins, as recently proposed (Schorey & Harding, 2016; Szempruch *et al.*, 2016; Ofir-Birin *et al.*, 2018; Demarta-Gatsi *et al.* 2019). IgE-HRF may be interesting with regards to the relatively unexplored presence and role of allergy in fish (*i.e.* IgE has not been identified in teleosts). Although allergy in fish has not been investigated *per se*, the concept of hypersensitivity has been explored and there is a complete review on the different described types of hypersensitivity in fish by Jurd (1987). More recently, a type IV hypersensitivity reaction was firstly described in Rainbow Trout during the study by Jirillo *et al.* (2007). The results from the *N. perurans* transcriptome and past evidence of these specific and antigen-driven immune hypersensitivity reactions in fish, presents a platform to undertake further studies with reference to fish disease, such as AGD. Furthermore, this future work could be potentially linked to the generalised down-regulation observed in Chapter 4 in the highly AGD-infected fish, supporting a theory of on-going immunomodulation by the parasite. Thus, the first attempt to characterise the *N. perurans* transcriptome has provided a robust list of vaccine candidates providing a platform for further vaccine development, examination of immune responses of fish to parasitic infections and mucosal health research.

Additional molecular techniques, such as qPCR, was applied for the *in vivo* work in the detection of amoebae with different swab materials. However, another novel aspect was studied during this experimental chapter. The swabbing of different gill arches to establish the preferred colonisation of *N. perurans* during an AGD infection. Even though there were variations in the two different trials, there were statistically significant differences found during these *in vivo* trials when sampling each gill arch. Lower *Ct* values were obtained, denoting greater loads, in gill arches 3-4 rather than on the traditionally sampled gill arch 2. The detection of higher amoebal loads in gill arches 3-4 could be due to a wide range of factors such as less water-flow, making the attachment to the gill epithelium easier, as occurs in some gill

monogean parasites (Etile *et al.*, 2018). Due to this work focusing on the swab materials rather than the spatial distribution of the parasites, samples were not taken to pursue this experimental work. However, the lower *Ct* values appear to provide evidence of a clear tendency for the third and fourth gill arches to present higher numbers of amoebae when sampling. Moreover, if less of the gill surface is swabbed through concentration on key arches, lower handling of fish could translate into less stress for fish (Assefa & Abunna, 2018). Future work should be focused on the quantification of amoebal load through histopathological sections in order to be able to confirm that this approach could lead to a timelier detection of amoebae and to establish a clear pattern for the spatial distribution of this parasite during an infection.

Final conclusions

In conclusion, this thesis has developed a range of tools for the characterisation of the host-pathogen interactions. The examination of different swab materials and the swabbing of different gill arches have provided some insight of the potential enhancement of better detection of amoebae during an AGD-infection. In addition, with respect to the interactions between the host and *N. perurans*, gill mucus was studied through the comparison of a series of fixatives, which culminated in confirmation of methacarn fixation as an improved technique for the preservation of the mucus coat along the gill epithelium. These findings supplemented the ones observed in the following chapter, in which the effect of hydrogen peroxide was explored through gene expression and immunohistochemistry. A potential effect of this oxidising agent appears to be the instigation of a T-cell response due to the loss of mucosal coat. A study of AGD-infected fish presented interesting results, which have raised some important questions into the quality of the biological material and the effect of gill damage in gene / transcript expression. Lastly, cultured amoebae were subjected to transcriptomic analysis and a list of potential vaccine candidates was generated by a reverse vaccinology approach targeting the *N. perurans*

transcriptome. Additional AGD-infected gill was also subjected to this analysis. Even though the starting material was not of high-quality, the information within this chapter provided some good targets offering the possibility of producing recombinant proteins and subsequent *in vivo* testing, with the ultimate goal of producing a successful vaccine against this parasite in Atlantic salmon. The work presented in this thesis work has fostered the development of a number of new tools, methods and approaches, which together provide an excellent platform for future research concerning AGD and fish mucosal health more widely.

Appendices

I. Protocol for the cryopreservation of *N. perurans*

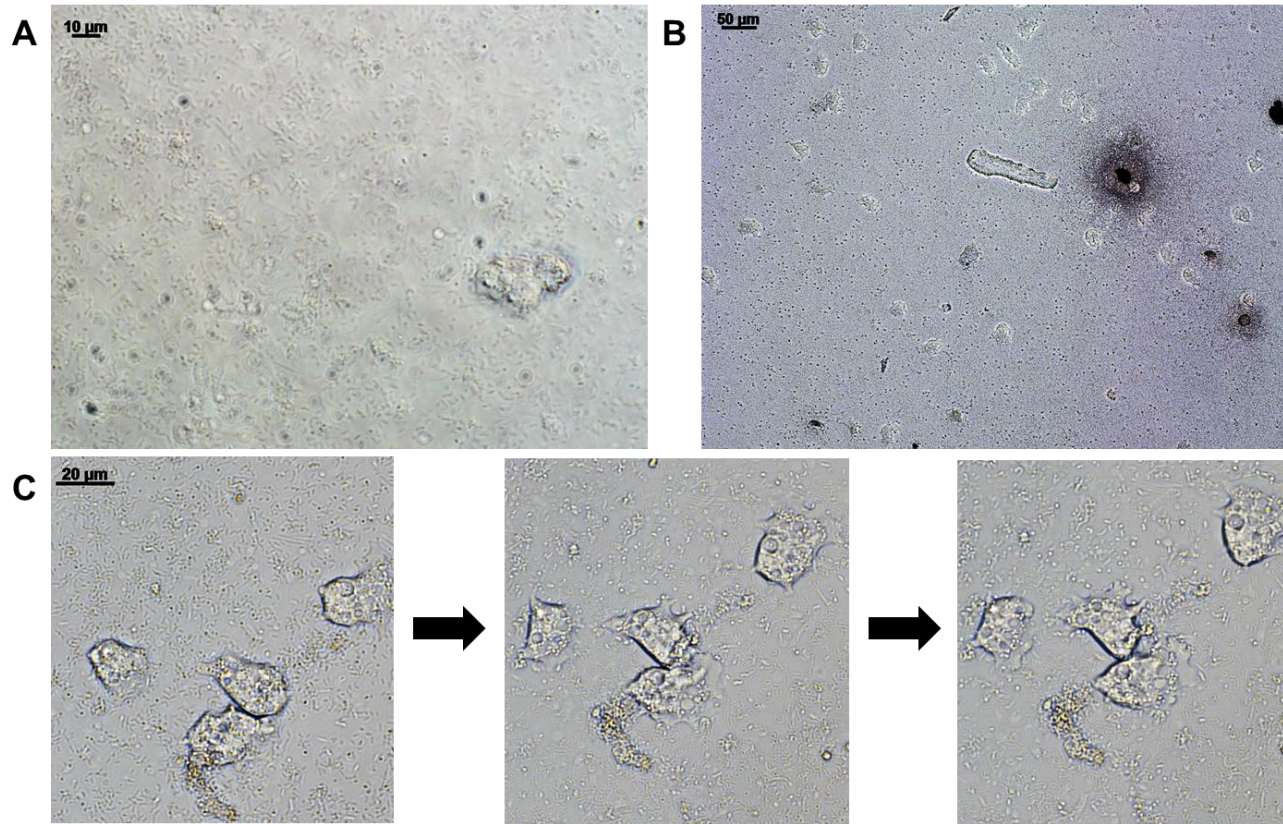
Cryopreservation methodology

A volume of 5mL from an early subculture (3-4 days) was taken and centrifuged at 200g for 10min. Following this, pellets were resuspended in 5 mL of freezing medium. Five replicates were maintained in DMEM (7.5% DMSO (Dimethyl sulfoxide, Sigma, UK), 20% FCS (Foetal calf/bovine serum, Sigma, UK) and DMEM (Dulbecco's Modified Eagle Medium, Sigma, UK)) and another five replicates were maintained in FSW (7.5% DMSO, 20% FCS and FSW). Then, they were aliquoted in ten cryovials (Nunc[®], Denmark) and store in the CoolCell[®] SV2 (Corning[®], UK) at -70°C for 24 h.

After the freezing period, samples were thawed in a 37°C bath for 2-3 min until almost all the ice is melted and diluted 15 mL of 15 °C fresh medium (FSW). A 6-well plate (Corning[®], UK) was seeded with 1 mL from the 15 mL dilution and additional 3 mL of FSW were added, diluting the concentration of FCS and DMEM for the first five replicates. The same protocol was followed for the other five cryovials.

Preliminary results from the cryopreservation of *N. perurans*

The viability of *N. perurans* trophozoites was assessed after 3 days (Appendix Fig. 1A) and after 13 days (Appendix Fig. 1B). Viability was assessed by checking trophozoites movement as showed in Appendix Figure 1C. These results were impossible to replicate, however.



Appendix Figure 1. Single satisfactory attempt while applying the protocol in Section I of this Appendix. A. Viable trophozoite after 3 days of culture. High bacterial contamination can be observed. B. Viable trophozoites after 13 days of thawing the cryopreserved samples with high bacterial contamination. C. Confirmation of *N. perurans* trophozoites viability through the assessment of its movement across the culture flasks. Image taken by light microscopy with microscope Olympus BX53M and images were taken with Olympus SC100 camera.

II. Annotation of the amoebae-cultured transcriptome with matching cell membrane proteins before blasting against the host's transcriptome. In blue and green the proteins that didn't match salmon's transcriptome

Appendix Table 1. Annotation of the amoebae-cultured transcriptome with matching cell membrane proteins before blasting against the host's transcriptome (73 proteins in total). Highlighted in grey the proteins that did not match salmon's transcriptome.

| Transcript ID | Cell location | Protein name |
|-----------------|---------------|--|
| Trans_g8639_i1 | Cell membrane | Endoplasmic reticulum-Golgi intermediate compartment protein 3 |
| Trans_g8730_i1 | Cell membrane | ABC transporter C family member 11 |
| Trans_g8812_i1 | Cell membrane | ABC transporter ATP-binding protein NatA |
| Trans_g9010_i1 | Cell membrane | Major facilitator superfamily domain-containing protein 1 |
| Trans_g9064_i1 | Cell membrane | cAMP-dependent protein kinase type I-alpha regulatory subunit |
| Trans_g9085_i1 | Cell membrane | Putative metabolite transport protein NicT |
| Trans_g9352_i1 | Cell membrane | Sarcoplasmic/endoplasmic reticulum calcium ATPase 2 |
| Trans_g9362_i1 | Cell membrane | Molybdenum import ATP-binding protein ModC |
| Trans_g9362_i2 | Cell membrane | Molybdenum import ATP-binding protein ModC |
| Trans_g9529_i1 | Cell membrane | Putative phospholipid-transporting ATPase 9 |
| Trans_g10170_i1 | Cell membrane | Bifunctional fatty acid conjugase/Delta(12)-oleate desaturase |
| Trans_g10496_i1 | Cell membrane | Transmembrane protein 104 |
| Trans_g11625_i1 | Cell membrane | Guanine nucleotide-binding protein alpha-2 subunit |

| | | |
|-----------------|---------------|--|
| Trans_g12398_i1 | Cell membrane | Vacuole membrane protein 1 homolog |
| Trans_g12511_i1 | Cell membrane | Guanine nucleotide-binding protein alpha-2 subunit |
| Trans_g12511_i2 | Cell membrane | Guanine nucleotide-binding protein alpha-2 subunit |
| Trans_g13033_i1 | Cell membrane | Calcium-transporting ATPase 2 |
| Trans_g13033_i2 | Cell membrane | Calcium-transporting ATPase 2 |
| Trans_g13451_i2 | Cell membrane | Phosphatidylcholine:ceramide cholinephosphotransferase 3 |
| Trans_g13451_i3 | Cell membrane | Phosphatidylcholine:ceramide cholinephosphotransferase 3 |
| Trans_g13622_i1 | Cell membrane | Pyrophosphate-energized membrane proton pump 2 |
| Trans_g13656_i1 | Cell membrane | Receptor like protein 21 |
| Trans_g13687_i1 | Cell membrane | P2X receptor D |
| Trans_g13687_i3 | Cell membrane | P2X receptor D |
| Trans_g13780_i2 | Cell membrane | Vacuolar protein sorting-associated protein 45 |
| Trans_g13993_i2 | Cell membrane | ABC transporter C family member 11 |
| Trans_g14064_i1 | Cell membrane | ABC transporter C family member 11 |
| Trans_g14064_i3 | Cell membrane | Cystic fibrosis transmembrane conductance regulator |
| Trans_g14244_i1 | Cell membrane | Guanine nucleotide-binding protein alpha-2 subunit |
| Trans_g14255_i1 | Cell membrane | Guanine nucleotide-binding protein alpha-2 subunit |
| Trans_g14255_i2 | Cell membrane | Guanine nucleotide-binding protein alpha-2 subunit |
| Trans_g14255_i3 | Cell membrane | Guanine nucleotide-binding protein alpha-2 subunit |
| Trans_g78_i1 | Cell membrane | Alpha-soluble NSF attachment protein |

| | | |
|----------------|---------------|---|
| Trans_g78_i2 | Cell membrane | Alpha-soluble NSF attachment protein |
| Trans_g1313_i1 | Cell membrane | Primary amine oxidase |
| Trans_g1674_i2 | Cell membrane | Triose phosphate/phosphate translocator |
| Trans_g1710_i1 | Cell membrane | ABC transporter C family member 11 |
| Trans_g1710_i3 | Cell membrane | ABC transporter C family member 11 |
| Trans_g1795_i1 | Cell membrane | ABC transporter ATP-binding protein NatA |
| Trans_g2401_i1 | Cell membrane | Zinc transporter ZIP8 |
| Trans_g2519_i2 | Cell membrane | Piezo-type mechanosensitive ion channel component |
| Trans_g3244_i1 | Cell membrane | Piezo-type mechanosensitive ion channel component |
| Trans_g3674_i1 | Cell membrane | Putative phospholipid-transporting ATPase 9 |
| Trans_g4082_i1 | Cell membrane | Glucosidase 2 subunit alpha |
| Trans_g4595_i1 | Cell membrane | Autophagy-related protein 9A |
| Trans_g5214_i1 | Cell membrane | ABC transporter C family member 11 |
| Trans_g5375_i1 | Cell membrane | Sel1-repeat-containing protein YbeQ |
| Trans_g5448_i1 | Cell membrane | Aldehyde dehydrogenase family 9 member A1 |
| Trans_g5562_i1 | Cell membrane | Putative sulfate transporter YbaR |
| Trans_g5670_i1 | Cell membrane | ABC transporter ATP-binding protein NatA |
| Trans_g5769_i1 | Cell membrane | Protein DD3-3 |
| Trans_g6060_i1 | Cell membrane | Vacuole membrane protein 1 homolog |
| Trans_g6103_i1 | Cell membrane | Geranylgeranyl pyrophosphate synthase 11 |

| | | |
|-----------------|---------------|---|
| Trans_g6495_i1 | Cell membrane | AP-4 complex subunit epsilon-1 |
| Trans_g6724_i1 | Cell membrane | Cystinosin homolog |
| Trans_g6869_i1 | Cell membrane | Sodium channel protein 1 brain |
| Trans_g7176_i1 | Cell membrane | Uncharacterized aarF domain-containing protein kinase At5g05200 |
| Trans_g8073_i1 | Cell membrane | Guanine nucleotide-binding protein alpha-2 subunit |
| Trans_g8256_i1 | Cell membrane | Cytochrome b5 isoform B |
| Trans_g8324_i1 | Cell membrane | Putative integrin alpha FG-GAP repeat-containing protein |
| Trans_g15112_i1 | Cell membrane | Integrator complex subunit 11 |
| Trans_g15208_i1 | Cell membrane | Sarcoplasmic/endoplasmic reticulum calcium ATPase 2 |
| Trans_g15835_i1 | Cell membrane | Putative ZDHHC-type palmitoyltransferase 5 |
| Trans_g15858_i3 | Cell membrane | CBL-interacting protein kinase 3 |
| Trans_g16250_i1 | Cell membrane | Endoplasmic reticulum-Golgi intermediate compartment protein 3 |
| Trans_g16738_i1 | Cell membrane | Lysine-specific demethylase JMJ703 |
| Trans_g16976_i3 | Cell membrane | Myosin ID heavy chain |
| Trans_g17024_i1 | Cell membrane | Cell surface glycoprotein 1 |
| Trans_g17025_i1 | Cell membrane | Sarcoplasmic/endoplasmic reticulum calcium ATPase 2 |
| Trans_g17025_i2 | Cell membrane | Sarcoplasmic/endoplasmic reticulum calcium ATPase 2 |
| Trans_g17026_i1 | Cell membrane | Sarcoplasmic/endoplasmic reticulum calcium ATPase 2 |
| Trans_g17198_i1 | Cell membrane | Putative phospholipid-transporting ATPase 9 |
| Trans_g17221_i1 | Cell membrane | Bumetanide-sensitive sodium-(potassium)-chloride cotransporter |

Appendix Table 2. Annotation of the amoebae-cultured transcriptome with matching extracellular proteins before blasting against the host's transcriptome (62 proteins in total). Highlighted in grey the proteins that did not match salmon's transcriptome.

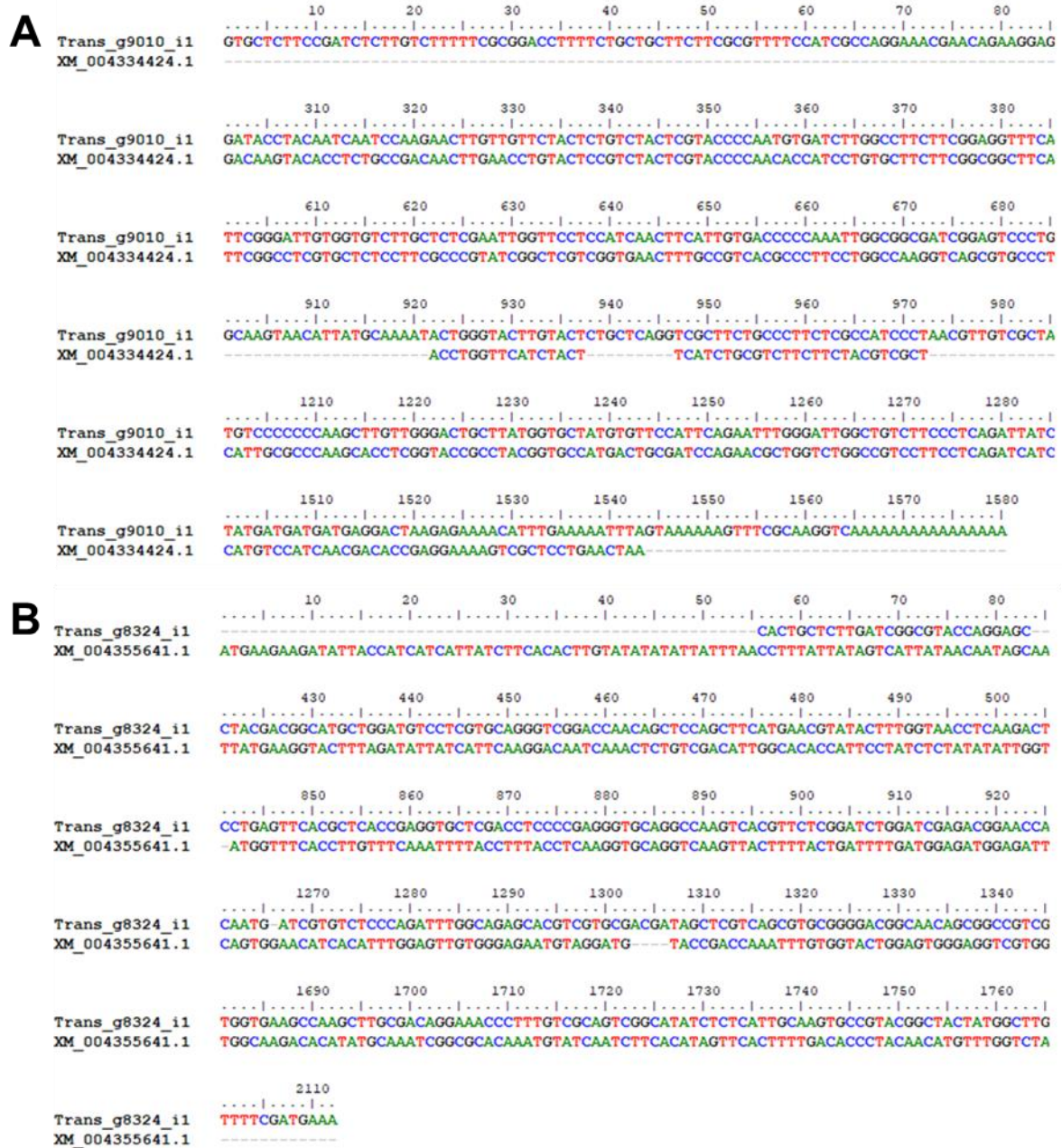
| Transcript ID | Cell location | Protein name |
|----------------------|----------------------|---|
| Trans_g194_i1 | Extracellular | Glutamyl-tRNA(Gln) amidotransferase subunit A |
| Trans_g542_i1 | Extracellular | CBL-interacting protein kinase 3 |
| Trans_g999_i1 | Extracellular | Deoxyribonuclease-2-alpha |
| Trans_g1428_i2 | Extracellular | Papain family cysteine protease |
| Trans_g1759_i1 | Extracellular | Aldehyde oxidase 1 |
| Trans_g1912_i3 | Extracellular | UPF0577 protein KIAA1324 |
| Trans_g1945_i5 | Extracellular | Protein TMA108 |
| Trans_g2151_i1 | Extracellular | Carboxylesterase 3A |
| Trans_g2432_i1 | Extracellular | Phospholipase B-like protein G |
| Trans_g2536_i1 | Extracellular | Carboxypeptidase B2 |
| Trans_g2558_i1 | Extracellular | Uroporphyrinogen decarboxylase |
| Trans_g3481_i1 | Extracellular | Choline-sulfatase |
| Trans_g3600_i1 | Extracellular | Carboxylesterase 3A |
| Trans_g3950_i1 | Extracellular | Polyketide synthase 1 |
| Trans_g3966_i1 | Extracellular | Carboxypeptidase Y |
| Trans_g4459_i1 | Extracellular | Carboxylesterase 3A |

| | | |
|----------------|---------------|---------------------------------------|
| Trans_g4530_i1 | Extracellular | Putative dioxygenase SSO1533 |
| Trans_g4530_i2 | Extracellular | Putative dioxygenase SSO1533 |
| Trans_g5068_i1 | Extracellular | Carboxypeptidase Y |
| Trans_g6336_i1 | Extracellular | Dihydropteridine reductase |
| Trans_g6336_i2 | Extracellular | Dihydropteridine reductase |
| Trans_g6362_i1 | Extracellular | Tripeptidyl-peptidase 1 |
| Trans_g6362_i2 | Extracellular | Tripeptidyl-peptidase 1 |
| Trans_g6387_i1 | Extracellular | E3 ubiquitin-protein ligase RNF19A |
| Trans_g6763_i2 | Extracellular | WD repeat-containing protein 19 |
| Trans_g7517_i2 | Extracellular | CTP synthase 1-A |
| Trans_g7829_i1 | Extracellular | Tripeptidyl-peptidase 1 |
| Trans_g7911_i1 | Extracellular | Putative dioxygenase VC_1345 |
| Trans_g8766_i4 | Extracellular | Carboxypeptidase Y |
| Trans_g8766_i5 | Extracellular | Carboxypeptidase Y |
| Trans_g8766_i6 | Extracellular | Carboxypeptidase Y |
| Trans_g8922_i1 | Extracellular | Tripeptidyl-peptidase 1 |
| Trans_g8925_i1 | Extracellular | NADH-quinone oxidoreductase subunit F |
| Trans_g9423_i1 | Extracellular | Periplasmic trehalase |
| Trans_g9734_i1 | Extracellular | Dipeptidyl peptidase 2 |
| Trans_g9829_i1 | Extracellular | Cathepsin D |

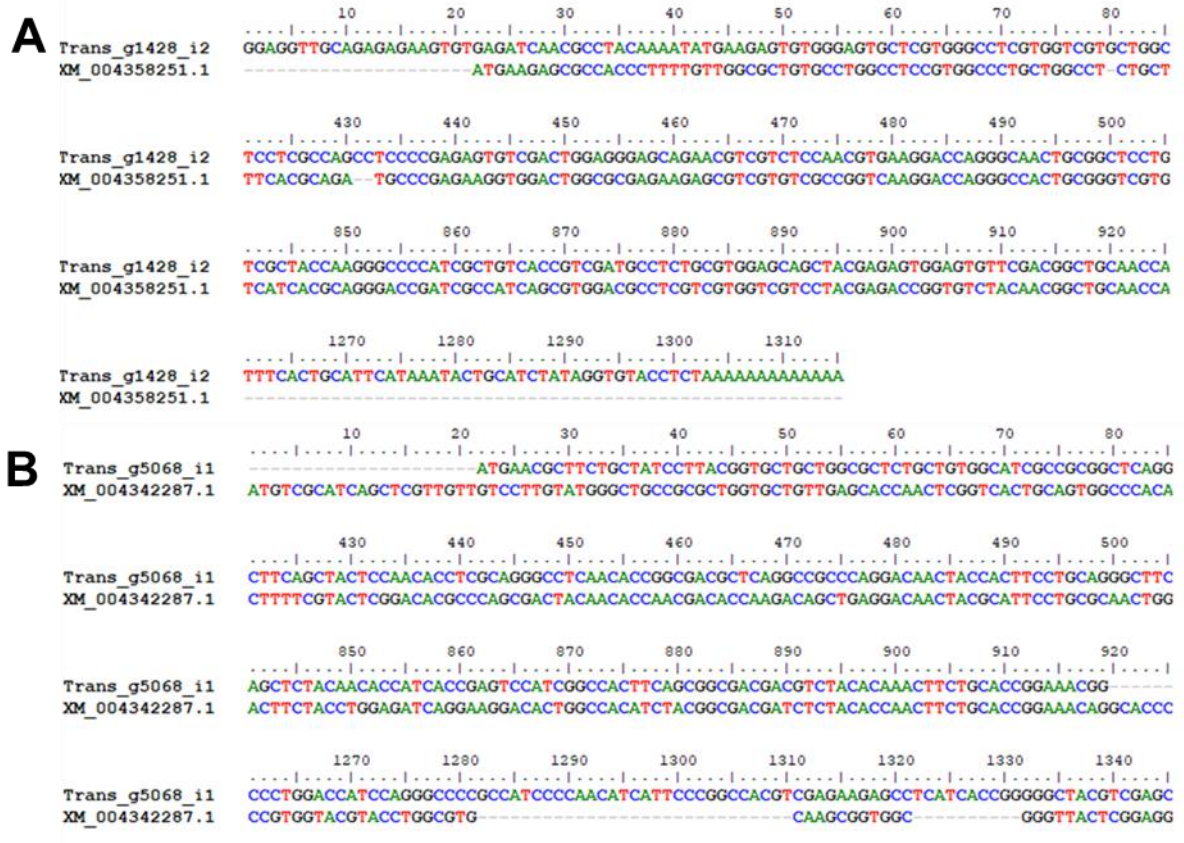
| | | |
|-----------------|---------------|---|
| Trans_g10621_i3 | Extracellular | Tripeptidyl-peptidase 1 |
| Trans_g11484_i1 | Extracellular | Glucosidase 2 subunit alpha |
| Trans_g12122_i1 | Extracellular | Probable beta-hexosaminidase ARB_01353 |
| Trans_g12122_i2 | Extracellular | Probable beta-hexosaminidase ARB_01353 |
| Trans_g12122_i3 | Extracellular | Probable beta-hexosaminidase ARB_01353 |
| Trans_g12132_i1 | Extracellular | Elongation factor-like GTPase 1 |
| Trans_g12132_i2 | Extracellular | Elongation factor-like GTPase 1 |
| Trans_g12132_i3 | Extracellular | Elongation factor-like GTPase 1 |
| Trans_g12132_i4 | Extracellular | Elongation factor-like GTPase 1 |
| Trans_g12342_i1 | Extracellular | Pantetheinase |
| Trans_g12342_i4 | Extracellular | Pantetheinase |
| Trans_g12346_i1 | Extracellular | Putative glucosylceramidase 1 |
| Trans_g12355_i1 | Extracellular | Endoplasmic reticulum chaperone BiP |
| Trans_g12369_i1 | Extracellular | Fimbrin-2 |
| Trans_g12740_i1 | Extracellular | GDP-Man:Man(3)GlcNAc(2)-PP-Dol alpha-1 |
| Trans_g13466_i1 | Extracellular | Rab GDP dissociation inhibitor alpha |
| Trans_g13895_i2 | Extracellular | ATP-dependent (S)-NAD(P)H-hydrate dehydratase 1 |
| Trans_g15171_i1 | Extracellular | Protein psiK |
| Trans_g15206_i1 | Extracellular | Thioredoxin-1 |
| Trans_g15206_i2 | Extracellular | Thioredoxin-1 |

| | | |
|-----------------|---------------|---------------------------------|
| Trans_g15655_i1 | Extracellular | Tripeptidyl-peptidase 1 |
| Trans_g15791_i1 | Extracellular | Phosphoglucomutase |
| Trans_g16506_i4 | Extracellular | Probable cysteine desulfurase 1 |
| Trans_g16658_i1 | Extracellular | Tripeptidyl-peptidase 1 |
| Trans_g17086_i1 | Extracellular | Acyloxyacyl hydrolase |
| Trans_g17086_i2 | Extracellular | Acyloxyacyl hydrolase |

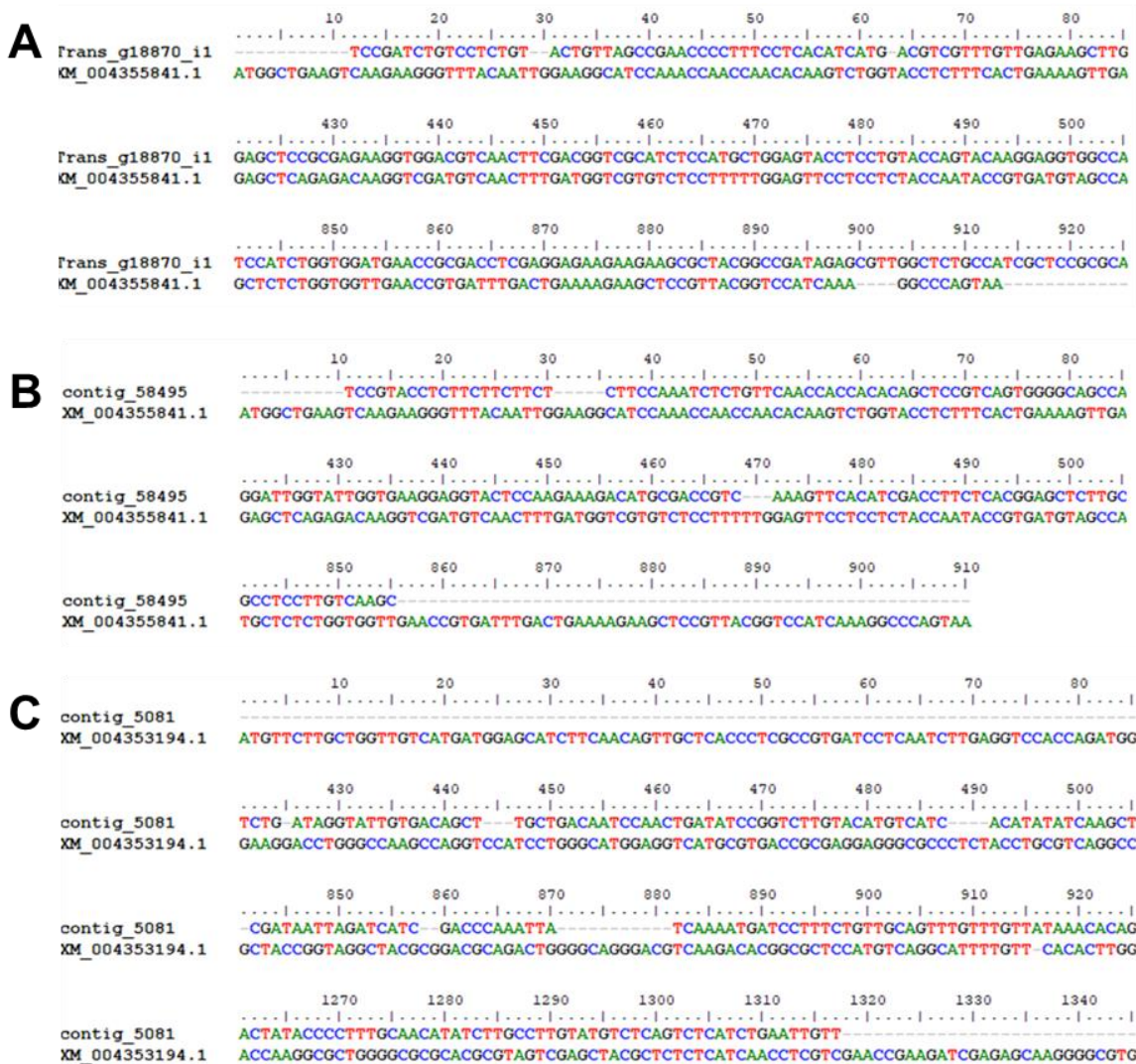
III. Alignments of all the mRNA sequences with the *N. perurans* transcriptome



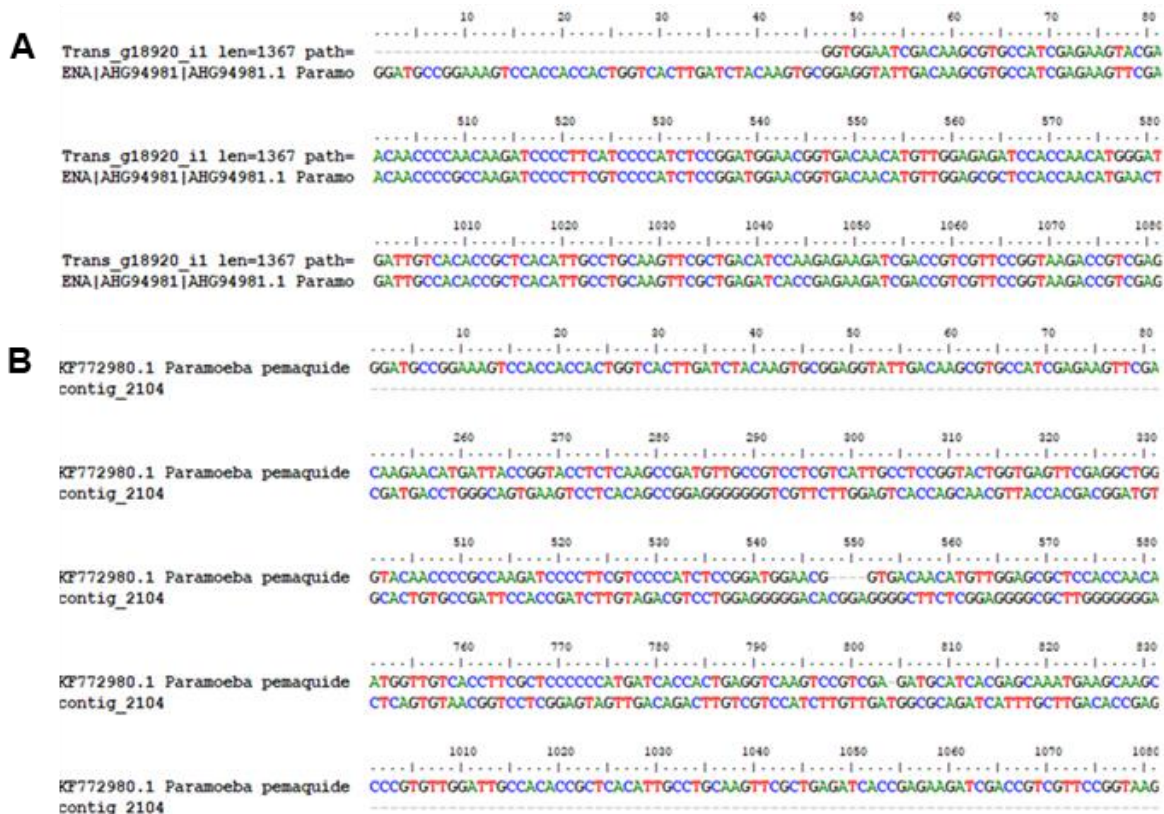
Appendix Figure 2. Alignment of transcripts with cell membrane proteins. (A) *Trans_g9010_i1* from the cultured *N. perurans* transcriptome assembly with the mRNA sequence of the *A. castellanii* transporter, major facilitation subfamily protein (XM_004334424.1) and (B) *Trans_g8324_i1* transcript from the cultured *N. perurans* transcriptome assembly with mRNA sequence of the *D. fasciculatum* integrin alpha FG-GAP (XM_004355641.1).



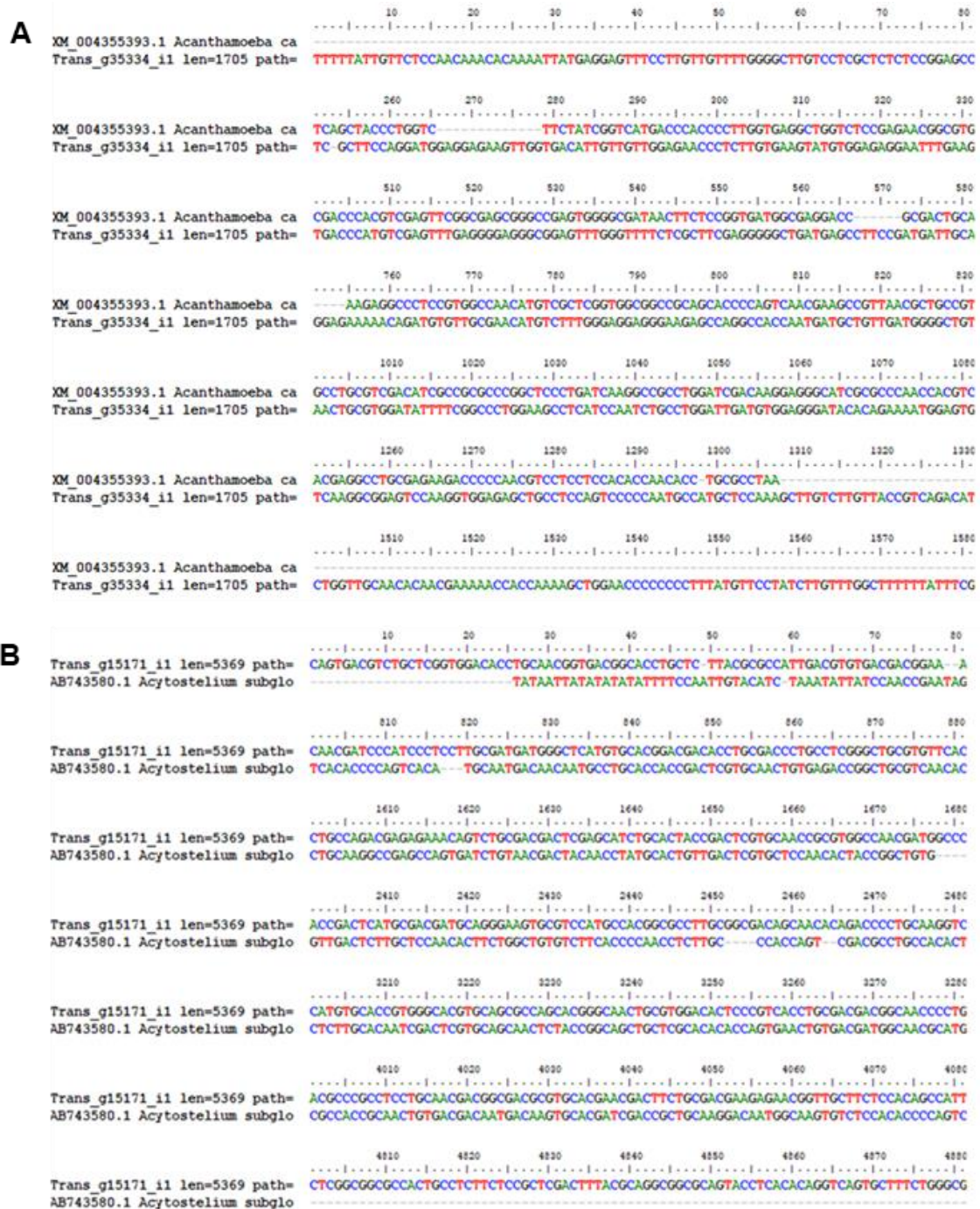
Appendix Figure 3. Alignment of transcripts with the extracellular proteins. (A) *Trans_g1428_i2* transcript from the cultured *N. perurans* transcriptome assembly with mRNA sequence of the *A. castellanii* Papain family cysteine protease (XM_004358251.1) and (B) *Trans_g5068_i1* from the cultured *N. perurans* transcriptome assembly transcript with mRNA sequence of the *A. castellanii* Carboxypeptidase Y (XM_004342287.1).



Appendix Figure 4. Alignment of transcripts of the AGD-infected gills transcriptome. (A) *Trans_g18870_i1* transcript from the cultured *N. perurans* transcriptome with mRNA sequence of the *T. lacteum* Actin bundling protein (XM_004355841.1), (B) *contig_58495* transcript from the AGD-infected gills transcriptome assembly with mRNA sequence of the *T. lacteum* Actin bundling protein (XM_004355841.1) and (C) *contig_5081* transcript from the AGD-infected gills transcriptome assembly with mRNA sequence of *A. castellanii* the Reverse transcriptase (XM_004353194.1).



Appendix Figure 6. Alignment of transcripts (A) *Trans_g18920_i1* from the cultured amoebae transcriptome assembly with mRNA sequence of the Elongation factor alpha 1 (KF772980.1) and (B) the transcript *contig_2104* from the AGD-infected gills transcriptome assembly with mRNA sequence of the Elongation factor alpha 1 (KF772980.1).



Appendix Figure 7. Alignment of transcripts (A) *Trans_g35334_i1* from the cultured amoebae transcriptome assembly with mRNA sequence of the *A. castellanii* Encystation-mediating serine proteinase (XM_004355393.1) and (B) *Trans_g15171_i1* from the cultured amoebae transcriptome assembly with the *A. subglobosum* mRNA sequence of the Extracellular matrix protein A (AB743580.1).

References

- Adams, M. B. & Nowak, B. F. (2001). Distribution and structure of lesions in the gills of Atlantic salmon, *Salmo salar* L., affected with amoebic gill disease. *Journal of Fish Diseases*, 24(9), 535-542. doi:10.1046/j.1365-2761.2001.00330.x.
- Adams, M. B. & Nowak, B. F. (2003). Amoebic gill disease: sequential pathology in cultured Atlantic salmon, *Salmo salar* L. *Journal of Fish Diseases*, 26(10), 601-614. doi: 10.1046/j.1365-2761.2003.00496.x.
- Adams, M. B. & Nowak, B. F. (2004). Experimental amoebic gill disease of Atlantic salmon, *Salmo salar* L.: further evidence for the primary pathogenic role of *Neoparamoeba* spp. (Page, 1987). *Journal of Fish Diseases*, 27(2), 105-113. doi: 10.1111/j.1365-2761.2004.00522.x.
- Adams, M. B. & Nowak, B. F. (2004a). Sequential pathology after initial freshwater bath treatment for amoebic gill disease in cultured Atlantic salmon, *Salmo salar* L. *Journal of Fish Diseases*, 27(3), 163-173. doi: 10.1111/j.1365-2761.2004.00531.x.
- Adams, M. B., Crosbie, P. B. B. & Nowak, B. F. (2012). Preliminary success using hydrogen peroxide to treat Atlantic salmon, *Salmo salar* L., affected with experimentally induced amoebic gill disease (AGD). *Journal of Fish Diseases*, 35(11), 839-848. doi: 10.1111/j.1365-2761.2012.01422.x.
- Adams, A. & Subasinghe, R. (2019). Use of Fish Vaccines in Aquaculture (Including Methods of Administration). *Veterinary Vaccines for Livestock*.
- Adams, A. (2019). Progress, challenges and opportunities in fish vaccine development. *Fish and Shellfish Immunology*, 90, 210-214. doi: 10.1016/j.fsi.2019.04.066.
- Akbari, M., Taghizadeh, V., Heidarieh, M., & Hajimoradloo, A. (2017). The key role of Tumor Necrosis Factor alpha (TNF- α) in vaccinated rainbow trout via irradiated *Ichthyophthirius multifiliis* trophont. *Veterinarski arhiv*, 87(2), 229-237.
- Akhlaghi, M., Munday, B. L., Rough, K. & Whittington, R. J. (1996). Immunological aspects of amoebic gill disease in salmonids. *Diseases of Aquatic Organisms*, 25(1-2), 23-31. doi: 10.3354/dao025023.

- Alafag, J. I. I., Moon, E. K., Hong, Y. C., Chung, D. I., & Kong, H. H. (2006). Molecular and biochemical characterization of a novel actin bundling protein in *Acanthamoeba*. *The Korean Journal of Parasitology*, 44(4), 331. doi: 10.3347/kjp.2006.44.4.331.
- Alexander, J. B. & Ingram, G. A. (1992). Non-cellular nonspecific defence mechanisms of fish. *Annual Review of Fish Diseases*, 2, 249-279. doi: 10.1016/0959-8030(92)90066-7.
- Allan-Wojtas, P., Farnworth, E. R., Modler, H. W. & Carbyn, S. (1997). A solvent-based fixative for electron microscopy to improve retention and visualization of the intestinal mucus blanket for probiotics studies. *Microscopy Research and Technique*, 36(5), 390-399. doi:10.1002/(sici)1097-0029(19970301)36:5<390::aid-jemt9>3.0.co;2-p.
- Almagro-Armenteros, J. J., Sønderby, C. K., Sønderby, S. K., Nielsen, H. & Winther, O. (2017). DeepLoc: prediction of protein subcellular localization using deep learning. *Bioinformatics*, 33(21), 3387-3395. doi: 10.1093/bioinformatics/btx431.
- Almeida, G. M., Laanto, E., Ashrafi, R. & Sundberg, L. R. (2019). Bacteriophage adherence to mucus mediates preventive protection against pathogenic bacteria. *Mbio*, 10(6). doi: 10.1128/mBio.01984-19.
- Altschul, S. F., Gish, W., Miller, W., Myers, E. W. & Lipman, D. J. (1990). Basic local alignment search tool. *Journal of Molecular Biology*, 215(3), 403-410. doi: 10.1016/S0022-2836(05)80360-2.
- Alvarez-Pellitero, P. (2008). Fish immunity and parasite infections: from innate immunity to immunoprophylactic prospects. *Veterinary Immunology and Immunopathology*, 126(3-4), 171-198. doi: 10.1016/j.vetimm.2008.07.013.
- Anderson, D. P. & Klontz, G. W. (1970). Precipitating antibody against *Aeromonas salmonicida* in serums of inbred albino rainbow trout (*Salmo gairdneri*). *Journal of the Fisheries Board of Canada*, 27(8), 1389-1393. doi: 10.1139/f70-164.
- Anderson, J. L. (1985). Market interactions between aquaculture and the common-property commercial fishery. *Marine Resource Economics*, 2(1), 1-24. doi: 10.1086/mre.2.1.42628874.

- Andreoni, F., Amagliani, G. & Magnani, M. (2016). Selection of vaccine candidates for fish pasteurellosis using reverse vaccinology and an *in vitro* screening approach. *Methods in Molecular Biology*, 1404, 181-92. doi: 10.1007/978-1-4939-3389-1_12.
- Andreoni, F., Boiani, R., Serafini, G., Amagliani, G., Dominici, S., Riccioni, G. & Magnani, M. (2013). Isolation of a novel gene from *Photobacterium damsela* subsp. piscicida and analysis of the recombinant antigen as promising vaccine candidate. *Vaccine*, 31(5), 820-826. doi: 10.1016/j.vaccine.2012.11.064.
- Aranishi, F. & Nakane, M. (1997). Epidermal proteases of the *Japanese eel*. *Fish Physiology and Biochemistry*, 16(6), 471-478. doi: 10.1023/A:100773680.
- Arme, C. & Halton, D. W. (1972). Observations on the occurrence of *Diclidophora merlangi* (Trematoda: Monogenea) on the gills of whiting, *Gadus merlangus*. *Journal of Fish Biology*, 4, 27-32. doi: 10.1111/j.1095-8649.1972.tb05649.x.
- Asakawa, M. (1970). Histochemical studies of the mucus on the epidermis of eel, *Anguilla japonica*. *Nippon Suisan Gakkaishi*, 36, 83-87.
- Assefa, A. & Abunna, F. (2018). Maintenance of fish health in aquaculture: review of epidemiological approaches for prevention and control of infectious disease of fish. *Veterinary Medicine International*. doi: 10.1155/2018/5432497.
- Aujla, S. J., Chan, Y. R., Zheng, M., Fei, M., Askew, D. J., Pociask, D. A. & Husain, S. (2008). IL-22 mediates mucosal host defense against Gram-negative bacterial pneumonia. *Nature Medicine*, 14(3), 275. doi: 10.1038/nm1710.
- Aujla, S. J., Dubin, P. J. & Kolls, J. K. (2007). Th17 cells and mucosal host defense. *Seminars in Immunology*, 19(6), 377-382. doi: 10.1016/j.smim.2007.10.009.
- Aurrecoechea, C., Brestelli, J., Brunk, B. P., Carlton, J. M., Dommer, J., Fischer, S. & Harb, O. S. (2008). GiardiaDB and TrichDB: integrated genomic resources for the eukaryotic protist pathogens *Giardia lamblia* and *Trichomonas vaginalis*. *Nucleic Acids Research*, 37(1), 526-530. doi: 10.1093/nar/gkn631.
- Avendaño-Herrera, R., Magariños, B., Irgang, R. & Toranzo, A. E. (2006). Use of hydrogen peroxide against the fish pathogen *Tenacibaculum maritimum* and its effect on infected turbot (*Scophthalmus maximus*). *Aquaculture*, 257(1-4), 104-110. doi: 10.1016/j.aquaculture.2006.02.043
- Bakthavatsalam, D., Brock, D. A., Nikravan, N. N., Houston, K. D., Hatton, R. D. & Gomer, R. H. (2008). The secreted *Dictyostelium* protein CfaD is a chalone. *Journal of Cell Science*, 121(15), 2473-2480. doi: 10.1242/jcs.026682.

- Baliga, P., Shekar, M. & Venugopal, M. N. (2018). Potential Outer Membrane Protein Candidates for Vaccine Development against the Pathogen *Vibrio anguillarum*: A Reverse Vaccinology Based Identification. *Current Microbiology*, 75(3), 368-377. doi: 10.1007/s00284-017-1390-z.
- Bassity, E. & Clark, T. G. (2012). Functional identification of dendritic cells in the teleost model, rainbow trout (*Oncorhynchus mykiss*). *PLoS One*, 7(3), e33196. doi: 10.1371/journal.pone.0033196.
- Beck, B. H. & Peatman, E. (2015). Mucosal health in aquaculture. *Academic Press*. Cambridge, MA, USA, 2015.
- Béné, C., Barange, M., Subasinghe, R., Pinstруп-Andersen, P., Merino, G., Hemre, G. I. & Williams, M. (2015). Feeding 9 billion by 2050—Putting fish back on the menu. *Food Security*, 7(2), 261-274. doi: 10.1007/s12571-015-0427-z.
- Benedicenti, O., Collins, C., Wang, T., McCarthy, U. & Secombes, C. J. (2015). Which Th pathway is involved during late stage amoebic gill disease? *Fish and Shellfish Immunology*, 46(2), 417-425. doi: 10.1016/j.fsi.2015.07.002.
- Benhamed, S., Guardiola, F. A., Mars, M. & Esteban, M. Á. (2014). Pathogen bacteria adhesion to skin mucus of fishes. *Veterinary Microbiology*, 171(1-2), 1-12. doi: 10.1016/j.vetmic.2014.03.008.
- Ben-Othman, R., Guizani-Tabbane, L. & Dellagi, K. (2008). *Leishmania* initially activates but subsequently down-regulates intracellular mitogen-activated protein kinases and nuclear factor- κ B signaling in macrophages. *Molecular Immunology*, 45(11), 3222-3229. doi: 10.1016/j.molimm.2008.02.019.
- Bergh, Ø., Børsheim, K. Y., Bratbak, G. & Heldal, M. (1989). High abundance of viruses found in aquatic environments. *Nature*, 340(6233), 467. doi: 10.1038/340467a0.
- Bergmann, S. M. & Kempter, J. (2011). Detection of koi herpesvirus (KHV) after re-activation in persistently infected common carp (*Cyprinus carpio* L.) using non-lethal sampling methods. *Bulletin of the European Association of Fish Pathologists*, 31(3), 92-100.
- Bertholet, S., Reed, S. G. & Rappuoli, R. (2014). Reverse vaccinology applied to TB. In *The Art & Science of Tuberculosis Vaccine Development*. N. M. Nor, A. Acosta, and M. E. Sarmiento, Eds., pp. 413–431, Oxford University Press, Pulau Pinang, Malaysia, 2nd edition.

- Birlanga, V. B., McCormack, G., Ijaz, U. Z., McCarthy, E., Smith, C. & Collins, G. (2020). Dynamic Gill and Mucous Microbiomes Track an Amoebic Gill Disease Episode in Farmed Atlantic Salmon. doi: 10.21203/rs.3.rs-29747/v1.
- Black, E. A., Whyth, J. N. C., Bagshaw, J. W. & Ginther, N. G. (1991). The effects of *Heterosigma akashiwo* on juvenile *Oncorhynchus tshawytscha* and its implications for fish culture. *Journal of Applied Ichthyology*, 7(3), 168-175. doi: 10.1111/j.1439-0426.1991.tb00523.x.
- Boateng, J. S., Matthews, K. H., Stevens, H. N. & Eccleston, G. M. (2008). Wound healing dressings and drug delivery systems: a review. *Journal of Pharmaceutical Sciences*, 97(8), 2892-2923. doi: 10.1002/jps.21210.
- Bohle, H., Henríquez, P., Grothusen, H., Navas, E., Sandoval, A., Bustamante, F. & Mancilla, M. (2014). Comparative genome analysis of two isolates of the fish pathogen *Piscirickettsia salmonis* from different hosts reveals major differences in virulence-associated secretion systems. *Genome Announcement.*, 2(6), e01219-14. doi: 10.1128/genomeA.01219-14.
- Bolger, A. M., Lohse, M. & Usadel, B. (2014). Trimmomatic: a flexible trimmer for Illumina sequence data. *Bioinformatics*, 30(15), 2114-2120. doi: 10.1093/bioinformatics/btu170.
- Bollard, J. E., Vanderwee, M. A., Smith, G. W., Tasman-Jones, C., Gavin, J. B. & Lee, S. P. (1986). Preservation of mucus in situ in rat colon. *Digestive Diseases and Sciences*, 31(12), 1338-1344. doi: 10.1007/bf01299812.
- Boman, H. G. (1991). Antibacterial peptides: key components needed in immunity. *Cell*, 65(2), 205-207. doi: 10.1016/0092-8674(91)90154-Q.
- Bordas, M. A., Balebona, M. C., Zorrilla, I., Borrego, J. J. & Morin, M. A. (1996). Kinetics of Adhesion of Selected Fish-Pathogenic *Vibrio* Strains to Skin Mucus of Gilt-Head Sea Bream (*Sparus aurata* L.). *Applied and Environmental Microbiology*, 62(10), 3650–3654.
- Boshra, H., Li, J. & Sunyer, J. O. (2006). Recent advances on the complement system of teleost fish. *Fish and Shellfish Immunology*, 20(2), 239-262. doi: 10.1016/j.fsi.2005.04.004.
- Boutin, S., Bernatchez, L., Audet, C. & Derôme, N. (2013). Network analysis highlights complex interactions between pathogen, host and commensal microbiota. *PloS One*, 8(12), e84772. doi: 10.1371/journal.pone.0084772.

- Bowers, J. M., Speare, D. J., & Burka, J. F. (2002). The effects of hydrogen peroxide on the stress response of Atlantic Salmon (*Salmo salar*). *Journal of Veterinary Pharmacology and Therapeutics*, 25(4), 311-313. doi: 10.1046/j.1365-2885.2002.00413.x.
- Bridle, A. R., Butler, R., & Nowak, B. F. (2003). Immunostimulatory CpG oligodeoxynucleotides increase resistance against amoebic gill disease in Atlantic salmon, *Salmo salar* L. *Journal of Fish Diseases*, 26(6), 367-371.
- Bridle, A. R., Carter, C. G., Morrison, R. N., & Nowak, B. F. (2005). The effect of β -glucan administration on macrophage respiratory burst activity and Atlantic salmon, *Salmo salar* L., challenged with amoebic gill disease—evidence of inherent resistance. *Journal of Fish Diseases*, 28(6), 347-356. doi: 10.1111/j.1365-2761.2005.00636.x
- Bridle, A. R., Morrison, R. N., Cunningham, P. M. C. & Nowak, B. F. (2006). Quantitation of immune response gene expression and cellular localisation of interleukin-1 β mRNA in Atlantic salmon, *Salmo salar* L., affected by amoebic gill disease (AGD). *Veterinary Immunology and Immunopathology*, 114(1-2), 121-134. doi: 10.1016/j.vetimm.2006.08.002.
- Bridle, A. R., Crosbie, P. B. B., Cadoret, K. & Nowak, B. F. (2010). Rapid detection and quantification of *Neoparamoeba perurans* in the marine environment. *Aquaculture*, 309(1-4), 56–61. doi: 10.1016/j.aquaculture.2010.09.018.
- Bridle, A. R., Davenport, D. L., Crosbie, P. B., Polinski, M. & Nowak, B. F. (2015). *Neoparamoeba perurans* loses virulence during clonal culture. *International Journal for Parasitology*, 45(9-10), 575-578. doi: 10.1016/j.ijpara.2015.04.005.
- Brinchmann, M. F. (2016). Immune relevant molecules identified in the skin mucus of fish using-omics technologies. *Molecular BioSystems*, 12(7), 2056-2063. doi: 10.1039/c5mb00890e.
- Brock D.A. & Gomer R.H. (2005). A secreted factor represses cell proliferation in *Dictyostelium*. *Development*, 132(20), 4553–4562. doi:10.1242/ dev.02032.
- Brudeseth, B. E., Wiulsrød, R., Fredriksen, B. N., Lindmo, K., Løkling, K. E., Bordevik, M. & Gravningen, K. (2013). Status and future perspectives of vaccines for industrialised fin-fish farming. *Fish & Shellfish Immunology*, 35(6), 1759-1768. doi: 10.1016/j.fsi.2013.05.029.

- Bruno, D. W. & Raynard, R. S. (1994). Studies on the use of hydrogen peroxide as a method for the control of sea lice on Atlantic salmon. *Aquaculture International*, 2(1), 10-18. doi: 10.1007/BF00118529.
- Buchfink, B., Xie, C. & Huson, D. H. (2015). Fast and sensitive protein alignment using DIAMOND. *Nature Methods*, 12(1), 59. doi: 10.1038/nmeth.3176.
- Buchmann, K. (2012). Fish immune responses against endoparasitic nematodes—experimental models. *Journal of Fish Diseases*, 35(9), 623-635. doi:10.1111/j.1365-2761.2012.01385.x.
- Burridge, L., Weis, J. S., Cabello, F., Pizarro, J. & Bostick, K. (2010). Chemical use in salmon aquaculture: a review of current practices and possible environmental effects. *Aquaculture*, 306(1-4), 7-23. doi:10.1016/j.aquaculture.2010.05.020.
- Bury, N. R., Schnell, S. & Hogstrand, C. (2014). Gill cell culture systems as models for aquatic environmental monitoring. *Journal of Experimental Biology*, 217(5), 639-650. doi: 10.1242/jeb.095430.
- Bushnell, B. (2017). *BBMap Software Package*. Available at sourceforge.net/projects/bbmap/.
- Butler, R. & Nowak, B. F. (2004). *In vitro* interactions between *Neoparamoeba* spp. and Atlantic salmon epithelial cells. *Journal of Fish Diseases*, 27(6), 343-349. doi: 10.1111/j.1365-2761.2004.00550.x.
- Butt, A. M., Tahir, S., Nasrullah, I., Idrees, M., Lu, J. & Tong, Y. (2012). *Mycoplasma genitalium*: a comparative genomics study of metabolic pathways for the identification of drug and vaccine targets. *Infection, Genetics and Evolution*, 12(1), 53-62. doi: 10.1016/j.meegid.2011.10.017.
- Caceci, T. (1984). Scanning electron microscopy of goldfish, *Carassius auratus*, intestinal mucosa. *Journal of Fish Biology*, 25(1), 1-12. doi: 10.1111/j.1095-8649.1984.tb04845.x.
- Cadoret, K., Bridle, a. R., Leef, M. J. & Nowak, B. F. (2013). Evaluation of fixation methods for demonstration of *Neoparamoeba perurans* infection in Atlantic salmon, *Salmo salar* L., gills. *Journal of Fish Diseases*, 36(10), 831–839. doi: 10.1111/jfd.12078.
- Caffrey, C. R., Scory, S. & Steverding, D. (2000). Cysteine Proteinases of Trypanosome Parasites Novel Targets for Chemotherapy. *Current Drug Targets*, 1(2), 155-162. doi: 10.2174/1389450003349290.

- Cain, K. D., Jones, D. R. & Raison, R. L. (2000). Characterisation of mucosal and systemic immune responses in rainbow trout (*Oncorhynchus mykiss*) using surface plasmon resonance. *Fish and Shellfish Immunology*, 10(8), 651-666. doi: 10.1006/fsim.2000.0280.
- Cain, R. & Steele, H. (1953). The Use of Calcium Alginate Soluble Wool for the Examination of Cleansed Eating Utensils. *Canadian Journal of Public Health/Revue Canadienne De Sante'e Publique*, 44(12), 464-467.
- Cano, I., Taylor, N. G., Bayley, A., Gunning, S., McCullough, R., Bateman, K. & Paley, R. K. (2019). *In vitro* gill cell monolayer successfully reproduces in vivo Atlantic salmon host responses to *Neoparamoeba perurans* infection. *Fish and Shellfish Immunology*, 86, 287-300. doi: 0.1016/j.fsi.2018.11.029.
- Castro, R., Bernard, D., Lefranc, M. P., Six, A., Benmansour, A. & Boudinot, P. (2011). T cell diversity and TcR repertoires in teleost fish. *Fish and Shellfish Immunology*, 31(5), 644-654. doi: 10.1016/j.fsi.2010.08.016.
- Cebra, J. J. (1999). Influences of microbiota on intestinal immune system development. *The American journal of clinical nutrition*, 69(5), 1046s-1051s. doi: 10.1093/ajcn/69.5.1046s.
- Chalmers, L., Taylor, J. F., Roy, W., Preston, A. C., Migaud, H. & Adams, A. (2017). A comparison of disease susceptibility and innate immune response between diploid and triploid Atlantic salmon (*Salmo salar*) siblings following experimental infection with *Neoparamoeba perurans*, causative agent of amoebic gill disease. *Parasitology*, 144(9), 1229-1242. doi: 10.1017/S0031182017000622.
- Chapman, L. J., Lanciani, C. A. & Chapman, C. A. (2000). Ecology of a diplozoon parasite on the gills of the African cyprinid *Barbus neumayeri*. *African Journal of Ecology*, 38(4), 312-320. doi: 10.1046/j.1365-2028.2000.00252.x.
- Chaudhuri, R., Ahmed, S., Ansari, F. A., Singh, H. V. & Ramachandran, S. (2008). MalVac: database of malarial vaccine candidates. *Malaria Journal*, 7(1), 184. doi: 10.1186/1475-2875-7-184.
- Chaudhuri, R., Kulshreshtha, D., Raghunandan, M. V. & Ramachandran, S. (2014). Integrative immunoinformatics for Mycobacterial diseases in R platform. *Systems and Synthetic Biology*, 8(1), 27-39. doi: 10.1007/s11693-014-9135-9.

- Chiang, M. H., Sung, W. C., Lien, S. P., Chen, Y. Z., Lo, A. F. Y., Huang, J. H. & Chong, P. (2015). Identification of novel vaccine candidates against *Acinetobacter baumannii* using reverse vaccinology. *Human Vaccines and Immunotherapeutics*, 11(4), 1065-1073. doi: 10.1080/21645515.2015.1010910.
- Christie, A. E. (2014). *In silico* characterization of the peptidome of the sea louse *Caligus rogercresseyi* (Crustacea, Copepoda). *General and Comparative Endocrinology*, 204, 248-260. doi: 10.1016/j.ygcen.2014.05.031.
- Christoffersen, T. B., Kania, P. W., von Gersdorff Jørgensen, L. & Buchmann, K. (2017). Zebrafish *Danio rerio* as a model to study the immune response against infection with *Ichthyophthirius multifiliis*. *Journal of Fish Diseases*, 40(6), 847-852. doi: 10.1111/jfd.12543.
- Chu, W. M. (2013). Tumor necrosis factor. *Cancer Letters*, 328(2), 222-225. doi: 10.1016/j.canlet.2012.10.014.
- Clark, A. & Nowak, B. F. (1999). Field investigations of amoebic gill disease in Atlantic salmon, *Salmo salar* L., in Tasmania. *Journal of Fish Diseases*, 22(6), 433-443. doi: 10.1046/j.1365-2761.1999.00175.x.
- Clark, G., Powell, M. & Nowak, B. (2003). Effects of commercial freshwater bathing on reinfection of Atlantic salmon, *Salmo salar*, with amoebic gill disease. *Aquaculture*, 219(1-4), 135-142. doi: 10.1016/S0044-8486(03)00020-6.
- Coet-Zee, H. L., Kotze, S. H. & Lourens, N. (1995). Characterization of mucus glycoproteins in the intestinal mucosa of the African elephant (*Loxodonta africana*) following lectin histochemistry. *Onderstepoort Journal of Veterinary Research*, 62, 187-192.
- Cole, A. M., Darouiche, R. O., Legarda, D., Connell, N. & Diamond, G. (2000). Characterization of a fish antimicrobial peptide: gene expression, subcellular localization, and spectrum of activity. *Antimicrobial Agents and Chemotherapy*, 44(8), 2039-2045. doi: 10.1128/aac.44.8.2039-2045.2000.
- Collins, C., Hall, M., Fordyce, M. J. & White, P. (2019). Survival and growth in vitro of *Paramoeba perurans* populations cultured under different salinities and temperatures. *Protist*, 170(2), 153-167. doi: 10.1016/j.protis.2018.11.003.

- Connaris, S. & Greenwell, P. (1997). Glycosidases in mucin-dwelling protozoans. *Glycoconjugate Journal*, 14(7), 879-882. doi: 10.1023/A:101855440.
- Cook, M., Elliot, N., Campbell, G., Patil, J. G., Holmes, B., Lim, V. & Prideaux, C. (2008). Amoebic gill disease (AGD) vaccine development phase II-Molecular basis of host parasite interactions in Amoebic Gill Disease.
- Cook, M., Maynard, B., Crosbie, P., Prideaux, C. & Elliott, N. (2012). AGD Vaccine Phase III: Sea-based trials, vaccine refinement and commercialisation. *The Seafood CRC Company Ltd, the Fisheries Research and Development Corporation and CSIRO Marine and Atmospheric Research, Australia*.
- Costa, M. M., Maehr, T., Diaz-Rosales, P., Secombes, C. J. & Wang, T. (2011). Bioactivity studies of rainbow trout (*Oncorhynchus mykiss*) interleukin-6: effects on macrophage growth and antimicrobial peptide gene expression. *Molecular Immunology*, 48(15-16), 1903-1916. doi:10.1016/j.molimm.2011.05.027.
- Crafford, D., Luus-Powell, W. & Avenant-Oldewage, A. (2014). Monogenean parasites from fishes of the Vaal Dam, Gauteng Province, South Africa. I. Winter survey versus summer survey comparison from *Labeo capensis* (Smith, 1841) and *Labeo umbratus* (Smith, 1841) hosts. *Acta Parasitologica*, 59, 17–24. doi:10.2478/s11686-014-0205-7.
- Crampton, A. & Vanniasinkam, T. (2007). Parasite vaccines: the new generation. *Infection, Genetics and Evolution*, 7(5), 664-673. doi: 10.1016/j.meegid.2007.06.004.
- Crosbie, P. B. B., Bridle, a. R., Cadoret, K. & Nowak, B. F. (2012). *In vitro* cultured *Neoparamoeba perurans* causes amoebic gill disease in Atlantic salmon and fulfils Koch's postulates. *International Journal for Parasitology*, 42(5), 511–515. doi: 10.1016/j.ijpara.2012.04.002.
- Dash, S., Das, S. K., Samal, J. & Thatoi, H. N. (2018). Epidermal mucus, a major determinant in fish health: a review. *Iranian Journal of Veterinary Research*, 19(2), 72-81. doi: 10.22099/IJVR.2018.4849.
- Davey, J. T. (1980). Spatial distribution of the copepod parasite *Lernanthropus kroyeri* on the gills of bass, *Dicentrarchus labrax* (L.). *Journal of the Marine Biological Association of the United Kingdom*, 60(4), 1061-1067. doi: 10.1017/S0025315400042107.

- David, V., Flegontov, P., Gerasimov, E., Tanifuji, G., Hashimi, H., Logacheva, M. D. & Lukeš, J. (2015). Gene loss and error-prone RNA editing in the mitochondrion of *Perkinsella*, an endosymbiotic kinetoplastid. *MBio*, 6(6), e01498-15. doi: 10.1128/mBio.01498-15.
- Davidson, G. A., Lin, S. H., Secombes, C. J. & Ellis, A. E. (1997). Detection of specific and 'constitutive' antibody secreting cells in the gills, head kidney and peripheral blood leucocytes of dab (*Limanda limanda*). *Veterinary Immunology and Immunopathology*, 58(3-4), 363-374. doi: 10.1016/s0165-2427(97)00017-2.
- Davies, M. N. & Flower, D. R. (2007). Harnessing bioinformatics to discover new vaccines. *Drug Discovery Today*, 12(9-10), 389-395. doi: 10.1016/j.drudis.2007.03.010.
- De Oliveira, S., Reyes-Aldasoro, C. C., Candel, S., Renshaw, S. A., Mulero, V. & Calado, Â. (2013). Cxcl8 (IL-8) mediates neutrophil recruitment and behavior in the zebrafish inflammatory response. *The Journal of Immunology*, 190(8), 4349-4359. doi: 10.4049/jimmunol.1203266.
- Del Tordello, E., Rappuoli, R. & Delany, I. (2017). Reverse vaccinology: exploiting genomes for vaccine design. In *Human Vaccines*, 65-86. doi: 10.1517/14712598.2.8.895.
- Delves, P. J., Martin, S. J., Burton, D. R., & Roitt, I. M. (2017). *Essential Immunology*. John Wiley & Sons.
- Dereeper, A., Guignon, V., Blanc, G., Audic, S., Buffet, S., Chevenet, F. & Claverie, J. M. (2008). Phylogeny.fr: robust phylogenetic analysis for the non-specialist. *Nucleic Acids Research*, 36(suppl_2), W465-W469. doi: 10.1093/nar/gkn180.
- Desmettre P. & Martinod S. Research and development. In: Pastoret P.P., Blancou J., Vannier P., Verschueren C., editors. *Veterinary Vaccinology*. Elsevier Press; Amsterdam, The Netherlands: 1997. pp. 175–194.
- Diaz, A. O., Garcia, A. M. & Goldemberg, A. L. (2010). Glycoproteins histochemistry of the gills of *Odontesthes bonariensis* (Teleostei, Atherinopsidae). *Journal of Fish Biology*, 77, 1665-1673. doi: 10.1111/j.1095-8649.2010.02803.x.
- Dickerson, H. W. & Findly, R. C. (2014). Immunity to *Ichthyophthirius* infections in fish: a synopsis. *Developmental and Comparative Immunology*, 43(2), 290-299. doi: 10.1016/j.dci.2013.06.004.

- Dijkstra, J. M., Köllner, B., Aoyagi, K., Sawamoto, Y., Kuroda, A., Ototake, M. & Fischer, U. (2003). The rainbow trout classical MHC class I molecule Onmy-UBA* 501 is expressed in similar cell types as mammalian classical MHC class I molecules. *Fish and Shellfish Immunology*, 14(1), 1-23. doi: 10.1006/fsim.2001.0407.
- Donati, C. & Rappuoli, R. (2013). Reverse vaccinology in the 21st century: improvements over the original design. *Annals of the New York Academy of Sciences*, 1285(1), 115-132. doi: 10.1111/nyas.12046.
- Douglas-Helders, M., Saksida, S., Raverty, S., & Nowak, B. F. (2001). Temperature as a risk factor for outbreaks of amoebic gill disease in farmed Atlantic salmon (*Salmo salar*). *Bulletin of the European Association of Fish Pathologists*, 21(3), 114-116.
- Douglas-Helders, G. M., Weir, I. J., O'brien, D. P., Carson, J. & Nowak, B. F. (2004). Effects of husbandry on prevalence of amoebic gill disease and performance of reared Atlantic salmon (*Salmo salar* L.). *Aquaculture*, 241(1-4), 21-30. doi: 10.1016/j.aquaculture.2004.07.026.
- Downes, J., Henshilwood, K., Collins, E., Ryan, A., O'Connor, I., Rodger, H. & Ruane, N. (2015). A longitudinal study of amoebic gill disease on a marine Atlantic salmon farm utilising a real-time PCR assay for the detection of *Neoparamoeba perurans*. *Aquaculture Environment Interactions*, 7(3), 239–251. doi: 10.3354/aei00150.
- Downes, J. K., Rigby, M. L., Taylor, R. S., Maynard, B. T., MacCarthy, E., Connor, I. O. & Cook, M. T. (2017). Evaluation of Non-destructive Molecular Diagnostics for the Detection of *Neoparamoeba perurans*, 4 (3), 1–9. <http://doi.org/10.3389/fmars.2017.00061>.
- Doytchinova, I. A. & Flower, D. R. (2008). Bioinformatic approach for identifying parasite and fungal candidate subunit vaccines. *The Open Vaccine Journal*, 1(1), 4. doi: 10.2174/1875035400801010022.
- Duchaud, E., Boussaha, M., Loux, V., Bernardet, J. F., Michel, C., Kerouault, B. & Bessieres, P. (2007). Complete genome sequence of the fish pathogen *Flavobacterium psychrophilum*. *Nature Biotechnology*, 25(7), 763. doi: 10.1038/nbt1313.
- Duff, D. C. B. (1942) The oral immunization of trout against *Bacterium salmonicida*. *Journal of Immunology*, 44, 87–93.

- Dyková, I., & Novoa, B. (2001). Comments on diagnosis of amoebic gill disease (AGD) in turbot, *Scophthalmus maximus*. *Bulletin of the European Association of Fish Pathologists*, 21(1), 40-44.
- Dzika, E. (1999). Microhabitats of *Pseudodactylogyrus anguillae* and *P. bini* (Monogenea: Dactylogyridae) on the gills of large-size European eel *Anguilla anguilla* from Lake Gaj, Poland. *Folia Parasitologica*, 46(4), 33-36.
- Earle, K. A., Billings, G., Sigal, M., Lichtman, J. S., Hansson, G. C., Elias, J. E. & Sonnenburg, J. L. (2015). Quantitative imaging of gut microbiota spatial organization. *Cell Host and Microbe*, 18(4), 478-488. doi: 10.1016/j.chom.2015.09.002.
- Easy, R. H., & Ross, N. W. (2009). Changes in Atlantic salmon (*Salmo salar*) epidermal mucus protein composition profiles following infection with sea lice (*Lepeophtheirus salmonis*). *Comparative Biochemistry and Physiology Part D: Genomics and Proteomics*, 4(3), 159-167. doi: 10.1016/j.cbd.2009.02.001.
- Edman, U., Meza, I., & Agabian, N. (1987). Genomic and cDNA actin sequences from a virulent strain of *Entamoeba histolytica*. *Proceedings of the National Academy of Sciences*, 84(9), 3024-3028. doi: 10.1073/pnas.84.9.3024.
- Eichinger, L., Pachebat, J. A., Glöckner, G., Rajandream, M. A., Sucgang, R., Berriman, M. & Tungal, B. (2005). The genome of the social amoeba *Dictyostelium discoideum*. *Nature*, 435(7038), 43. doi: 10.1038/nature03481.
- El-Gebali, S., Mistry, J., Bateman, A., Eddy, S. R., Luciani, A., Potter, S. C. & Sonnhammer, E. L. L. (2018). The Pfam protein families database in 2019. *Nucleic Acids Research*, 47(D1), D427-D432. doi: 10.1093/nar/gky995.
- Ellis, A. E. (2001). Innate host defense mechanisms of fish against viruses and bacteria. *Developmental and Comparative Immunology*, 25(8-9), 827-839. doi: 10.1016/s0145-305x(01)00038-6.
- Enenkel, C. & Wolf, D. H. (1993). BLH1 codes for a yeast thiol aminopeptidase, the equivalent of mammalian bleomycin hydrolase. *Journal of Biological Chemistry*, 268(10), 7036-7043.
- Engel, J. C., Doyle, P. S., Hsieh, I. & McKerrow, J. H. (1998). Cysteine protease inhibitors cure an experimental *Trypanosoma cruzi* infection. *Journal of Experimental Medicine*, 188(4), 725-734. doi: 10.1084/jem.188.4.725.

- Estensoro, I., Caldach-giner, J. A., Pe, J., Kaushik, S. & Sitja, A. (2013). Mucins as Diagnostic and Prognostic Biomarkers in a Fish-Parasite Model. *Transcriptional and Functional Analysis*, 8(6), 1–9. doi: 10.1371/journal.pone.0065457.
- Etile, S. S. & N'douba, V. (2018). Occurrence of Gill Monogenean Parasites in Redbelly tilapia, *Tilapia zillii* (Teleostei: Cichlidae) from Lobo River, Côte d'Ivoire. *Journal of Animal and Plant Sciences*, 35(3), 5674-5688.
- Evans, D. H., Piermarini, P. M. & Choe, K. P. (2005). The multifunctional fish gill: dominant site of gas exchange, osmoregulation, acid-base regulation, and excretion of nitrogenous waste. *Physiological Reviews*, 85(1), 97-177. doi: 10.1152/physrev.00050.2003.
- Fallon, P. G., Jolin, H. E., Smith, P., Emson, C. L., Townsend, M. J., Fallon, R. & McKenzie, A. N. (2002). IL-4 induces characteristic Th2 responses even in the combined absence of IL-5, IL-9, and IL-13. *Immunity*, 17(1), 7-17. doi: 10.1016/s1074-7613(02)00332-1.
- FAO (2020). The State of World Fisheries and Aquaculture (SOFIA), 2020. <http://www.fao.org/state-of-fisheries-aquaculture>
- Fast M.D., Sims D.E., Burka J.F., Mustafa A. & Ross N.W. (2002) Skin morphology and humoral non-specific defence parameters of mucus and plasma in rainbow trout, coho and Atlantic salmon. *Comparative Biochemistry and Physiology*, A132, 645–657. doi: 10.1016/s1095-6433(02)00109-5.
- Feehan, C. J., Johnson-Mackinnon, J., Scheibling, R. E., Lauzon-Guay, J. S. & Simpson, A. G. (2013). Validating the identity of *Paramoeba invadens*, the causative agent of recurrent mass mortality of sea urchins in Nova Scotia, Canada. *Diseases of Aquatic Organisms*, 103(3), 209-227. doi: 10.3354/dao02577.
- Feng, X. G., Sui, C. Y., Yuan, C. X., Shao, D. H., Chen, J. X. & Lin, J. J. (2007). Application of reverse vaccinology in *Schistosoma* vaccine development: advances and prospects. *Zhongguo Ji Sheng Chong Xue Yu Ji Sheng Chong Bing Za Zhi= Chinese Journal of Parasitology & Parasitic Diseases*, 25(3), 237-247.
- Feng, Z., Hensley, L., McKnight, K. L., Hu, F., Madden, V., Ping, L. & Lemon, S. M. (2013). A pathogenic picornavirus acquires an envelope by hijacking cellular membranes. *Nature*, 496(7445), 367–371. doi: 10.1038/nature12029.

- Ferrando, S., Bottaro, M., Gallus, L., Girosi, L., Vacchi, M. & Tagliafierro, G. (2006). Observations of crypt neuron-like cells in the olfactory epithelium of a cartilaginous fish. *Neuroscience Letters*, 403(3), 280-282. doi: 10.1016/j.neulet.2006.04.056.
- Ferri, D. & Liquori, G.E. (1992). Characterization of secretory cell glycoconjugates in the alimentary tract of the ruin lizard (*Podarcis sicula*) by means of lectin histochemistry. *Acta Histochemica*, 93, 341-349. doi: 10.1111/j.1463-6395.2010.00451.x.
- Findlay, V. L., Helders, M., Munday, B. L. & Gurney, R. (1995). Demonstration of resistance to reinfection with *Paramoeba* sp. by Atlantic salmon, *Salmo salar* L. *Journal of Fish Diseases*, 18(6), 639-642. doi: 10.1111/j.1365-2761.1995.tb00370.x.
- Findlay, V. L., Zilberg, D., & Munday, B. L. (2000). Evaluation of levamisole as a treatment for amoebic gill disease of Atlantic salmon, *Salmo salar* L. *Journal of Fish Diseases*, 23(3), 193-198. doi: 10.1046/j.1365-2761.2000.00238.x.
- Fischer, J., Klein, P.J., Vierbuch EN, M., Skutta, B., Uhlenbruck, G. & Fischer, R. (1984). Characterization of glycoconjugates of human gastrointestinal mucosa by lectins. I. Histochemical distribution of lectin binding sites in normal alimentary tract as well as in benign and malignant gastric neoplasms. *Journal of Histochemistry and Cytochemistry*, 32, 681- 689. doi: 10.1177/32.7.6330198.
- Fischer, U., Utke, K., Somamoto, T., Köllner, B., Ototake, M. & Nakanishi, T. (2006). Cytotoxic activities of fish leucocytes. *Fish and Shellfish Immunology*, 20(2), 209-226. doi: 10.1016/j.fsi.2005.03.013.
- Fletcher, T. C., Jones, R. & Reid, L. (1976). Identification of glycoproteins in goblet cells of epidermis and gill of plaice (*Pleuronectes platessa* L.), flounder (*Platichthys flesus* (L.)) and rainbow trout (*Salmo gairdneri* Richardson). *The Histochemical Journal*, 8(6), 597-608. doi: 10.1007/BF01003961.
- Flik, G., Kaneko, T., Greco, A. M., Li, J. & Fenwick, J. C. (1997). Sodium dependent ion transporters in trout gills. *Fish Physiology and Biochemistry*, 17(1-6), 385-396. doi: 10.1023/A:10077688.
- Florent, R. L., Becker, J. A. & Powell, M. D. (2007). Efficacy of bithionol as an oral treatment for amoebic gill disease in Atlantic salmon *Salmo salar* (L.). *Aquaculture*, 270(1-4), 15-22. doi: 10.1016/j.aquaculture.2007.04.082.

- Florent, R. L., Becker, J. A., & Powell, M. D. (2007a). Evaluation of bithionol as a bath treatment for amoebic gill disease caused by *Neoparamoeba* spp. *Veterinary Parasitology*, 144(3-4), 197-207.
- Forlenza, M., Scharsack, J. P., Kachamakova, N. M., Taverne-Thiele, A. J., Rombout, J. H. & Wiegertjes, G. F. (2008). Differential contribution of neutrophilic granulocytes and macrophages to nitrosative stress in a host–parasite animal model. *Molecular Immunology*, 45(11), 3178-3189. doi: 10.1016/j.molimm.2008.02.025.
- Frankic, A. & Hershner, C. (2003). Sustainable aquaculture: developing the promise of aquaculture. *Aquaculture International*, 11(6), 517-530. doi: 10.1023/B:AQUI.0000013264.38692.91.
- Fringuelli, E., Gordon, A. W., Rodger, H., Welsh, M. D. & Graham, D. A. (2012). Detection of *Neoparamoeba perurans* by duplex quantitative Taqman real-time PCR in formalin-fixed, paraffin-embedded atlantic salmonid gill tissues. *Journal of Fish Diseases*, 35(10), 711–724. doi: 10.1111/j.1365-2761.2012.01395.x.
- Fuglem, B., Jirillo, E., Bjerkås, I., Kiyono, H., Nochi, T., Yuki, Y. & Koppang, E. O. (2010). Antigen-sampling cells in the salmonid intestinal epithelium. *Developmental and Comparative Immunology*, 34(7), 768-774. doi: 10.1016/j.dci.2010.02.007.
- Gaikowski, M. P., Rach, J. J. & Ramsay, R. T. (1999). Acute toxicity of hydrogen peroxide treatments to selected life stages of cold-, cool-, and warmwater fish. *Aquaculture*, 178(3-4), 191-207. doi: 10.1016/S0044-8486(99)00123-4.
- Gajria, B., Bahl, A., Brestelli, J., Dommer, J., Fischer, S., Gao, X. & Pinney, D. F. (2007). ToxoDB: an integrated *Toxoplasma gondii* database resource. *Nucleic Acids Research*, 36(suppl_1), D553-D556. doi: 10.1093/nar/gkm981.
- Garcia, S. M. & Rosenberg, A. A. (2010). Food security and marine capture fisheries: characteristics, trends, drivers and future perspectives. *Philosophical Transactions of the Royal Society B: Biological Sciences*, 365(1554), 2869-2880. doi: 10.1098/rstb.2010.0171.
- Gardner, M. J., Hall, N., Fung, E., White, O., Berriman, M., Hyman, R. W. & Paulsen, I. T. (2002). Genome sequence of the human malaria parasite *Plasmodium falciparum*. *Nature*, 419(6906), 498. doi: 10.1038/nature01097.

- Gjessing, M. C., Thoen, E., Tengs, T., Skotheim, S. A. & Dale, O. B. (2017). Salmon gill poxvirus, a recently characterized infectious agent of multifactorial gill disease in freshwater-and seawater-reared Atlantic salmon. *Journal of Fish Diseases*, 40(10), 1253-1265. doi: 10.1111/jfd.12608.
- Gomez, D., Sunyer, J. O. & Salinas, I. (2013). The mucosal immune system of fish: the evolution of tolerating commensals while fighting pathogens. *Fish and Shellfish Immunology*, 35(6), 1729-1739. doi: 10.1016/j.fsi.2013.09.032.
- Gonçalves, D. D. S., Ferreira, M. D. S. & Guimarães, A. J. (2019). Extracellular Vesicles from the Protozoa *Acanthamoeba castellanii*: Their Role in Pathogenesis, Environmental Adaptation and Potential Applications. *Bioengineering*, 6(1), 13. doi: 10.3390/bioengineering6010013.
- Good, M. F., Staniscic, D., Xu, H., Elliott, S. & Wykes, M. (2004). The immunological challenge to developing a vaccine to the blood stages of malaria parasites. *Immunological Reviews*, 201(1), 254-267. doi: 10.1111/j.0105-2896.2004.00178.x.
- Goodswen, S. J., Kennedy, P. J., & Ellis, J. T. (2017). On the application of reverse vaccinology to parasitic diseases: a perspective on feature selection and ranking of vaccine candidates. *International Journal for Parasitology*, 47(12), 779-790. doi: 10.1016/j.ijpara.2017.08.004.
- Gorgoglione, B., Wang, T., Secombes, C. J. & Holland, J. W. (2013). Immune gene expression profiling of proliferative kidney disease in rainbow trout *Oncorhynchus mykiss* reveals a dominance of anti-inflammatory, antibody and T helper cell-like activities. *Veterinary Research*, 44(1), 55. doi: 10.1186/1297-9716-44-55.
- Grabherr, M. G., Haas, B. J., Yassour, M., Levin, J. Z., Thompson, D. A., Amit, I. & Chen, Z. (2011). Full-length transcriptome assembly from RNA-Seq data without a reference genome. *Nature Biotechnology*, 29(7), 644. doi: 10.1038/nbt.1883.
- Grell, K. G. & Benwitz, G (1970). Ultrastruktur mariner Amöben I. *Paramoeba eilhardi* Schaudinn. *Archiv für Protistenkunde* 112, 119–137.
- Griffith, J. W., Sokol, C. L. & Luster, A. D. (2014). Chemokines and chemokine receptors: positioning cells for host defense and immunity. *Annual Review of Immunology*, 32, 659-702. doi: 10.1146/annurev-immunol-032713-120145.
- Grimnes, A. & Jakobsen, P. J. (1996). The physiological effects of salmon lice infection on post-smolt of Atlantic salmon. *Journal of Fish Biology*, 48(6), 1179-1194. doi: 10.1111/j.1095-8649.1996.tb01813.x.

- Gross, K. A., Powell, M. D., Butler, R., Morrison, R. N. & Nowak, B. F. (2005). Changes in the innate immune response of Atlantic salmon, *Salmo salar* L., exposed to experimental infection with *Neoparamoeba* sp. *Journal of Fish Diseases*, 28(5), 293-299. doi: 10.1111/j.1365-2761.2005.00633.x.
- Guardiola, F. A., Cuesta, A., Abellán, E., Meseguer, J. & Esteban, M. A. (2014). Comparative analysis of the humoral immunity of skin mucus from several marine teleost fish. *Fish and Shellfish Immunology*, 40(1), 24-31. doi: 10.1016/j.fsi.2014.06.018.
- Gunnarsson, G. S., Karlsbakk, E., Blindheim, S., Plarre, H., Imsland, A. K., Handeland, S. & Nylund, A. (2017). Temporal changes in infections with some pathogens associated with gill disease in farmed Atlantic salmon (*Salmo salar* L.). *Aquaculture*, 468, 126-134. doi: 10.1016/j.aquaculture.2016.10.011.
- Guo, X., Barroso, L., Lyster, D. M., Petri Jr, W. A., & Houpt, E. R. (2011). CD4+ and CD8+ T cell-and IL-17-mediated protection against *Entamoeba histolytica* induced by a recombinant vaccine. *Vaccine*, 29(4), 772-777. doi: 10.1016/j.vaccine.2010.11.013.
- Hall, T. A. (1999, January). BioEdit: a user-friendly biological sequence alignment editor and analysis program for Windows 95/98/NT. In *Nucleic Acids Symposium Series*, 41, 95-98.
- Handy, R. D. & Eddy, F. B. (1991). The absence of mucus on the secondary lamellae of unstressed rainbow trout, *Oncorhynchus mykiss* (Walbaum). *Journal of Fish Biology*, 38(1), 153-155. doi: 10.1111/j.1095-8649.1991.tb03100.x.
- Handy, E. (1999). Microhabitats of *Pseudodactylogyrus anguillae* and *P. bini* (Monogenea: Dactylogyridae) on the gills of large-size European eel *Anguilla anguilla* from Lake Gaj, Poland. *Folia Parasitologica*, 46(4), 33-36.
- Hanek, G. & Fernando, C. H. (1978). Spatial distribution of gill parasites of *Lepomis gibbosus* (L.) and *Ambloplites rupestris* (Raf.). *Canadian Journal of Zoology*, 56, 1235-1240. doi: 10.1139/z78-175.
- Harrell, L. W., Etlinger, H. M. & Hodgins, H. O. (1976). Humoral factors important in resistance of salmonid fish to bacterial disease. II. Anti-*Vibrio anguillarum* activity in mucus and observations on complement. *Aquaculture*, 7(4), 363-370. doi: 10.1016/0044-8486(76)90133-2.

- Harris, J. O., Powell, M. D., Attard, M. & Green, T. J. (2004). Efficacy of chloramine-T as a treatment for amoebic gill disease (AGD) in marine Atlantic salmon (*Salmo salar* L.). *Aquaculture Research*, 35(15), 1448-1456.
- Hatten, F., Fredriksen, Å., Hordvik, I. & Endresen, C. (2001). Presence of IgM in cutaneous mucus, but not in gut mucus of Atlantic salmon, *Salmo salar*. Serum IgM is rapidly degraded when added to gut mucus. *Fish and Shellfish Immunology*, 11(3), 257-268. doi: 10.1006/fsim.2000.0313.
- Haugland, G. T., Olsen, A.-B., Rønneseth, A. & Andersen, L. (2016). Lumpfish (*Cyclopterus lumpus* L.) develop amoebic gill disease (AGD) after experimental challenge with *Paramoeba perurans* and can transfer amoebae to Atlantic salmon (*Salmo salar* L.). *Aquaculture*, 2013, 1–8. doi: 10.1016/j.aquaculture.2016.04.001.
- Heidel, A. J., Lawal, H. M., Felder, M., Schilde, C., Helps, N. R., Tunggal, B. & Platzer, M. (2011). Phylogeny-wide analysis of social amoeba genomes highlights ancient origins for complex intercellular communication. *Genome Research*, 21(11), 1882-1891. doi: 10.1101/gr.121137.111.
- Hellio, C., Pons, A. M., Beaupoil, C., Bourgougnon, N. & Le Gal, Y. (2002). Antibacterial, antifungal and cytotoxic activities of extracts from fish epidermis and epidermal mucus. *International Journal of Antimicrobial Agents*, 20(3), 214-219. doi: 10.1016/s0924-8579(02)00172-3.
- Hemerly, J. P., Oliveira, V., Del Nery, E., Morty, R. E., Andrews, N. W., Juliano, M. A. & Juliano, L. (2003). Subsite specificity (S3, S2, S1', S2'and S3') of oligopeptidase B from *Trypanosoma cruzi* and *Trypanosoma brucei* using fluorescent quenched peptides: comparative study and identification of specific carboxypeptidase activity. *Biochemical Journal*, 373(3), 933-939. doi: 10.1042/bj20030342.
- Henriksen, M. M. M., Kania, P. W., Buchmann, K. & Dalsgaard, I. (2015). Effect of hydrogen peroxide and/or *Flavobacterium psychrophilum* on the gills of rainbow trout, *Oncorhynchus mykiss* (W albaum). *Journal of Fish Diseases*, 38(3), 259-270. doi: 10.1111/jfd.12232.
- Herrero, A., Thompson, K. D., Ashby, A., Rodger, H. D. & Dagleish, M. P. (2018). Complex gill disease: an emerging syndrome in farmed Atlantic salmon (*Salmo salar* L.). *Journal of Comparative Pathology*, 163, 23-28. doi: 10.1016/j.jcpa.2018.07.004.

- Higgins, M. (1950). A Comparison of the Recovery Rate of Organisms from Cotton-Wool and Calcium Alginate Wool Swabs. *Monthly Bull. Ministry of Health & Pub. Health Lab. Service* (directed by Med. Res. Council), 9, 50-51.
- Hishida, Y., Ishimatsu, A. & Oda, T. (1997). Mucus blockade of lamellar water channels in yellowtail exposed to *Chattonella marina*. *Fisheries Science*, 63(2), 315-316. doi: 10.2331/fishsci.63.315.
- Hiyoshi, H., Kodama, T., Saito, K., Gotoh, K., Matsuda, S., Akeda, Y. & Iida, T. (2011). VopV, an F-actin-binding type III secretion effector, is required for *Vibrio parahaemolyticus*-induced enterotoxicity. *Cell Host and Microbe*, 10(4), 401-409. doi: 10.1016/j.chom.2011.08.014.
- Hollingsworth, M. A. & Swanson, B. J. (2004). Mucins in cancer: protection and control of the cell surface. *Nature Reviews Cancer*, 4(1), 45. doi: 10.1038/nrc1251.
- Howat, W. J., & Wilson, B. A. (2014). Tissue fixation and the effect of molecular fixatives on downstream staining procedures. *Methods*, 70(1), 12-19. doi: 10.1016/j.ymeth.2014.01.022.
- Hsu, K. L. & Mahal, L. K. (2006). A lectin microarray approach for the rapid analysis of bacterial glycans. *Nature Protocols*, 1(2), 543. doi: 10.1038/nprot.2006.76.
- Humbert, W., Kirsch, R. & Meister, M.F. (1984). Scanning electron microscopic study of the oesophageal mucous layer in the eel, *Anguilla anguilla* L. *Journal of Fish Biology*, 25(1), 117-122. doi: 10.1111/j.1095-8649.1984.tb04856.x.
- Hwang, B. O., Kim, Y. K. & Nam, Y. K. (2016). Effect of hydrogen peroxide exposures on mucous cells and lysozymes of gill tissues of olive flounder *Paralichthys olivaceus*. *Aquaculture Research*, 47(2), 433-444. doi: 10.1111/are.12504.
- Hytterød, S., Andersen, L., Hansen, H., Blindheim, S. H., Poppe, T. T., Kristoffersen, A. B. & Mo, T. A. (2017). AGD-behandlingsstrategier-dose-respons-studier med hydrogenperoksid og ferskvann. *Veterinærinstituttets Rapportserie nr. 10-2017*.
- Ingerslev, H. C., Cunningham, C. & Wergeland, H. I. (2006). Cloning and expression of TNF- α , IL-1 β and COX-2 in an anadromous and landlocked strain of Atlantic salmon (*Salmo salar* L.) during the smolting period. *Fish and Shellfish Immunology*, 20(4), 450-461. doi: 10.1016/j.fsi.2005.06.002.

- Ingerslev, H. C., Pettersen, E. F., Jakobsen, R. A., Petersen, C. B. & Wergeland, H. I. (2006a). Expression profiling and validation of reference gene candidates in immune relevant tissues and cells from Atlantic salmon (*Salmo salar* L.). *Molecular Immunology*, 43(8), 1194-1201. doi: 10.1016/j.molimm.2005.07.009.
- Isaza, C. E., Zhong, X., Rosas, L. E., White, J. D., Chen, R. P. Y., Liang, G. F. C. & Chan, M. K. (2008). A proposed role for *Leishmania* major carboxypeptidase in peptide catabolism. *Biochemical and Biophysical Research Communications*, 373(1), 25-29. doi: 10.1016/j.bbrc.2008.05.162.
- Janeway Jr, C. A. & Medzhitov, R. (2002). Innate immune recognition. *Annual Review of Immunology*, 20(1), 197-216. doi: 10.1146/annurev.immunol.20.083001.084359.
- Jenkins, P. G., Wrathmell, A. B., Harris, J. E. & Pulsford, A. L. (1994). Systemic and mucosal immune responses to enterically delivered antigen in *Oreochromis mossambicus*. *Fish and Shellfish Immunology*, 4(4), 255-271. doi: 10.1006/fsim.1994.102.
- Jensen, L. B. (2015). Nutritional and environmental impacts on skin and mucus condition in Atlantic salmon (*Salmo salar* L.). University of Bergen (2015), Doctoral thesis.
- Jiang, R. H., de Bruijn, I., Haas, B. J., Belmonte, R., Löbach, L., Christie, J. & Dumas, B. (2013). Distinctive expansion of potential virulence genes in the genome of the oomycete fish pathogen *Saprolegnia parasitica*. *PLoS Genetics*, 9(6). doi: 10.1371/journal.pgen.1003272.
- Jiang, X. B., Wang, Z. D., Zhu, Y., Zhang, X. L., Cui, X. F., Yao, K., & Yin, K. S. (2009). Inhibition of CD8+ T lymphocytes attenuates respiratory syncytial virus-enhanced allergic inflammation. *Respiration*, 77(1), 76-84. doi: 10.1159/000158871.
- Jirillo, F., Passantino, G., Massaro, M. A., Cianciotta, A., Crasto, A., Perillo, A. & Jirillo, E. (2007). *In vitro* elicitation of intestinal immune responses in teleost fish: evidence for a type IV hypersensitivity reaction in rainbow trout. *Immunopharmacology and Immunotoxicology*, 29(1), 69-80. doi: 10.1080/08923970701282544.

- Johansson, M. E. & Hansson, G. C. (2012). Preservation of mucus in histological sections, immunostaining of mucins in fixed tissue, and localization of bacteria with FISH. *Methods in Molecular Biology*, 842, 229-35. doi: 10.1007/978-1-61779-513-8_13
- Johansson, M. E. & Hansson, G. C. (2016). Immunological aspects of intestinal mucus and mucins. *Nature Reviews Immunology*, 16(10), 639. doi: 10.1038/nri.2016.88.
- Johansson, M. E., Phillipson, M., Petersson, J., Velcich, A., Holm, L. & Hansson, G. C. (2008). The inner of the two Muc2 mucin-dependent mucus layers in colon is devoid of bacteria. *Proceedings of the National Academy of Sciences of the United States of America*, 105(39), 15064–15069. doi: 10.1073/pnas.0803124105.
- John, D. T. & John, R. A. (2006). Viability of pathogenic *Naegleria* and *Acanthamoeba* isolates during 10 years of cryopreservation. *Folia Parasitologica*, 53(4), 311. doi: 10.14411/fp.2006.038
- John, L., John, G. J. & Kholia, T. (2012). A reverse vaccinology approach for the identification of potential vaccine candidates from *Leishmania* spp. *Applied Biochemistry and Biotechnology*, 167(5), 1340-1350. doi: 10.1007/s12010-012-9649-0.
- Johnson, S. C., Constible, J. M. & Richard, J. (1993). Laboratory investigations on the efficacy of hydrogen peroxide against the salmon louse *Lepeophtheirus salmonis* and its toxicological and histopathological effects on Atlantic salmon *Salmo salar* and chinook salmon *Oncorhynchus tshawytscha*. *Diseases of Aquatic Organisms*, 17(3), 197-204.
- Jones, D. (2012). Reverse vaccinology on the cusp: an upcoming decision for Novartis's Bexsero--the first vaccine against meningococcus B--could substantiate reverse vaccinology. *Nature Reviews Drug Discovery*, 11(3), 1-3. doi: 10.1038/nrd3679.
- Jones, D. R., Hannan, C. M., Russell-Jones, G. J. & Raison, R. L. (1999). Selective B cell non-responsiveness in the gut of the rainbow trout (*Oncorhynchus mykiss*). *Aquaculture*, 172(1-2), 29-39. doi: 10.1016/s0044-8486(98)00445-1.
- Jones, P., Binns, D., Chang, H. Y., Fraser, M., Li, W., McAnulla, C. & Pesseat, S. (2014). InterProScan 5: genome-scale protein function classification. *Bioinformatics*, 30(9), 1236-1240. doi: 10.1093/bioinformatics/btu031.

- Judice, W. A., Puzer, L., Cotrin, S. S., Carmona, A. K., Coombs, G. H., Juliano, L. & Juliano, M. A. (2004). Carboxydiptidase activities of recombinant cysteine peptidases: cruzain of *Trypanosoma cruzi* and CPB of *Leishmania mexicana*. *European Journal of Biochemistry*, 271(5), 1046-1053. doi: 10.1111/j.1432-1033.2004.04008.x.
- Jurd, R. D. (1987). Hypersensitivity in fishes: A review. *Journal of Fish Biology*, 31, 1-7. doi: 10.1111/j.1095-8649.1987.tb05285.x.
- Kanehisa, M., Sato, Y., Furumichi, M., Morishima, K. & Tanabe, M. (2019). New approach for understanding genome variations in KEGG. *Nucleic Acids Research*, 47(D1), D590-D595. doi: 10.1093/nar/gky962.
- Kanoi, B. N. & Egwang, T. G. (2007). New concepts in vaccine development in malaria. *Current Opinion in Infectious Diseases*, 20(3), 311-316. doi: 10.1097/QCO.0b013e32816b5cc2.
- Kantyka, T., Shaw, L. N. & Potempa, J. (2011). Papain-like proteases of *Staphylococcus aureus*. *Advances in Experimental Medicine and Biology*, 712, 1–14. doi: 10.1007/978-1-4419-8414-2_1.
- Karnaky, K. J. (1998). Osmotic and ionic regulation. In *The Physiology of Fishes* (ed. D. H. Evans), 157–176.
- Kent, M. L., Sawyer, T. K. & Hedrick, R. P. (1988). *Paramoeba pemaquidensis* (Sarcomastigophora: Paramoebidae) infestation of the gills of coho salmon *Oncorhynchus kisutch* reared in sea water. *Diseases of Aquatic Organisms*, 5(3), 163-169. doi: 10.3354/dao005163.
- Khacho, M., Mekhail, K., Pilon-Larose, K., Pause, A., Côté, J. & Lee, S. (2008). eEF1A is a novel component of the mammalian nuclear protein export machinery. *Molecular Biology of the Cell*, 19(12), 5296-5308. doi: 10.1091/mbc.e08-06-0562.
- Khader, S. A., Gaffen, S. L. & Kolls, J. K. (2009). Th17 cells at the crossroads of innate and adaptive immunity against infectious diseases at the mucosa. *Mucosal Immunology*, 2(5), 403. doi: 10.1038/mi.2009.100.
- Kiemer, M. C. & Black, K. D. (1997). The effects of hydrogen peroxide on the gill tissues of Atlantic salmon, *Salmo salar* L. *Aquaculture*, 153(3-4), 181-189. doi:10.1016/S0044-8486(97)00037-9.
- Kilvington, S. & White, D. (1991). A simple method for the cryopreservation of free-living amoebae belonging to the genera *Naegleria* and *Acanthamoeba*. *European Journal of Protistology*, 27(2), 115-118. doi: 10.1016/S0932-4739(11)80332-9.

- Kim, Y. S., Yoon, N. K., Karisa, N., Seo, S. H., Lee, J. S., Yoo, S. S. & Ahn, J. (2019). Identification of novel immunogenic proteins against *Streptococcus parauberis* in a zebrafish model by reverse vaccinology. *Microbial Pathogenesis*, 127, 56-59. doi: 10.1016/j.micpath.2018.11.053.
- Klöck, G., Frank, H., Houben, R., Zekorn, T., Horcher, A., Siebers, U. & Zimmermann, U. (1994). Production of purified alginates suitable for use in immunisolated transplantation. *Applied Microbiology and Biotechnology*, 40(5), 638-643. doi: 10.1007/BF00173321.
- Kneafsey, B., O'Shaughnessy, M. & Condon, K. C. (1996). The use of calcium alginate dressings in deep hand burns. *Burns*, 22(1), 40-43. doi: 10.1016/0305-4179(95)00066-6.
- Koppang, E. O., Hordvik, I., Bjerkås, I., Torvund, J., Aune, L., Thevarajan, J. & Endresen, C. (2003). Production of rabbit antisera against recombinant MHC class II β chain and identification of immunoreactive cells in Atlantic salmon (*Salmo salar*). *Fish and Shellfish Immunology*, 14(2), 115-132. doi: 10.1006/fsim.2002.0424.
- Koppang, E. O., Fischer, U., Moore, L., Tranulis, M. A., Dijkstra, J. M., Köllner, B. & Hordvik, I. (2010). Salmonid T cells assemble in the thymus, spleen and in novel interbranchial lymphoid tissue. *Journal of Anatomy*, 217(6), 728-739. doi: 10.1111/j.1469-7580.2010.01305.x.
- Kopylova, E., Noé, L. & Touzet, H. (2012). SortMeRNA: fast and accurate filtering of ribosomal RNAs in metatranscriptomic data. *Bioinformatics*, 28(24), 3211-3217. doi: 10.1093/bioinformatics/bts611.
- Lafferty, K. D., Harvell, C. D., Conrad, J. M., Friedman, C. S., Kent, M. L., Kuris, A. M. & Saksida, S. M. (2015). Infectious diseases affect marine fisheries and aquaculture economics. *Annual Review of Marine Science*, 7, 471-496. doi: 10.1146/annurev-marine-010814-015646.
- Langmead, B. & Salzberg, S. L. (2012). Fast gapped-read alignment with Bowtie 2. *Nature Methods*, 9(4), 357. doi: 10.1038/nmeth.1923.
- Larsen, J. L. & Pedersen, K. (1997). Vaccination strategies in freshwater salmonid aquaculture. *Developments in Biological Standardization*, 90, 391-400.

- Latendresse, J. R., Warbritton, A. R., Jonassen, H. & Creasy, D. M. (2002). Fixation of testes and eyes using a modified Davidson's fluid: comparison with Bouin's fluid and conventional Davidson's fluid. *Toxicologic Pathology*, 30(4), 524-533. doi: 10.1080/01926230290105721.
- Lazado, C. C., Caipang, C. M. A. & Estante, E. G. (2015). Prospects of host-associated microorganisms in fish and penaeids as probiotics with immunomodulatory functions. *Fish and Shellfish Immunology*, 45(1), 2-12. doi: 10.1016/j.fsi.2015.02.023.
- Lazado, C. C., Timmerhaus, G., Pedersen, L. F., Pittman, K., Soleng, M., Haddeland, S. & Hytterød, S. (2019). Peracetic acid as a potential treatment for amoebic gill disease (AGD) in Atlantic salmon-Stage 1. *Nofima rapportserie*.
- Lee, M. M., Schurch, S., Roth, S. H., Jiang, X., Cheng, S., Bjarnason, S. & Green, F. H. Y. (1995). Effects of acid aerosol exposure on the surface properties of airway mucus. *Experimental Lung Research*, 21(6), 835-851. doi: 10.3109/01902149509031766.
- Lee, L. E. J., Dayeh, V. R., Schirmer, K. & Bols, N. C. (2009). Applications and potential uses of fish gill cell lines: examples with RTgill-W1. *In Vitro Cellular & Developmental Biology-Animal*, 45(3-4), 127-134. doi: 10.1007/s11626-008-9173-2.
- Lee, Y. K., & Mazmanian, S. K. (2010). Has the microbiota played a critical role in the evolution of the adaptive immune system?. *Science*, 330(6012), 1768-1773. doi: 10.1126/science.1195568
- Leist, D. P., Nettleton, G. S. & Feldhoff, R. C. (1986). Determination of lipid loss during aqueous and phase partition fixation using formalin and glutaraldehyde. *Journal of Histochemistry & Cytochemistry*, 34, 437-441. doi: 10.1177/34.4.3081623.
- Leon-Coria, A., Kumar, M. & Chadee, K. (2019). The delicate balance between *Entamoeba histolytica*, mucus and microbiota. *Gut Microbes*, 1-8. doi: 10.1080/19490976.2019.1614363.
- Levine, M. M., & Sztein, M. B. (2004). Vaccine development strategies for improving immunization: the role of modern immunology. *Nature immunology*, 5(5), 460-464. doi: 10.1038/ni0504-460.

- Li, H. & Durbin, R. (2009). Fast and accurate short read alignment with Burrows–Wheeler transform. *Bioinformatics*, 25(14), 1754-1760. doi: 10.1093/bioinformatics/btp324.
- Li, W., Wang, H. Q., He, R. Z., Li, Y. W., Su, Y. L. & Li, A. X. (2016). Major surfome and secretome profile of *Streptococcus agalactiae* from Nile tilapia (*Oreochromis niloticus*): insight into vaccine development. *Fish and Shellfish Immunology*, 55, 737-746. doi: 10.1016/j.fsi.2016.06.006.
- Liang, S. C., Tan, X. Y., Luxenberg, D. P., Karim, R., Dunussi-Joannopoulos, K., Collins, M. & Fouser, L. A. (2006). Interleukin (IL)-22 and IL-17 are coexpressed by Th17 cells and cooperatively enhance expression of antimicrobial peptides. *Journal of Experimental Medicine*, 203(10), 2271-2279. doi: 10.1084/jem.20061308.
- Lieke, T., Meinelt, T., Hoseinifar, S. H., Pan, B., Straus, D. L. & Steinberg, C. E. (2019). Sustainable aquaculture requires environmental-friendly treatment strategies for fish diseases. *Reviews in Aquaculture*. doi: 10.1111/raq.12365.
- Lilehaug, A. (1997). Vaccination strategies in seawater cage culture of salmonids. *Developments in Biological Standardization*, 90, 401-408.
- Lima, P. C., Botwright, N. A., Harris, J. O. & Cook, M. (2014). Development of an in vitro model system for studying bacterially expressed dsRNA-mediated knockdown in *Neoparamoeba* genus. *Marine Biotechnology*, 16(4), 447-455. doi: 10.1007/s10126-014-9561-4.
- Lima, P. C., Taylor, R. S. & Cook, M. (2017). Pseudocyst formation in the marine parasitic amoeba *Neoparamoeba perurans*: A short-term survival strategy to abrupt salinity variation. *Journal of Fish Diseases*, 40(8), 1109-1113. doi: 10.1111/jfd.12588.
- Linden, S. K., Sutton, P., Karlsson, N. G., Korolik, V. & McGuckin, M. A. (2008). Mucins in the mucosal barrier to infection. *Mucosal Immunology*, 1(3), 183. doi: 10.1038/mi.2008.5.
- Liu, F., Tang, X., Sheng, X., Xing, J. & Zhan, W. (2017). Comparative study of the vaccine potential of six outer membrane proteins of *Edwardsiella tarda* and the immune responses of flounder (*Paralichthys olivaceus*) after vaccination. *Veterinary Immunology and Immunopathology*, 185, 38-47. doi: 10.1016/j.vetimm.2017.01.008.

- Liu, X., Sun, J. & Wu, H. (2017a). Glycolysis-related proteins are broad spectrum vaccine candidates against aquacultural pathogens. *Vaccine*, 35(31), 3813-3816. doi: 10.1016/j.vaccine.2017.05.066.
- Llewellyn, J. (1956). The host-specificity, micro-ecology, adhesive attitudes, and comparative morphology of some trematode gill parasites. *Journal of the Marine Biological Association of the United Kingdom*, 35(1), 113-127. doi: 10.1017/S0025315400009000.
- Llewellyn, M. S., Leadbeater, S., Garcia, C., Sylvain, F. E., Custodio, M., Ang, K. P. & Derome, N. (2017). Parasitism perturbs the mucosal microbiome of Atlantic Salmon. *Scientific reports*, 7, 43465. doi: 10.1038/srep43465.
- López-Camarillo, C., Lopez-Casamichana, M., Weber, C., Guillen, N., Orozco, E. & Marchat, L. A. (2009). DNA repair mechanisms in eukaryotes: special focus in *Entamoeba histolytica* and related protozoan parasites. *Infection, Genetics and Evolution*, 9(6), 1051-1056. doi: 10.1016/j.meegid.2009.06.024.
- Lovy, J., Speare, D. J., Stryhn, H. & Wright, G. M. (2008). Effects of dexamethasone on host innate and adaptive immune responses and parasite development in rainbow trout *Oncorhynchus mykiss* infected with *Loma salmonae*. *Fish and Shellfish Immunology*, 24(5), 649-658. doi: 10.1016/j.fsi.2008.02.007.
- Lozano, R., Naghavi, M., Foreman, K., Lim, S., Shibuya, K., Aboyans, V. & AlMazroa, M. A. (2012). Global and regional mortality from 235 causes of death for 20 age groups in 1990 and 2010: a systematic analysis for the Global Burden of Disease Study 2010. *The Lancet*, 380(9859), 2095-2128. doi: 10.1016/S0140-6736(12)61728-0.
- Lugo-Villarino, G., Balla, K. M., Stachura, D. L., Bañuelos, K., Werneck, M. B. & Traver, D. (2010). Identification of dendritic antigen-presenting cells in the zebrafish. *Proceedings of the National Academy of Sciences*, 107(36), 15850-15855. doi: 10.1073/pnas.1000494107.
- Lumsden, J. S., Ferguson, H. W., Ostland, V. E. & Byrne, P. J. (1994). The mucous coat on gill lamellae of rainbow trout (*Oncorhynchus mykiss*). *Cell and Tissue Research*, 275(1), 187-193. doi: 10.1007/BF00305386.

- Lumsden, J. S., Ostland, V. E., MacPhee, D. D. & Ferguson, H. W. (1995). Production of gill-associated and serum antibody by rainbow trout (*Oncorhynchus mykiss*) following immersion immunization with acetone-killed *Flavobacterium branchiophilum* and the relationship to protection from experimental challenge. *Fish and Shellfish Immunology*, 5(2), 151-165. doi: 10.1016/S1050-4648(05)80024-5.
- Ma, J., Bruce, T. J., Jones, E. M. & Cain, K. D. (2019). A review of fish vaccine development strategies: Conventional methods and modern biotechnological approaches. *Microorganisms*, 7(11), 569. doi: 10.3390/microorganisms7110569.
- MacDonald, S. M., Rafnar, T., Langdon, J. & Lichtenstein, L. M. (1995). Molecular identification of an IgE-dependent histamine-releasing factor. *Science*, 269(5224), 688-690. doi: 10.1126/science.7542803.
- Madrid, J.F., Ballesta, J., Castells, M.T., Marin, J.A. & Pastor, L.M. (1989). Characterization of glycoconjugates in the intestinal mucosa of vertebrates by means of lectin histochemistry. *Acta Histochemica et Cytochemica*, 22, 1-14. doi: 10.1267/ahc.22.1.
- Maetz, J. (1971). Fish gills: mechanisms of salt transfer in fresh water and sea water. *Philosophical Transactions of the Royal Society of London. B, Biological Sciences*, 262(842), 209-249. doi: 10.1098/rstb.1971.0090.
- Mahendran, R., Jeyabaskar, S., Sitharaman, G., Michael, R. D. & Paul, A. V. (2016). Computer-aided vaccine designing approach against fish pathogens *Edwardsiella tarda* and *Flavobacterium columnare* using bioinformatics softwares. *Drug Design, Development and Therapy*, 10, 1703. doi: 10.2147/DDDT.S95691.
- Mansell, B., Powell, M. D., Ernst, I. & Nowak, B. F. (2005). Effects of the gill monogenean *Zeuxapta seriolae* (Meserve, 1938) and treatment with hydrogen peroxide on pathophysiology of kingfish, *Seriola lalandi* Valenciennes, 1833. *Journal of Fish Diseases*, 28(5), 253-262. doi: 10.1111/j.1365-2761.2005.00625.x.
- Marcos-López, M., Ruiz, C. E., Rodger, H. D., O'Connor, I., MacCarthy, E. & Esteban, M. Á. (2017). Local and systemic humoral immune response in farmed Atlantic salmon (*Salmo salar* L.) under a natural amoebic gill disease outbreak. *Fish & Shellfish Immunology*, 66, 207-216. doi: 10.1016/j.fsi.2017.05.029.

- Marcos-López, M., Rodger, H. D., O'Connor, I., Braceland, M., Burchmore, R. J., Eckersall, P. D. & MacCarthy, E. (2017a). A proteomic approach to assess the host response in gills of farmed Atlantic salmon *Salmo salar* L. affected by amoebic gill disease. *Aquaculture*, 470, 1-10. doi: 10.1016/j.aquaculture.2016.12.009.
- Marcos-López, M., Calduch-Giner, J. A., Mirimin, L., MacCarthy, E., Rodger, H. D., O'Connor, I. & Piazzon, M. C. (2018). Gene expression analysis of Atlantic salmon gills reveals mucin 5 and interleukin 4/13 as key molecules during amoebic gill disease. *Scientific Reports*, 8. doi: 10.1038/s41598-018-32019-8.
- Marcos-Lopez, M., Espinosa, C. R., Rodger, H. D., O'Connor, I., MacCarthy, E. & Esteban, M. A. (2018). Oxidative stress is associated with late-stage amoebic gill disease in farmed Atlantic salmon (*Salmo salar* L.). *Journal of Fish Diseases*, 41(2), 383-7. doi: 10.1111/jfd.12699.
- Marcos-López, M. & Rodger, H. D. (2020). Amoebic gill disease and host response in Atlantic salmon (*Salmo salar* L.): A review. *Parasite immunology*, 42(8), e12766. doi: 10.1111/pim.12766.
- Mariuzza, R. A., Velikovskiy, C. A., Deng, L., Xu, G. & Pancer, Z. (2010). Structural insights into the evolution of the adaptive immune system: the variable lymphocyte receptors of jawless vertebrates. *Biological Chemistry*, 391(7), 753-760. doi: 10.1515/BC.2010.091.
- Marshall, W. S. & Bryson, S. E. (1998). Transport mechanisms of seawater teleost chloride cells: an inclusive model of a multifunctional cell. *Comparative Biochemistry and Physiology Part A: Molecular & Integrative Physiology*, 119(1), 97-106. doi: 10.1016/s1095-6433(97)00402-9.
- Martínez-Castillo, M., Cárdenas-Guerra, R. E., Arroyo, R., Debnath, A., Rodríguez, M. A., Sabanero, M. & Shibayama, M. (2017). Nf-GH, a glycosidase secreted by *Naegleria fowleri*, causes mucin degradation: an *in vitro* and *in vivo* study. *Future Microbiology*, 12(9), 781-799. doi: 10.2217/fmb-2016-0230.
- Martinsen, K. H., Thorisdottir, A. & Lillehammer, M. (2018). Effect of hydrogen peroxide as treatment for amoebic gill disease in Atlantic salmon (*Salmo salar* L.) in different temperatures. *Aquaculture Research*, 49(5), 1733-1739. doi: 10.1111/are.13627.

- Matejusová, I., Simková, A., Sasal, P. & Gelnar, M. (2003). Microhabitat distribution of *Pseudodactylogyrus anguillae* and *Pseudodactylogyrus bini* among and within gill arches of the European eel (*Anguilla anguilla* L.). *Parasitology Research*, 89(4), 290-296. doi: 10.1007/s00436-002-0682-8.
- Matthews, C. G. G., Richards, R. H., Shinn, A. P. & Cox, D. I. (2013). Gill pathology in Scottish farmed Atlantic salmon, *Salmo salar* L., associated with the microsporidian *Desmozoon lepeophtherii* Freeman et Sommerville, 2009. *Journal of Fish Diseases*, 36(10), 861-869. doi: 10.1111/jfd.12084.
- Matthews, R. A. (2005). *Ichthyophthirius multifiliis* Fouquet and ichthyophthiriosis in freshwater teleosts. *Advances in Parasitology*, 59, 159-241. doi: 10.1016/S0065-308X(05)59003-1.
- Mays, E. T., Feldhoff, R. C. & Nettleton, G. S. (1984). Determination of protein loss during aqueous and phase partition fixation using formalin and glutaraldehyde. *Journal of Histochemistry and Cytochemistry*, 32, 1107–1127. doi: 10.1152/ajplung.1997.273.5.11036.
- McCarthy, U., Hall, M., Schrittwieser, M., Ho, Y. M., Collins, C., Feehan, L., et al. (2015). “Assessment of the viability of *Neoparamoeba perurans* following exposure to hydrogen peroxide (SARF SP005),” in A study commissioned by the Scottish Aquaculture Research Forum (SARF). Available online at: <http://www.sarf.org.uk/>
- Medzhitov, R. & Janeway, C. A. (2002). Decoding the patterns of self and nonself by the innate immune system. *Science*, 296(5566), 298-300. doi: 10.1126/science.1068883.
- Medzhitov, R. (2007). Recognition of microorganisms and activation of the immune response. *Nature*, 449(7164), 819. doi:10.1038/nature06246.
- Meeker, N. D. & Trede, N. S. (2008). Immunology and zebrafish: spawning new models of human disease. *Developmental and Comparative Immunology*, 32(7), 745-757. doi: 10.1016/j.dci.2007.11.011.
- Meeusen, E. N., Walker, J., Peters, A., Pastoret, P. P. & Jungersen, G. (2007). Current status of veterinary vaccines. *Clinical Microbiology Reviews*, 20(3), 489-510. doi: 10.1128/CMR.00005-07.

- Menna-Barreto, R. F., Beghini, D. G., Ferreira, A. T., Pinto, A. V., De Castro, S. L. & Perales, J. (2010). A proteomic analysis of the mechanism of action of naphthoimidazoles in *Trypanosoma cruzi* epimastigotes *in vitro*. *Journal of Proteomics*, 73(12), 2306-23. doi: 10.1016/j.jprot.2010.07.002.
- Meyerholz, D. K., Rodgers, J., Castilow, E. M. & Varga, S. M. (2009). Alcian Blue and Pyronine Y histochemical stains permit assessment of multiple parameters in pulmonary disease models. *Veterinary Pathology*, 46(2), 325–328. doi: 10.1354/vp.46-2-325.
- Mitchell, A. L., Attwood, T. K., Babbitt, P. C., Blum, M., Bork, P., Bridge, A. & Gough, J. (2018). InterPro in 2019: improving coverage, classification and access to protein sequence annotations. *Nucleic Acids Research*, 47(D1), D351-D360. doi: 10.1093/nar/gky1100.
- Mitchell, S. O. & Rodger, H. D. (2011). A review of infectious gill disease in marine salmonid fish. *Journal of Fish Diseases*, 34(6), 411-432. doi: 10.1111/j.1365-2761.2011.01251.x.
- Mo, Z. Q., Li, Y. W., Wang, H. Q., Wang, J. L., Ni, L. Y., Yang, M. & Dan, X. M. (2016). Comparative transcriptional profile of the fish parasite *Cryptocaryon irritans*. *Parasites and Vectors*, 9(1), 630. doi: 10.1186/s13071-016-1919-1.
- Monaghan, S. J., Thompson, K. D., Adams, A. & Bergmann, S. M. (2015). Sensitivity of seven PCR s for early detection of koi herpesvirus in experimentally infected carp, *C yprinus carpio* L., by lethal and non-lethal sampling methods. *Journal of Fish Diseases*, 38(3), 303-319.
- Moncada, D., Keller, K. & Chadee, K. (2005). *Entamoeba histolytica*-secreted products degrade colonic mucin oligosaccharides. *Infection and immunity*, 73(6), 3790-3793. doi: 10.1128/IAI.73.6.3790-3793.2005.
- Monte, M. M., Zou, J., Wang, T., Carrington, A. & Secombes, C. J. (2011). Cloning, expression analysis and bioactivity studies of rainbow trout (*Oncorhynchus mykiss*) interleukin-22. *Cytokine*, 55(1), 62-73. doi: 10.1016/j.cyto.2011.03.015.
- Moon, E. K., Chung, D. I., Hong, Y. C. & Kong, H. H. (2008). Characterization of a serine proteinase mediating encystation of *Acanthamoeba*. *Eukaryotic Cell*, 7(9), 1513-1517. doi: 10.1128/EC.00068-08.

- Morita, H., Toh, H., Oshima, K., Yoshizaki, M., Kawanishi, M., Nakaya, K. & Murakami, M. (2011). Complete genome sequence and comparative analysis of the fish pathogen *Lactococcus garvieae*. *PLoS One*, 6(8). doi: 10.1371/journal.pone.0023184.
- Morrison, R. N., Cooper, G. A., Koop, B. F., Rise, M. L., Bridle, A. R., Adams, M. B. & Nowak, B. F. (2006). Transcriptome profiling the gills of amoebic gill disease (AGD)-affected Atlantic salmon (*Salmo salar* L.): a role for tumour suppressor p53 in AGD pathogenesis? *Physiological Genomics*, 26(1), 15-34. doi: 10.1152/physiolgenomics.00320.2005.
- Morrison, R. N., Koppang, E. O., Hordvik, I., & Nowak, B. F. (2006a). MHC class II+ cells in the gills of Atlantic salmon (*Salmo salar* L.) affected by amoebic gill disease. *Veterinary Immunology and Immunopathology*, 109(3-4), 297-303. doi: 10.1016/j.vetimm.2005.08.026.
- Morrison, R. N. & Nowak, B. F. (2008). Immunohistochemical detection of anterior gradient-2 in the gills of amoebic gill disease-affected Atlantic salmon, *Salmo salar* L. *Journal of Fish Diseases*, 31(9), 699-705. doi: 10.1111/j.1365-2761.2008.00934.x.
- Morrison, R. N., Young, N. D., & Nowak, B. F. (2012). Description of an Atlantic salmon (*Salmo salar* L.) type II interleukin-1 receptor cDNA and analysis of interleukin-1 receptor expression in amoebic gill disease-affected fish. *Fish & Shellfish Immunology*, 32(6), 1185-1190. doi: 10.1016/j.fsi.2012.03.005.
- Mottram, J. C., Coombs, G. H. & Alexander, J. (2004). Cysteine peptidases as virulence factors of *Leishmania*. *Current Opinion in Microbiology*, 7(4), 375-381. doi: 10.1016/j.mib.2004.06.010.
- Mowry, R. W. (1956). Alcian blue techniques for the histochemical study of acidic carbohydrates. *Journal of Histochemistry and Cytochemistry*, 4, 403-407.
- Munday, B.L. (1986). Diseases of salmonids. In: *Proceedings of the Workshop on Diseases of Australian Fish and Shellfish*, 127-141. doi: 10.1111/j.1365-2761.1987.tb01088.x.
- Munday, B. L., Foster, C. K., Roubal, F. R. & Lester, R. J. G. (1990). Paramoebic gill infection and associated pathology of Atlantic salmon, *Salmo salar*, and rainbow trout, *Salmo gairdneri*, in Tasmania. *Pathology in Marine Science*, 215-222.

- Munday, B. L., Lange, K., Foster, C., Lester, R. J. G. & Handler, J. (1993). Amoebic gill disease of sea-caged salmonids in Tasmanian waters. *Tasmanian Fisheries Research*, 28, 14-19.
- Munday, B. L., Zilberg, D. & Findlay, V. (2001). Gill disease of marine fish caused by infection with *Neoparamoeba pemaquidensis*. *Journal of Fish Diseases*, 24(9), 497–507. doi: 10.1046/j.1365-2761.2001.00329.x.
- Murray, C.K. & Fletcher, T.C., (1976). The immunohistochemical localization of lysozyme in plaice (*Pleuronectes platessa* L.) tissues. *Journal of Fish Biology*, 9, 329-334. doi: 10.1111/j.1095-8649.1976.tb04681.x.
- Nagashima, Y., Kikuchi, N., Shimakura, K. & Shiomi, K., (2003). Purification and characterization of an antibacterial factor in the skin secretion of rock fish *Sebastes schlegeli*. *Comparative Biochemistry and Physiology - Part C: Toxicology and Pharmacology*, 136, 63–71. doi: 10.1016/S1532-0456(03)00174-1.
- Naka, H., Dias, G. M., Thompson, C. C., Dubay, C., Thompson, F. L. & Crosa, J. H. (2011). Complete genome sequence of the marine fish pathogen *Vibrio anguillarum* harboring the pJM1 virulence plasmid and genomic comparison with other virulent strains of *V. anguillarum* and *V. ordalii*. *Infection and Immunity*, 79(7), 2889-2900. doi: 10.1128/IAI.05138-11.
- Nakanishi, T., Toda, H., Shibasaki, Y. & Somamoto, T. (2011). Cytotoxic T cells in teleost fish. *Developmental and Comparative Immunology*, 35(12), 1317-1323. doi: 10.1016/j.dci.2011.03.033.
- Nho, S. W., Hikima, J. I., Cha, I. S., Park, S. B., Jang, H. B., del Castillo, C. S. & Jung, T. S. (2011). Complete genome sequence and immunoproteomic analyses of the bacterial fish pathogen *Streptococcus parauberis*. *Journal of Bacteriology*, 193(13), 3356-3366. doi: 10.1128/JB.00182-11.
- Niemirowicz, G., Fernández, D., Solà, M., Cazzulo, J. J., Avilés, F. X. & Gomis-Rüth, F. X. (2008). The molecular analysis of *Trypanosoma cruzi* metalloprotease 1 provides insight into fold and substrate specificity. *Molecular Microbiology*, 70(4), 853-866. doi: 10.1111/j.1365-2958.2008.06444.x.
- Nieuwenhuizen, N., Lopata, A. L., Jeebhay, M. F., De'Broski, R. H., Robins, T. G. & Brombacher, F. (2006). Exposure to the fish parasite *Anisakis* causes allergic airway hyperreactivity and dermatitis. *Journal of Allergy and Clinical Immunology*, 117(5), 1098-1105. doi: 10.1371/journal.pntd.0004845.

- Nigam, A. K., Kumari, U., Mittal, S. & Mittal, A. K. (2012). Comparative analysis of innate immune parameters of the skin mucous secretions from certain freshwater teleosts, inhabiting different ecological niches. *Fish Physiology and Biochemistry*, 38(5), 1245-1256. doi:10.1007/s10695-012-9613-5.
- Nishimura, S. I., Furuike, T., Matsuoka, K., Maruyama, K., Nagata, K., Kurita, K. & Tokura, S. (1994). Synthetic Glycoconjugates. 4. Use of Omega-(Acrylamido) alkyl Glycosides for the Preparation of Cluster Glycopolymers. *Macromolecules*, 27(18), 4876-4880. doi: 10.1021/ma00096a004.
- Norwegian Ministry of Health and Care Services. National Strategy against Antimicrobial Resistance 2015–2020. Oslo, Norway: Norwegian Ministry of Health and Care Services, 2015, Available at: <https://www.regjeringen.no/contentassets/5eaf66ac392143b3b2054aed90b85210/antibiotic-resistance-engelsklavopploslig-versjon-for-nett-10-09-15.pdf>
- Novinec, M. & Lenarcic, B. (2013). Papain-like peptidases: structure, function, and evolution. *Biomolecular Concepts* 4, 287–308. doi: 10.1515/bmc-2012-0054.
- Nowak, B. F. & Munday, B.L. (1994) Histology of gills of Atlantic salmon during the first few months following transfer to sea water. *Bulletin of the European Association of Fish Pathologists*, 14, 77– 81.
- Nowak, B. F. (2012). Neoparamoeba perurans. *Fish Parasites, Pathobiology and Protection*, 2012, 1-18.
- Nowak, B., Valdenegro-Vega, V., Crosbie, P. & Bridle, A. (2014). Immunity to amoeba. *Developmental & Comparative Immunology*, 43(2), 257-267. doi: 10.1016/j.dci.2013.07.021.
- Nowak, B., Valdenegro-Vega, V., Crosbie, P. & Bridle, A. (2014). Immunity to amoeba- *Developmental and Comparative Immunology*, 43(2), 257–267. doi: 10.1016/j.dci.2013.07.021.
- Ofir-Birin, Y., Abou Karam, P., Rudik, A., Giladi, T., Porat, Z. & Regev-Rudzki, N. (2018). Monitoring extracellular vesicle cargo active uptake by imaging flow cytometry. *Frontiers in Immunology*, 9, 1–9. doi: 10.3389/fimmu.2018.01011.
- Okazaki, K. & Yumura, S. (1995). Differential association of three actin-bundling proteins with microfilaments in *Dictyostelium amoebae*. *European Journal of Cell Biology*, 66(1), 75-81.

- Oldham, T., Rodger, H. & Nowak, B. F. (2016). Incidence and distribution of amoebic gill disease (AGD) - An epidemiological review. *Aquaculture*, 457, 35–42. doi: 10.1016/j.aquaculture.2016.02.013.
- Olsen, M. M., Kania, P. W., Heinecke, R. D., Skjoedt, K., Rasmussen, K. J. & Buchmann, K. (2011). Cellular and humoral factors involved in the response of rainbow trout gills to *Ichthyophthirius multifiliis* infections: molecular and immunohistochemical studies. *Fish and Shellfish Immunology*, 30(3), 859-869. doi: 10.1016/j.fsi.2011.01.010.
- Ouaissi, A., Da Silva, A. C., Guevara, A. G., Couthino, M. & Guilvard, E. (2001). *Trypanosoma cruzi*-induced host immune system dysfunction: a rationale for parasite immunosuppressive factor (s) encoding gene targeting. *BioMed Research International*, 1(1), 11-17. doi: 10.1155/S1110724301000055.
- Overton, K., Samsing, F., Oppedal, F., Dalvin, S., Stien, L. H. & Dempster, T. (2018). The use and effects of hydrogen peroxide on salmon lice and post-smolt Atlantic salmon. *Aquaculture*, 486, 246-252. doi: 10.1016/j.aquaculture.2017.12.041.
- Page, F. C. (1973). *Paramoeba*: a common marine genus. *Hydrobiologia* 41, 183–188.
- Page, F. C. (1983). Three freshwater species of Mayorella (Amoebida) with a cuticle. *Archiv für Protistenkunde*, 127(2), 201-221.
- Pallavi, B., Shankar, K. M. & Abhiman, P. B. (2016). *In silico* prediction of potential vaccine candidates of *Lernaea cyprinacea*: An ectoparasite of Indian major carps. *Indian Journal of Biotechnology*, 15, 601-603.
- Panpradist, N., Toley, B. J., Zhang, X., Byrnes, S., Buser, J. R., Englund, J. A. & Lutz, B. R. (2014). Swab sample transfer for point-of-care diagnostics: characterization of swab types and manual agitation methods. *PloS One*, 9(9). doi: 10.1371/journal.pone.0105786.
- Parsons, H., Nowak, B., Fisk, D. & Powell, M. (2001). Effectiveness of commercial freshwater bathing as a treatment against amoebic gill disease in *Atlantic salmon*. *Aquaculture*, 195(3-4), 205-210. doi: 10.1016/S0044-8486(00)00567-6.
- Parussini, F., García, M., Mucci, J., Agüero, F., Sánchez, D., Hellman, U. & Cazzulo, J. J. (2003). Characterization of a lysosomal serine carboxypeptidase from *Trypanosoma cruzi*. *Molecular and Biochemical Parasitology*, 131(1), 11-23. doi: 10.1016/s0166-6851(03)00175-0.

- Pennacchi, Y., Leef, M. J., Crosbie, P. B. B., Nowak, B. F. & Bridle, A. R. (2014). Evidence of immune and inflammatory processes in the gills of AGD-affected Atlantic salmon, *Salmo salar* L. *Fish and Shellfish Immunology*, 36(2), 563-570. doi: 10.1016/j.fsi.2013.12.013.
- Perkins, F. O. & Castagna, M. (1971). Ultrastructure of the Nebenkörper or 'secondary nucleus' of the parasitic amoeba *Paramoeba pernicioso* (Amoebida, Paramoebidae). *Journal of Invertebrate Pathology* 17, 186–193.
- Perry, S. F. (1997). The chloride cell: structure and function in the gills of freshwater fishes. *Annual Review of Physiology*, 59(1), 325-347. doi: 10.1146/annurev.physiol.59.1.325.
- Petri, W. A., Smith, R. D., Schlesinger, P. H., Murphy, C. F. & Ravdin, J. I. (1987). Isolation of the galactose-binding lectin that mediates the *in vitro* adherence of *Entamoeba histolytica*. *The Journal of Clinical Investigation*, 80(5), 1238-1244. doi: 10.1172/JCI113198.
- Phu, T. M., Phuong, N. T., Dung, T. T., Hai, D. M., Son, V. N., Rico, A. & Dalsgaard, A. (2016). An evaluation of fish health-management practices and occupational health hazards associated with *Pangasius catfish* (*Pangasianodon hypophthalmus*) aquaculture in the Mekong Delta, Vietnam. *Aquaculture Research*, 47(9), 2778-2794. doi: 10.1111/are.12728.
- Pickering, A. D. & Macey, D. J. (1977). Structure, histochemistry and the effect of handling on the mucous cells of the epidermis of the char *Salvelinus alpinus* (L.). *Journal of Fish Biology*, 10(5), 505-512. doi: 10.1111/j.1095-8649.1977.tb04083.x.
- Poppe, T. T. & Mo, T. A. (1993). Systemic, granulomatous hexamitosis of farmed Atlantic salmon: interaction with wild fish. *Fisheries Research*, 17(1-2), 147-152. doi: 10.1016/0165-7836(93)90014-X.
- Powell, M. D., Speare, D. J. & Wright, G. M. (1994). Comparative ultrastructural morphology of lamellar epithelial, chloride and mucous cell glycocalyx of the rainbow trout (*Oncorhynchus mykiss*) gill. *Journal of Fish Biology*, 44(4), 725-730. doi: 10.1111/j.1095-8649.1994.tb01248.x.
- Powell, M. D., Parsons, H. J. & Nowak, B. F. (2001). Physiological effects of freshwater bathing of Atlantic salmon (*Salmo salar*) as a treatment for amoebic gill disease. *Aquaculture*, 199(3-4), 259-266. doi: 10.1016/S0044-8486(01)00573-7.

- Powell, M. D. & Clark, G. A. (2004). Efficacy and toxicity of oxidative disinfectants for the removal of gill amoebae from the gills of amoebic gill disease affected Atlantic salmon (*Salmo salar* L.) in freshwater. *Aquaculture Research*, 35(2), 112-123. doi: 10.1111/j.1365-2109.2004.00989.x
- Powell, M. D., Attard, M., Harris, J. O., Roberts, S. D. & Leef, M. J. (2005). Why fish die-the treatment and pathophysiology of AGD. *FRDC Project*, (2001/205).
- Powell, M. D., Speare, D. J. & Burka, J. F. (1992). Fixation of mucus on rainbow trout (*Oncorhynchus mykiss* Walbaum) gills for light and electron microscopy. *Journal of Fish Biology*, 41, 813–824. doi: 10.1111/j.1095-8649.1992.tb02709.x.
- Press, C. M. & Lillehaug, A. (1995). Vaccination in European salmonid aquaculture: a review of practices and prospects. *British Veterinary Journal*, 151(1), 45-69. Doi: 10.1016/S0007-1935(05)80064-8.
- Pritam, M., Singh, G., Swaroop, S., Singh, A. K. & Singh, S. P. (2019). Exploitation of reverse vaccinology and immunoinformatics as promising platform for genome-wide screening of new effective vaccine candidates against *Plasmodium falciparum*. *BMC Bioinformatics*, 19(13), 468. doi: 10.1186/s12859-018-2482-x.
- Proudfoot, N. J., Furger, A. & Dye, M. J. (2002). Integrating mRNA processing with transcription. *Cell*, 108(4), 501-512. doi: 10.1016/S0092-8674(02)00617-7.
- Puiu, D., Enomoto, S., Buck, G. A., Abrahamsen, M. S. & Kissinger, J. C. (2004). CryptoDB: the *Cryptosporidium* genome resource. *Nucleic Acids Research*, 32(suppl_1), D329-D331. doi: 10.1093/nar/gkh050.
- Qi, Z., Zhang, Q., Wang, Z., Zhao, W., Chen, S. & Gao, Q. (2015). Molecular cloning, expression analysis and functional characterization of interleukin-22 in So-iny mullet, *Liza haematocheila*. *Molecular Immunology*, 63(2), 245-252. doi: 10.1016/j.molimm.2014.07.006.
- Quast, C., Priesse, E., Yilmaz, P., Gerken, J., Schweer, T., Yarza, P. & Glöckner, F. O. (2012). The SILVA ribosomal RNA gene database project: improved data processing and web-based tools. *Nucleic Acids Research*, 41(D1), D590-D596. doi: 10.1093/nar/gks1219.
- Quintana-Hayashi, M. P., Padra, M., Padra, J. T., Benktander, J. & Lindén, S. K. (2018). Mucus-pathogen interactions in the gastrointestinal tract of farmed animals. *Microorganisms*, 6(2), 55. doi: 10.3390/microorganisms6020055.

- Rach, J. J., Schreier, T. M., Howe, G. E. & Redman, S. D. (1997). Effect of species, life stage, and water temperature on the toxicity of hydrogen peroxide to fish. *The Progressive Fish-Culturist*, 59(1), 41-46. doi: 10.1577/1548-8640(1997)059<0041:eoslsa>2.3.co;2.
- Rakoff-Nahoum, S., & Medzhitov, R. (2009). Toll-like receptors and cancer. *Nature Reviews Cancer*, 9(1), 57-63. doi: 10.1038/nrc2541.
- Ramakrishnaiah, V., Thumann, C., Fofana, I., Habersetzer, F., Pan, Q., de Ruiter, P. E. & van der Laan, L. J. (2013). Exosome-mediated transmission of hepatitis C virus between human hepatoma Huh7.5 cells. *Proceedings of the National Academy of Sciences of the United States of America*, 110(32), 13109–13113. doi: 10.1073/pnas.1221899110.
- Ramirez-Gonzalez, R. H., Bonnal, R., Caccamo, M. & MacLean, D. (2012). Bio-samtools: Ruby bindings for SAMtools, a library for accessing BAM files containing high-throughput sequence alignments. *Source Code for Biology and Medicine*, 7(1), 6. doi: 10.1186/1751-0473-7-6.
- Rappuoli, R. (2000). Reverse vaccinology. *Current Opinion in Microbiology*, 3(5), 445-450. doi: 10.1016/s1369-5274(00)00119-3.
- Rappuoli, R. & Aderem, A. (2011). A 2020 vision for vaccines against HIV, tuberculosis and malaria. *Nature*, 473(7348), 463. doi: 10.1038/nature10124.
- Rappuoli, R. (2014). Vaccines, emerging viruses, and how to avoid disaster. *BMC Biology*, 12(1), 100. doi: 10.1186/s12915-014-0100-6.
- Rappuoli, R., Pizza, M., Del Giudice, G. & De Gregorio, E. (2014). Vaccines, new opportunities for a new society. *Proceedings of the National Academy of Sciences*, 111(34), 12288-12293. doi: 10.1073/pnas.1402981111.
- Rashid, M. I., Rehman, S., Ali, A. & Andleeb, S. (2019). Fishing for vaccines against *Vibrio cholerae* using *in silico* pan-proteomic reverse vaccinology approach. *PeerJ*, 7, doi: 10.7717/peerj.6223.
- Ravdin, J. I., Murphy, C. F., Salata, R. A., Guerrant, R. L., & Hewlett, E. L. (1985). N-Acetyl-D-galactosamine-inhibitable adherence lectin of *Entamoeba histolytica*. I. Partial purification and relation to amoebic virulence *in vitro*. *Journal of Infectious Diseases*, 151(5), 804-815. doi: 10.1093/infdis/151.5.804.

- Rawlings, N. D., Pearl, L. H. & Buttle, D. J. (1992). The baculovirus *Autographa californica nuclear* polyhedrosis virus genome includes a papain-like sequence. *Biological Chemistry Hoppe-Seyler*, 373, 1211–1216. doi: 10.1515/bchm3.1992.373.2.1211.
- Régnier, P. & Marujo, P. E. (2013). Polyadenylation and Degradation of RNA in Prokaryotes. In *Madame Curie Bioscience Database* [Internet]. Landes Bioscience. Available at: <https://www.ncbi.nlm.nih.gov/books/NBK6253/>
- Reichert, J. S., McNeight, S. A. & Rudel, H. W. (1939). Determination of hydrogen peroxide and some related peroxygen compounds. *Industrial & Engineering Chemistry Analytical Edition*, 11(4), 194-197. doi: 10.1021/ac50132a007.
- Reite, O. B. & Evensen, Ø. (2006). Inflammatory cells of teleostean fish: a review focusing on mast cells/eosinophilic granule cells and rodlet cells. *Fish & shellfish immunology*, 20(2), 192-208.
- Ringø, E., Dimitroglou, A., Hoseinifar, S. H. & Davies, S. J. (2014). Prebiotics in finfish: an update. *Aquaculture Nutrition: Gut health, Probiotics and Prebiotics*, 360-400. doi: 10.1002/9781118897263.ch14.
- Roberts, S. D. & Powell, M. D. (2003). Comparative ionic flux and gill mucous cell histochemistry: effects of salinity and disease status in Atlantic salmon (*Salmo salar* L.). *Comparative Biochemistry and Physiology Part A: Molecular and Integrative Physiology*, 134(3), 525-537. doi: 10.1016/s1095-6433(02)00327-6.
- Roberts, S. D. & Powell, M. D. (2005). The viscosity and glycoprotein biochemistry of salmonid mucus varies with species, salinity and the presence of amoebic gill disease. *Journal of Comparative Physiology B*, 175(1), 1-11. doi: 10.1007/s00360-004-0453-1.
- Roberts, S. D. & Powell, M. D. (2008). Freshwater bathing alters the mucous layer of marine Atlantic salmon *Salmo salar* L. *Journal of Fish Biology*, 72(7), 1864-1870. doi: 10.1111/j.1095-8649.2008.01853.x.
- Rodger, H. D. & McArdle, J. F. (1996). An outbreak of amoebic gill disease in Ireland. *Veterinary Record*, 139(14), 348–349. doi: 10.1136/vr.139.14.348.
- Rodger, H. D. (2014). Amoebic gill disease (AGD) in farmed salmon (*Salmo salar*) in Europe. *Fish Veterinary Journal*, 24, 16–26.

- Rodger, H.D. (2007). Gill disorders: an emerging problem for farmed Atlantic salmon (*Salmo salar*) in the marine environment? *Fish Veterinary Journal*, 9(1), 38–48.
- Rodger, H. D., Murphy, K., Mitchell, S. O. & Henry, L. (2011). Gill disease in marine farmed Atlantic salmon at four farms in Ireland. *Veterinary Record*, 168(25), 668-668. doi: 10.1136/vr.d3020.
- Rodger, H. D. (2016). Fish disease causing economic impact in global aquaculture. In *Fish Vaccines* (pp.1-34). Springer, Basel.
- Röhe, I., Hüttner, F. J., Plendl, J., Drewes, B., & Zentek, J. (2018). Comparison of different histological protocols for the preservation and quantification of the intestinal mucus layer in pigs. *European Journal of Histochemistry*, 62(1). doi: 10.4081/ejh.2018.2874.
- Rombout, J. H., Taverne, N., van de Kamp, M. & Taverne-Thiele, A. J. (1993). Differences in mucus and serum immunoglobulin of carp (*Cyprinus carpio* L.). *Developmental and Comparative Immunology*, 17(4), 309-317. doi: 10.1016/0145-305x(93)90003-9.
- Rombout, J. H., Yang, G. & Kiron, V. (2014). Adaptive immune responses at mucosal surfaces of teleost fish. *Fish and Shellfish Immunology*, 40(2), 634-643. doi: 10.1016/j.fsi.2014.08.020.
- Ross, A. J. & Klontz, G. W. (1965). Oral Immunization of Rainbow Trout (*Salmo gairdneri*) Against an Etiologic Agent of "Redmouth Disease". *Journal of the Fisheries Board of Canada*, 22(3), 713-719. doi: 10.1139/f65-063.
- Roubal, F. R., Bullock, A. M., Robertson, D. A. & Roberts, R. J. (1987). Ultrastructural aspects of infestation by *Ichthyobodo necator* (Henneguy, 1883) on the skin and gills of the salmonids *Salmo salar* L. and *Salmo gairdneri* Richardson. *Journal of Fish Diseases*, 10(3), 181-192. doi: 10.1111/j.1365-2761.1987.tb01060.x.
- Rozas, M., Bohle, H., Ildefonso, R. & Bustos, P. (2011). Development of PCR assay for detection of *Neoparamoeba perurans* and comparison of histological diagnosis. *Bulletin of European Association of Fish Pathologists*, 31, 211-218.
- Rozas-Serri, M. (2019). Gill diseases in marine salmon aquaculture with an emphasis on amoebic gill disease. *Atlantic*, 32(33), 34-35. doi: 10.1079/PAVSNNR201914032.

- Russell, S., Hayes, M. A. & Lumsden, J. S. (2009). Immunohistochemical localization of rainbow trout ladderlectin and intelectin in healthy and infected rainbow trout (*Oncorhynchus mykiss*). *Fish and Shellfish Immunology*, 26(1), 154-163. doi: 10.1016/j.fsi.2008.03.001.
- Sajid, M. & McKerrow, J. H. (2002). Cysteine proteases of parasitic organisms. *Molecular and Biochemical Parasitology*, 120(1), 1-21. doi: 10.1016/S0166-6851(01)00438-8.
- Salinas, I. (2015). The mucosal immune system of teleost fish. *Biology*, 4(3), 525-539. doi: 10.3390/biology4030525.
- Sanchez, J. G., Speare, D. J., Sims, D. E. & Johnson, G. J. (1997). Adaptation of a fluorocarbon-based non-aqueous fixation regime for the ultrastructural study of the teleost epithelial mucous coat. *Journal of Comparative Pathology*, 117(2), 165-170. doi: 10.1016/S0021-9975(97)80033-3.
- Sang, Y. & Blecha, F. (2008). Antimicrobial peptides and bacteriocins: alternatives to traditional antibiotics. *Animal Health Research Reviews*, 9(2), 227-235. doi: 10.1017/S1466252308001497.
- Saraiva, M. & O'garra, A. (2010). The regulation of IL-10 production by immune cells. *Nature Reviews Immunology*, 10(3), 170. doi: 10.1038/nri2711.
- Sarkar, N. (1997). Polyadenylation of mRNA in prokaryotes. *Annual Review of Biochemistry*, 66(1), 173-197. doi: 10.1146/annurev.biochem.66.1.173.
- Saurabh, S. & Sahoo, P. K. (2008). Lysozyme: an important defence molecule of fish innate immune system. *Aquaculture Research*, 39(3), 223-239. doi: 10.1111/j.1365-2109.2007.01883.x.
- Schlenk, D., & Benson, W. H. (2001). Fish immunotoxicology. In *Target Organ Toxicity in Marine and Freshwater Teleosts*, 107-150. CRC Press.
- Schmieder, R. & Edwards, R. (2011). Quality control and preprocessing of metagenomic datasets. *Bioinformatics*, 27(6), 863-864. doi: 10.1093/bioinformatics/btr026.
- Schorey, J. S. & Harding, C. V. (2016). Extracellular vesicles and infectious diseases: New complexity to an old story. *The Journal of Clinical Investigation*, 126(4), 1181–1189. doi: 10.1172/jci81132.
- Schroeder Jr, H. W. & Cavacini, L. (2010). Structure and function of immunoglobulins. *Journal of Allergy and Clinical Immunology*, 125(2), S41-S52. doi: 10.1016/j.jaci.2009.09.046.

- Schuster, F. L. (2002). Cultivation of pathogenic and opportunistic free-living amebas. *Clinical Microbiology Reviews*, 15(3), 342-354. doi: 10.1128/CMR.15.3.342-354.2002.
- Secombes, C. J. & Fletcher, T. C. (1992). The role of phagocytes in the protective mechanisms of fish. *Annual Review of Fish Diseases*, 2, 53-71. doi: 10.1016/0959-8030(92)90056-4.
- Segal, H. C., Hunt, B. J. & Gilding, K. (1998). The effects of alginate and non-alginate wound dressings on blood coagulation and platelet activation. *Journal of Biomaterials Applications*, 12(3), 249-257. doi: 10.1177/088532829801200305.
- Sellon, R. K., Tonkonogy, S., Schultz, M., Dieleman, L. A., Grenther, W., Balish, E. D. & Sartor, R. B. (1998). Resident enteric bacteria are necessary for development of spontaneous colitis and immune system activation in interleukin-10-deficient mice. *Infection and immunity*, 66(11), 5224-5231. doi: 10.1128/IAI.66.11.5224-5231.1998.
- Seo, S. A., Yong, T. S. & Im, K. I. (1992). The maintenance of free-living amoebae by cryopreservation. *The Korean Journal of Parasitology*, 30(2), 151-153. doi: 10.3347/kjp.1992.30.2.151.
- Shefat, S. H. T. (2018). Vaccines for use in finfish aquaculture. *Acta Scientifical Pharmaceutical Sciences*, 2, 15-19.
- Shephard, K. L. (1994). Functions for fish mucus. *Reviews in Fish Biology and Fisheries*, 4(4), 401-429. doi: 10.1007/BF00042888.
- Shinn, A. P., Pratoomyot, J., Bron, J. E., Paladini, G., Brooker, E. E. & Brooker, A. J. (2015). Economic costs of protistan and metazoan parasites to global mariculture. *Parasitology*, 142(1), 196-270. doi: 10.1017/S0031182014001437.
- Sies, H., Berndt, C. & Jones, D. P. (2017). Oxidative stress. *Annual Review of Biochemistry*, 86, 715-748. doi: 10.1146/annurev-biochem-061516-045037.
- Simpson, R. J., Lim, J. W., Moritz, R. L. & Mathivanan, S. (2009). Exosomes: Proteomic insights and diagnostic potential. *Expert Review of Proteomics*, 6(3), 267-283. doi: 10.1586/epr.09.17.
- Sims, D. E. & Horne, M. M. (1997). Heterogeneity of the composition and thickness of tracheal mucus in rats. *American Journal of Physiology-Lung Cellular and Molecular Physiology*, 273(5), L1036-L1041. doi: 10.1152/ajplung.1997.273.5.L1036.

- Sims, D. E., Westfall, J. A., Kiorpes, A. L. & Home, M. M. (1991). Preservation of tracheal mucus by nonaqueous fixative. *Biotechnical and Histochemistry*, 66(4), 173-180. doi: 10.3109/10520299109109965.
- Snieszko, S., Piotrowska, W., Kocylowski, B. & Marek, K. (1938). Badania bakteriologiczne i serologiczne nad bakteriami posocznicy karpi. *Rospr Biol. Zakresu Med. Wet.*, 16, 143-157.
- Sommerset, I., Krossøy, B., Biering, E. & Frost, P. (2005). Vaccines for fish in aquaculture. *Expert Review of Vaccines*, 4(1), 89-101. doi: 10.1586/14760584.4.1.89.
- Song, X., Hu, X., Sun, B., Bo, Y., Wu, K., Xiao, L. & Gong, C. (2017). A transcriptome analysis focusing on inflammation-related genes of grass carp intestines following infection with *Aeromonas hydrophila*. *Scientific Reports*, 7(1), 1-12. doi: 10.1038/srep40777.
- Speare, D. J. & Ferguson, H. W. (2006). Gills and pseudobranchs. In *Systemic Pathology of Fish*, pp. 24-63.
- Speare, D. J. & Mirsalimi, S. M. (1992). Pathology of the mucous coat of trout skin during an erosive bacterial dermatitis: a technical advance in mucous coat stabilization for ultrastructural examination. *Journal of Comparative Pathology*, 106(3), 201-211. doi: 10.1016/0021-9975(92)90049-Z.
- Steinel, N. C. & Bolnick, D. (2018). The fish adaptive immune response and its suppression by helminths. *The Journal of Immunology*, 200, Issue 1 Supplement.
- Sterud, E., Mo, T. A. & Poppe, T. T. (1998). Systemic spironucleosis in sea-farmed Atlantic salmon *Salmo salar*, caused by *Spironucleus barkhanus* transmitted from feral Arctic char *Salvelinus alpinus*? *Diseases of Aquatic Organisms*, 33(1), 63-66. doi: 10.3354/dao033063.
- St-Hilaire, S., Hill, M., Kent, M. L., Whitaker, D. J. & Ribble, C. (1997). A comparative study of muscle texture and intensity of *Kudoa thyrsites* infection in farm-reared Atlantic salmon *Salmo salar* on the Pacific coast of Canada. *Diseases of Aquatic Organisms*, 31(3), 221-225. doi: 10.3354/dao031221.
- Sudha, R., Katiyar, A., Katiyar, P., Singh, H. & Prasad, P. (2019). Identification of potential drug targets and vaccine candidates in *Clostridium botulinum* using subtractive genomics approach. *Bioinformation*, 15(1), 18-25. doi: 10.6026/97320630015018.

- Suydam, E. L. (1971). The micro-ecology of three species of monogenetic trematodes of fishes from the Beaufort-Cape Hatteras area. *Proceedings of the Helminthological Society of Washington*, 38, 240-6.
- Sveen, L. R., Grammes, F. T., Ytteborg, E., Takle, H. & Jørgensen, S. M. (2017). Genome-wide analysis of Atlantic salmon (*Salmo salar*) mucin genes and their role as biomarkers. *PloS One*, 12(12). doi: 10.1371/journal.pone.0189103.
- Swidsinski, A., Weber, J., Loening-baucke, V., Hale, L. P. & Lochs, H. (2005). Spatial Organization and Composition of the Mucosal Flora in Patients with Inflammatory Bowel Disease. *Journal of Clinical Microbiology*, 43(7), 3380–3389. doi: 10.1128/JCM.43.7.3380.
- Szempruch, A. J., Dennison, L., Kieft, R., Harrington, J. M. & Hajduk, S. L. (2016). Sending a message: Extracellular vesicles of pathogenic protozoan parasites. *Nature Reviews Microbiology*, 14(11), 669–675. doi: 10.1038/nrmicro.2016.110.
- Tang, Y., Wu, Y., Herlihy, S. E., Brito-Aleman, F. J., Ting, J. H., Janetopoulos, C. & Gomer, R. H. (2018). An autocrine proliferation repressor regulates *Dictyostelium discoideum* proliferation and chemorepulsion using the G protein-coupled receptor GrIH. *MBio*, 9(1). doi: 10.1128/mBio.02443-17.
- Tanifuji, G., Cenci, U., Moog, D., Dean, S., Nakayama, T., David, V. & Colp, M. (2017). Genome sequencing reveals metabolic and cellular interdependence in an amoeba-kinetoplastid symbiosis. *Scientific Reports*, 7(1), 11688. doi: 10.1038/s41598-017-11866-x.
- Taylor, R. S., Muller, W. J., Cook, M. T., Kube, P. D. & Elliott, N. G. (2009). Gill observations in Atlantic salmon (*Salmo salar*, L.) during repeated amoebic gill disease (AGD) field exposure and survival challenge. *Aquaculture*, 290(1-2), 1-8. doi: 10.1016/j.aquaculture.2009.01.030.
- Team, R. C. (2014). A language and environment for statistical computing. R Foundation for Statistical Computing, Vienna, Austria2014. Available at: <https://www.R-project.org>.
- Thomas, P., Mujawar, M. M., Upreti, R. & Sekhar, A. C. (2013). Improved recovery of *Bacillus* spores from nonporous surfaces with cotton swabs over foam, nylon, or polyester, and the role of hydrophilicity of cotton in governing the recovery efficiency. *Applied and Environmental Microbiology*, 79(1), 381-384. doi: 10.1128/AEM.02626-12.

- Thompson, K. D. (2017). Immunology: improvement of Innate and Adaptive Immunity. In *Fish Diseases*, 1-17. Academic Press.
- Toledo, O. M. S., Taniwaki, N. N., Saldiva, P. H. & Montes, G. S. (1996). Effect of aqueous and nonaqueous fixatives on the quantitative estimation of collagen-proteoglycan interaction in tissue sections. *Biotechnical and Histochemistry*, 71(3), 109-114. doi: 10.3109/10520299609117145.
- Tongsri, P., Meng, K., Liu, X., Wu, Z., Yin, G., Wang, Q. & Xu, Z. (2020). The predominant role of mucosal immunoglobulin IgT in the gills of rainbow trout (*Oncorhynchus mykiss*) after infection with *Flavobacterium columnare*. *Fish & Shellfish Immunology*. doi: 10.1016/j.fsi.2020.01.044.
- Torrecilhas, A. C., Schumacher, R. I., Alves, M. J. & Colli, W. (2012). Vesicles as carriers of virulence factors in parasitic protozoan diseases. *Microbes and Infection*, 14(15), 1465–1474. doi: 10.1016/j.micinf.2012.07.008.
- Touchon, M., Barbier, P., Bernardet, J. F., Loux, V., Vacherie, B., Barbe, V. & Duchaud, E. (2011). Complete genome sequence of the fish pathogen *Flavobacterium branchiophilum*. *Applied and Environmental Microbiology*, 77(21), 7656-7662. doi: 10.1128/AEM.05625-11.
- Tredinnick, J. E. & Tucker, J. (1951). The use of calcium alginate wool for swabbing dairy equipment. In *Proceedings of the Society for Applied Bacteriology*. Vol. 14, No. 1, pp. 85-88. Oxford, UK: Blackwell Publishing Ltd.
- Turgut, E., Shinn, A. & Wootten, R. (2006). Spatial distribution of *Dactylogyrus* (Monogenan) on the gills of the host fish. *Turkish Journal of Fisheries and Aquatic Sciences*, 6, 93–98.
- Turner, J. C., Harry, K., Lofland, D. & Madhusudhan, K. T. (2010). The Characterization of the Absorption and Release Properties of Various Clinical Swabs. In *26th Clinical Virology Symposium*, Florida, USA.
- Ulmer, J. B., Mason, P. W., Geall, A. & Mandl, C. W. (2012). RNA-based vaccines. *Vaccine*, 30(30), 4414-4418. doi: 10.1016/j.vaccine.2012.04.060.
- Uribe, C., Folch, H., Enriquez, R. & Moran, G. (2011). Innate and adaptive immunity in teleost fish: a review. *Veterinárni Medicína*, 56(10), 486–503. doi: 10.1016/j.pestbp.2010.09.001.

- Urushihara, H., Kuwayama, H., Fukuhara, K., Itoh, T., Kagoshima, H., Shin, T. & Kuroki, Y. (2015). Comparative genome and transcriptome analyses of the social amoeba *Acytostelium subglobosum* that accomplishes multicellular development without germ-soma differentiation. *BMC Genomics*, 16(1), 80. doi: 10.1186/s12864-015-1278-x.
- Valdenegro-Vega, V. A. C. (2014). Using the mucosal response to recombinant *Neoparamoeba perurans* attachment proteins to design an experimental vaccine against amoebic gill disease (AGD). Doctoral thesis, University of Tasmania. Available at: <https://eprints.utas.edu.au/22402/>
- Valdenegro-Vega, V. A., Crosbie, P. B., Cook, M. T., Vincent, B. N. & Nowak, B. F. (2014a). Administration of recombinant attachment protein (r22C03) of *Neoparamoeba perurans* induces humoral immune response against the parasite in Atlantic salmon (*Salmo salar*). *Fish and Shellfish Immunology*, 38(2), 294-302. doi: 10.1016/j.fsi.2014.03.034.
- Valdenegro-Vega, V. A., Crosbie, P., Bridle, A., Leef, M., Wilson, R. & Nowak, B. F. (2014b). Differentially expressed proteins in gill and skin mucus of Atlantic salmon (*Salmo salar*) affected by amoebic gill disease. *Fish and Shellfish Immunology*, 40(1), 69-77. doi: 10.1016/j.fsi.2014.06.025.
- Valdenegro-Vega, V. A., Cook, M., Crosbie, P., Bridle, A. R. & Nowak, B. F. (2015). Vaccination with recombinant protein (r22C03), a putative attachment factor of *Neoparamoeba perurans*, against AGD in Atlantic salmon (*Salmo salar*) and implications of a co-infection with *Yersinia ruckeri*. *Fish and Shellfish Immunology*, 44(2), 592-602. doi: 10.1016/j.fsi.2015.03.016.
- Valderrama, D. & Anderson, J. L. (2010). Market interactions between aquaculture and common-property fisheries: Recent evidence from the Bristol Bay sockeye salmon fishery in Alaska. *Journal of Environmental Economics and Management*, 59(2), 115-128. doi: 10.1016/j.jeem.2009.12.001.
- Van Boeckel, T. P., Brower, C., Gilbert, M., Grenfell, B. T., Levin, S. A., Robinson, T. P. & Laxminarayan, R. (2015). Global trends in antimicrobial use in food animals. *Proceedings of the National Academy of Sciences*, 112(18), 5649-5654. doi: 10.1073/pnas.1503141112.
- Van Haastert, P. J. (2011). Amoeboid cells use protrusions for walking, gliding and swimming. *PloS One*, 6(11). doi: 10.1371/journal.pone.0027532.

- Van Kessel, M. A., Mesman, R. J., Arshad, A., Metz, J. R., Spanings, F. T., van Dalen, S. C. & Klaren, P. H. (2016). Branchial nitrogen cycle symbionts can remove ammonia in fish gills. *Environmental Microbiology Reports*, 8(5), 590-594. doi: 10.1111/1758-2229.12407.
- Vera, L. M. & Migaud, H. (2016). Hydrogen peroxide treatment in Atlantic salmon induces stress and detoxification response in a daily manner. *Chronobiology International*, 33(5), 530-542. doi: 10.3109/07420528.2015.1131164.
- Vercruyse, J., Schetters, T. P. M., Knox, D. P., Willadsen, P. & Claerebout, E. (2007). Control of parasitic disease using vaccines: an answer to drug resistance? *Revue Scientifique et Technique-Office International des Epizooties*, 26(1), 105. doi: 10.20506/rst.26.1.1728.
- Vigano, S., Utzschneider, D. T., Perreau, M., Pantaleo, G., Zehn, D. & Harari, A. (2012). Functional avidity: a measure to predict the efficacy of effector T cells? *Clinical and Developmental Immunology*, 2012. doi: 10.1155/2012/153863.
- Villavedra, M., To, J., Lemke, S., Birch, D., Crosbie, P., Adams, M. & Wallach, M. (2010). Characterisation of an immunodominant, high molecular weight glycoprotein on the surface of infectious *Neoparamoeba* spp., causative agent of amoebic gill disease (AGD) in Atlantic salmon. *Fish & Shellfish Immunology*, 29(6), 946-955. doi: 10.1016/j.fsi.2010.07.036.
- Vincent, B. N., Morrison, R. N. & Nowak, B. F. (2006). Amoebic gill disease (AGD)-affected Atlantic salmon, *Salmo salar* L., are resistant to subsequent AGD challenge. *Journal of Fish Diseases*, 29(9), 549-559. doi: 10.1111/j.1365-2761.2006.00751.x.
- Vincent, A. T., Gauthier, J., Derome, N. & Charette, S. J. (2019). The Rise and Fall of Antibiotics in Aquaculture. In *Microbial Communities in Aquaculture Ecosystems* (pp. 1-19). Springer, Cham.
- Vishnu, U. S., Sankarasubramanian, J., Gunasekaran, P. & Rajendhran, J. (2017). Identification of potential antigens from non-classically secreted proteins and designing novel multipeptide vaccine candidate against *Brucella melitensis* through reverse vaccinology and immunoinformatics approach. *Infection, Genetics and Evolution*, 55, 151-158. doi: 10.1016/j.meegid.2017.09.015.

- Wang, Z. J., Liu, X. H., Jin, L., Pu, D. Y., Huang, J. & Zhang, Y. G. (2016). Transcriptome profiling analysis of rare minnow (*Gobiocypris rarus*) gills after waterborne cadmium exposure. *Comparative Biochemistry and Physiology Part D: Genomics and Proteomics*, 19, 120-128. doi: 10.1016/j.cbd.2016.05.003.
- Waterhouse, R. M., Seppey, M., Simão, F. A., Manni, M., Ioannidis, P., Klioutchnikov, G. & Zdobnov, E. M. (2017). BUSCO applications from quality assessments to gene prediction and phylogenomics. *Molecular Biology and Evolution*, 35(3), 543-548. doi: 10.1093/molbev/msx319.
- Watts, J., Schreier, H., Lanska, L. & Hale, M. (2017). The rising tide of antimicrobial resistance in aquaculture: sources, sinks and solutions. *Marine Drugs*, 15(6), 158. doi: 10.3390/md15060158.
- Wlodarska, M., Willing, B. P., Bravo, D. M. & Finlay, B. B. Phytonutrient diet 646 supplementation promotes beneficial Clostridia species and intestinal mucus 647 secretion resulting in protection against enteric infection. *Scientific Reports*, 5(648), 9253.
- Wolf, K., Markiw, M. E. & Hiltunen, J. K. (1986). Salmonid whirling disease: *Tubifex tubifex* (Müller) identified as the essential oligochaete in the protozoan life cycle. *Journal of Fish Diseases*, 9(1), 83-85. doi: 10.1111/j.1365-2761.1986.tb00984.x.
- Wolfe, K. G., Plumb, J. A. & Morrison, E. E. (1998). Lectin binding characteristics of the olfactory mucosa of channel catfish: potential factors in attachment of *Edwardsiella ictaluri*. *Journal of Aquatic Animal Health*, 10(4), 348-360. doi: 10.1577/1548-8667(1998)010<0348:lbcoto>2.0.co;2.
- Wright D.W., Nowak B.F., Oppedal F, Bridle A. & Dempster T. (2015) Depth distribution of the amoebic gill disease agent, *Neoparamoeba perurans*, in salmon sea-cages. *Aquaculture Environment Interactions*, 7, 67–74. doi: 10.3354/aei00137.
- Wynne, J. W., O'Sullivan, M. G., Cook, M. T., Stone, G., Nowak, B. F., Lovell, D. R. & Elliott, N. G. (2008). Transcriptome analyses of amoebic gill disease-affected Atlantic salmon (*Salmo salar*) tissues reveal localized host gene suppression. *Marine biotechnology*, 10(4), 388-403. doi 10.1007/s10126-007-9075-4.

- Xu Z., Parra D., Gomez D., Salinas I., Zhang Y.-A., Jørgensen L.v.G., Heinecke R.D., Buchmann K., LaPatra S. & Sunyer J.O. (2013) Teleost skin, an ancient mucosal surface that elicits gut-like immune responses. *Proceedings of the National Academy of Sciences of the United States of America*, 110, 13097–13102. doi: 10.1073/pnas.1304319110.
- Xu, Z., Takizawa, F., Parra, D., Gómez, D., von Gersdorff Jørgensen, L., LaPatra, S. E. & Sunyer, J. O. (2016). Mucosal immunoglobulins at respiratory surfaces mark an ancient association that predates the emergence of tetrapods. *Nature Communications*, 7, 10728. doi: 10.1038/ncomms10728.
- Xu, D. H., Moreira, G. S., Shoemaker, C. A., Zhang, D. & Beck, B. H. (2017). Expression of immune genes in systemic and mucosal immune tissues of channel catfish vaccinated with live theronts of *Ichthyophthirius multifiliis*. *Fish and Shellfish Immunology*, 66, 540-547. doi: 10.1016/j.fsi.2017.05.051.
- York, R. & Gossard, M. H. (2004). Cross-national meat and fish consumption: exploring the effects of modernization and ecological context. *Ecological Economics*, 48(3), 293-302. doi: 10.1016/j.ecolecon.2003.10.009.
- Young, N. D., Dyková, I., Snekvik, K., Nowak, B. F. & Morrison, R. N. (2008). *Neoparamoeba perurans* is a cosmopolitan aetiological agent of amoebic gill disease. *Diseases of Aquatic Organisms*, 78(3), 217-223. doi: 10.3354/dao01869.
- Young, N. D., Crosbie, P. B. B., Adams, M. B., Nowak, B. F. & Morrison, R. N. (2008a). *Neoparamoeba perurans* n. sp., an agent of amoebic gill disease of Atlantic salmon (*Salmo salar*). *International Journal for Parasitology*, 37(13), 1469-1481. doi: 10.1016/j.ijpara.2007.04.018.
- Young, N. D., Dyková, I., Nowak, B. F. & Morrison, R. N. (2008b). Development of a diagnostic PCR to detect *Neoparamoeba perurans*, agent of amoebic gill disease. *Journal of Fish Diseases*, 31(4), 285-295. doi: 10.1111/j.1365-2761.2008.00903.x.
- Young, N. D., Cooper, G. A., Nowak, B. F., Koop, B. F., & Morrison, R. N. (2008c). Coordinated down-regulation of the antigen processing machinery in the gills of amoebic gill disease-affected Atlantic salmon (*Salmo salar* L.). *Molecular Immunology*, 45(9), 2581-2597. doi: 10.1016/j.molimm.2007.12.023.

- Young, N. D., Dyková, I., Crosbie, P. B., Wolf, M., Morrison, R. N., Bridle, A. R. & Nowak, B. F. (2014). Support for the coevolution of *Neoparamoeba* and their endosymbionts, *Perkinsela* amoebae-like organisms. *European Journal of Protistology*, 50(5), 509-523. doi: 10.1016/j.ejop.2014.07.004.
- Yu, H., Li, Q., Kolosov, V. P., Perelman, J. M. & Zhou, X. (2010). Interleukin-13 induces mucin 5AC production involving STAT6/SPDEF in human airway epithelial cells. *Cell Communication and Adhesion*, 17(4-6), 83-92. doi: 10.3109/15419061.2010.551682.
- Yue, J., Zhu, C., Zhou, Y., Niu, X., Miao, M., Tang, X. & Liu, Y. (2018). Transcriptome analysis of differentially expressed unigenes involved in flavonoid biosynthesis during flower development of *Chrysanthemum morifolium* 'Chuju'. *Scientific Reports*, 8(1), 1-14. doi: 10.1038/s41598-018-31831-6.
- Zanin, M., Baviskar, P., Webster, R. & Webby, R. (2016). The interaction between respiratory pathogens and mucus. *Cell host & microbe*, 19(2), 159-168. doi: 10.1016/j.chom.2016.01.001.
- Zeng, Z., Wu, X., Chen, F., Yu, J., Xue, L., Hao, Y. & Hu, P. (2011). Polymorphisms in prostate stem cell antigen gene rs2294008 increase gastric cancer risk in chinese. *Molecular Carcinogenesis*, 50, 353-8. doi.org/10.1002/mc.20718.
- Zerlotini, A., Aguiar, E. R., Yu, F., Xu, H., Li, Y., Young, N. D. & Kissinger, J. C. (2012). SchistoDB: an updated genome resource for the three key schistosomes of humans. *Nucleic Acids Research*, 41(D1), D728-D731. doi: 10.1093/nar/gks1087.
- Zhang, Y. A., Salinas, I., Li, J., Parra, D., Bjork, S., Xu, Z. & Sunyer, J. O. (2010). IgT, a primitive immunoglobulin class specialized in mucosal immunity. *Nature Immunology*, 11(9), 827. doi: 10.1038/ni.1913.
- Zilberg, D. & Munday, B. L. (2000). Pathology of experimental amoebic gill disease in Atlantic salmon, *Salmo salar* L., and the effect of pre-maintenance of fish in sea water on the infection. *Journal of Fish Diseases*, 23(6), 401-407. doi: 10.1046/j.1365-2761.2000.00252.x.
- Zilberg, D., Findlay, V. L., Girling, P. & Munday, B. L. (2000). Effects of treatment with levamisole and glucans on mortality rates in Atlantic Salmon (*Salmo salar* L.) suffering from amoebic gill. *Bulletin of the European Association of Fish Pathologists*, 20(1), 23.

- Zilberg, D. & Munday, B. L. (2001). Responses of Atlantic salmon, *Salmo salar* L., to *Paramoeba* antigens administered by a variety of routes. *Journal of Fish Diseases*, 24(3), 181-183. doi: 10.1046/j.1365-2761.2001.00280.x.
- Zou, H. K., Hoseinifar, S. H., Miandare, H. K. & Hajimoradloo, A. (2016). *Agaricus bisporus* powder improved cutaneous mucosal and serum immune parameters and up-regulated intestinal cytokines gene expression in common carp (*Cyprinus carpio*) fingerlings. *Fish and Shellfish Immunology*, 58, 380-386. doi: 10.1016/j.fsi.2016.09.050.